Interaction between SO_2 fumigation and drought stress on growth, photosynthesis and symbiotic nitrogen fixation in soybean, studied in an Open-top chamber facility.

Thesis submitted in partial fulfilment of the degree *Masters in Environmental Science (M.Env.Sci)* in the School of Environmental Sciences, North-West University, Potchefstroom Campus, South Africa.

E. Heyneke

(B.Sc.)

Supervisor: **Prof GHJ Krüger**

Co-supervisor: **Dr PDR van Heerden**

2008

Potchefstroom Campus



Open-top chamber facility, Potchefstroom campus

"Where air pollution is not seen as a serious problem, it might be due to a lack of information" …Lars Nordberg (2002).

Acknowledgements

I wish to sincerely thank and acknowledge the contribution and skill of the following persons:

- my supervisor, Prof. Gert Krüger, to whom I am greatly indebted for his valued advice, contribution, support and remarkable leadership.
- my co-supervisor, Dr. Riekert van Heerden, for his expert opinion and advice.
- Dr Jacques Berner, for helping me with the measurement of leaf water potential and for guidance in the laboratory.
- Riaan, for his skilful assistance with measurement and data attainment.
- Pieter, for helping to construct the chambers and helping with the maintenance and technical operation of the OTCs.
- Misha, for assistance with ureide analysis.
- Shorty, for maintaining the OTC site and for always lending a helping hand when pots had to be filled or moved around.
- Prof Leon van Rensburg and Prof. Kobus Pienaar, for additional financial assistance.
- Prof. Reto Strasser (Bioenergetics Laboratory, University of Geneva), for his patience and fruitful discussions regarding the fluorescence data.
- Dr. Anine Jordaan, for her assistance with the interpretation of TEM micrographs.
- Miss Wilna Pretorius and Dr Lowrens Tiedt, for assistance with the preparations for TEM work.
- Mr Willem du Pisanie and Owen Pretorius (EKSOM) for the loan of the SO_2 analyser used to conduct preliminary studies and the regular servicing of the analyser.
- The Instrument Making Department of the North-West University, particularly Mr Pieter Erasmus, Mr Hans Grobler and Mr Johann Broodryk.
- Mr Chris Albertyn and his team at C&M consulting Engineers; André Loubser and Jaco van Brakel for their professional and skilful expertise in constructing the OTC fumigation and sampling system.
- Miss Elma Verwey, for assembly and repair of the OTC sheeting.

- Mr Pietman Jordaan, for his skilful and professional service in producing the technical drawings of the OTC system.
- Mr Johnathan Taylor and Miss Louisemarie Combrink for the language provision.
- My parents for their love, support, sacrifices and eagerness to provide me with this opportunity.
- My brother Willie, for always being there to help carry heavy instruments and potted plants and for keeping me company.
- My family and friends for their love and support.
- The love of my life, Florian, and his family, Erich, Lucy and Alex Putz, for their love and support throughout my study.
- I gratefully acknowledge the financial support from the following South African organisations: National Research Foundation, South Africa; the Protein Research Foundation, the Oil and Protein Seeds Development Trust and the North-West University (Potchefstroom Campus) for making money available to erect such a state-of-the-art OTC growth facility on the campus.

I hereby declare that this thesis presented for the degree *Masters in Environmental Science (M. Env. Sci.)*, at the North-West University (Potchefstroom Campus), is my independent work and has not previously been presented for a degree at any other university or faculty.

Abstract

Interaction between SO_2 fumigation and drought stress on growth, photosynthesis and symbiotic nitrogen fixation in soybean

Air pollution emissions from South Africa are expected to increase in the short to medium term because of increased industrial activities and expected growth in socio-economic development. The developing world faces a more significant challenge regarding air pollution control with its growing efforts at promoting industrial development. Agriculture plays a critical role in food security and in the economic growth of developing countries. The Highveld region is responsible for more than 90 % of South Africa's air pollution emissions (Rorich & Galpin, 1998). Also, the North-eastern Free State, the North-West Province and the Mpumalanga Highveld region can be considered collectively as the "breadbasket" of South Africa. It is therefore extremely important to establish evidence for the threat that SO_2 may pose to crop production (Marshall *et al.,* 1998). While the impacts of air pollution have received considerable attention in North America and Europe, there has been little recognition of this issue in developing countries – including South Africa (Marshall *et al.*, 2000). To date, no detailed research to this end has been undertaken in South Africa. The study of the physiological and biochemical basis of SO_2 impacts on crop plants and the determination of critical levels under South African conditions is of paramount importance. Without this, the quantification of impacts and the rational management of air pollution will remain bogged down by speculation and uninformed perceptions.

The current research wishes to make a contribution in this regard. For this study, a battery of open top chambers was successfully commissioned and optimised in which a series of elevated levels of SO_2 (0, 50, 150 and 300 ppb SO_2) could be administered to assess the effects of SO_2 on plants as these would occur under natural conditions in the field. An external (outside) plot was included to assess the chamber effect. It is known that there is a close relationship between air quality guidelines and dose-response relationships (Sanders *et al.*, 1995). By following the development of visual injury symptoms in this study, it could be concluded that low concentrations of SO_2 can reduce photosynthetic capacity without any accompanying visual injury being apparent after as much as 14 days of exposure. SO_2 exposure brought about large decreases in the accumulation of biomass in well watered and drought stressed *Brassica oleracea* and *Glycine max* plants. Besides

biomass in drought stressed plants was reduced even more than in well watered plants, and showed that shoot growth were inhibited more than root growth. Yield reduction of up to 57 % was calculated for plants exposed to the highest SO_2 concentration and simultaneously subjected to drought stress. The yield reduction probably arose as a result of the increased stomatal conductance in drought stressed plants; drought stress thus not only caused a greater flux of SO_2 into the leaf, but also resulted in a reduction in the water use efficiency of the plants. Reductions in water use efficiency were also apparent in SO_2 exposed *Brassica oleracea*, despite the decreased stomatal conductance and transpiration rate these plants presented. Even though the test plants displayed distinctive stomatal responses toward SO_2, further analysis of the gas exchange data demonstrated that the SO_2-induced inhibition of photosynthesis in both *Brassica oleracea* and *Glycine max*, was mainly due to limitation of mesophyll (biochemical) processes and, to a lesser extent, due to stomatal limitations. Dose response relationships plotted from photosynthetic gas exchange data emphasised that SO_2 is a potent inhibitor of photosynthesis and can be described as highly phytotoxic. Analysis of the CO_2 response of the test plants exposed to different SO_2 concentrations revealed a severe inhibition in the maximal rate of CO_2 assimilation (J_{max}; regeneration capacity of RuBP) and carboxylation efficiency (CE; Rubisco activity). *In vitro* measurement of Rubisco activity in *Glycine max* corroborated this finding. The photosynthetic light response data indicated that the maximum quantum yield and light-saturated rate of photosynthesis in intact leaves of plants exposed to SO_2 were severely reduced. Although the reduction occurred at all SO_2 levels applied, the magnitude of these reductions could be ascribed for the most part to the SO_2 concentration administered. The chlorophyll content decreased significantly at all treatment levels after 35 days' fumigation with SO_2 in well watered and drought stressed *Brassica oleracea* and *Glycine max*. Root nodule ureide content decreased drastically in *Glycine max* at all SO_2 concentration levels. It could be assumed that the decreased chlorophyll content and the sharp reduction in the ureide content contributed to the decreases in growth and yield production. Analysis of the *chlorophyll a* fluorescence OKJIP transients measured in parallel with gas exchange showed that several biophysical parameters of photosystem II were affected in the test plants exposed to SO_2. The parameters most severely affected were the density of active reaction centres, electron transport and the performance index. *Chlorophyll a* fluorescence data showed an initial stimulation in well watered plants that were exposed to the lowest SO_2 concentration. No stimulations of any fluorescence parameters were evident in drought stressed plants. The *chlorophyll a* fluorescence data supported

the gas exchange data, confirming that the inhibition of CO_2 assimilation is due to impaired formation of end electron acceptors, ATP and NADPH. *Chlorophyll a* fluorescence also revealed inhibition on the electron acceptor side of PSII, namely the oxygen evolving complex. Ultrastructural investigation of the leaf material of the *Glycine max* plants revealed that SO_2-induced damage occurred mainly in the chloroplasts. Changes in chloroplast shape, damage to internal membranes and damage to the thylakoids were the most notable changes that occurred after 35 days' fumigation with 300 ppb SO_2. In each case, the effect of SO_2 in combination with drought was of great severity, indicating that drought-induced partial stomatal closure does not relieve damage caused by SO_2. The implication of the data obtained has for crop production in highly industrialised regions of the Mpumalanga Highveld of South Africa is discussed.

Opsomming

Interaksie van SO_2 begassing en droogtestres op groei, fotosintese en simbiotiese stikstoffiksering in soja

Daar word voorspel dat lugbesoedelingsemissies in en vanuit Suid-Afrika op die kort- en mediumtermyne gaan toeneem as gevolg van 'n toename in nywerheidsaktiwiteite en die verwagte groei in sosio-ekonomiese ontwikkeling. Die ontwikkelende wêreld staar 'n besondere belanrike uitdaging in die gesig ten opsigte van die beheer van lugbesoedeling met die doel om nywerheidsontwikkeling te bevorder. Landbou speel 'n kritieke rol in voedselsekuriteit en ook in die ekonomiese groei van ontwikkelende lande. Die Hoëveldstreek is verantwoordelik vir meer as 90 % van Suid-Afrika se lugbesoedelingsemissies (Rorich & Galpin, 1998). Verder word die Noord-Oos Vrystaat, die Noordwesprovinsie en die Mpumalanga-Hoëveld beskou as die "broodmandjie" van Suid-Afrika. Om hierdie rede is dit van besondere belang om bewyse vir die bedreiging wat SO_2 vir gewasproduksie inhou, te verskaf (Marshall *et al.*, 1998). Waar die impak van lugbesoedeling reeds deeglik onder die loep geneem is in Noord-Amerika en Europa, het dié aspek nog min aandag geniet in ontwikkelende lande – met inbegrip van Suid-Afrika (Marshall *et al.*, 2000). Tot op hede is nog geen omvattende navorsing oor hierdie onderwerp in Suid-Afrika gedoen nie. Die bestudering van die fisiologiese en biochemiese grondslag van SO_2-effekte op gewasse, asook bepaling van kritiese vlakke, is noodsaaklik. Sonder hierdie inligting sal die kwantifisering van impakte en die rasionele bestuur van lugbesoedeling belemmer word deur spekulasie en oningeligte menings.

Die huidige navorsing maak 'n bydrae in hierdie opsig. Vir die bestudering van die effek van SO_2 is 'n battery ooptopkamers ("open top chambers") suksesvol in werking gestel en geoptimiseer vir die deurlopende blootstelling van proefplante aan verhoogde SO_2-konsentrasies (0, 50, 150 en 300 ppb SO_2) onder toestande so na as moontlik aan die natuurlike. 'n Eksterne (buite-) perseel is ingesluit om die kamereffek te bepaal. Dit is bekend dat daar 'n nou verband bestaan tussen lugbesoedelingsriglyne en dosis-responsverhoudings (Sanders *et al.*, 1995). Deur die ontwikkeling van sigbare skadesimptome noukeurig te volg, kon die afleiding gemaak word dat lae konsentrasies SO_2 fotosintese rem in die afwesigheid van

sigbare letsels na so min as 14 dae blootstelling. Blootstelling aan SO_2 het gelei tot groot afnames in die biomassatoename van benatte en droogtegestremde *Brassica oleracea* en *Glycine max* plante. Trouens, selfs 'n verhoogde afname in die biomassa van droogtegestremde plante teenoor dié wat goed benat is, het voorgekom. Daar is ook bevind dat bogrondse groei meer as ondergrondse groei gerem was. 'n Vermindering van 57 % in opbrengs is bepaal vir droogtegestremde plante wat aan die hoogste SO_2-konsentrasie blootgestel is. Hierdie vermindering in opbrengs is waarskynlik te wyte aan die gepaardgaande toename in stomatale geleiding van die droogtegestremde plante wat veroorsaak het dat nie alleen meer SO_2 in die blare beland het nie, maar dat ook die watergebruikseffektiwiteit afgeneem het. Hierdie SO_2-geïnduseerde afname in watergebruikseffektiwiteit het ook voorgekom in *Brassica oleracea*, ten spyte van die afname in stomatale geleiding en transpirasietempo. Nieteenstaande die proefplante se unieke stomatale response ten opsigte van SO_2, het verdere analise van die gaswisselingsdata getoon dat die SO_2-geïnduseerde remming van fotosintese in beide *Brassica oleracia* en *Glycine max* hoofsaaklik toegeskryf kon word aan 'n beperking van mesofil (biochemiese) prosesse en, tot 'n mindere mate, aan stomatale beperking. Die fotosintetiese gaswisselingsdata ten opsigte van dosisresponsverhoudings het beklemtoon dat SO_2 'n sterk remmer van fotosintese is en as hoogs fitotoksies beskryf kan word. Ontleding van die CO_2-respons van proefplante blootgestel aan verskillende SO_2-konsentrasies, is besonder sterk gerem ten opsigte van die maksimale CO_2-assimileringstempo (J_{max}; regenereringskapasiteit van RuBP) en die karboksileringseffektiwiteit (CE; Rubisco-aktiwiteit). *In vitro*-bepaling van die Rubisco-aktiwiteit in *Glycine max* het hierdie bevinding ondersteun. Die fotosintetiese ligresponsdata het gedui op 'n groot afname in die maksimumkwantumopbrengs en die ligversadigingstempo van fotosintese van intakte blare van plante aan SO_2 blootgestel. Genoemde afnames was konsentrasie-afhanklik. Die chlorofilinhoud het ook drasties afgeneem in beide goedbenatte en droogte gestremde *Brassica oleracea* en *Glycine max* plante na 35 dae blootstelling aan SO_2. Die nodule ureidinhoud van *Glycine max* het ook drasties afgeneem na blootstelling by alle SO_2 konsentrasies. Daarmee dan die veronderstelling dat die skerp afname in chlorofilinhoud sowel as die drastiese afname in ureidinhoud bygedra het tot die afnames in groei en opbrengs. Ontleding van die *chlorofil a*-fluoressensie-OKJIP-stygingskromme wat parallel aan gaswisseling gemeet is, het getoon dat verskeie biofisiese parameters van die fotosisteem II funksie van die proefplante beïnvloed is. Die parameters wat die ergste beïnvloed is, was die digtheid van die aktiewe reaksiesentrums,

elektrontransport en die vitaliteitsindeks. Die *chlorofil a*-fluoressensiedata het 'n aanvanklike stimulasie by goedbenatte plante wat aan die laagste SO_2-konsentrasie, blootgestel is, getoon. Geen stimulering van enige fluoressensieparameters het voorgekom in die droogtegestremde plante nie. Die *chlorofil a*-fluoressensiedata het die gaswisselingsdata goed ondersteun en bevestig dat die inhibisie van CO_2-assimilering te wyte is aan doeltreffendheid van die vorming van eind-elektronontvangers, soos NADPH. Daar kon aangetoon word dat *chlorofil a*-fluoressensie aan die elektronontvangerkant van PSII, naamlik die suurstofvrystellingskompleks, geïnhibeer is. 'n Ultrastrukturele ondersoek van die blaarmateriaal van die *Glycine max*-plante het aan die lig gebring dat SO_2-geïnduseerde skade hoofsaaklik in die chloroplaste plaasgevind het. Veranderinge van die chloroplaststruktuur, beskadiging van interne membrane en skade aan die tillakoïede, was van die mees opvallende veranderinge na 35 dae van begassing met 300 ppb SO_2. Dit het geblyk dat die nadelige effek van SO_2 in kombinasie met droogtestremming vererger het, wat daarop gedui het dat droogte-geïnduseerde gedeeltelike sluiting van die stomata nie die skade aangerig deur SO_2, verlig nie. Die implikasie van die data vir gewasproduksie in die gekonsentreerde nywerheidsgebiede van die Mpumalanga-Hoëveld, word bespreek.

TABLE OF CONTENTS

Chapter 1 Literature review 1

1.1 Background 1

1.2 Introduction 4

1.3 Chemistry of SO_2 5

1.4 Biochemical effects of SO_2 6

1.4.1 Foliar injury engendered by SO_2 exposure 7

1.4.2 SO_2 effects on plant biomass accumulation and yield 8

1.4.3 SO_2 effects in combination with co-stress 9

1.4.4 SO_2 effects on stomatal metabolism 9

1.5 Hypotheses 11

1.5.1 Aim of the Study 11

Chapter 2 Introduction to open-top chambers 13

2.1 Open-top chamber construction and operation 13

2.1.1 Basic design features of open-top chambers (OTCs) 14

2.1.2 Chamber frame and chamber film cladding 15

2.1.3 Filter blower units and OTC ventilation 18

2.1.4 Filtration 22

2.1.5 Fumigation practice 23

2.1.6 Analysis of pollutant concentrations / Monitoring pollutant concentration 25

2.2 The environment inside open-top chambers 28

2.2.1 Radiation environment 28

2.2.2 Thermal environment 29

2.3 Detailed measurements of environmental conditions inside and outside OTCs at NWU 30

2.4 Experimental layout 32

Chapter 3 Material and methods 33

3.1 Plant cultivation 33

3.1.1 Cultivation of *Glycine max* plants - summer annual (2007/8) 33
3.1.2 Cultivation of *Brassica oleracea* plants - summer annual (2007/8) 35
3.2 Experimental design and treatment factors 35
3.3 Soil moisture measurements and calculation of plant available water 36
3.3.1 Soil water potential 36
3.4 Non-destructive plant analysis 37
3.4.1 Plant growth and development 37
3.4.2 Chlorophyll content index 38
3.4.3 Stomatal conductance (Gs) 38
3.4.4 Overview of photosynthetic gas exchange kinetics 38
3.4.5 Measurement of photosynthetic gas exchange 43
3.4.6 Overview of light response kinetics 44
3.4.7 Measurement of photosynthetic light response kinetics 46
3.4.8 Fast-phase *chlorophyll a* fluorescence kinetics 47
3.4.8.1 Overview of *chlorophyll a* fluorescence kinetics 47
3.4.8.2 Analysis of the *chlorophyll a* fluorescence transients by the JIP-test 48
3.4.9 Measurement of *chlorophyll a* fluorescence induction kinetics 54
3.5 Destructive plant analysis 55
3.5.1 Leaf water potential 55
3.5.2 Biomass accumulation and allocation 57
3.5.3 Yield attributes 57
3.5.4 Rubisco enzyme analysis 57
3.5.5 Nodule ureide content 58
3.6 Statistical analysis 59
Chapter 4 Results and discussion 60
4.1 Meteorological conditions in the chambers 60
4.2 Verification of water regime of the different treatments, i.e. "well watered" and "drought stressed" 63

4.2.1 *Brassica oleracea*....64

4.2.2 *Glycine max*....65

4.3 Growth....66

4.3.1 Plant development - Plastochron index....66

4.3.2 Foliar injury....68

4.3.3 Effects of SO_2 on the leaf ultrastructure of *Glycine max*....70

4.3.4 Biomass accumulation....72

4.3.4.1 Effects of SO_2 on biomass accumulation in *Brassica oleracea*....72

4.3.4.2 Effects of SO_2 on biomass accumulation in *Glycine max*....74

4.3.5 Yield attributes....75

4.3.5.1 Effect of SO_2 on yield attributes of *Glycine max*....75

4.3.6 Chlorophyll content index (CCI)....79

4.3.6.1 Effects of SO_2 on chlorophyll content index in *Brassica oleracea*....79

4.3.6.2 Effects of SO_2 on chlorophyll content index in *Glycine max*....80

4.3.7 Effect of SO_2 on nodule ureide content in *Glycine max*....81

4.3.8 Effect of SO_2 on Rubisco activity in *Glycine max*....82

4.4 Physiological response parameters....84

4.4.1 Effect of SO_2 on photosynthetic gas exchange in *Brassica oleracea*....84

4.4.2 Effect of SO_2 on photosynthetic gas exchange in *Glycine max*....98

4.4.3 Effect of SO_2 on photosynthetic light response in *Glycine max*....116

4.4.2 Effects of SO_2 on stomatal conductance....127

4.4.4.1 Effects of SO_2 on stomatal conductance in *Brassica oleracea*....127

4.4.4.2 Effects of SO_2 on stomatal conductance in

Glycine max.....128

4.4.5 Effects of SO_2 on fast phase *chlorophyll a* fluorescence kinetics.....129

4.4.5.1 Effects of SO_2 on fast phase *chlorophyll a* fluorescence kinetics in *Brassica oleracea*.....130

4.4.5.2 Effects of SO_2 on fast phase *chlorophyll a* fluorescence kinetics in *Glycine max*.....135

Chapter 5 Discussion.....152

5.1 Meteorological growth conditions in the open-top chambers.....152

5.2 Growth.....152

5.3 Biomass accumulation.....153

5.4 Yield.....154

5.5 Chlorophyll content.....154

5.6 Photosynthesis.....155

5.7 Constraints on photosynthesis.....163

5.7.1 Stomatal constraints.....165

5.8 The influence of the chamber effect.....166

Chapter 6: Concluding comments and future perspectives.....167

Future perspectives.....171

References.....172

List of abbreviations

ACC	Aminocyclopropane carboxylic acid
A_{350}	CO_2 assimilation rate at ambient CO_2 concentration (350 µmol mol^{-1})
A_0	CO_2 assimilation rate at an intercellular CO_2 concentration of 350 µmol mol^{-1}, or above, where no stomatal limitation is present
A_{max}	Light saturated rate of photosynthsis
ABS/CS_M	Phenomenological energy flux (per excited cross section of leaf) for light absorption
ABS/RC	The specific energy flux (per PSII reaction centre) for light absorption
C_a	Atmospheric CO_2 concentration
CCI	Chlorophyll content index
CE	Carboxylation efficiency
C_i	Intercellular CO_2 concentration
CS	Excited cross section of leaf
δ	probability for formation of end electron acceptors
DF	Driving force for photosynthesis
dw	Dry weight
ET	Electron transport
ET_0/CS_M	Phenomenological energy flux (per excited cross section of leaf) for electron transport
ET_0/RC	Specific energy flux (per PSII reaction centre) for electron transport
F_V/F_M	Quantum yield of primary photochemistry
fw	Fresh weight
g_s	Stomatal conductance
I_c	Light compensation point
J_{max}	Maximum CO_2 assimilation rate at saturating CO_2 concentration
ℓ	Relative stomatal limitation of photosynthesis

OEC	Oxygen Evolving Complex
OTC	Open-top chamber
PAR	Photosynthetic active radiation
PEA	Plant Efficiency Analyser
PFD	Photon flux density
PI_{ABS}	Performance index expressed on absorption basis
PLC	Photosynthetic leaf chamber
ppb	parts per billion
ppm	parts per million
PQ	Plastoquinone
PSI	Photosystem I
PSII	Photosystem II
PVPP	Polyvinylpolypyrrollidone
Φ_{max}	Maximum quantum yield of photosynthesis
φ_{EO}	Quantum yield of electron transport
φR_O	Quantum efficiency of the formation of reducing equivalents
ψ_0	Efficiency of converting a trapped exciton to electron transport further than Q_A^- into the electron transport chain
Ψ_L	Leaf water potential
Ψsoil	Soil matric potential
Q_A	Primary bound quinone
Q_A^-	Primary bound quinone in reduced state
Q_B	Secondary bound quinone
Q_B^-	Secondary bound quinone in reduced state
RC	Photosystem II reaction centre
RC/ABS	The density of active PSII reaction centres on a chlorophyll basis
RC/CS_M	The density of active PSII reaction centres per excited cross section
Γ	CO_2 compensation concentration

RuBP	Ribulose-1,5-bisphosphate
Rubisco	Ribulose-1,5-bisphosphate carboxylase/oxygenase
SO_2	Sulphur dioxide
SO_3^{2-}	Sulphite
HSO_3^-	Bisulphite
TR	Trapping of excitation energy
TR_0/CS_M	The phenomenological energy flux (per excited cross section of leaf) for trapping
TR_0/RC	The specific energy flux (per PSII reaction centre) for trapping
WUE	Water use efficiency

List of Figures

Figure 1.1: Spatial and temporal average SO_2 concentration isopleth.....2

Figure 2.1: Battery of twelve OTCs at experimental site.....14

Figure 2.2: Transmission spectrum of PVC sheeting 16

Figure 2.3: Ventilation unit, air ducting and chamber dimension.....17

Figure 2.4: Ventilation performance graph 20

Figure 2.5: Virtual position of ventilation unit.....21

Figure 2.6: Photograph of actual system.....21

Figure 2.7: Filtration unit 22

Figure 2.8: Liquid SO_2 and air compressor.....23

Figure 2.9: Needle valve connected to rotameters.....24

Figure 2.10: .Scheme of OTC fumigation system.....25

Figure 2.11: Sample line fitted with disk filter.....26

Figure 2.12: Manifold of 2/3-way solenoid valves.....26

Figure 2.13: Scheme of OTC sampling system.....27

Figure 2.14 Relative humidity and temperature sensor.....31

Figure 2.15: Solar radiation and automatic precipitation meter.....31

Figure 2.16: Layout of chambers on experimental site.....32

Figure 3.1: Soybean seedlings in temperature controlled greenhouse 34

Figure 3.2: Schematic presentation of pot-reservoir system.....34

Figure 3.3: Tensiometers used to record soil water potential.....37

Figure 3.4: A:C_i response curve.....42

Figure 3.5: A:Q response curve.....46

Figure 3.6: Measuring of photosynthetic gas exchange.....47

Figure 3.7: Polyphasic *chlorophyll a* flurescence transient.....50

Figure 3.8: Energy cascade from solar radiation to electron transport.....53

Figure 3.9: Measurement of leaf water potential 57

Figure 4.1: Mean SO_2 concentrations in OTCs.....61

Figure 4.2: Mean hourly soil water potential.....62

Figure 4.3: Leaf water potential in *Brassica oleracea*.....64

Figure 4.4: Leaf water potential in *Glycine max*.....65

Figure 4.5: Plastochron index in *Glycine max*.....66

Figure 4.6: Visible leaf injury symptoms in *Brassica oleracea*.....68

Figure 4.7: Visual leaf injury symptoms in *Glycine max*.....69

Figure 4.8: Visual leaf injury symptoms in *Glycine max* 69

Figure 4.9: Visual leaf injury symptoms in *Glycine max*.....69

Figure 4.10: TEM graphs of adaxial mesophyll cells of *Glycine max* leaves..... 71

Figure 4.11: TEM graphs of adaxial mesophyll cells of *Glycine max* leaves 71

Figure 4.12: TEM graphs of adaxial mesophyll cells of *Glycine max* leaves.....72

Figure 4.13: Shoot and root biomass accumulation in *Brassica oleracea*.....73

Figure 4.14: Shoot and root biomass accumulation in *Glycine max* 75

Figure 4.15: Seed development inside pods of *Glycine max* 79

Figure 4.16: Chlorophyll content index in *Brassica oleracea* 80

Figure 4.17: Clorophyll content index in *Glycine max*.....81

Figure 4.18: Root nodule ureide content in *Glycine max* 82

Figure 4.19: Initial and total *in vitro* Rubisco activity measured in *Glycine max*.....83

Figure 4.20: A:C_i curve of well watered *Brassica oleracea* after 35 days 85

Figure 4.21: Mesophyll related parameters of drought stressed *Brassica oleracea* after 35 days 88

Figure 4.22: Mesophyll related parameters of drought stressed *Brassica oleracea* after 35 days 89

Figure 4.23: A:C_i curve of well watered *Brassica oleracea* after 50 days 92

Figure 4.24: Mesophyll related parameters of drought stressed *Brassica oleracea* after 50 days 95

Figure 4.25: Mesophyll related parameters of drought stressed *Brassica oleracea* after 50 days 96

Figure 4.26: A:C_i response curve in *Glycine max* before fumigation commenced 98

Figure 4.27: A:C_i response curve in well watered *Glycine max* after 7 days 101

Figure 4.28: A:C_i response curve in drought stressed *Glycine max* after 7 days 104

Figure 4.29: A:C_i response curve in well watered *Glycine max* after 28 days 108

Figure 4.30: 3-D A:C_i response curve of *Glycine max* after 7 days 110

Figure 4.31: A:C_i response curve in drought stressed *Glycine max* after 28 days 112

Figure 4.32: 3-D A:C_i response curve of *Glycine max* after 28 days 114

Figure 4.33: A:Q curves in well watered *Glycine max* after 14 days 116

Figure 4.34: A:Q curves in drought stressed *Glycine max* after 14 days. 119

Figure 4.35: 3D- A:Q curves in *Glycine max* after 14 days 121

Figure 4.36: A:Q curves in well watered *Glycine max* after 35 days.....122

Figure 4.37: A:Q curves in drought stressed *Glycine max* after 35 days.....124

Figure 4.38: 3D- A:Q curves in *Glycine max* after 14 days.....127

Figure 4.39: Stomatal conductance in *Brassica oleracea*.....128

Figure 4.40: Stomatal conductance in *Glycine max* 129

Figure 4.41: Specific and phenomenological energy fluxes in well watered *Brassica oleracea* 131

Figure 4.42: Specific and phenomenological energy fluxes in drought stressed *Brassica oleracea* 131

Figure 4.43: Performance index total after 28 and 35 days in *Brassica oleracea*.. 132

Figure 4.44: Driving force total after 28 and 35 days in *Brassica oleracea*.....135

Figure 4.45: Raw *chlorophyll a* fluorescence transients in well watered *Glycine max*..... 137

Figure 4.46: Raw *chlorophyll a* fluorescence transients in drought stressed Glycine max.....137

Figure 4.47: *Chlorophyll a* fluorescence transients normalised between 0.05 and 2ms for well watered *Glycine max*..... 138

Figure 4.48: *Chlorophyll a* fluorescence transients normalised between 0.05 and 2ms for drought stressed *Glycine max*.....138

Figure 4.49: Specific and phenomenological energy fluxes in well watered *Glycine max* 140

Figure 4.50: Specific and phenomenological energy fluxes in drought stressed *Glycine max* 141

Figure 4.51: Energy pipeline models in *Glycine max* after 28 days..... 142

Figure 4.52: Performance index total after 28 and 35 days in *Glycine max*.....143

Figure 4.53: Driving force total after 28 and 35 days in *Glycine max*.....145

Figure 4.54: Relative variable *chlorophyll a* fluorescence transients in well watered *Glycine max* after 14 days..... 148

Figure 4.55: Relative variable *chlorophyll a* fluorescence transients in drought stressed *Glycine max* after 14 days.....149

Figure 4.56: Relative variable chlorophyll a fluorescence transients in well watered *Glycine max* after 28 days.....150

Figure 4.57: Relative variable chlorophyll a fluorescence transients in drought stressed *Glycine max* after 28 days. 151

Figure 5.1: Scheme of inhibition sites in the chloroplast.....162

List of Tables

Table 2.1: Computer simulated calculations of ducting diameter.....19

Table 3.1: Timetable of event during growth of *Glycine max*.....35

Table 3.2: JIP-test formulae.....53

Table 4.1: Vegetative and reproductive responses of well watered *Glycine max*.....77

Table 4.2: Vegetative and reproductive responses of drought stressed *Glycine max*.....78

Table 4.3: Gas exchange parameters of well watered *Brassica oleracea* after 35 days.....86

Table 4.4: Gas exchange parameters of drought stressed *Brassica oleracea* after 35 days.....90

Table 4.5: Gas exchange parameters of well watered *Brassica oleracea* after 50 days.....93

Table 4.6: Gas exchange parameters of drought stressed *Brassica oleracea* after 50 days.....97

Table 4.7: Gas exchange parameters of *Glycine max* before fumigation commenced.....100

Table 4.8: Gas exchange parameters of well watered *Glycine max* after 7 days.....103

Table 4.9: Gas exchange parameters of drought stressed *Glycine max* after 7 days.....107

Table 4.10: Gas exchange parameters of well watered *Glycine max* after 28 days.....111

Table 4.11: Gas exchange parameters of drought stressed *Glycine max* after 7 days.....115

Table 4.12: Light response parameters of well watered *Glycine max* after 14 days.....118

Table 4.13: Light response parameters of drought stressed *Glycine max* after 14 days 120

Table 4.14: Light response parameters of well watered *Glycine max* after 35 days 123

Table 4.15: Light response parameters of drought stressed *Glycine max* after 35 days 126

Chapter 1

Literature review

1.1 Background

Air pollution is one of the most pressing and urgent problems globally; it is also a problem that does not respect political or geographical boundaries. As a consequence, long-distance transport and dispersal of air pollutants from industrial areas may intrude into remote rural areas far from the actual pollution source. Although sulphur dioxide emissions from industry are no longer a major issue in Europe and North America, due to the imposition of strict regulatory legislation, there is growing evidence of the pollutant effects of sulphur dioxide in developing countries.

South Africa has an extremely energy-intensive economy, and contributes substantially to pollution through its coal-fired power stations. The "Highveld" region (i.e. the interior plateau at a mean altitude of 1 700 m encompassing Gauteng, western Mpumalanga and the North-West provinces) forms the heartland of South Africa's fast-growing economy. Annual mean SO_2 concentrations in this region are more than ten times higher than background concentrations in southern Africa. Daily SO_2 concentrations of up to 60 ppb have been reported at the Elandsfontein monitoring site in the centre of the Mpumalanga Highveld (Turner, 1990). In this region, South Africa's considerable mineral wealth is exploited to the full by various mining and industrial operations. In addition, at least 98% of South Africa's electricity is generated in this region by coal-fired power stations. The Highveld region is responsible for more than 90% of South Africa's air pollution emissions. Coal-fired power stations alone emitted 1 167 000 tonnes of sulphur dioxide (SO_2) during 1994 (Rorich & Galpin, 1998).

The Highveld region is therefore particularly problematic in this regard, and the air pollutant dispersion conditions in this region have been described "as among the most unfavourable anywhere in the world" (Tyson *et al.*, 1998). The unique air circulation patterns and stable atmospheric layers, in which vertical distribution of air pollutants is very limited, are largely to blame for this (Van Tienhoven & Scholes, 2003). As a consequence, the ground-level concentrations of sulphur dioxide (SO_2) and ozone (O_3) frequently exceed critical levels, compared to European and North American air quality standards. An annual mean concentration of 11.5 parts per billion (ppb) SO_2 is the European critical level or threshold at which a 5% yield

reduction can be expected for agricultural crops (Ashmore & Marshall, 1998). Various monitoring sites on the Highveld (Figure 1.1) have exceeded this critical level in the past.

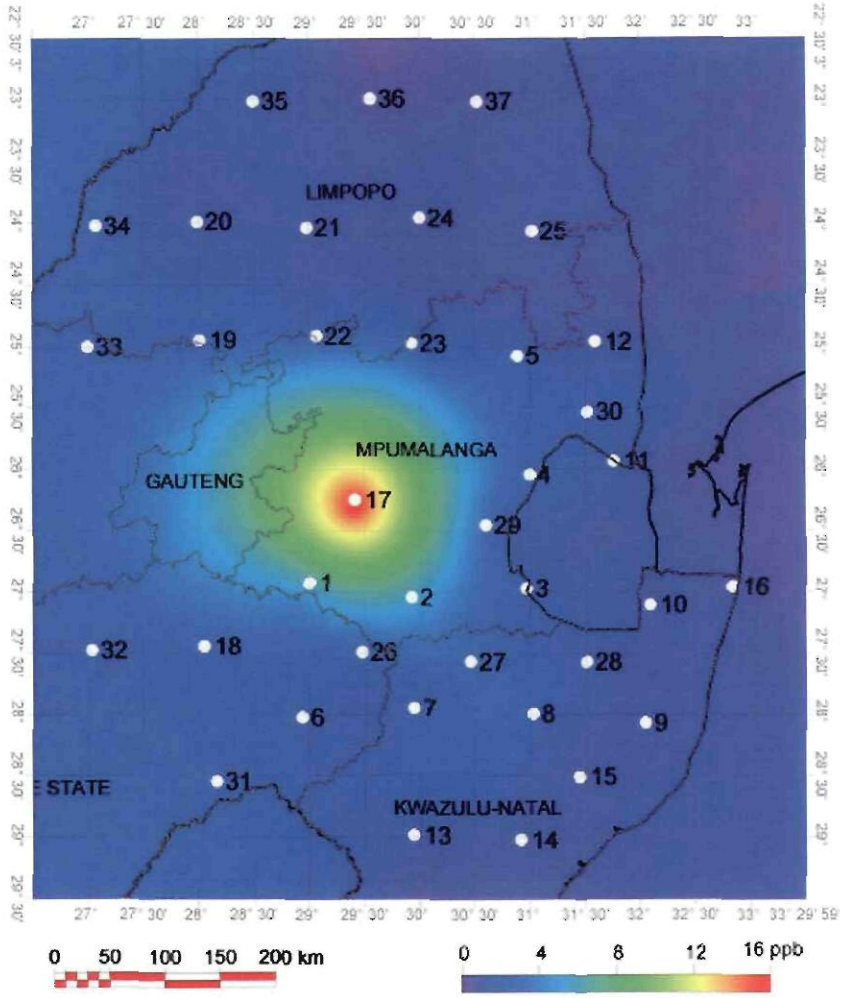


Figure 1.1 Spatial and temporal averaged concentration isopleths for SO_2 (ppb) recorded during January 2005 to May 2006, showing sulphur dioxide concentrations over the South African Highveld region; home to ten ESKOM power stations, five of which are the largest in the world. Passive samplers were chemically analysed by the School of Chemistry, North-West University (Potchefstroom Campus) (Josipovic, 2007).

To make matters even worse, SO_2 emissions are expected to rise dramatically in the near future, especially in fast-developing countries such as South Africa due to technological limitations on the control of emissions, increased numbers of motor

vehicles and the need to supply in the rapidly growing national electricity demand. This must be seen as a major concern because the yield losses of economically important agricultural crops have been well documented in the vicinity of urban and industrial areas in India where SO_2 was the principal pollutant (Agrawal, 2000).

The susceptibility of natural vegetation and crop plants to SO_2 and O_3 is well documented, especially in northern hemisphere countries. Visual symptoms and substantial reductions in crop yield have been reported (Benton *et al.*, 2000) However, the impacts of air pollution on crop production in South Africa in general, and in the Highveld region in particular, are still poorly understood (Van Tienhoven & Scholes, 2003). Only a few superficial studies have been conducted to date and results have mostly been inconclusive. Limitations inherent to air pollution research, such as inadequate control/measurement of low application dosages (in the parts per billion range) as well as rudimentary fumigation techniques/infrastructure are the main reasons for this. Furthermore, fundamental problems associated with adopting data obtained from studies conducted in northern hemisphere countries persist. South Africa's climatic conditions are quite different from those in Europe and North America, and considerable climatic variations that exist within South Africa's boundaries; such as droughts and other stress factors that may modulate the response of plants to air pollutants, are much more prevalent than in the northern hemisphere. Finally, the stable whirlpool of air that recirculates over the southern African region traps and accumulates air pollutants (Van Tienhoven & Scholes, 2003).

A rapid increase in pollutant emissions is predicted over the coming years in many developing countries, South Africa included (Marshall *et al.*, 1998). No such research has been undertaken in the past in southern Africa and it is thus of paramount importance that the response of crops be assessed for South African conditions (Marshall *et al.*, 1998).

Periods of drought, as frequently experienced in South Africa, together with the direct effects of air pollutants such as SO_2 could have substantial effects on crop production. More than 80% of South Africa is classified as semi-arid with average annual precipitation being less than 500 mm. It is not surprising therefore that the average yield of oilseed such as soybean is much lower than in various other parts in the world. Along with changes in temperatures and shifts in precipitation patterns, emerging climate change is predicted to reduce annual rainfall in many agricultural

systems and also to increase the frequency of droughts (IPCC, 2001). Increased water demands by the ever-growing industrial sector, urban population rise and demands to maintain environmental flows and water quality will continue to reduce water availability for irrigated agriculture. Elevated SO_2 concentration is said to cause stomatal closure, thereby decreasing transpiration at the same time that carbon assimilation is increased (Darrall, 1989). Therefore, because soil water availability is a major environmental factor for plant growth, it is of particular importance to analyse possible interactions of elevated SO_2 concentrations and water supply in terms of net photosynthesis (A), stomatal conductance (Gs) and water use efficiency (WUE).

1.2 Introduction

The effects of SO_2 on plants were some of the earliest studied phenomena of toxic gasses. Sulphur dioxide has caused damage since the beginning of the smelting of sulphur-containing ores over 4 000 years ago, and has turned out to be one of the most prominent phytotoxic by-products of fossil fuel burning.

Among the sulphur gasses, SO_2 is considered to be the most important phytotoxic molecule (Legge *et al.*, 1998). The main anthropogenic sources of SO_2 are stationary or point sources involved in fossil fuel combustion and liquefaction, metal smelting and oil and natural gas processing (Cullis & Hirschler, 1980; Brimblecombe *et al.*, 1989). Eighty three per cent of the estimated 194 million tonnes of SO_2 emitted annually is due to fossil fuel combustion (Watson *et al.*, 1990).

SO_2 is an air pollutant which can have positive effects on physiological and growth characteristics of plants at low concentrations, especially in plants growing in sulphur deficient soil (Darall, 1989), when the sulphate might be metabolised to fulfil the demand for sulphur as a nutrient (De Kok, 1990). At the same time, increased uptake of SO_2 can cause toxicity and reduce growth and productivity of plants due to accumulation of sulphite or sulphate (Darall, 1989; Agrawal & Verma, 1997). In contrast to the cases for SO_2 damage to forests, there are only a few well-documented examples of the adverse effects of ambient SO_2 exposures on crop plants. SO_2, as in the case of fluoride, is an accumulative pollutant in plant tissue (Bell & Treshow, 2002). In general, acute and/or chronic exposures to SO_2 can result in a reduction of the photosynthetic rate (Winner *et al.*, 1985). In this regard, Pratt *et*

al. (1983) showed an accumulation of total S in SO_2-fumigated soybean plants and a reduction in leaf total chlorophyll content. Although there are a few reports of short-term SO_2-induced stimulation of photosynthesis, there is a measure of uncertainty as to whether such studies were satisfactorily able to account for CO_2 loss by photorespiration. In contrast to the effects of the primary metabolic pathways, exposures to SO_2 can also alter secondary metabolism. For example, cell wall rigidity can be induced by direct exposure to SO_2 through increased production of phenols (Hyodo *et al.*, 1978) and peroxidases (Morgan & Fowler, 1972) and consequently increased oxidation of phenols (Biggs & Fry, 1987) influencing the elastic properties of the cell walls and thus water relations.

1.3 Chemistry of SO_2

Sulphur dioxide is a polyatomic molecule made up of one sulphur atom attached to two oxygen atoms. Sulphur dioxide has the ability to act as either a reducing or oxidising agent depending upon the pH of the medium in which it exists. Acidic solutions favour the formation of SO_3^{2-}. Sulphur dioxide is extremely soluble in water, causing it to dissolve completely upon contact with surface or tissue moisture of plants to establish the following equilibriums:

$$SO_2 + H_2O \longrightarrow H_2SO_3$$

$$H_2SO_3 \longrightarrow H^+ + HSO_3^- \quad , \quad pK = 1.76$$

$$HSO_3^- \longrightarrow H^+ + SO_3^{2-} \quad , \quad pK = 7.20$$

Like CO_2, SO_2 is a potentially acidic gas and reacts according to the above listed equilibriums, thereby releasing protons. Taking the pK values into consideration, one could mention that HSO_3^- anions dominate below pH 7 and the SO_3^{2-} anion above pH 7. Because protons are trapped by alkaline substances, the products of the reaction of SO_2 with water will accumulate particularly in alkaline cell compartments (Malhotra & Hocking, 1976). The release of protons in these compartments will cause the pH within these compartments to decrease. The extent of the decrease is a function of the flux of SO_2 into the leaf, the pH of the compartment and its buffering capacity (Malhotra & Hocking, 1976).

1.4 Biochemical effects of SO_2

Plant shoots form a sink for atmospheric sulphur gasses, which can be taken up directly by the foliage. SO_2 enters the leaf primarily through the stomata under conditions favourable to rapid CO_2 and water vapour exchange. This uptake by the unwetted foliage depends on the degree of opening of the stomata, since the resistance to gas is low. If the stomata are closed, SO_2 can overcome the cuticular resistance and thereby enter the leaf. Once inside the leaf, SO_2 encounters moist surfaces upon which, on account of its great solubility in water, it is readily absorbed and rapidly dissolves in the aqueous phase of the cell wall; and at apoplastic pH value, it reacts with water and dissociates into toxic sulphite anions such as bisulphate (HSO_3^-) and sulphite (SO_3^{2-}) (Pfanz *et al.*, 1990). Sulphurous acid decreases the cytoplasmic pH, stimulating the cytoplasmic pH-stat mechanisms which counter acidification (Pfantz *et al.*, 1987b; Pfantz & Heber, 1986). If the decrease in pH caused by SO_2 cannot be compensated for by cellular mechanisms, then metabolism will be affected. Numerous examples related to changes in pH can be mentioned, such as the sensitivity of photosynthesis to changes in pH and the role that the proton concentration plays as a controlling factor for the light activation of the Calvin cycle enzymes (Hopkins, 1999). Atmospheric SO_2 may cross the plasmalemma and enter the symplasm either in the form of sulphate, mainly by active carrier mediated transport, or in the form of SO_2 (aq) by diffusion of sulphate (Rennenberg, 1984). It is trapped in this compartment by its reaction with water to yield bisulphite. Within the chloroplast, bisulphite will be further converted to sulphite because of the pH value of the stroma (pH 8.8) (Kurkdjian & Guern, 1989). Sulphite can be rapidly converted to the non-toxic sulphate (SO_4^{2-}) in the apoplast (Pfanz *et al.*, 1990) leading to an S influx into the leaf cells through the transpiration stream (Wolfenden *et al.*, 1991; Rennenberg & Herschbach, 1996). Excessive sulphate is transferred into the vacuole. Sulphite can be oxidised extra- and intracellularly by the reaction of peroxidase with hydrogen peroxide and apoplastic phenolics or non-enzymatically catalysed by metal ions or superoxide radicals, and subsequently reduced and assimilated again (Pfanz *et al.*, 1990; Takahama *et al.*, 1993). The detoxification of sulphite to sulphate, which takes place through light-initiated reactions mediated by the photosynthetic electron transport chain, leads to the formation of superoxide anions (O_2^-), hydroxyl radicals (OH) and hydrogen peroxide H_2O_2) (Asada, 1980). These highly oxidant molecular species together with toxic sulphite can disrupt membranes and damage lipids, proteins and pigments of the thylakoid membranes (Wellburn, 1985; Winner *et al.*, 1985). Plants exposed to SO_2

can also re-emit part of that absorbed sulphur as hydrogen sulphide (H_2S). The conversion of SO_4^{2-} and SO_3^- to H_2S is a light-mediated process thought to occur in the chloroplast. Sulphite may directly enter the sulphur reduction pathway where it is reduced to sulphide, and incorporated/assimilated into cysteine and other sulphur-containing compounds. This overall process of the loss of S into the atmosphere can be viewed as a means of reducing excess sulphur and control its S nutrition via homeostatic regulation of the cell cysteine concentration (Rennenberg & Herschbach, 1996).

1.4.1 Foliar injury engendered by SO_2 exposure

Injury to plants caused by SO_2 is first visible on the more sensitive foliage rather than on the stems, buds and reproductive parts. The expanse of injury caused by SO_2 is determined by biotic and abiotic factors, as well as the concentration, duration and the frequency of exposure. That taken into consideration, it should be noted that the SO_2 concentration, duration and the frequency of exposure are determined by meteorological conditions, which play a significant role in determining the adverse response of the vegetation to SO_2 exposure. For example, in the vicinity of point sources, meteorological conditions favourable for the promotion of surface level atmospheric inversions can expose vegetation to relatively high levels of SO_2 (Boubel *et al.*, 1994).

Foliar injury/symptoms can develop in response to either acute or chronic exposure. Acute SO_2 exposure can be characterised as exposure that is of short duration of a few minutes to hours, which is of sufficient concentration to result in the expression of necrotic injury to the foliage. Legge *et al.* (1998) describe acute SO_2 injury on broad-leaved plants to consist of bifacial, marginal and or interveinal necrosis and chlorosis on leaves at the full stage of development. Depending on the species, the necrotic areas can range in colour from white to reddish-brown and even black. The margins of the necrotic areas are irregular and occasionally darkly pigmented. On the other hand, monocotyledonous plants show acute injury as necrotic and chlorotic streaks that start at the tip of the leaf and spread downwards. Foliar injury symptoms reported in corn are seen as whitish-tan and brownish-red marginal and interveinal necrosis that start at the leaf tips and margins, spreading towards the mid-rib. Acute SO_2 symptoms are almost certainly best described for conifers, in which acute injury appeared on second-year needles and older and consisted of a tan to reddish-brown necrosis that spread from the needle tips downwards towards the needle base

preceded by chlorosis. Premature needle drop of the older needles is also documented to occur commonly (Darral, 1989; Legge *et al.*, 1998). These acute foliar symptoms can be ascribed to the acidic nature of the water droplets present on the leaf following absorption of SO_2 to form sulphuric acid (H_2SO_4). These water droplets cause necrotic areas with regular margins that reflect the outline of the acidified water droplets. Alternatively, chronic SO_2 exposure is viewed as exposures of low SO_2 concentration that occur during the entire growth cycle of the plant with intermittent or random peak levels (Krupa, 1996). As noted for acute leaf injury, chronic exposure to SO_2 may result in marginal and/or interveinal chlorosis in broad-leaved plants and can cause chlorosis in second-year and older conifer needles that ultimately brings about premature fall colouration and premature needle abscission (Legge *et al.*, 1998). Although thus far acute and chronic exposure was discussed as occurring separately, this is not always the case. Acute SO_2 exposure can occur on top of chronic symptoms or co-occur on the same or different foliage on the same plant. This has been reported to take place in the vicinity of point sources (Legge & Krupa, 2002). Acute and/or chronic exposure to SO_2 can result in changes in the physical nature and chemical composition of the epicuticular waxes (Percy *et al.*, 1994).

1.4.2 SO_2 effects on plant biomass accumulation and yield

Even though foliar injury symptoms may be evident when plants are chronically exposed to SO_2, it is important to consider that reductions in the rate of plant growth and productivity (biomass) may occur without the development of visible chronic foliar injury symptoms (Crittenden & Read, 1978). Reduction in yield has also been reported without the development of visible symptoms when plants were treated with low concentrations of SO_2 for a long duration (Godzik & Krupa, 1982). Strong yield reductions of soybean (up to 48%) were reported by Sprügel *et al.* (1980), who fumigated the crop during 18 days for 5 $h.day^{-1}$ with 90 – 370 ppb SO_2. On the contrary, Deepak and Agrawal (1999) reported increases in morphological characteristics and biomass and suggested that the plants derived some metabolic advantage from low doses of SO_2 to meet their sulphur requirements in the early stages of growth. Beneficial effects of SO_2 have also been reported by Tingey *et al.* (1980); Olszyk *et al.* (1986) and Clarke and Murray (1990). Although its been shown that exposure to low concentrations of SO_2 may stimulate plant growth, it should be considered that these increases in growth may stimulate plants so that they outgrow their resource base, leading to an insufficient supply of water, nutrients (other than

sulphur), and light. Other authors reported reductions in dry matter accumulation and fruit yield and have also reported that plants revealed decreases in almost all growth parameters (Krishnayya & Date, 1996). Decreases in shoot biomass of various plants due to SO_2 exposure have also been reported by many investigators (Convill *et al.,* 1983; Koch *et al.,* 1987; Rajput *et al.,* 1995; Agrawal & Verma, 1997). Exposure of plants to 0.06 ppm SO_2 resulted in loss of yield and this was correlated with reduced photosynthetic rate (Keller, 1984; Darrall, 1986).

1.4.3 SO_2 effects in combination with co-stress

Air pollution stress seldom occurs in isolation. The response of plants to air pollutants should be investigated in a "multi-stress" context to understand how air pollutants affect plants and to predict how air pollution impacts will be modified by elements of climate change (Winner, 1994). Although drought also represents a stress factor, it has been reported that drought can in principle be protective by limiting the direct impact of SO_2 through stomatal closure. However, if produced in combination with air pollutants during prolonged exposure, it results in damage that neither of the stresses alone would cause (Heber *et al.,* 1989b). Many plant responses to air pollution have also been characterised as forms of stress "compensation" (Winner, 1994). Reduction in the root-to-shoot ratio that commonly occurs when plants are exposed to SO_2 is one example of a compensatory response to air pollution (Mooney *et al.,* 1988). Mooney *et al.* (1988) reported a reduction in total biomass at the end of the experimental period, but also reported that most of the biomass loss occurred for the non-photosynthetic tissue below ground. Although the SO_2 treatment reduced photosynthesis, the shift in the root-to-shoot ratio enhanced the productivity above ground, which would not have occurred had the root-to-shoot ratio not shifted. It is important to keep in mind that there are limits for shifting partitioning of carbon and other resources beyond which plants simply cannot go. In addition, reductions in root-to-shoot ratio caused by air pollution may reduce the capacity of plants to grow with co-occurring stresses such as drought. It is not yet possible to grow plants with environmental stresses while restricting their compensatory capacity (Winner, 1994).

1.4.4 SO_2 effects on stomatal metabolism

Stomata play an important role in regulating the physiological processes in the leaf, and primarily serve as a pathway for the exchange of gasses between the intercellular surfaces and the atmosphere. Stomatal movements are known to be caused by changes in the guard cell turgor arising from the movement of K^+ and H^+ with electroneutrality being maintained by movement of Cl^- or internal production of malate (Outlaw, 2003; Raschke, 1979; McAinsh *et al.*, 2002). Stomatal responses to SO_2 and other air pollutants have been extensively reviewed (Darrall, 1989; Saxe, 1990; Wellburn, 1994; McAinsh, 2002; Mansfield, 1998; Robinson *et al.,* 1998). There is now abundant evidence that SO_2 can affect control mechanisms of stomata even at very low concentrations. Air pollutants may affect stomata directly or indirectly. There is evidence that air pollutants can influence the stomata directly by reducing the ability of guard cells to respond to stimuli such as ABA (Darrall, 1989; Saxe, 1990; Wellburn, 1994; McAinsh, 2002; Mansfield, 1998; Robinson *et al.,* 1998). Atkinson *et al.* (1991) showed that exposure of spring barley to low concentrations (35 ppb) of SO_2 had very little effect on stomatal opening; however, the stomata of the exposed leaves closed slower and less completely than those of the control plants in response to ABA. Black and Unsworth (1979) demonstrated stomatal closure in *Vicia faba* as a result of exposure to $0.35\mu l.l^{-1}$ SO_2. Air pollutants such as SO_2 may influence stomata indirectly through damage to the subsidiary cells, or the epidermal cells instead, or by altering the cell wall structure within the stomatal apparatus, resulting in reductions in the mechanical resistance towards the guard cells that lead to wider stomatal apertures (Maier-Maercker & Koch, 1986; Maier-Maercker, 1989). Roa *et al.* (1983) observed a decrease in the free thiol content in the epidermal region and whole leaf when plants were exposed to concentrations of SO_2. According to the study that Roa *et al.* (1983) conducted, exposure to SO_2 inhibits the light-dependant build-up of free thiols in the epidermis and whole leaves of pea plants, but more importantly, it found that the free thiol content of the epidermis was more sensitive to SO_2 than that of the entire leaf.

The closing of stomata as a result of exposure to higher SO_2 concentrations has frequently been reported for a wide variety of species (Heath, 1980; Mudd & Kozlowski, 1975). Stomatal closure induced by exposure to SO_2 occurs due to a combination of immediate effects on the activity of certain key enzymes in the epidermis, and delayed effects arising from the inhibition of photosynthesis in the mesophyll (Roa *et al.,* 1983). Decreased photosynthesis in the mesophyll probably

led to an accumulation of CO_2 in the intercellular spaces which affected stomatal movement (Raschke, 1979).

As human activities continues to modify the chemistry of the earth's atmosphere, those concerned about managing agricultural resources, forests and wild lands must develop a better predictive understanding of plant responses to air pollutants. To date, the responses of plants to air pollutants have been studied extensively within a number of volumes and articles; however, current understanding is insufficient for resource managers, biologists, and policy makers to predict the specific effects of air pollutants on plant physiology and growth.

1.5 Hypothesis

All studies agree that a closing of stomata protects plants against further uptake of injurious SO_2. However, under these circumstances, the residual (mesophyll) resistance has been found to be larger than the stomatal resistance, thereby diminishing the relative importance of the protection by stomatal closure. Growing plants under conditions of water deprivation - inducing drought - could cause stomatal closure and reduce the direct entry of SO_2 into the leaf and thereby reduce inhibition.

1.5.1 Aim of the study

In this study the effect of SO_2 on photosynthesis in *Brassica oleracea* and *Glycine max* has been studied with a view to resolve the mechanism of injury induced by SO_2. The purpose of this investigation was to examine the effects of SO_2 in actively growing *Brassica oleracea* (cabbage) and *Glycine max* (soybean) plants that were well watered (~80% of field capacity) or subjected to drought stress (~20% of field capacity) by:

a) determining the effect of SO_2 on growth, biomass accumulation and yield attributes
b) determining the effect of SO_2 on stomatal conductance
c) determining the effect of SO_2 on chlorophyll content
d) measuring photosynthetic gas exchange and evaluate the contribution of stomatal and non-stomatal constraints towards injury

e) analysing fast phase *chlorophyll a* fluorescence kinetics, to evaluate the effect on primary photochemistry and give insight into the possible sites of inhibition
f) determining the *in vitro* Rubisco activity in soybean
g) determining the effects of SO_2 on the ureide content in soybean root nodules

A series of SO_2 exposure concentrations were employed in well-watered and drought-stressed *Brassica oleracea* and *Glycine max* plants to determine whether water availability affected SO_2 responses and, if so, how responses between the winter crop *Brassica oleracea* and the summer crop *Glycine max* differed.

Chapter 2

Introduction to Open-Top Chambers

2.1 Open Top Chamber construction and operation

Open-Top Chambers (OTCs) have been in use for the last 20 years; they were first utilised in the United States to investigate the relationship of crop growth and yield to gaseous air pollutants *in situ* (Heagle *et al.,* 1973; Mandl *et al.,* 1973). Since then, they have seen widespread application at numerous sites in the UK, operating in various European programmes to standardise protocols, generating valuable exposure-response relationships for a number of species (Jäger *et al.,* 1993). Various designs have been described in the past (Heagle *et al.,* 1973; Mandl *et al.,* 1973; Heagle *et al.,* 1989; Dunin & Greenwood, 1986; Weigel & Jäger, 1988); in particular, cylindrical chambers with open tops which can be placed over sections of a field crop have been extensively utilised to investigate the effects that air quality has on yield (Heagle *et al.*, 1973; Mandl *et al.,* 1973).

OTCs are a widely accepted design to enclose vegetation, allowing air quality to be modified whilst maintaining natural climatic conditions close to ambient conditions in the field, since the response of plants to air pollutants is highly dependent on the surrounding environment. OTCs were originally considered for excluding trace pollutants, such as ozone (O_3) and sulphur dioxide (SO_2) from plants, but it was soon realised that OTCs could also provide an enclosure within which known concentrations of an air pollutant (fumigant) could be uniformly administered (Heagle *et al.,* 1973; Weinstock *et al.,* 1982) thus offering an means for monitoring growth responses of plants to known concentrations of air pollutants at a single site (Heagle *et al.,* 1979).



Figure 2.1 A battery of 12 OTCs erected at an experimental site on the premises of the North-West University, Potchefstroom, RSA. The insert shows the air-conditioned instrumentation room that houses the SO_2 gas analysers, gas fumigation system and the PLC computer system logging the data. The meteorological instrumentation for measuring ambient meteorology, i.e. rainfall, relative humidity, solar radiation, temperature and wind speed and direction are mounted on the side of the room. Probes measuring PDF, humidity and temperature are also mounted in two OTCs.

2.1.1 Basic design features of Open-Top Chambers (OTCs)

The OTCs used in this study consist of a cylindrical aluminium framework (specially built by Hydro Arch, Secunda, RSA) covered with transparent sheeting and a rain cap at the top to exclude ambient rain that may pose problems, seeing that rainfall may be unusually high or low during a season, and may not fall uniformly across all chambers or within a particular chamber (Figure 2.3). Rainfall chemistry is also another uncontrolled variable that may affect plants and needs to be considered. The opening between the top of the chamber and the rain cap allows air movement

through the chamber, hence the name Open-Top Chamber (OTC). A large axial fan with a high capacity output with variable speed control, fitted inside a fan box positioned outside the chambers, ventilates two OTCs. Ambient air is blown through a stainless steel duct which divides horizontally into two PVC tubes and enters at the base of each of the two chambers through a vertical Perspex tube that serves as a manifold onto which two toroids could be positioned. Perforated, flexible lay-flat tubing, situated 1 meter and 1.2 meters respectively from the base of the chamber, surrounds the inside of the chamber wall, to form the suspended toroids. The air was vented through perforations in the suspended toroids into the cylindrical chamber, creating an inward and upward flow to exit through the opening at the top. Positive pressure created by the air entering from the base of the chamber minimised the ingress of ambient air with its pollutants through the open top of the chamber, which could result in the loss of the treatment control (Buckingham *et al.,* 1981).

2.1.2 Chamber frame and chamber film cladding

The chamber frame comprises six upright aluminium channel pillars, three channelled hoops and four top-angled L-sections to support the chamber's rain cap. The channel bars were bolted to the channelled hoops through spacer brackets to sustain the channelled frames and make the structure more rigid. Tightening of the bolts onto the channelled frame could cause bending of the frame that might tear and cause the chamber to collapse when force is applied. UV-stabilised transparent PVC sheeting 400 μm thick (Block & Levington, Johannesburg, RSA) was chosen to cover the chambers. The PVC sheeting could be tensioned in the channels of the horizontal hoops with tie-down ratchets. The sheeting was chosen with great care, since the nature of this material is critical in determining the quality and quantity of radiation/irradiance inside the chamber. A transmission spectrum (Figure 2.2) of the PVC sheeting revealed that more than 90% of photosynthetic active radiation (PAR) (400 nm – 700 nm wavelength) (Figure 2.2) is transmitted. The aluminium frame made the chamber light and resistant to corrosion and also provided support for the PVC covering. The resulting chamber was 2.2 m in height and 1.7 m in diameter. Covered with the PVC sheeting, the chamber succumbed 5 m^3. The chambers were fitted with a rain cap to exclude rain, thus enabling control of water regime of the potted test plants during the course of the experiments.

OTCs need to be firmly anchored to the ground to avoid catastrophic failure during storm conditions when lateral forces approaching 2000 N may be applied to the structure. Large ground pegs were used and provided adequate anchorage.

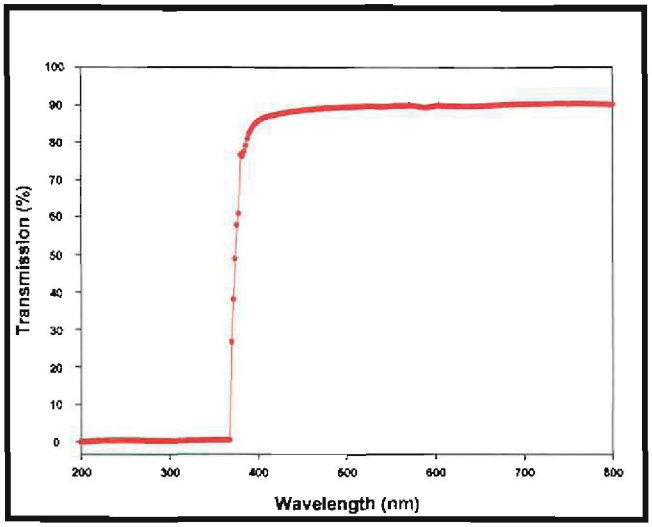


Figure 2.2. Transmission spectrum of the PVC sheeting measured with a spectrophotometer (380 – 700 nm), revealing more than 90% transmission of photosynthetic active radiation.

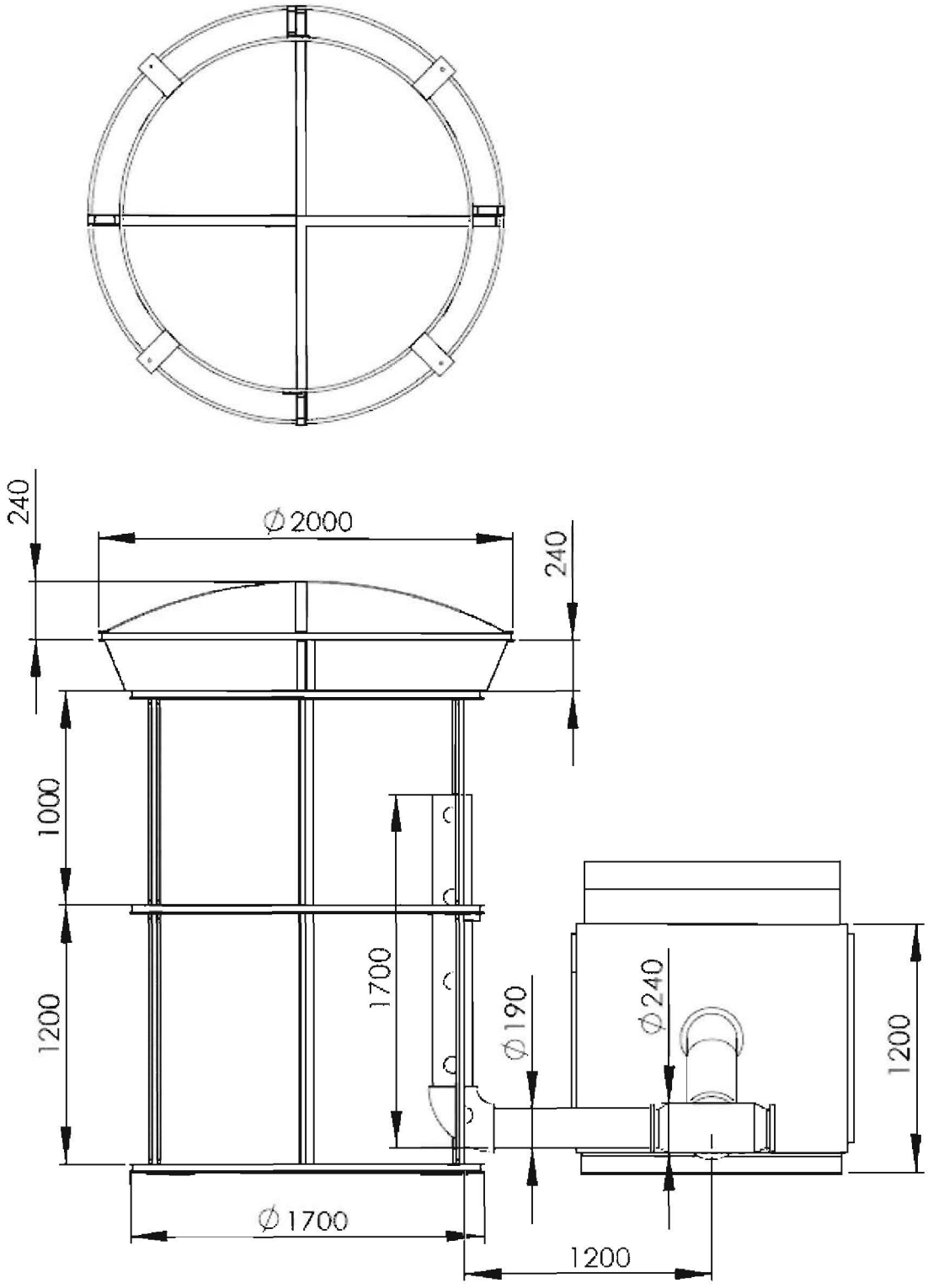


Figure 2.3 Schematic representation showing the ventilation unit, air ducting and chamber dimensions.

2.1.3 Filter blower units and OTC ventilation

Mechanical ventilation was provided by a 3 Kw, 380 V large axial fan motor (Trojan Fans Ltd., RSA) with a backward curved centrifugal impeller (355 mm diameter) with variable speed drive. The fan was fitted downstream inside a weatherproof fan-box containing three different filter systems. The large diameter fan impeller promoted high efficiency, robustness regarding motor overload and low noise for a given air flow rate (Figure 2.4). This high capacity ventilation unit provided sufficient ventilation for two OTCs (Figure 2.5).

The ventilation units (Freudenberg Nonwovens (Pty) Ltd.) were positioned at a distance remote from the chambers. The chambers were placed parallel in two rows of six chambers, 1.5 m apart; each row facing northwards, in order to avoid shadows of the ventilation units and chambers intercepting illumination; i.e. no shadows were cast on the adjacent chambers at any time. Air coming from the ventilation unit, divided into large (25 cm in diameter) opaque air ducts through a T-junction and entered at the base of each chamber, suspending the air through two perforated toroids. The large diameter of the air ducts connecting the ventilation unit to the chambers was necessary to minimise frictional losses and pressure drops. Flanges connected the opaque ducting to the fan outlet. All air ducts were cut and welded with precision by the Instrument Making Department, NWU, Potchefstroom, RSA.

A transparent Perspex tube (19 cm in diameter) served as a manifold to which the transparent flexible lay-flat tubes (toroids) could be attached and positioned 50 cm and 65 cm respectively from the base of the chamber, surrounding the inside of the chamber wall. An angle bent at the end of the opaque duct partly entering the chamber kept the transparent Perspex manifold upright and parallel to the chamber wall. The Perspex manifold allowed precise orientation of the lay-flat tubing to ensure uniform air ventilation into the plant canopy. 26 exit holes of 17 mm diameter each spaced 200 mm from one another (calculated using a computer air flow simulation model), were punched into each of the 200 µm thick transparent polyethylene film tubes (lay-flat tubing), and made up the air outlet surface. The exit jet velocity at the outlet surfaces of the toroid was around 10 $m.s^{-1}$, which corresponded to an air exchange rate of about 3 air $changes.min^{-1}$ through the chamber. Uniform ventilation over the plant canopy was ensured by the upper toroid facing diagonally inwards and the bottom toroid facing horizontally into the canopy. The number of holes, their diameter and their circumferential spacing were

determined from the total air speed and static pressure in the toroid. An air-flow computer simulation model was used to determine the diameter of air ducts and the number and size of the orifices on the toroid (see calculation Table 2.1 – M Tech Industrial (Pty) Ltd.). The suspended toroids proved to be more advantageous than the ground plenum employed on the original OTC design/configuration (Heagle *et al.*, 1979; Olszyk *et al.*, 1980; Weinstock *et al.*, 1982), which resulted in inadequate dispersion in the centre of the chamber. The air flow through all the ventilation units was measured regularly with a TA 45 thermal anemometer (Airflow Developments Ltd., Buckinghamshire, HP12 3QP, England) and kept at the same rate for all chambers by the aid of electronic motor speed controllers (WEG Model CFW - 08) fitted to each ventilation unit for precise control of the fan speed. This made the precise control of the ventilation rate possible. The ventilation units were in operation 10hr.day^{-1} until senescence of plants (early January 2008).

Table 2.1 Computer-simulated calculations that were used to determine the diameter of the ducting. The total pressure drop from the inlet of pipe 1 to the outlet of the ventilation hole in the toroid is 812 Pa. The air velocity close to the inlet of the toroid is 12.9 m.s^{-1}. This velocity is higher than the 10 m.s^{-1} stated in table 2.1., but is only applicable for the first 600 mm of the toroid. Thereafter the velocity inside the toroid drops to 9.9 m.s^{-1}, and then to 1 m.s^{-1} between successive holes. The high quantity of the holes ensures proper ventilation and dispersion over the plant canopy in the OTCs.

Part description		Inside diameter (mm)	Length (m)	Mass flow rate (Kg.s^{-1})	Air flow velocity (m.s^{-1})
Pipe 1	stainless steel duct	240	1.0	0.538	11.7
Pipe 2	PVC ducts	185	1.0	0.269	9.8
Pipe 3		185	1.0	0.269	9.8
Pipe 4	Perspex manifolds	185	1.5	0.269	9.8
Pipe 5		185	1.5	0.269	9.8
Pipe 6	one of two toroids	127 mm (flat) 80.8 mm (expanded)	5.4	0.135	9.93

TROJAN FANS
FOCUSED ON DEPENDABILITY

PERFORMANCE GRAPH Printed: 2006/08/28

OurReference: 605035k1	**Customer: Freudenberg Nonwovens (Pty) Ltd**		
Our Item: 1	**Customer Ref: Plate Fan**		
FAN SERIES:	**BC90**	**AIR DENSITY:**	**1.00** kg/m³
FAN SIZE:	**355C/0.8**	**FAN SPEED:**	**2 890** r/min
IMPELLER DIAMETER:	**355 mm**	**DUTY VOLUME:**	**1.66** Am³/s
INLET TYPE:	**Single Inlet**	**DUTY PRESSURE:**	**620.00** Pa

Average Open Inlet Sound Level @ Distance of 3.0 m 73 dBA Average Breakout Sound Level @ Distance of 3.0 m 61 dBA

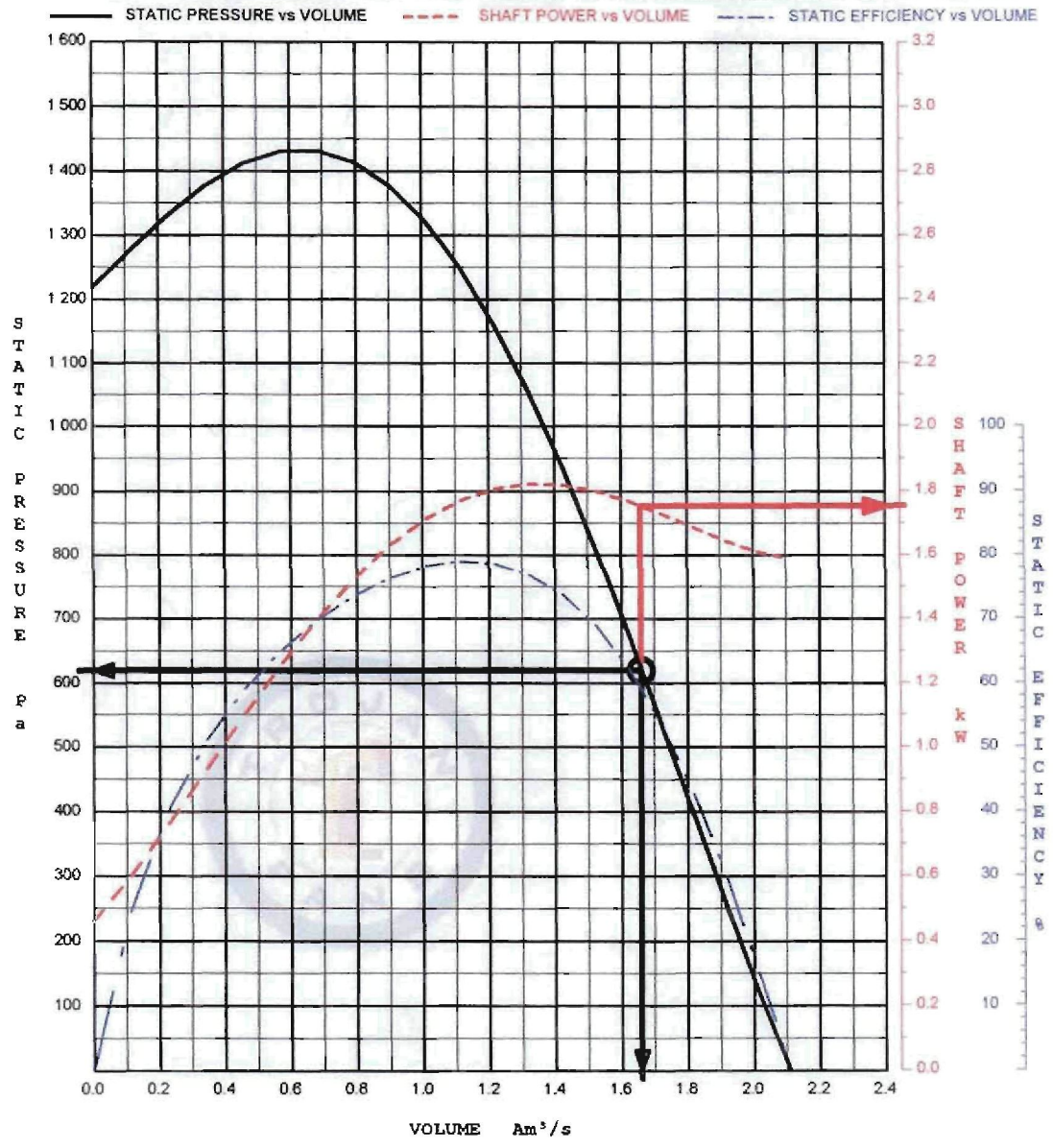


Figure 2.4 Graph showing the performance of the ventilation unit with blower capacity being most efficient between 0.9 – 1.66 $m^3.s^{-1}$.

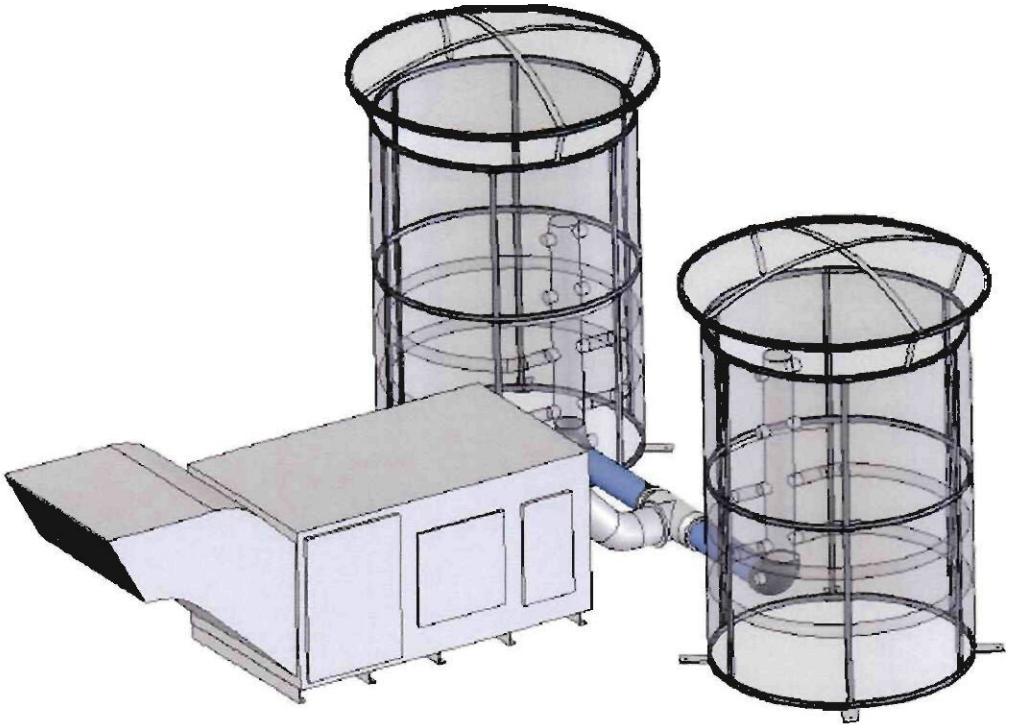


Figure 2.5 3-D drawing showing the virtual position of the ventilation unit to the OTCs it serves.



Figure 2.6 Photograph of the actual system.

2.1.4 Filtration

Following the direction of incoming air into the ventilation units (Figure 2.7), the first filter, consisting of two aluminium panels, retained coarse-grained impurities; the second, consisting of six exchangeable cartridges which are filled with a fine-grained charcoal-Purafil blend (Purafil ®, Georgia, USA), removed gaseous pollutants such as O_3, SO_2 and NO_2 from the air. The third filter, formed by two aluminium panels fitted with a zigzagged cloth-like filter, retained finer particles coming from the charcoal/Purafil blend media. Air entering the control chambers (0 ppb SO_2 treatment) was filtered through Purafil CP blend media containing activated carbon and 8% potassium permanganate to absorb and oxidise a wide variety of gaseous contaminants. The ventilation units which supplied the chambers, representing the SO_2 fumigation treatments (50, 150 and 300 ppb SO_2), were operational with dust filters only. Prior to the start of the experiments the filter-cartridges were refilled with new Purafil media.

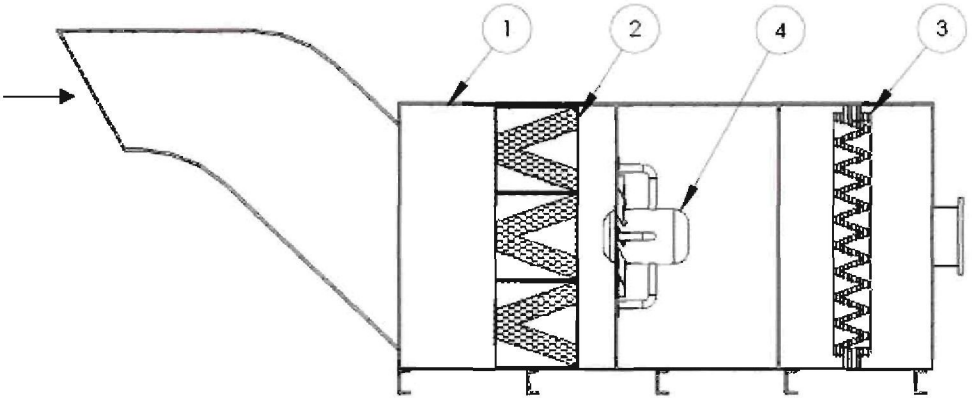


Figure 2.7 Schematic representation of a typical ventilation unit amplifying the components located inside the weatherproof fan box: (1) Rough filter retaining coarse-grained impurities, (2) 6 exchangeable cartridges filled with fine-grained charcoal-Purafil blend, (3) zigzagged cloth-like filter, retaining finer particles coming from the charcoal/Purafil blend media, and (4) 3 Kw Volt axial fan.

2.1.5 Fumigation practice

Anhydrous liquid SO_2 contained in a temperature-controlled pressurised cylinder (8 Kg) (kept at 33 °C with a thermal blanket to increase the vapour pressure) was diluted to 20% with dry compressed air generated by a compressor (Figure 2.8). The gas mixture was captured in a mixing-chamber (Figure 2.9). The SO_2 pressure from the cylinder as well as the air pressure from the compressor was regulated by individual regulators (Figure 2.10). Rotameters regulated the single-stage dilution step. A non-return valve fitted to the mixing chamber, leading to outside the instrumentation room, served as an overflow to prohibit pressure build-up. A trap was installed to capture any SO_2 that was not yet in gas phase and residue coming from the regulator, before it passed through the rotameters. From the mixing chamber the diluted SO_2 gas passed into a distribution chamber from where it divided to follow ten separate paths through an array of needle valves of ten rotameters, with which the SO_2 concentration for each chamber could be regulated or re-adjusted according to the air flow rate (Figures 2.9 and 2.10). The SO_2 gas was distributed to the different chambers through ¼" Teflon tubing and was injected into the air stream at the rear of the fan so that turbulence in the air flow through the ducting system would aid in mixing the diluted SO_2 and filtered air properly before it entered the OTCs.



Figure 2.8 Liquid SO_2, kept at 33 °C with a thermostatic blanket to raise the pressure, diluted to 20% by air provided by a compressor.

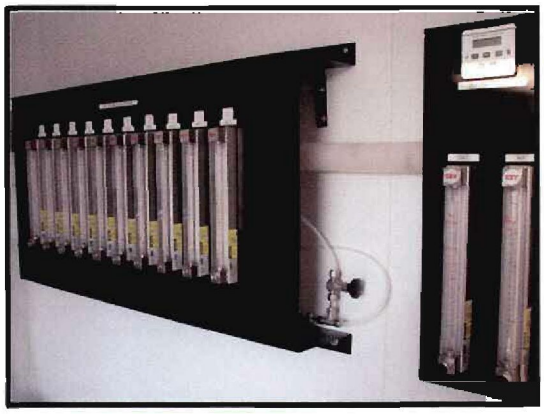


Figure 2.9 An array of needle valves connected to a series of rotameters for the precise control of the SO_2 concentrations of the different treatments in the OTCs.

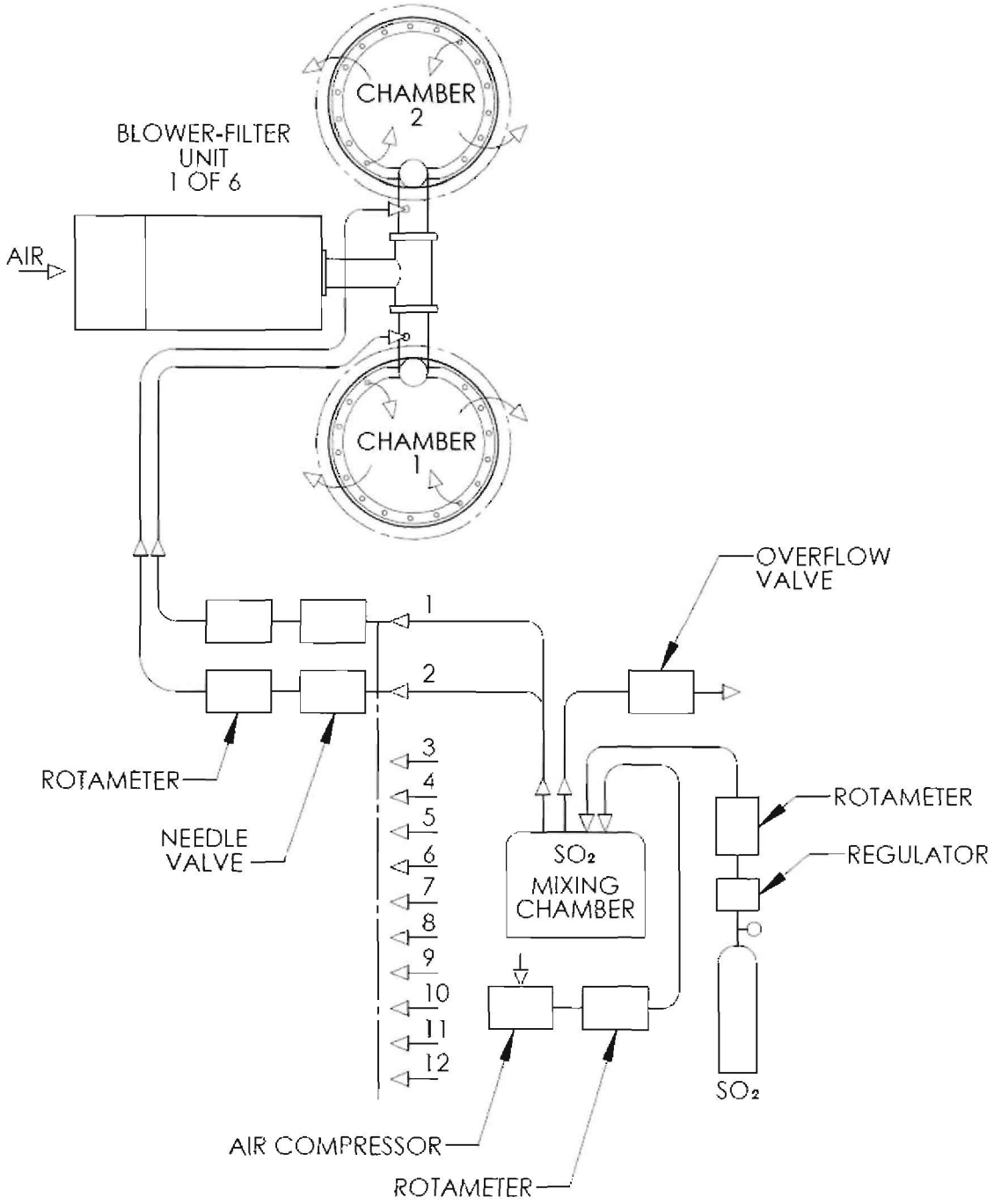


Figure 2.10 Scheme of the OTC fumigation system indicating the path of diluted SO_2 from the distribution chamber through an array of needle valves of ten rotameters, with which the SO_2 concentration for each chamber could be regulated or re-adjusted according to the air flow rate.

2.1.6 Analysis of pollutant concentrations / Monitoring pollutant concentrations

Pollutant (e.g. SO_2) concentrations were measured in an air sample taken from the middle of each chamber from an area of approximately 0.5 m^2 and at a height of 10-15 cm above the plant canopy. To prevent dust from entering the sample stream, each Teflon sample line was fitted with a disk filter holder (Figure 2.11). The air samples from each chamber were extracted by supporting vacuum pumps (Gillian GILAIR-3 air sampling systems, Sensidyne, Florida, USA) over a manifold of 2/3-way solenoid valves controlled by a PLC process controller. The 12 solenoid valves switched intermittently between chambers and allowed a particular air sample to be collected in a stainless steel chamber. The air sample was then diverted to two automatic SO_2 fluorescent analysers (Teledyne Instruments Ltd., Model 100A, San Diego, CA), with their own built-in vacuum pumps extracting air samples from the flow created by the supporting vacuum pumps. The SO_2 concentration of the air in the chamber was measured by the SO_2 analysers and the analogue output signals from the SO_2 analysers were logged on a multi-channel logging device (ScadaLog) connected to the same PLC which controlled the intermittent switching of the solenoid valves (Figure 2.13). The data logger also collected status signals from the PLC to link an analyser's output signal to a specific OTC (Figure 2.12). The valves were programmed to remain open for 15 minutes to allow sufficient time for the analyser to stabilise. Thereafter it switched to the next set of solenoid valves. A valid reading was recorded every five minutes so that the average SO_2 concentration in each OTC was measured for a period of 15 minutes during any given 60-minute period. The readings from the SO_2 analysers, the meteorological instruments, as well as the information from the PLC, were stored on a data logger and processed on a laptop computer with the aid of dedicated software. The gas analysers were calibrated frequently, and the calibration was performed against a VE-3M-Environment S.A., Dynamic Calibration System (Field Standard, FS-01) and a certified bottled source (SO_2 "Field Standard" gas cylinder) (C&M Consulting Engineers CC, Pretoria, RSA). All gas-carrying lines were made of Teflon. The SO_2 analysers, PLC, data logger, SO_2 cylinder and air compressor were housed in an air-conditioned instrumentation room (see insert Figure 2.1).



Figure 2.11 The Teflon sample line fitted with a disk filter to prevent dust from settling in the Teflon tubing.

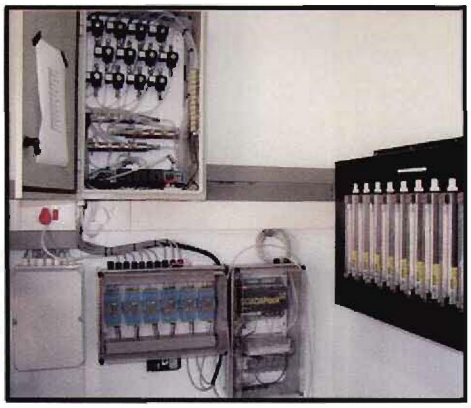


Figure 2.12 A manifold of 2/3-way solenoid valves controlling the different sample lines fed to the analyser by aid of vacuum pumps. The PLC and data logger controlling and logging the analogue output signals are visible in the bottom of the photograph.

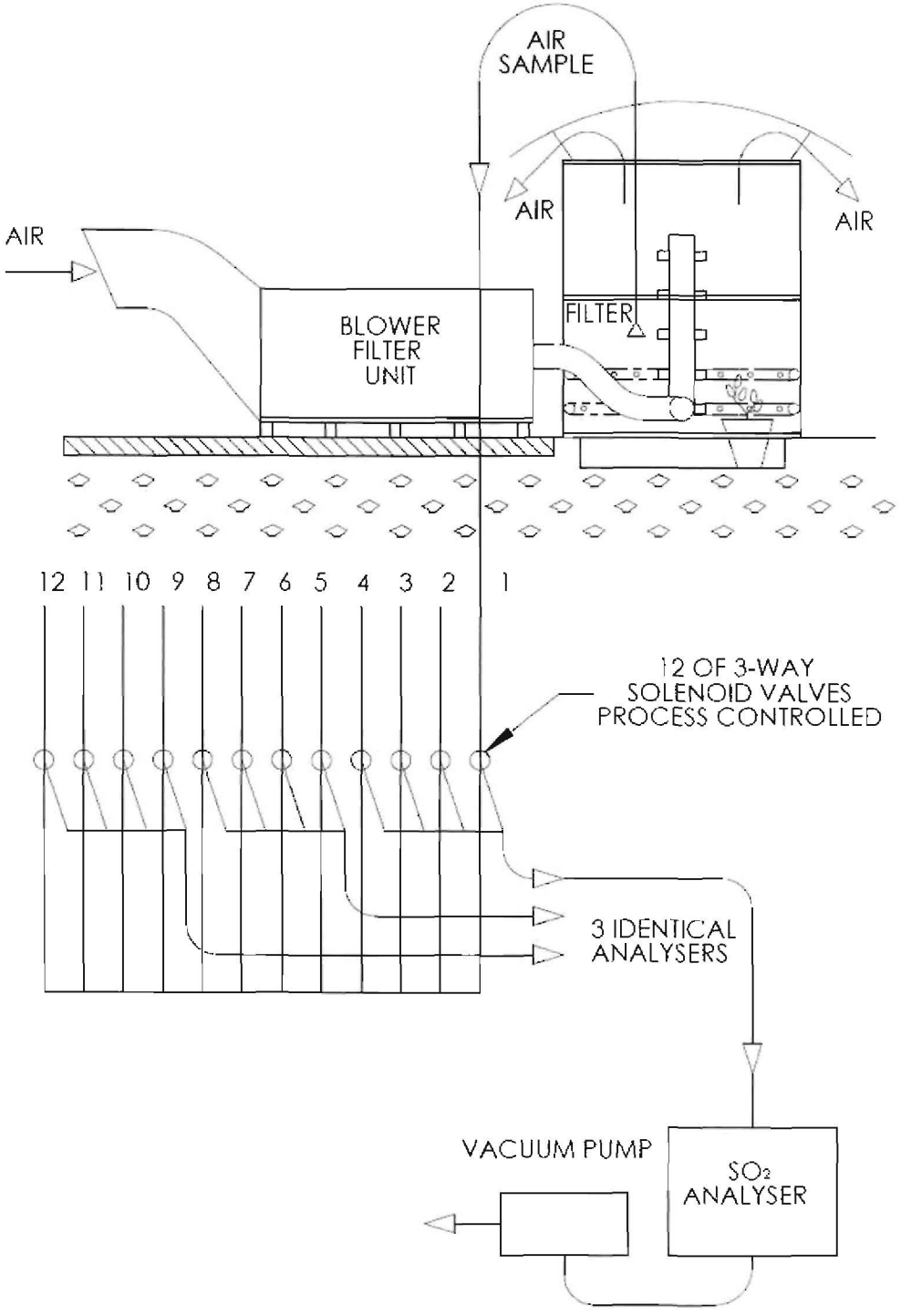


Figure 2.13 Scheme of the OTC air sampling system showing the indraw-path of a particular air sample over a manifold of 2/3-way solenoid valves controlled by a PLC process controller. The air samples were analysed by one of three analysers with the output signal from the SO_2 analysers logged continuously on a multi-channel logging device (SCADALOG).

2.2 The environment inside Open-Top Chambers.

The diversity of OTC designs as well as the differing climatic conditions in which these chambers have been used, encouraged the research in the chamber microclimate in order to ensure valid comparisons of experimental data (Adaros *et al.,* 1989; Drake *et al.,* 1989; Whitehead *et al.,* 1995; Norris *et al.,* 1996; Norris & Bailey, 1996). Various methods have been introduced to control the microclimate inside OTCs (Weinstock *et al.,* 1982; Unsworth, 1982; Adaros *et al.,*1988; Sanders *et al.,* 1991; Worington & Colls, 1998).

OTCs influence the plant environment by modifying both the physical climatic parameters such as light intensity, air temperature, relative humidity, wind speed and the concentration of chemical components such as gaseous pollutants and CO_2. It has been shown that some chamber designs may change water use (Olszyk *et al.,* 1980; Leuning & Foster, 1990) and water-use efficiency of the vegetation by up to 50% (Denmead *et al.*, 1993). To evaluate the microclimate within any chamber, a comparison between the chamber environment and ambient environment is necessary.

2.2.1 Radiation environment

OTCs alter the net radiation (R_n) in reducing the solar energy by absorbing/intercepting energy in the covering material and the framework. It is known that the chamber frame and cladding material modify the light flux incident on the plant canopy. Heagle *et al.* (1989) and Drake *et al.* (1989) reported a reduction of 10-20% in the solar flux within plastic-clad covered OTCs. Furthermore, UV stabilisers found in the plastic cladding affect the UV region (below 380 nm) of the spectrum substantially (Drake *et al.,* 1989). Although reductions in solar radiation occur when light is transmitted through the covers or intercepted by the framework, net radiation is generally increased inside an OTC due to the emission of long-wave radiation by the covers (Unsworth, 1986).

The net radiation (R_n) is given by:

$$R_n = S_t - rS_t + L_d - L_u,$$

where S_t represents the incoming and outgoing solar radiation over the canopy and r reflects a fraction r = 0.2 of the solar radiation fluxes at noon on a cloudless day; L_d

represents the downward long-wave radiation and L_u the upward long-wave radiation.

Chambers largely alter the downward long-wave radiation L_d that comes from the chamber walls which are closer to air temperature than the atmosphere which, when cloudless, behaves like a radiator at 20° C below air temperature. Upward long-wave radiation L_u is not altered much because the temperatures of plant canopies inside the chambers are usually within a few degrees of those outside the chambers (Unsworth, 1986).

Several studies conducted in the northern hemisphere on the internal radiation environment of OTCs have shown that spatial variation of short-wave radiation does occur. It is known that positional effects and flux densities were greater in the southern position of the chamber (Heggestad *et al.,* 1980; Heagle *et al.,* 1989; Jetten, 1992), and significant diurnal and seasonal variation of internal light levels also occurred (Weinstock *et al.,* 1982). Heagle *et al.* (1979) noted that levels of photosynthetically active radiation (PAR), that is the radiation in the 400 -700 nm waveband - essential for plant growth, were greater in the chambers than in the ambient environment at certain times during sunny days because of the reflection from the cylindrical OTCs plastic covering. Worthington and Colls (1998) applied a computer simulation to study the light distribution inside OTCs in detail and found that both transmission and glancing-angle reflection characteristics of the cladding can influence the solar flux distribution at the floor of the chamber. Increased radiation intensity due to the focussing effect by the PVC chamber walls on sunny days causes an increase in the global radiation levels within the chamber (Jetten, 1992). Weinstock *et al.* (1982); Olszyk *et al.* (1980) and Mandl *et al.* (1989) noted that the PVC covering focuses light in some areas of the chamber and that recorded PAR levels varied considerably at two particular times of day. The importance of differential irradiance was affirmed by Heck *et al.* (1988) who noted differences in yield at different positions inside the chambers. Unsworth (1986) made it evident that in some plant species, development can be greatly influenced by the light quality inside OTCs and that characterisation of light quality is desirable.

2.2.2 Thermal environment

Temperature rise within the chamber is primarily governed by absorbed solar radiation, the ventilation rate and the air flow regime within the chamber. The rate of

heat loss from foliage, imposed by convection, depends strongly on the air movement within the chamber. The thin layer of air close to the leaf surface that controls this convective heat loss is described as the boundary layer resistance (R_b). In OTCs, the boundary layer resistance is determined by the ventilation rate (air change per minute) within the chambers which is directed/influenced/controlled by the speed of the blower as well as the incursion of ambient air through the top of the chamber. It is known that plants growing in OTCs lose heat more rapidly than plants growing in the open. Convection from the foliage heats the air above the canopy so that in general the air inside the chamber will be at a different temperature than air above the same crop growing in the field. This is because the chamber environment differs from ambient conditions due to differences in net radiation, and because of different air flow through the canopy. Heagle *et al.* (1979) reported temperature increases reaching 2° C during midday on sunny days. Unsworth (1986) and Weinstock (1982) revealed that temperature differences at night-time were almost non-existent and that the very small temperature increase inside the OTCs was caused by radiant heating generated by the blowers. Norris and Baily (1996a) acknowledged the importance of air speed within the chamber to create boundary layer resistance for foliage which is comparable to plants grown in the field. Norris *et al.* (1996) stated that the temperature rise within OTCs is governed primarily by the solar energy absorbed, the rate of ventilation and the air flow regime in the chamber. Norris *et al.* (1996) also indicated that a slight temperature increase will always exist within an OTC, even when very high ventilation rates are employed.

2.3 Detailed measurements of environmental conditions inside and outside our OTCs at the NWU.

Climatological conditions inside and outside the chambers were continuously recorded (Figures 2.14 and 2.15). Light quantity inside and outside the chambers was monitored with solar radiation sensors (LI-COR sensor, Model 70201, R.M. Young Company, USA), placed above the canopy in the chamber (Figure 2.14b). Temperature and relative humidity of air inside and outside were measured with a Pt 100 relative humidity and temperature sensors (Relative humidity/Temperature probe, 0-1 V output, Model 41382 VC/VF, R.M. Young Company, USA). The temperature sensors were located close to the light sensor and protected from sun rays with a naturally ventilated radiation shield (Figure 2.14a).

In the recording of climatic conditions inside the chamber, wind speed, wind direction and precipitation were also measured (Figure 2.15). All meteorological measurements were recorded every five seconds and five minute averages were stored. The instruments measuring ambient conditions were mounted on a mast which was itself mounted onto the instrumentation room (Figure 2.15).



Figure 2.14 Photograph showing the relative humidity and temperature sensor (left) and solarimeter (right) mounted to the chamber frame.



Figure 2.15 Solar radiation meter and automatic precipitation meter with tip bucket mounted to the instrumentation room shown in the photograph to the left and the wind speed/direction meter mounted to the tip of the post in the photograph on the right.

2.4 Experimental layout

The experimental layout (Figure 2.16) entailed two OTCs replicating one treatment, and three elevated SO_2 treatments so that a total of eight chambers of a battery of twelve OTCs were in use for the experiments described below (Chapter 3). Environmental modifications caused by patterns of air movement inside the chamber may be substantial, and thus it was deemed necessary to monitor the meteorological conditions inside the chamber with precision and compare them with ambient conditions to assess the chamber effect ("Boreas effect"). Circular plots having the same diameter to those of the chambers, but without the chamber frame, covering material and ventilation units, were prepared to represent ambient conditions. Measurements on plants grown inside these plots were compared with those of plants grown inside the chambers exposed to filtered ambient air. Two plots were used to replicate the ambient treatment. By comparing the chamber environment to the ambient air environment the extent to which plant development differed under the different conditions could be determined, and also whether the chamber environments altered the sensitivity of plants to pollutants and other possible stresses.

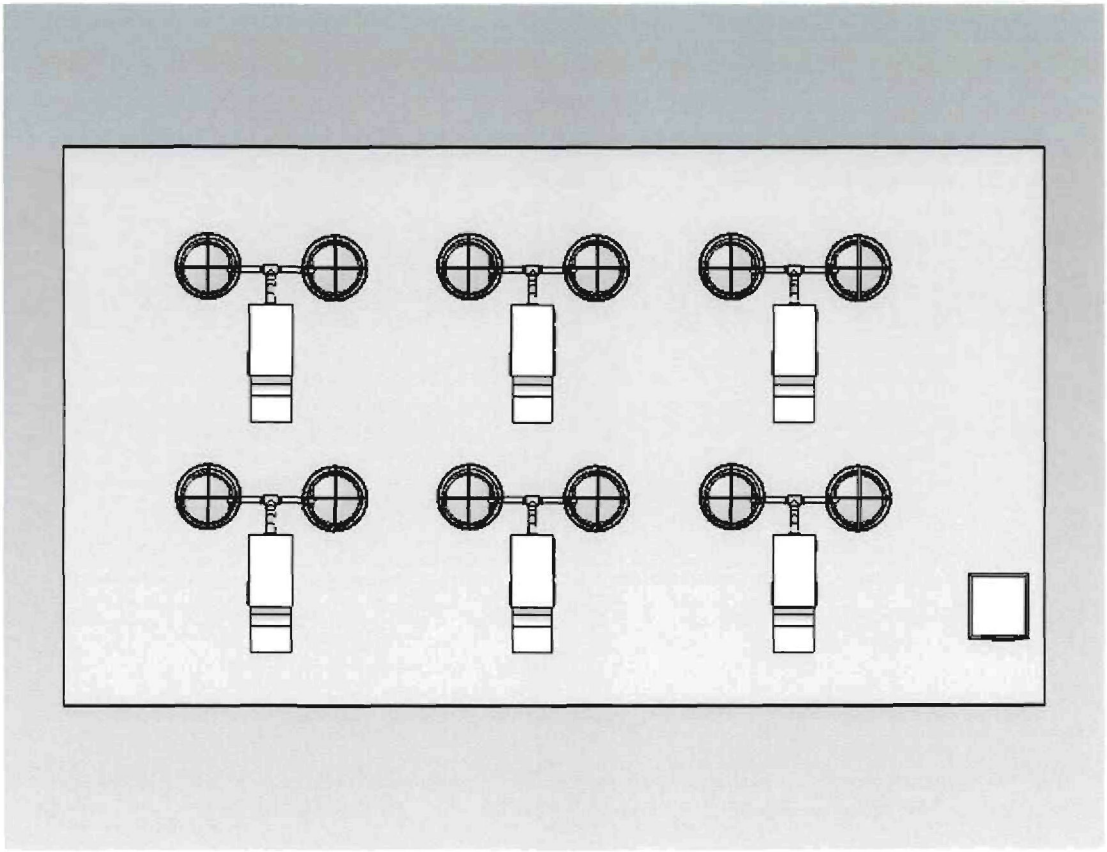


Figure 2.16 Layout of chambers on the experimental site.

Chapter 3

Material and Methods

3.1 Plant cultivation

3.1.1 Cultivation of *Glycine max* plants – summer annual (2007- 8)

Commercial seeds of soybean (*Glycine max* (L.) cv PAN809) obtained from the Agricultural Research Council, Potchefstroom, were inoculated with a culture of *Bradyrhizobium japonicum* strain WB74-5 and planted into 200ml plastic pots on 18 September 2007 to germinate in a greenhouse under standard agronomic conditions. The day/night temperature regime was 20/25 °C and 22/18 °C respectively and the photoperiod was 12/12h.day/night (Figure 3.1). Shortly after emergence, with primary leaves unfolded, seedlings were transplanted (one plant per pot) to 16 dm^3 (30 cm diameter) white plastic pots filled with a mixture of sand, soil and vermiculite (1:2:1) The plants were fertilised with a six-months slow release fertiliser containing 14N:9P:15K:2MgO (Plantacote® pluss, Aglukon Spezialdünger, GmbH & Co.KG, Heerdter Landstraße 199, D-40549, Düsseldorf, Germany). The plants were watered daily with tap water and twice with half-strength Hoagland's nutrient solution (Hoagland & Arnon, 1950) until seedlings were well established. Thereafter, the pots were positioned over plastic buckets, which served as water reservoirs. The reservoirs were connected to a water tap through a network of PVC tubing that allowed easy refilling of the reservoirs when required. The pots fitted into the reservoirs in such a way that the base of the pot was not in contact with the water in the reservoir. Water uptake by the soil medium in the pots took place through special glass fibre wicks (Thoenes Dichtungstechnik GmbH, Germany) placed at different levels in the soil of the pots with one end protruding through the drainage holes in the base of the pot, hanging into the water in the reservoir. Through the glass fibre wicks water was supplied to the soil by simple capillary action, enabling maintenance of near-constant soil water content inside the pots. The glass fibre wicks were cut into specific lengths and layered in a clockwise direction at different, evenly spaced depths within each pot to ensure uniform wetting of the soil (Figure 3.2). The efficiency of wicks to supply water to the soil of the potted plants was evaluated beforehand. In our evaluation of the suitability of this system, results have proven that one glass fibre wick can provide a reasonable water supply to induce drought stress and three glass fibre wicks can supply adequate water so that no drought

conditions or respiration as a consequence of excessive watering are established in the pots.



Figure 3.1 Established soybean (*Glycine max* (L.) cv PAN809) seedlings cultivated in a temperature-controlled greenhouse, just before transplanting them into 16 dm^3 pots with wick irrigation system.

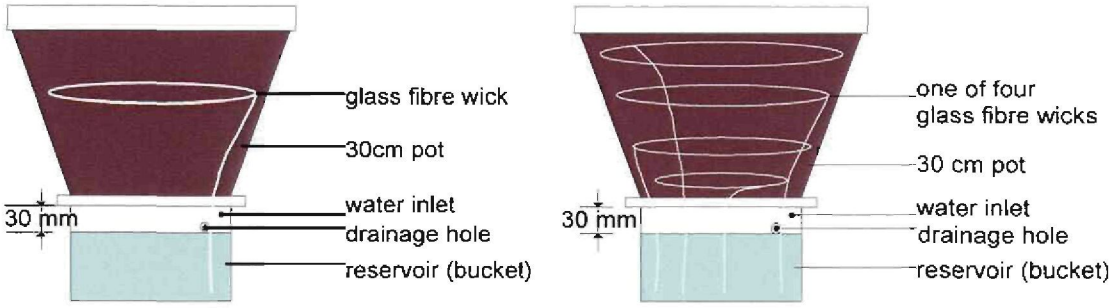


Figure 3.2 Schematic presentations of the pot-reservoir irrigation system used for controlling water supply to the soil through special glass fibre wicks. The wick system was tested for its suitability to induce mild drought stress in soybean by simply reducing the number of glass fibre wicks supplying water to the soil. Four glass fibre wicks were used to serve as a control, maintaining the water regime at 80% of field capacity in the pot and one glass fibre wick, situated near the middle of the pot, to induce water stress conditions, sustaining the water regime at 20% of field capacity.

Table 3.1 Timetable of events during the growth of the soybean (*Glycine max*) crop 2007-8

Event	Date
Sowing	18 September 2007
Emergence of seedlings	23 September 2007
Hoagland's nutrient solution applied	25 September – 8 October 2007
Transplantation to 16 dm^3 pots	5 October 2007 (13*)
Moving into OTCs	8 October 2007 (16*)
OTC fans switched on	10 October 2007 (18*)
SO_2 fumigation started	8 November 2007 (47*)
Drought stress treatment started	13 November 2007 (52*)
Insecticide applied	23 October 2007
Calibration of SO_2 analysers (2^{nd})	25 October 2007
Midseason harvest	28 November 2007 (67*)
SO_2 fumigation terminated	10 January 2008 (110*)
Final harvest	10 February 2008

* d.a.e., Days after emergence

3.1.2 Cultivation of *Brassica oleracea* – winter annual (2007)

Five-week-old seedlings of *Brassica oleracea* (cabbage) were obtained from a local nursery and transplanted directly to 16 dm^3 (30 cm diameter) white plastic pots filled with a mixture of sand, soil and vermiculite (1:2:1). The plants were fertilised with slow-release fertiliser and watered daily until well established. Thereafter the plants were watered only by the irrigation system described in section 3.3.1.

3.2 Experimental design and treatment factors

SO_2 fumigation was carried out using a state of the art Open-Top Chamber facility (OTC) situated on the experimental site of the North-West University, Potchefstroom. Fumigation of *Brassica oleracea* commenced one week after transplanting of seedlings and lasted for three months until 1 October 2007. Fumigation of *Glycine max* plants started on 8 November 2007 at 14h00, 47 days after emergence and continued until grain maturity (10 February 2008). The general experimental design included four SO_2-level treatments, namely: 0 ppb; 50 ppb, 150 ppb and 300 ppb at

two watering regimes. The control (0 ppb SO_2) was provided by plants grown in chambers ventilated with filtered air and an additional non-chamber/'chamber-less' plot was established in ambient air in order to evaluate the 'boreas effect/chamber effect' on the crop. All treatments were replicated twice, i.e. 8 OTCs were used. Eight potted plants served as pseudo-replications within each chamber. Plants were fumigated with SO_2 for 9 $hr.day^{-1}$, 7 day wk^{-1}. The fumigation took place from 08h00 until 17h00 every day, except on days with rain (34 days). The interaction of SO_2 and drought (water supply) was tested by selecting four of the eight potted plants per OTC for the drought stress treatment.

3.3 Soil moisture measurements and calculation of plant available water

3.3.1 Soil water potential

Plant turgor and transpiration from the crop canopy are maintained by the soil water availability and consequent uptake thereof by the roots at the soil-root interface (Beadle *et al.*, 1993). Plant physiological response - and ultimately biomass and yield production - depends in essence on the efficient use of irrigation and a solid understanding of soil water status. The major component of soil water potential (ψ_{soil}), namely matric potential (τ_{soil}) is predominantly influenced by the surface tension of capillary forces originating from the liquid–air interfaces that exist on the finer pores (Beadle *et al.*, 1993).

Soil water potential can be expressed as:

$$\psi_{soil} = \tau_{soil} + \pi_{soil}$$

Tensiometers are widely used for measuring the moisture availability. A tensiometer is an air-tight, water-filled tube with a porous ceramic tip at the base. Small pores at the ceramic tip allow water to move in and out, but prevent the entry of air. When inserted into the soil, water will move out of the water-filled tube into the soil to create vacuum in the tube which is diverted to a signal that could be recorded by the logging device.

Tensiometers recorded soil water potential in six pots of the first control chamber which were also fitted with sensors of the meteorological instruments. The tensiometers were carefully inserted, one per pot at a depth of 20 cm in the root zone. The logging device receiving the signal, could record up to 3 000 values (Figure 3.3).



Figure 3.3 One of six tensiometers used to record soil water potential near the plant root zone. The logging device with high storage capacity appears at the bottom of the photograph.

3.4. Non destructive plant analysis

3.4.1 Plant growth and development

The vegetative development of *Glycine max* plants was measured daily prior to the onset of SO_2 fumigation. The plastochron index, an easy non-destructive measure, (Erickson & Michelini, 1957) was used to quantify the vegetative development of the plants. All trifoliate leaves with central leaflets exceeding a reference length of 25 mm (L_{ref}) were counted. The length of the youngest central leaflet longer than or equal to 25 mm, as well as the length of the central leaflet (shorter than 25 mm) on the next trifoliate leaf was measured. The plastochron index of each plant was calculated using the following formula:

$$\textbf{Plastochron index} = n + (\log L_n - \log L_{ref})/(\log L_n - \log L_{n+1})$$

where n = number of trifoliate leaves with central leaflets longer than the reference length of 25 mm (L_{ref}), L_n = length of the central leaflet on trifoliate leaf L_n (which, by definition, is longer than or equal to L_{ref}) and L_{n+1} = length of the central leaflet on trifoliate leaf L_{n+1} (which, by definition, is shorter than L_{ref}). Establishing the

plastochron index for *Brassica olearcea* was not possible due to its rosette-like growth form, and characteristic compact cluster.

3.4.2 Chlorophyll content index

The chlorophyll content index (CCI) of leaves of *Brassica oleracea* and *Glycine max* was measured before the start of the SO_2 treatment and then weekly thereafter. CCI was measured with a hand-held chlorophyll content meter (CCM-200, Opti-Sciences, Inc., USA).

3.4.3 Stomatal conductance (Gs)

A steady state leaf porometer (SC-1, Decagon Devices, Pullman, WA) was used to measure stomatal conductance. This steady state technique measures the vapour flux from the leaf surface to the atmosphere. A fixed diffusion path is clamped to the surface of the leaf. The vapour flux is determined from the vapour pressure gradient in the diffusion path and the known vapour conductance through the fixed path. Stomatal conductance was calculated from the known vapour flux and the conductance in the diffusion path. All measurements of stomatal conductance were conducted weekly on the lower (abaxial) epidermis on the central leaflet of the trifoliate leaflet in *Glycine max* plants. Initial experiments determined the position of measurement on the leaf to minimise variability of the resistance recorded under constant conditions.

3.4.4 Overview of photosynthetic gas exchange kinetics

Since the dry matter of plants is derived from photosynthetic carbon fixation, photosynthesis may be seen as the key physiological process involved in air pollution-induced crop losses. Measurement of CO_2 assimilation is an effective non-destructive, non-invasive method for studying short-term effects on carbon gain of individual organs. This information provides additional information to effects on long-term carbon gain, which is analysed as the final biomass.

The approach of measuring photosynthetic gas exchange in plants is in essence based on Fick's first law of diffusion - which states that the rate of diffusion is directly proportional to the cross-sectional area of the diffusion path and to the concentration or vapour pressure gradient, and that it is inversely proportional to the length of the diffusion path.

To study CO_2 assimilation in plants, a number of measurements, terms and units are employed (Von Caemmerer & Farquhar, 1981): The evaporation rate (E) is defined using Fick's law and can be calculated as the ratio $(e_i - e_a)/Pr$, where e_i and e_a are the vapour pressures of water inside the leaf and in the air, respectively, and Pr is the atmospheric pressure, and portrays the difference of water vapour concentration between the inside and the outside of the leaf expressed as a mole fraction. The CO_2 assimilation rate (A) is expressed as the amount of CO_2 assimilated per unit leaf area and time ($\mu mol\ CO_2\ m^{-2}\ s^{-1}$). The stomatal conductance (g_s) represents the flux of CO_2 through the stomata, with the same units as for A.

When a portable open-circuit photosynthesis system is used to measure CO_2 assimilation, air is pumped from the photosynthetic leaf chamber (PLC) or cuvette enclosing a leaf into an infrared gas analyser which continuously measures the CO_2 concentration in the air stream. The CO_2 concentration of the air stream will decrease if the leaf inside the PLC assimilates CO_2. The CO_2 assimilation rate equals the change in the amount of CO_2 in the air stream per unit time. Changes in temperature and pressure are compensated for in the calculation of the CO_2 assimilation rate, but humidity has to be controlled, since a rise in transpiration will cause an increase in the amount of water vapour, resulting in dilution of CO_2 in the air stream (Long & Hällgren, 1993).

CO_2 first has to diffuse through the boundary layer on the leaf surface before it is able to enter the leaf. The boundary layer conductance will be at least an order of a magnitude greater than the highest possible g_s under field conditions (Long, 1985). In the Parkinson-type PLC (used in most portable photosynthesis systems) the boundary layer resistance is minimised and kept constant by the fan of the PLC, which keeps the turbulence high, resulting in the removal of the boundary layer. If only diffusion is taken into consideration, the intercellular CO_2 concentration (C_i) can be calculated by the following formula:

$$\mathbf{C_i = C_a - A/g_i}$$

where g_i represents the total conductance, i.e. boundary layer as well as stomatal conductance, and C_a is the atmospheric CO_2 concentration.

The volumetric net efflux of gas (predominantly water vapour) from a photosynthesising leaf will normally exceed the total influx so that a pressure gradient will exist, driving mass flow of gasses (including CO_2) out of the leaf and so

depressing C_i relative to C_a. This will occur even in the absence of any consumption of CO_2 within the mesophyll. Thus, taking the transpiration into account, the intercellular CO_2 concentration (C_i) can be calculated by the following formula:

$$C_i = (g_1 - E/2) \cdot C_a - A / g_1 + E/2$$

where g_i represents the total conductance, i.e. the boundary layer as well as stomatal conductance, E represents the transpiration rate, A represents the assimilation rate and C_a is the atmospheric CO_2 concentration.

An *in vivo* screening of limitations on the photosynthetic CO_2 assimilation can be achieved by means of the construction of so-called CO_2 response ($A:C_i$) curves (Figure 3.3). The $A:C_i$ response curve, for which the rate of net CO_2 assimilation (A) is plotted against intercellular CO_2 concentration (C_i) over a range of different C_a values, gives the response of the photosynthetic apparatus of the leaf to intercellular CO_2 and thus is a measure of the mesophyll components of photosynthesis (i.e. the dark and light reactions). Photosynthetic CO_2 assimilation is measured at increasing CO_2 concentrations (C_a) in order to create an artificial situation where no stomatal limitation exists, i.e. $C_i = C_a$. The photosynthetic CO_2 assimilation rate under this condition is then used as reference point to calculate the percentage stomatal limitation (Farquhar & Sharkey, 1982; Von Caemmerer & Farquhar, 1981).

Such studies allow the quantitative assessment of different gas exchange parameters that can be used to quantify the effect of environmental factors on the different steps of photosynthetic CO_2 assimilation pathways. It is possible to separate limitations in the mesophyll from stomatal limitations by employing simultaneous measurements of CO_2 and water vapour fluxes. Separation of the effects on the CO_2 limiting phases is also possible (Farquhar & Sharkey, 1982; Long & Hällgren, 1993).

The supply and demand functions are effectively two simultaneous equations describing the response of $A:C_i$. The demand function, $A = CE(C_i - \Gamma)$, of an $A:C_i$ response expresses the rate of CO_2 assimilation in terms of the effectiveness [C_i] and the capacity of the system to assimilate CO_2 (Farquhar & Sharkey, 1982). The symbol Γ represents the CO_2 compensation concentration which can be defined as the point at which net efflux of CO_2 from the plant is zero, i.e. CO_2 fixed by photosynthesis and CO_2 produced by respiration balance each other. The supply function, $A = g_s(C_a - C_i)$, of an $A:C_i$ response expresses the rate of CO_2 assimilation

in terms of the difference in concentration between C_a and C_i (the driving force for the inward movement of CO_2) and the prevailing stomatal conductance (g_s) (Farquhar & Sharkey, 1982). The actual assimilation rate, A_{350}, is given by the simultaneous solution of the demand and the supply function, depicted graphically by the intersection of the corresponding two lines. That is, the point of intersection of the supply and demand functions gives the rate of assimilation and the intercellular CO_2 concentration that prevails under those ambient conditions that give rise to that particular stomatal conductance and activity of the mesophyll processes. This point is known as the operational point (Lange *et al.*, 1987).

The operational point can provide information on which of the component processes are limiting CO_2 assimilation. If the supply function intercepts the A:C_i curve on the initial linear portion, small changes in stomatal conductance (g_s) will cause noticeable changes in A under ambient conditions, and assimilation can be considered to be predominantly limited by the stomata. If the point of intersection is on the flat portion of the A:C_i curve, small changes in g_s will have little effect on A, and CO_2 assimilation will be limited by the rate of the mesophyll processes, rather than by stomatal conductance.

To determine the degree of stomatal limitation of photosynthesis, the following equation is employed:

$$\ell = (A_0 - A_{350})/A_0$$

where A_{350} = the CO_2 assimilation rate at ambient CO_2 concentration (C_a = 350 µmol mol^{-1}) and A_0 = the CO_2 assimilation rate where no stomatal limitation is present ($C_i \geq$ 350 µmol mol^{-1}) (Farquhar & Sharkey, 1982). Stomatal limitation (ℓ) represents the proportionate decrease in CO_2 assimilation rate that may be attributed to stomatal restrictions.

The apparent carboxylation efficiency of photosynthesis can be deduced from the initial linear response (CE) of the A:C_i response curve which is an *in vivo* estimation of Rubisco activity (Bolhàr-Nordenkampf & Öquist, 1993). Over the initial linear portion of the curve, CO_2 assimilation is limited by C_i and saturated with Ribulose biphosphate (RuBP). The maximal CO_2 assimilation rate at saturating C_i (J_{max}) can be regarded as a reliable indicator of the RuBP regeneration capacity of the leaf.

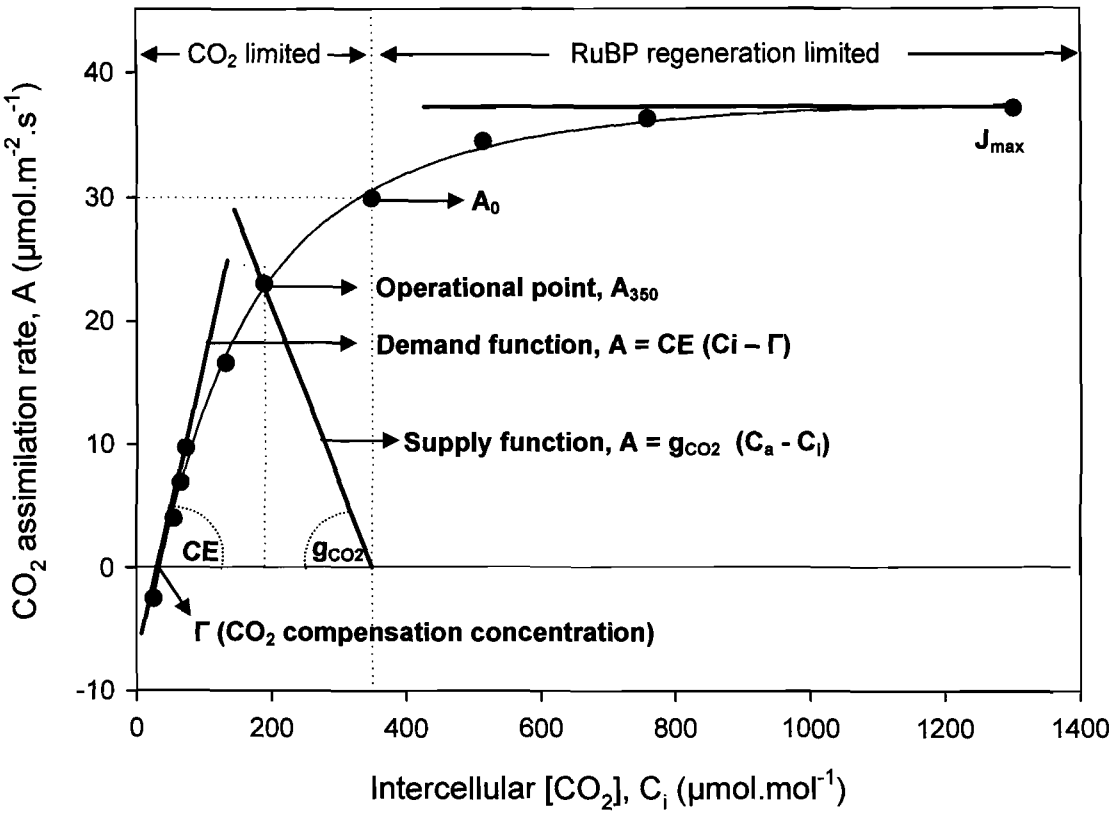


Figure 3.4 Response of CO_2 assimilation rate (A) vs. intercellular CO_2 concentration (C_i). A_{350} is the assimilation rate under atmospheric conditions, i.e. the point of simultaneous solution of the demand and supply functions. Carboxylation efficiency (CE) is represented by the initial slope of the demand function, the CO_2 compensation concentration (Γ) is the intercellular CO_2 level where the net usage of CO_2 equals zero, the maximum rate of assimilation (J_{max}) represents the rate of CO_2 assimilation at saturated levels of CO_2. A_0 is the rate of assimilation at the point where stomatal limitation is artificially eliminated by raising the ambient CO_2 concentration (C_a) to attain a resulting internal CO_2 concentration (C_i) of 350 µmol.mol^{-1} (Lange *et al.*, 1987). The solid points symbolise data generated with an infrared gas analysing system, to construct an A:C_i response curve.

3.4.5 Measurement of photosynthetic gas exchange

Photosynthetic gas exchange was measured in leaves situated on the 4th, 6th and 9th node on the stem of *Brassica oleracea*. Due to the unevenness of the lamina, great

care was taken when placing the leaf into the cuvette (PLC) to ensure that the gaskets of the cuvette sealed properly.

In the case of *Glycine max*, photosynthetic gas exchange was measured in fully expanded trifoliate leaves, of equivalent physiological age and crown position (see Table 3.3). Measurements were conducted on four randomly selected plants in each chamber of which two replicates were subjected to drought stress and two were watered close to field capacity. Leaf gas exchange measurements were carried out on cloud-free days and all measurements were made between 09h00 and 16h00 local time. A 2.5 cm^2 section of a leaf was clamped into a standard broad leaf photosynthetic leaf chamber (PLC) with light and temperature control. The light intensity (PPF) was kept at 1 200 µmol photons.m^{-2}.s^{-1} to ensure full activation of Rubisco (Taylor & Terry, 1984), while leaf temperature was kept at 26° C during measurements. To ensure steady–state activation of Rubisco, the leaf in the cuvette was acclimated to a CO_2 concentration of 360 µmol.mol^{-1} at a saturating net photosynthetic photon flux (PPF; 1200 µmol.m^{-2}.s^{-1}) for 10 minutes before measurement with an infrared gas analysis system (CIRAS-2, PP-Systems, Hertz, UK). After gas exchange reached a steady state, the intercellular CO_2 concentration (C_i) was manipulated by varying ambient CO_2 concentration (C_a). The linear slope of the response curve was constructed by lowering the ambient CO_2 concentration (C_a) in the cuvette from 360 µmol.mol^{-1} in five steps to 200, 100, 75, 50 and 25 µmol.mol^{-1}. C_a was again stabilised at 360 µmol.mol^{-1} to ensure open stomata and to verify the stability of the photosynthetic apparatus. This procedure allowed for comparison of post and pre-A_{net} (A_{360}) values at 360 µmol.mol^{-1}. Lastly, C_a was stepped up from 360 µmol.mol^{-1} in four steps to 500, 700, 1000 and 1500 µmol.mol^{-1}, allowing CO_2 assimilation rate (A) *vs.* intercellular CO_2 concentration (C_i) response curves to be generated (Singsaas *et al.*, 2001). A three-minute measuring period at each successive increment was sufficient to attain accurate values.

3.4.6 Overview of light response kinetics

The rate of CO_2 assimilation (A) to photon flux density (PFD) describes a curve or curvilinear progression that can be accurately defined in terms of (i) an initial rapid increase in A with increase in Q below the light-compensation point, termed the "Kok effect"; (ii) a longer linear phase in which ($\delta A/\delta Q$) is considered to represent the maximum quantum yield of photosynthesis (Φ_{max}); (*iii*) a transition from light limited to

light saturated photosynthesis described by the convexity (Θ) of the curve and (iv) the asymptote indicating the light-saturated rate of A (A_{max}) (Leverenz, 1987).

The typical light response curve may approximate to a rectangular hyperbola:

$$A = A_{max}.Q/ k_Q + Q$$

where k is the value of Q at which $A = A_{max}/2$

This value of A is termed the light-saturated rate of CO_2 uptake. Here the convexity (Θ) is zero.

The "Kok effect" indicated by an initial increase in A with Q through the light compensation point can be ascribed to increases in mitochondrial respiration at very low light (<20 μmol m^{-2} s^{-1} PFD) affecting net photosynthesis which results in an increase in the initial slope of the light-response curve (Sharp *et al.*, 1984). The "apparent Kok effect" is evident when the curvature did not result from the light saturation of photosynthesis, but rather as a result of changes in C_i. The "apparent Kok effect" was first described by Kirschbaum and Farquhar (1987) as a situation where photosynthesis responds to light independently of stomatal conductance during gas-exchange measurements and increases in CO_2 assimilation, without an accommodating change in stomatal conductance results in decreased C_i.

The light compensation point (I_c) is analogous to the compensation concentration of CO_2 discussed earlier in the chapter. The CO_2 compensation point reflects the balance between photosynthesis and respiration as a function of CO_2 concentration, and the light compensation point reflects that balance as a function of photon flux; in other words, the light compensation point signify the irradiance level at which photosynthetic CO_2 uptake and respiratory CO_2 release are in equilibrium, and no gas exchange is detectable (Hall *et al.*, 1993).

When (I_c) has been exceeded, there is at first a linear increase in CO_2 uptake, indicating a strict proportionality between available radiation and photosynthetic yield (photosynthetic efficiency (Φ_i) expressed in mol CO_2 per mol incident photons). The initial slope is assumed to correspond to the maximum apparent quantum yield of photosynthesis (Φ_{max}) when photosynthesis is light-limited, a situation diagnosed by a linear relationship between photosynthesis and photosynthetic photon flux density.; i.e. the efficiency of light utilisation by photosynthesis, the number of moles of CO_2

fixed per mole quanta absorbed by the leaf. The higher the apparent quantum yield (Φ_a), the steeper the slope in the range of the light response curve would be in terms of proportionality. Since light becomes less important as a factor limiting photosynthesis with increasing Q, the Φ_{max} can only be measured at low Q, when photosynthesis is strictly light-limited and proportional to Q. Beyond this point, a linear response of A to Q persists at between 50 and ~ 200 $\mu mol.m^{-2}.s^{-1}$. Only the linear region meets the assumptions that light is limiting and respiration is constant for calculating Φ_{max}. Including points from the Kok effect region would cause an overestimation of Φ, while including points from the transition region would cause an underestimation. The linear region of each light-response curve varied considerably among the light-response curves measured. Thus, the ranges of PFD valid for Φ analysis were determined by evaluating each light-response curve individually, using the computer program Photosynthesis Assistant. Since the Kok effect (Sharp *et al.*, 1984) was evident at the lowest two PFD levels in the data, these points were excluded from the Φ analysis. Quantum yield was calculated from each regression line fit to different numbers of points starting at low PFD.

A progressive decrease in the slope of the curve ($\delta A/\delta Q$) with increase in Q follows until a plateau is reached beyond the light saturated assimilation rate of CO_2 uptake (A_{max}). Once the saturation point has been reached, further increase in photon flux will no longer affect photosynthetic rates, indicating that factors such as electron transport reactions, Rubisco activity, or triose phosphate metabolism become limiting. At this stage photosynthesis is referred to as CO_2 limited, reflecting the inability of the carbon metabolism enzymes to keep pace with the absorbed light energy. Along these lines the light-saturated assimilation rate (A_{max}) may be considered as a measure of the photosynthetic capacity of the leaf (Hall *et al.*, 1993).

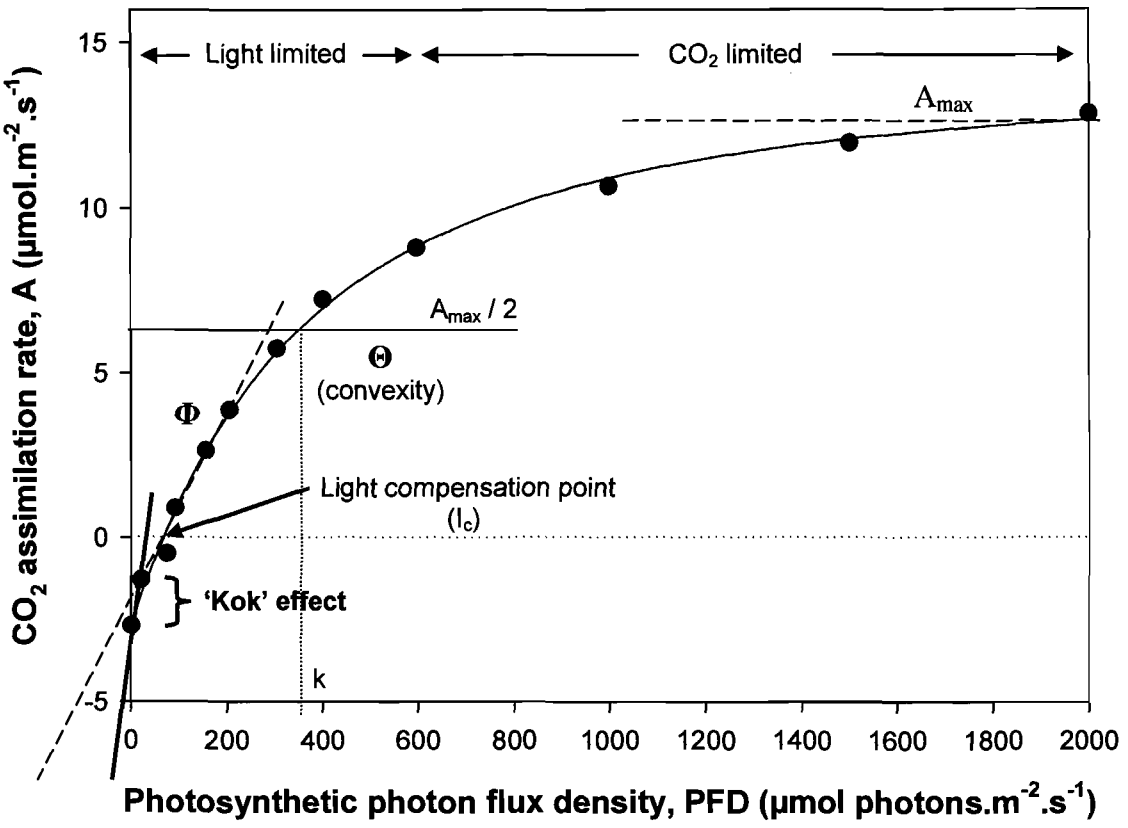


Figure3.5 **Light response curve of CO_2 assimilation rate (A) to photon flux density (Q). This illustrates all the possible phases of the curve: (i) the initial rapid increase (indicated as the bolded solid line) in A with increase in Q below the light compensation point, termed the "Kok effect". (However, based on only two data points, the "Kok effect" can be recognised.) (ii) A longer linear phase in which (δA/δQ) is considered to represent the maximum quantum yield of photosynthesis (Φ); (iii) a transition from light limited to light-saturated photosynthesis described by the convexity (Θ) of the curve and; (iv) the asymptote indicating the light-saturated rate of A, namely A_{max}. The light compensation point (I_c) (bolded arrow) indicates the irradiance level at which photosynthetic CO_2 uptake and respiratory CO_2 release are in equilibrium. The solid points represent data generated with an infrared gas analysis system from which light response curves could be constructed.**

3.4.7 Measurement of photosynthetic light response kinetics

Light response curves were generated on fully expanded trifoliate leaves of *Glycine max* of similar physiological age and crown position. The measurements were conducted twice during the course of the experiment. The CO_2 concentration inside the PLC was kept at 360 µmol.mol^{-1} to ensure open stomata and to verify the stability of the photosynthetic apparatus. The light intensity inside the cuvette was stepped up from 1 µmol.photons.m^{-2}.s^{-1} in ten successive steps to 25, 75, 100, 150, 200, 400, 600, 1 000, 1 500 and 2 000 µmol. photons.m^{-2}.s^{-1}.

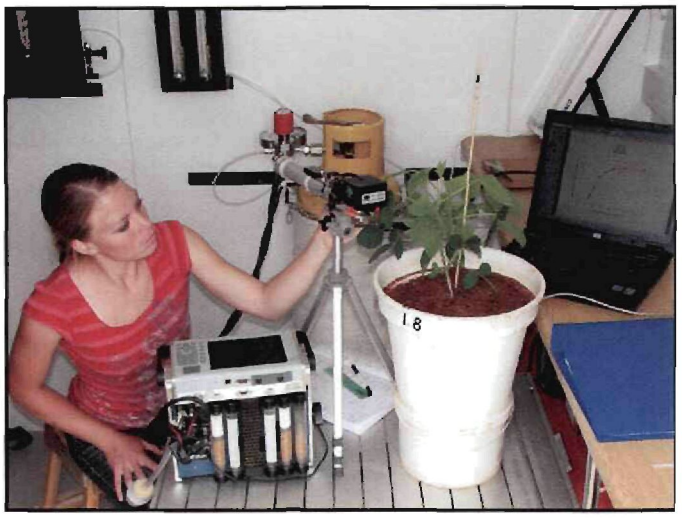


Figure 3.6 Measuring photosynthetic gas exchange in *Glycine max* for generating A:C$_i$ and A:Q curves using an automated PLC coupled to an IRGA. A 2.5 cm^3 section of a leaf of *Glycine max* was clamped into the cuvette and temperature and light conditions could be kept near constant while CO_2 levels or PFD were adjusted as required.

3.4.8 Fast-phase *chlorophyll a* fluorescence kinetics

3.4.8.1 Overview of *chlorophyll a* fluorescence kinetics

All dark adapted oxygenic photosynthetic material exhibit fluorescence upon illumination. The fluorescent emission occurs in the long-wavelength side of the red absorption band (Hopkins, 1999) and originates mostly from the minor antennae complexes CP-43 and CP 47 (Govindjee, 2004).

Light energy absorbed by pigments in plants, mostly chlorophyll molecules, can undergo one of three fates: (i) it can be used to drive photochemistry, i.e. photosynthesis (inductive resonance), (ii) excess energy can be dissipated as heat from the light harvesting complexes (LHC) of photosystem II (PSII), or (iii) it can be re-emitted as light-chlorophyll fluorescence. These three processes occur in competition with another in such a way that any increase in the efficiency of the one results in a decrease in yield in the other two (Maxwell & Johnson, 2000). By measuring the yield of chlorophyll fluorescence, information about the changes in the efficiency of photochemistry and heat dissipation can be gained. Since the decay processes of excited chlorophyll are competitive, changes in photosynthetic rate and/or dissipative heat will lead to complementary changes in emitted fluorescence intensity (Bolhàr-Nordenkampf & Öquist, 1993).

The spectrum of fluorescence is different from the spectrum of absorbed light, with the peak of fluorescence emission being of a longer wavelength than that of absorption (Hopkins,1999). Thus fluorescence yield can be quantified by exposing a leaf to light of a defined wavelength and measuring the amount of light re-emitted at a longer wavelength.

When a dark-adapted leaf is illuminated with a saturated light pulse, characteristic changes in the intensity of *chlorophyll a* fluorescence, known as the Kautsky effect, are observed (Kautsky & Hirsch, 1931). The Kautsky transient shows a fast rise (increase in chlorophyll fluorescence yield) completed in less than one second, with a subsequent slower decline towards a steady state. It is postulated that the rising phase of the transient reflects the primary reactions of photosynthesis and has subsequently been explained as a consequence of reduction of electron acceptors in the photosynthetic pathway, downstream of PSII, notably plastoquinone and predominantly Q_A (Krause & Weis, 1991). It was observed that changes in fluorescence emission were related to changes in photosynthetic rate (Kautsky & Hirsch, 1931). With the development of fluorimeters with high time resolution and high data acquisition capacity, additional and more accurate information about the kinetics of these transients was obtained (Schreiber & Neubauer, 1987; Strasser & Govindjee, 1992; Strasser *et al.*, 1995). The JIP-Test: Conversion of experimental signals to biophysical parameters and the performance index: The well-known fluorescence induction curve observed by Kautsky and Hirsch (1931) shows an initial O-P rise lasting for less than 1 second to several seconds depending on the actinic light intensity, an subsequent decrease labelled P – S occurring in the time range of

seconds to minutes. The detailed shape of the polyphasic O – P fluorescence transient was revealed only when the fluorescence signal was recorded with a high resolution (high time resolution and large data acquisition capacity) and the data was plotted on a logarithmic scale (Figure 2.5). The instrument used was the PEA-fluorimeter (Plant Efficiency Analyser, built by Hansatech Instruments, Ltd. Kings Lynn, UK.) (Strasser & Govindjee, 1992; Strasser *et al.*, 1995). Such a plot clearly revealed the steps J and I (Strasser & Govindjee, 1992) or I_1 and I_2 (Scheiber & Neubauer, 1997). When the OJIP (fast phase fluorescence transient) is measured with the Plant Efficiency Analyser (PEA, Hansatech Instruments Ltd., Kingslynn, UK), direct fluorescence is measured as opposed to modulated fluorescence as is the case with many other commercially available instruments. It was demonstrated that the fluorescence rise kinetics of the Kautsky transient is polyphasic when plotted on a logarithmic time scale (Figure 2.5), clearly exhibiting the steps J and I (Strasser & Govindjee, 1992) or I_1 and I_2 (Schreiber & Neubauer, 1987) between the initial O (F_0) and maximum P level ($F_P = F_M$).

Upon excitation with a saturated light pulse, a rapid initial rise occurs in fluorescence intensity from O to the first intermediate step J within ca. 2 ms. This phase is followed by a further rise to the second intermediate step I within ca. 30 ms and to the final peak P in ca. 200 ms. The OJIP fluorescence transient reflects the filling up of the electron acceptor side of PSII (Q_A, Q_B and PQ pool) with electrons from the donor side of PSII (Papageorgiou, 1975; Lavorel & Etienne, 1977; Strasser & Govindjee, 1992). The relationship of these events to the OJIP fluorescence transient was suggested by Strasser *et al.* (1995) to be the following: O, minimal *chlorophyll a* fluorescence yield (highest yield of photochemistry); O to J, reduction of Q_A to Q_A^- (photochemical phase, light intensity dependent); J to I to P, reduction of the PQ pool (non-photochemical phase). Since the OJIP fluorescence transient reflects the kinetics and heterogeneity involved in the filling up of the PQ pool with electrons, it can be used as a sensitive tool to investigate the function and structure of the photosynthetic apparatus *in vivo* (Strasser *et al.*, 1995). The shape of the OJIP fluorescence transient (Figure 2.5) has been found to be very sensitive to various types of stress (Krüger *et al.*, 1997; Lazár & Ilík, 1997; Tsimilli-Michael *et al.*, 1999; Van Heerden *et al.*, 2004; Strauss *et al.*, 2006).

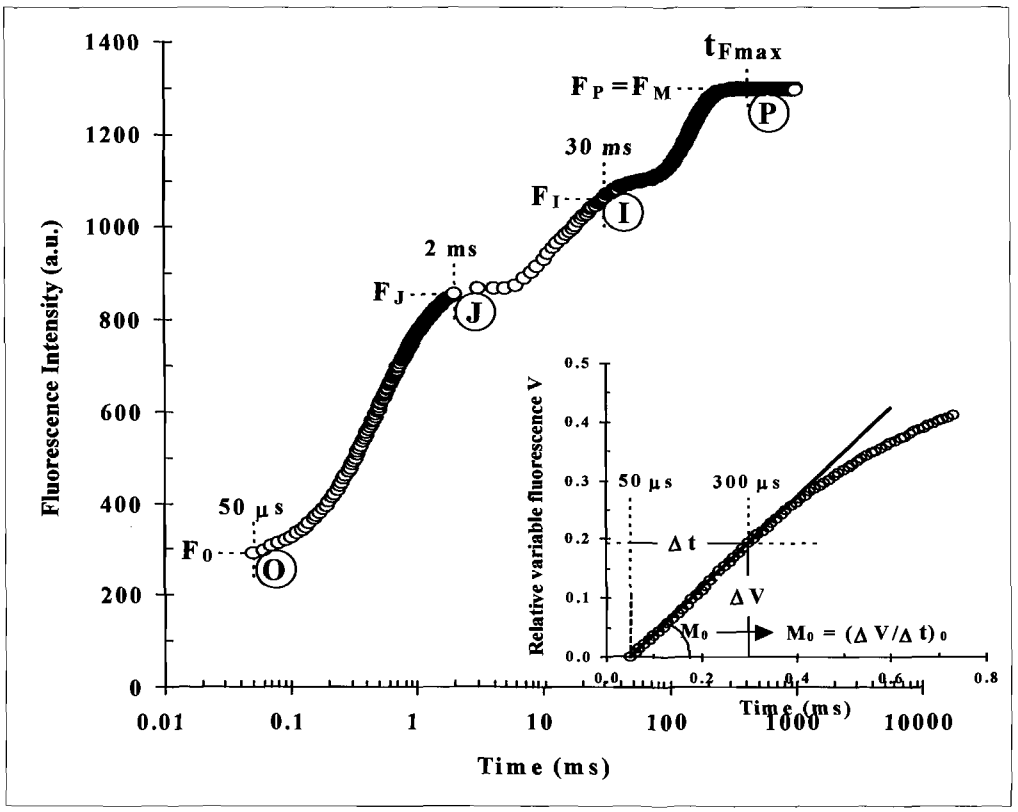


Figure 3.7: An example of a typical polyphasic *chlorophyll a* fluorescence transient OJIP emitted by higher plants representing the accumulation of reduced Q_A. The transient is plotted on a logarithmic time scale from 50 µs to 1 s. The labels refer to the fluorescence data used by the JIP-test for the calculation of various parameters quantifying PSII structure and function with the Biolyser software (Biolyser4HP version 3.06, RM Rodriquez, Bioenergetics Lab, Geneva, Switzerland). The labels are: the fluorescence intensity F_0 (at 50 µs); the fluorescence intensity F_J (at 2 ms); the fluorescence intensity F_I (at 30 ms) and the maximal fluorescence intensity $F_P = F_M$. The inserted figure shows the transient expressed as the relative variable fluorescence, $V = (F - F_0)/(F_M - F_0)$, on a linear time-scale and demonstrates how the initial slope (M_0) is calculated: $M_0 = (\delta_V/\delta_t)_0 = (V_{300\mu s})/(0.25\ ms)$ (from Strasser & Tsimilli-Michael *et al.*, 2000).

3.4.8.2 Analysis of the *chlorophyll a* fluorescence transient by the JIP-test

The key expression of the JIP-test is TR_0/RC, in other words, the maximal trapping flux at t = 0. This reflects the reduction of Q_A through a single turnover (re-oxidation

of Q_A^- blocked by DCMU), therefore only the photochemical reactions. This can be calculated by the initial slope of the fluorescence rise:

$$(dV/dt)_{0,DCMU} = M_{0,DCMU}$$

In the absence of DCMU, accumulation of Q_A^- (the net result of Q_A reduction by PSII and its reoxidation by PSI, in other words multiple turnovers of Q_A to Q_A^-) can be represented by the initial slope:

$$(dV/dt)_0 = M_0$$

The RC closing rate, i.e. M_0, increases while electron transport beyond Q_A resulting in Q_A^- tends to decrease it. The net rate of closing RCs is represented in the slope:

$$M_0 = TR_0/RC - ET_0/RC$$

A breakthrough was made by Strasser and Strasser (1995) when it was determined that $M_{0,DCMU}$ can be simulated by multiplying M_0 by $1/V_J$ (V_J is the relative change in fluorescence at F_J, calculated by $(F_J - F_0)/(F_M - F_0)$), thus:

$$M_{0,DCMU} = M_0/V_J$$

This implied that the maximal trapping flux could be simulated without the use of DCMU, making these measurements non-destructive and creating the opportunity to fully exploit the fluorescence transient.

The following data from the original measurements are used by the JIP-test for calculation of the energy fluxes through PSII and other fluorescence parameters: maximal fluorescence intensity (F_M); fluorescence intensity at 50 μs (considered as F_0); fluorescence intensity at 300 μs ($F_{300\mu s}$) required for calculation of the initial slope (M_0) of the relative variable fluorescence (V) kinetics; and the fluorescence intensity at 2 ms (the J step) denoted as F_J (Figure 2.5).

The JIP-test represents a translation of the original fluorescence data to biophysical parameters that quantify the stepwise flow of energy through PSII at the reaction centre (RC) as well as excited cross-section (CS) level (Strasser & Strasser, 1995; Force *et al.*, 2003; Strasser *et al.*, 2004). The parameters, which all refer to time zero (onset of fluorescence induction), are: (i) the specific energy fluxes (per reaction centre) for absorption (ABS/RC), trapping (TR_o/RC), dissipation at the level of the antenna chlorophylls (DI_o/RC) and electron transport (ET_o/RC); (ii) the flux ratios or yields, i.e. the maximum quantum yield of primary photochemistry ($\varphi_{Po} = TR_o/ABS =$

F_V/F_M), the efficiency ($\psi_o = ET_o/TR_o$) with which a trapped exciton can move an electron into the electron transport chain further than Q_A^-, the quantum yield of electron transport ($\varphi_{Eo} = ET_o/ABS = \varphi_{Po} \bullet \psi_o$); the quantum yield of the formation of reduction equivalents ($\varphi_{R0} = \varphi_{Eo} \bullet \delta$) (Strasser, 2006); (iii) the phenomenological energy fluxes (per excited cross section, CS) for absorption (ABS/CS), trapping (TR_o/CS), dissipation (DI_o/CS) and electron transport (ET_o/CS). The fraction of active PSII reaction centres per excited cross section (RC/CS) is also calculated. The formulae in Table 2.2 illustrate how each of the above-mentioned biophysical parameters can be calculated from the original fluorescence measurements.

The initial stage of photosynthetic activity of a RC complex is regulated by three functional steps, namely absorption of light energy (ABS), trapping of excitation energy (TR) and conversion of excitation energy to electron transport (ET) (Figure 3.8). Strasser *et al.* (2000) introduced a multi-parametric expression of these three independent steps contributing to photosynthesis, the so-called performance index (PI_{ABS}):

$$\mathbf{PI_{ABS} = RC/ABS \bullet \varphi_{P0}/(1-\varphi_{P0}) \bullet \psi_0/(1-\psi_0)}$$

This expression can be de-convoluted into three JIP-test parameters and estimated from the original fluorescence measurements as $RC/ABS = RC/TR_o \bullet TR_o/ABS = [(F_{2ms} - F_{50\mu s})/4(F_{300\mu s} - F_{50\mu s})] \bullet F_V/F_M$. The factor 4 is used to express the initial fluorescence rise per 1 ms. The expression RC/ABS shows the contribution to the PI_{ABS} due to the RC density on a chlorophyll basis. The contributions of the light reactions for primary photochemistry are estimated according to the JIP-test as $[\varphi_{Po}/(1-\varphi_{Po})] = TR_o/DI_o = k_P/k_N = F_V/F_o$. The contribution of the dark reactions are derived as $[\psi_o/(1-\psi_o)] = ET_o/(TR_o - ET_o) = (F_M - F_{2ms})/(F_{2ms} - F_{50\mu s})$. The JIP-test reveals changes in the behaviour of PSII that cannot be detected by the commonly used parameter $\varphi_{P0} = F_V/F_M$, (quantum efficiency of primary photochemistry) which is the least sensitive of all parameters (Strasser *et al.*, 2004). An additional parameter has been recently developed that gives an indication of the efficiency of the reduction of $NADP^+$ to NADPH, namely φ_{R0}, which is derived as follows (Strasser, 2006):

$$\mathbf{\varphi R_0 = \varphi P_0 \bullet \delta = \varphi P_0 \bullet (1-V_{i\,\{F30ms\}})/(1-V_{J\,\{F2ms\}})}$$

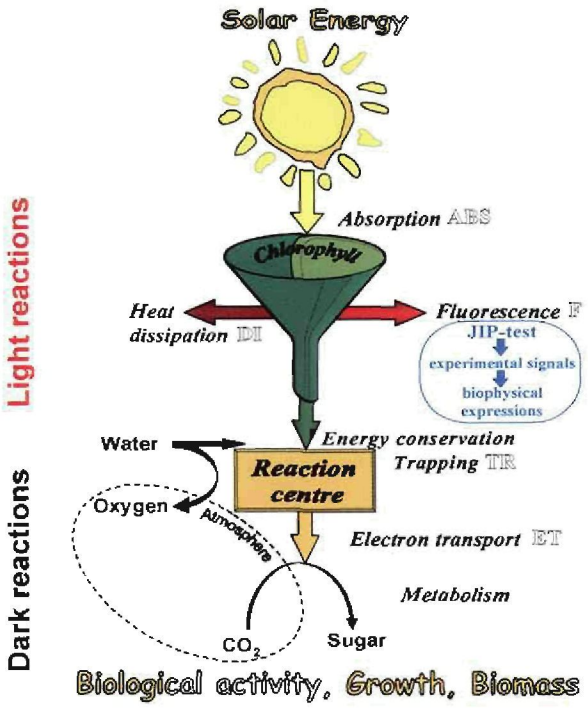


Figure 3.8 Schematic representation of the energy cascade, showing the major important events in the photosynthetic apparatus. The PI is an expression which combines the three main categories of forces driving photosynthesis, namely the concentration of reaction centers of PSII, the performance of the light reaction and the performance of the dark reaction (Epitalawage *et al.*, 2003).

Table 3.2 **Summary of the JIP-test formulae using data extracted from the *chlorophyll a* fluorescence transient OJIP (Modified from Strasser & Tsimilli-Michael, 2000).**

Extracted and Technical Fluorescence Parameters		
F_0	=	$F_{50\mu s}$, fluorescence intensity at 50μs
$F_{100\mu s}$	=	fluorescence intensity at 100μs
$F_{300\mu s}$	=	fluorescence intensity at 300μs
F_J	=	fluorescence intensity at the J-step (at 2ms)
F_I	=	fluorescence intensity at the I-step (at 30ms)
F_M	=	maximal fluorescence intensity
t_{F_M}	=	time to reach F_M , in ms
V_J	=	relative variable fluorescence at the J-step = $(F_{2ms} - F_0) / (F_M - F_0)$

$(dV / dt)_0 = M_0$	=	fractional rate of PS II reaction centre closure = 4 . $(F_{300} - F_0)/(F_M - F_0)$
Quantum Efficiencies or Flux Ratios or Yields		
$\varphi_{Po} = TR_0 / ABS$	=	$[1 - (F_0 / F_M)] = F_V / F_M$
$\varphi_{Eo} = ET_0 / ABS$	=	$[1 - (F_0 / F_M)] . \psi_0$
$\varphi_{Ro} = RE/ABS$	=	$(1-V_I)/(1-V_J) . \varphi_{Eo}$
$\psi_0 = ET_0 / TR_0$	=	$(1 - V_J)$
Specific Fluxes or Specific Activities		
ABS / RC	=	$M_0 . (1 / V_J) . (1 / \varphi_{Po})$
TR_0 / RC	=	$M_0 . (1 / V_J)$
ET_0 / RC	=	$M_0 . (1 / V_J) . \psi_0$
DI_0 / RC	=	$(ABS / RC) - (TR_0 / RC)$
Phenomenological Fluxes or Phenomenological Activities		
ABS / CS	=	ABS / CS_{Chl} = Chl / CS or $ABS / CS_0 = F_0$ or $ABS / CS_M = F_M$
TR_0 / CS	=	$\varphi_{Po} . (ABS / CS)$
ET_0 / CS	=	$\varphi_{Po} . \psi_0 . (ABS / CS)$
DI_0 / CS	=	$(ABS / CS) - (TR_0 / CS)$

Density of Reaction Centres		
RC / CS	=	$\varphi_{Po} . (V_J / M_0) . ABS / CS$
Performance Indices		
PI_{ABS}	=	$(RC / ABS) . [\varphi_{Po} / (1 - \varphi_{Po})] . [\psi_0 / (1 - \psi_0)]$
PI_{TOT}	=	$(RC/ABS) . [\varphi_{Po}/(1-\varphi_{Po})] . [\psi_0/(1-\psi_0)] . [\varphi_{Ro}/(1-\varphi_{Ro})]$
Driving Force		
DF_{ABS}	=	$\log [PI_{ABS}]$
DF_{TOT}	=	$\log [PI_{TOT}]$

3.4.9 Measurements of *chlorophyll a* fluorescence induction kinetics

Chlorophyll a fluorescence induction curves were recorded weekly on dark-adapted leaves of *Brassica oleracea* and *Glycine max* plants to assess the effect of SO_2 singly and in combination with drought stress. Measurements were recorded at night with a Handy Plant Efficiency Analyser (Handy-PEA, Hansatech Instruments Ltd., Kingslynn, UK). Each fluorescence induction transient was induced by red light (peak

650nm) of 2000 µmol photons.$m^{-2}.s^{-1}$ (sufficient excitation intensity to ensure complete closure of PSII reaction centres to obtain true fluorescence intensity of F_M) and recorded for 1 second on a 4 mm diameter area of a dark-adapted, attached leaf sample. The recorded OJIP transients were analysed by the JIP-test.

3.5 Destructive plant analysis

3.5.1 Leaf water potential

Plant water status strongly influences plant growth, particularly through its effect on the rate of photosynthesis in general; and biomass, since biomass production is directly proportional to the supply and use of water. Therefore, measurement of plant water status is an important part of understanding biomass production and in conjunction with the determination of soil water potential, can provide valuable information regarding its contribution to yield attributes.

Water potential (ψ), is defined as the potential energy (Joules) per unit mass of water (m^3) with reference to pure water at zero potential:

$$\Psi = \mu_w - \mu^*_w \; / \; V_w$$

where μ_w is the chemical potential, or free energy per mole, of water at some point in the system at constant temperature and pressure, μ^*_w is the chemical potential of pure water at the same temperature and at atmospheric pressure, and V_w is the partial molal volume of water. Thus, the quantity, $\mu_w - \mu^*_w$, represents the work involved in moving one mole of water from some point in the system to a pool of water at the same temperature and at atmospheric pressure.

The water potential for a plant cell (ψ) may be expressed as the sum of the three components:

$$\Psi = P + \pi + \tau$$

where P is the turgor potential arising from the pressure exerted on the cells by their walls, π is the osmotic potential arising from the measured dissolved solutes in the cell (negative value); τ is the matric potential which accounts for the reduction in free energy of water when it exits as a thin surface layer adsorbed onto the surface of the cell walls and other materials (Tyree & Jarvis, 1982).

The pressure chamber technique (Sholander *et al.*, 1965) was used to estimate leaf water potential in plants grown under two different water regimes. Although partly destructive, the pressure chamber technique is an easy, inexpensive method ideally suited for field studies and has been reviewed as the most widely used method for characterising plant water status.

Leaf water potential was measured in fully expanded trifoliate leaflets of the *Glycine max* plants for quantifying the plant water status grown under two watering regimes. Four plants were selected from each chamber and a leaf each from the 3rd, 4th and 5th nodes were harvested at the petiole. The excised leaf was placed with the petiole protruding through a rubber gasket into the chamber and sealed air tight to prevent leakage. Immediately prior to being excised from the plant, the leaf was enclosed in a plastic sheath to prevent water loss during the measuring period. A sharp razor blade was used to cut the leaf at the petiole precisely so that the length of the protruding end of the petiole was minimised to prevent evaporation from the exposed section. Re-cutting the petiole after the leaf was excised from the plant will cause net movement of water into the symplasm, which may result in a very high measurement of ψ. As long as the petiole has only been cut once, the water will re-fill the emptied xylem elements when pressure is increased inside the chamber and no net movement of water into the symplasitc tissue will be possible (Hall *et al.*, 1993). The concave groove of the soybean petiole, however, caused leakage of the pressurised air from the chamber and therefore a length of thinly rolled parafilm was used to fill the groove so that the petiole fitted tightly into the rubber gasket. In the case of *Brassica oleracea*, a section of the leaf lamina was cut with a sharp blade and sealed of in the chamber by using a rubber gasket with a slit (Figure 2.6). The pressure was slowly increased in the chamber by controlling the rate of pressurised air from a regulated cylinder so that the ψ disequilibria within the tissue symplasm was eradicated. The pressure created in the chamber caused the water interface in the xylem to return to where it was before detachment of the leaf. This pressure was equal and opposite to the tension created in the xylem of the intact plant.

Measurements were conducted during midday and the predawn period of the following day. Measuring leaf water potential at predawn provides a good estimate of the water stress situation the plant is currently experiencing.



Figure 3.9 Measuring leaf water potential on *Brassica oleracea*. A section of the leaf is excised over the main vein (left) and placed into an elastic rubber with a slit tightly fitting into the pressure chamber head (right).

3.5.2 Biomass accumulation and allocation

Twenty days after the treatments commenced, *Glycine max* plants were harvested for the midseason mean biomass quantification. The plants were carefully removed from each pot and the soil thoroughly removed from the roots. The shoots and roots of two plants per chamber were separated and dried at 60˚C for 48h or until constant mass. The dried shoots and roots were then weighed and the root to shoot ratios calculated. Biomass accumulation in *Brassica oleracea* was determined at the end of the treatment period and thus only a final harvest was done. Roots and shoots were separated, dried and the root to shoot ratios calculated.

3.5.3 Yield attributes

Yield attributes were only determined for *Glycine max* plants. Yield was determined in terms of number of immature and mature pods per plant and number of immature and mature seeds per pod. The pods were separated from the plant stems and dried at 60°C for 48h or until constant mass. The dried pods and stems were weighed and a pod to stem ratio calculated.

3.5.4 Rubisco enzyme analysis

Whole trifoliate leaves of *Glycine max* were sampled in liquid nitrogen after 29 days of SO_2 fumigation. Sampling was done around midday. Special care was taken not to

shade the portion of the leaf from which the sample was taken, in order to prevent deactivation of Rubisco. The collected leaf samples were stored at –84°C. The method of Keys and Parry (1990) was used to assay Rubisco activity. Each leaf was ground in liquid nitrogen, insoluble polyvinylpolypyrrollidone (PVPP) and proteinase inhibition cocktail (Sigma proteinase inhibition cocktail for plant extractions; containing 4-(2-aminoethyl) benzenesulfonyl fluoride, bestatin, pepstatinA, E-64, leupeptin and 1,10-phenanthroline), and then rapidly extracted with extraction buffer (pH 8.0) containing 100 mM bicine-NaOH, 20 mM $MgCl_2$ and 50 mM β-mercaptoethanol to form a crude extract. The crude extract was transferred to a pre-cooled micro centrifuge tube and centrifuged at 10 000 x g at 4°C for 1 min. Of the clarified supernatant 25 µl was then added to a glass scintillation vial containing assay buffer (pH 8.2 and the same composition as the abovementioned buffer but without β-mercaptoethanol), and substrate (RuBP and $NaH^{14}CO_2$). The enzyme reaction was stopped after 1 min with 200 µl formic acid (10 mM). This was done to determine initial activity (enzyme activity at the time of sampling). For total activity (activity after incubation in bicarbonate) the same clarified supernatant was used but substrate (RuBP) was added after a 3 min incubation period. All the acidified samples were dried in an oven. Water (4 ml) and 3.5 ml scintillation cocktail (Packard Ultima Gold) were then added. The incorporation of ^{14}C into 3-phosphoglycerate was determined by liquid scintillation spectrometry using a liquid scintillation analyser (Beckman, LS 6000TA). The soluble protein content of the original supernatants was determined according to the method of Bradford (1976).

3.5.5 Nodule ureide content

Nodules were harvested during the midseason harvest after 29 days of fumigation and stored at -84° C until the nodule ureide content was determined according to the method of Young and Conway (1942). Nodules were dried at 60° C for 48 hours before analysis. Nodules were weighed and ground to a power in liquid nitrogen and ureides extracted with 1 ml 0.2M NaOH. The ureide extracts were boiled for 20 min to convert all allantoin to allantoic acid and then cooled to room temperature and centrifuged at 10 000 x g and 4°C for 10 min. Of the supernatant, 50 µl were added to 350 µl H_2O. From this substrate 400 µl were added to 80 µl of 0.5N NaOH, vortexed and boiled for 10 min and immediately put on ice to cool down to room temperature. 160 µl phenylhidrazine/HCl were added and again vortexed and boiled for 2 min and put on ice to cool down to room temperature. Finally, 400 µl KFeCn/HCl were added to the mixture, vortexed and left at room temperature for 10

min after which the absorbance was read at 525nm. The urieid content was expressed on a dry weight basis.

3.6 Statistical analysis

Statistical analysis was conducted with the software package Statistica for Windows version 6 (StatSoft, Inc, USA). In data sets with parametric distribution, significant differences between treatment means were determined using Student's t-test.

Chapter 4

Results and discussion

4.1 Meteorological conditions in the chambers

The most important endeavour regarding the open top chamber growth conditions was to generate test atmospheres of elevated SO_2 concentrations and still maintain meteorological conditions close to the natural conditions in the field. The mean SO_2 concentrations (Figure 4.1a) are typical measurements recorded throughout a single day from the start of the dosing period (08h00), for a 9h.day^{-1} (until 17h00). The variability in SO_2 concentration increased during windy periods (data not shown) as an incursion through the opening at the top could cause dilution. Over the course of a single day of measurement of the diurnal temperature, relative humidity and solar radiation, the chamber effect could be evaluated and compared with ambient conditions as it would occur under natural conditions in the field.

Solar radiation

Figure 4.1b represents a comparison between solar radiation measured inside two of the eight open top chambers as well as ambient recorded for a 24h period. Quite large differences in solar radiation were detected between inside and outside the OTCs, due to shadowing caused by the frame uprights and the PVC sheeting. The difference was greatest towards the end of the season (data not shown). The UV stabilisers in both sides of the PVC sheeting blocked transmission in the UV region below 380nm (Chapter 2). (Transmission of the photosynthetically active spectrum (400-700nm) was approximately 90 % of PAR.)

Temperature

Concurrent air temperature values (Figure 4.1c) recorded with shielded thermometers located 1 m above the plant canopy inside the chambers, indicated that there was a clear relationship between the temperature difference and incident solar radiation (Figure 4.1b) around midday with a maximum temperature elevation in the chamber of 4.2 °C when solar radiation was approximately 1300 W.m^{-2}. At night, the difference between air temperature inside and outside the chambers was almost non-existent with the air temperature inside the chambers 1-2 °C higher than that of ambient. Overall, the mean elevation in temperature in the chambers was 2.3 °C.

Relative humidity

During the day, the relative humidity percentage inside the OTCs decreased by more than 20 % of that recorded ambient over midday (Figure 4.1d). This could be ascribed partly to the increase in temperature over midday (Figure 4.1c) and partly to the simulated ventilation inside the OTCs. Differences in percentage relative humidity between ambient and inside the OTCs were minimal in the early morning hours, when the ventilation units were not in operation.

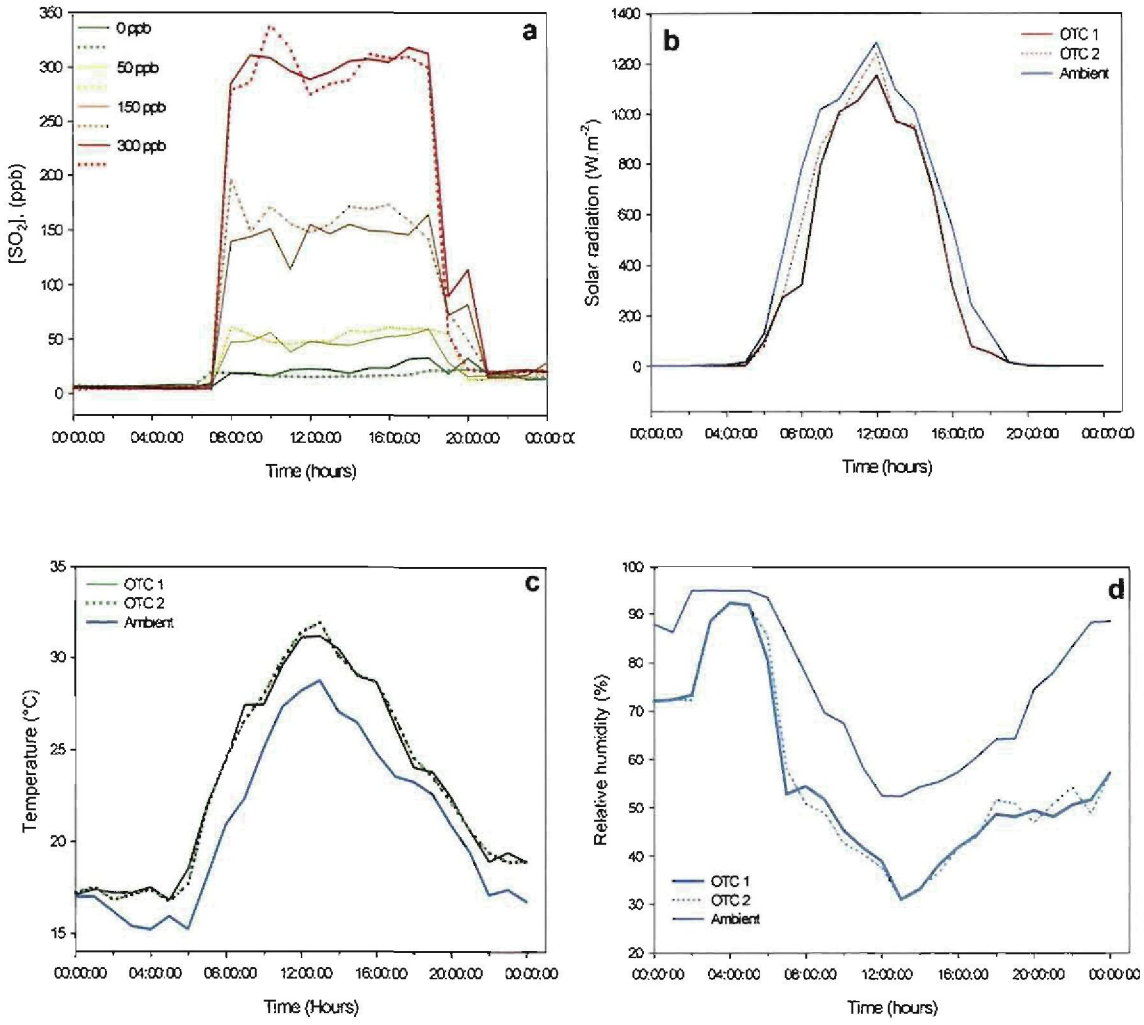


Figure 4.1 Mean SO_2 concentrations (ppb) (a) in eight open top chambers and, hourly mean values of solar irradiance (b), temperature (c) and relative humidity (d) in two of eight open top chambers measured on 22 November 2007. The solid blue line represents ambient conditions measured at a height of 6 m.

Soil water potential

Figure 4.2 illustrates the functionality of the pot reservoir system used to maintain soil water potential of the two water regimes at which the plants were grown. Even though the ventilation in the chambers dried the soil surface quicker during the day than during the night, the reservoir system could supply adequate water to the pots through the capillary action of the wicks to yield little variation in the soil water potential.

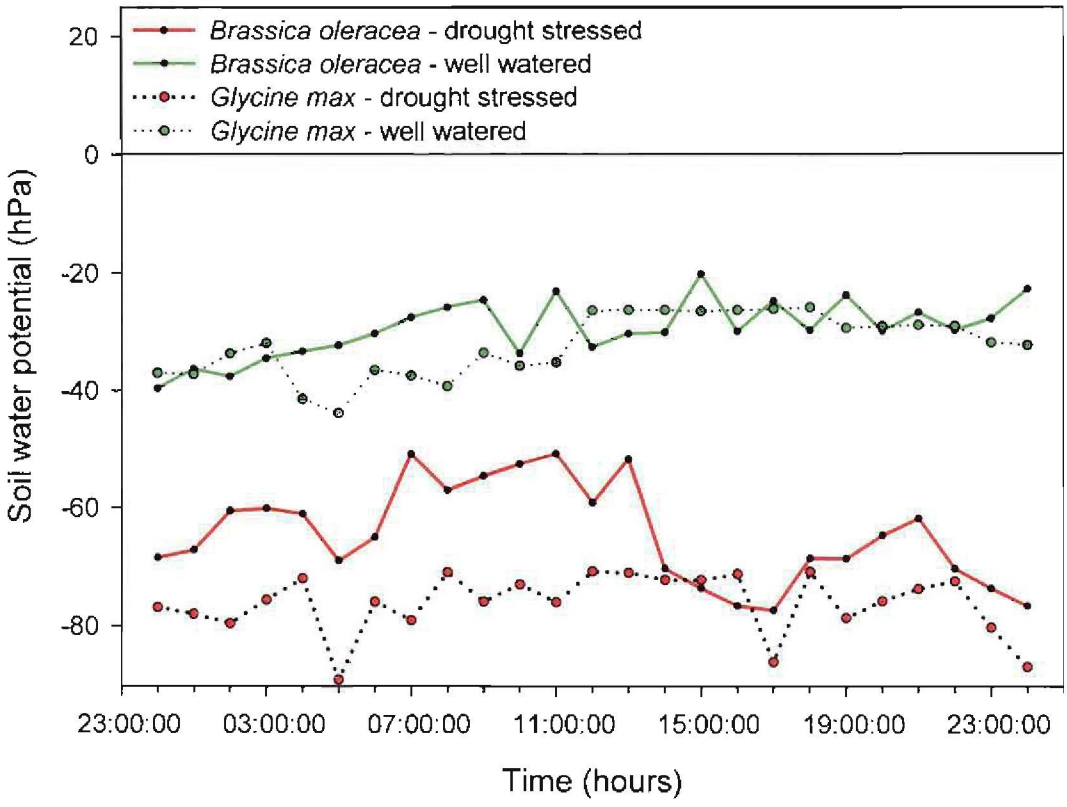


Figure 4.2 Soil water potential (hPa) mean hourly values measured at a depth of 20 cm for soil well watered to ~80 % of field capacity (green) and drought stressed soil watered to ~20 % of field capacity (red) for *Brassica oleracea* (solid) and *Glycine max* (dotted).

4.2 Verification of the water regime of the different treatments, i.e. "well watered" and "drought stressed":

4.2.1 *Brassica oleracea*

Under well watered conditions, the midday leaf water potential (Ψ_{MD}) values remained fairly constant at about -0.6 MPa decreasing to about -0.7 MPa after 35 days (Figures 4.3a and b) as the plants increased in size. Plants subjected to drought stress displayed a more negative Ψ_{MD} of about -1.4 MPa, decreasing to lower values after 35 days. Ψ_{MD} measured in drought stressed leaves after 21 days was 40 % more negative than that measured in the well watered leaves. After 35 days, the leaf water potential became even more negative, decreasing to more than 50 % compared to the well watered plants. Pre-dawn values measured in well watered leaves remained similar at all SO_2 treatments after 14 days' fumigation and subjection to drought stress. Drought stressed leaves displayed the same trend, but were 10 % smaller than the leaf water potential measured in well watered leaves. After 35 days' fumigation and subjection to drought stress, leaf water potential measured in drought stressed plants decreased by 5 % as compared to the values measured in drought stressed plants on day 14. Leaf water potential values measured pre-dawn did not display such a large difference between well watered and drought stressed plants as the differences observed with the measurements taken over midday. This is due to the fact that transpiration decreased during the dark period and the negative pressure in the xylem tissue could easily be cancelled.

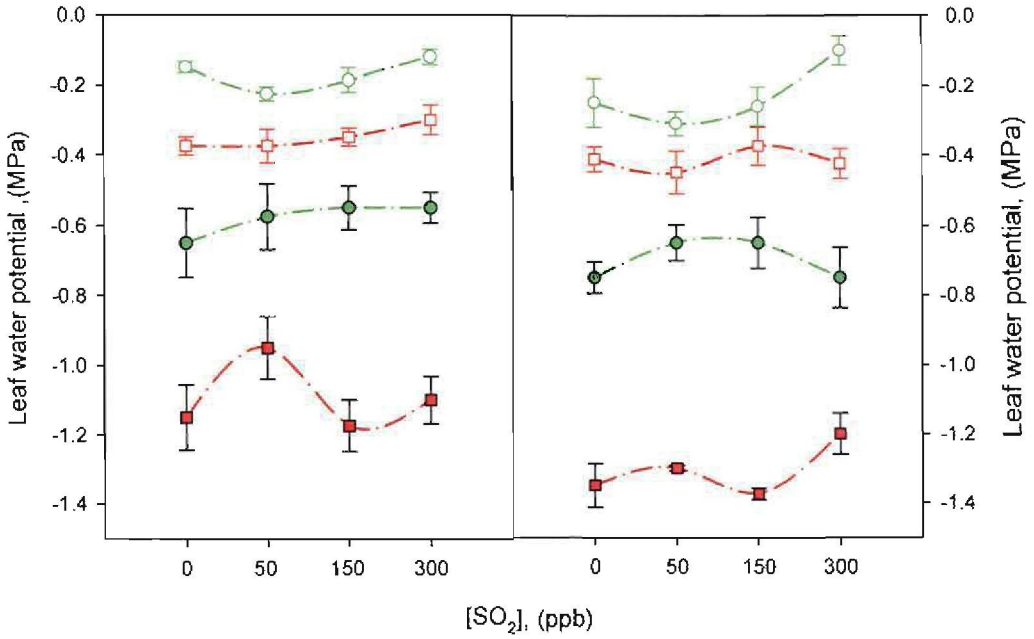


Figure 4.3 Pre-dawn (open symbols) and midday (solid symbols) leaf water potential (MPa) measured in well watered (green) and drought stressed (red) test plants (*Brassica oleracea*) after (a) 21 and (b) 35 days' fumigation at different SO_2 levels. Leaf water potential of samples was measured with a Scholander pressure chamber. Each value represents a mean (±SE), where n = 4.

4.2.2 *Glycine max*

When drought stress was introduced in combination with SO_2 fumigation simultaneously, leaf water potential decreased rapidly with increasing dosage. After 14 days' fumigation and drought stress, pre-dawn leaf water potential values decreased slightly with increasing SO_2 concentration (Figures 4.4a and b). After 28 days' fumigation with SO_2 in combination with drought, leaf water potential measured at pre-dawn decreased more rapidly (Figure 4.4b), while leaf water potential measured at pre-dawn in well watered plants grown in the presence of SO_2 remained nearly the same as the pre-dawn measure 14 days earlier. During dehydration, leaf water potential decreased much more rapidly in plants grown in the presence of SO_2 when compared to plants grown in SO_2-free air. On day 14 of fumigation with SO_2 and dehydration by drought (Figure 4.4a), leaf water potential measured over midday for plants grown in SO_2-free air was about 40 % more than that of plants grown in the

presence of SO_2. After 28 days of fumigation with SO_2 in combination with drought stress (Figure 4.4b), leaf water potential over midday measured for plants grown in the presence of SO_2 decreased even more, with as much as 57 %, but remained the same at the 150 ppb SO_2 treatment. Leaf water potential measured over midday in well watered plants in the presence of SO_2, decreased only slightly and remained nearly constant for the highest SO_2 treatment measured on day 14 (Figure 4.4a). After 28 days, leaf water potential of plants grown in the presence of SO_2 decreased slightly with increasing SO_2 concentration.

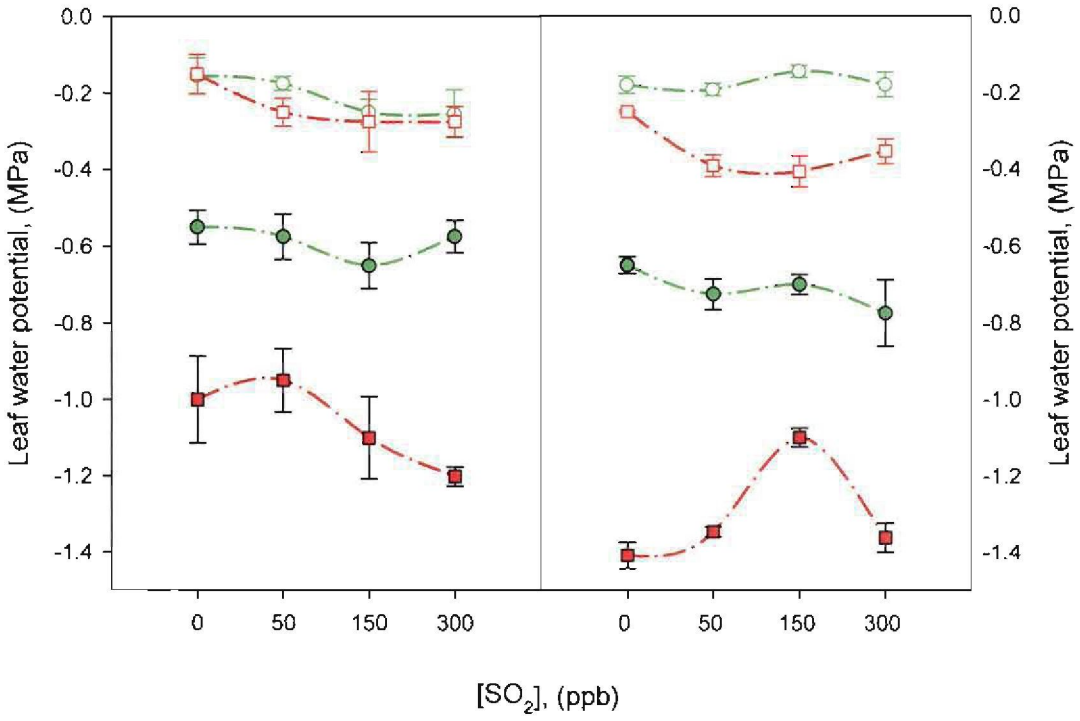


Figure 4.4 Pre-dawn (open symbols) and midday (solid symbols) leaf water potential (MPa) measured in well watered and drought stressed test plants (*Glycine max*) after (a) 14 and (b) 28 days of SO_2 fumigation at different levels. Leaf water potential of samples was measured with a Scholander pressure chamber.

4.3 Growth

4.3.1 Plant development – Plastochron index

In order to make reliable comparisons between different treatments, information regarding age and growth of the plants was necessary. The growth of the *Glycine max* plants used in the fumigation experiment is given in Figure 4.5 as analysed

according to the plastochron index. The growth rate of the seedlings from the different chambers was very similar before exposure to the different SO_2 concentrations and watering regimes. Even though the effect of SO_2 on growth rate was not determined, the approximately exponential growth of the seedlings suggests that possible changes in physiological conditions due to age variations should have little influence on the results. The ambient control plants were at the same growth stage before the plants were potted out, but growth progressed at a slower rate than those grown in the OTCs. This could be ascribed to the sheltering effect of the chambers when the night temperatures outside dropped below 15 °C.

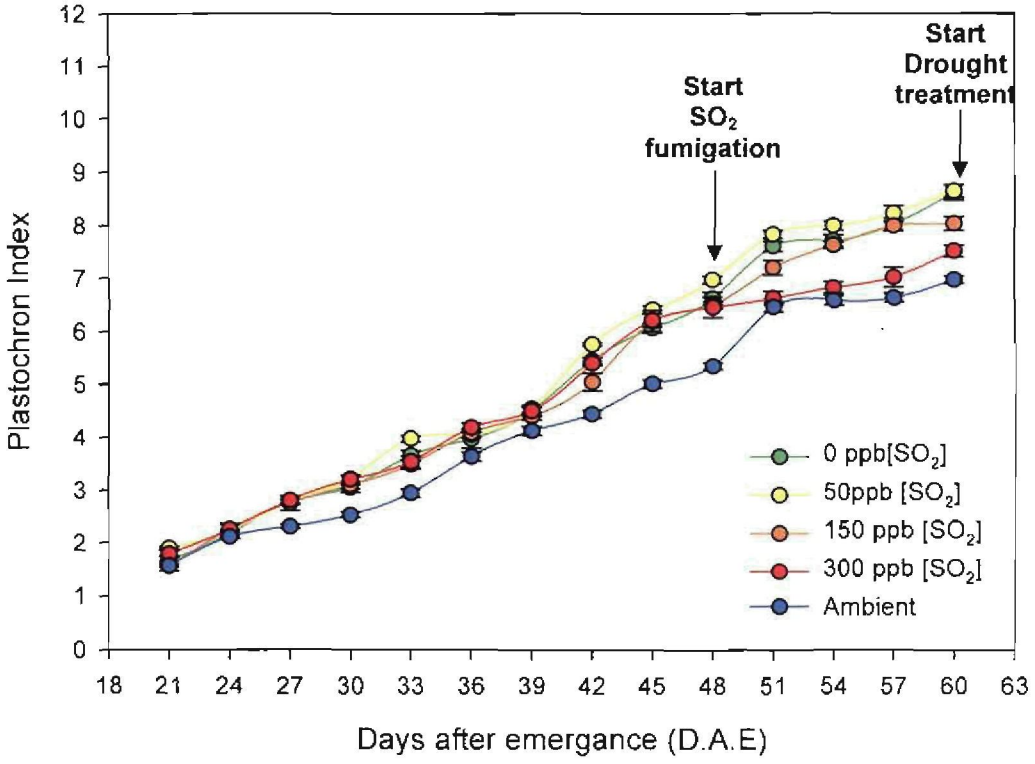


Figure 4.5 Figure 4.5 Plastochron index in *Glycine max* plants indicating that all plants that were grown in the OTCs were at the same stage of development before fumigation commenced. The arrow indicates the start of SO_2 fumigation (48 d.a.e). Each value represents a mean (±SE), where n = 8.

4.3.2 Foliar injury

Acute and/or chronic foliar SO_2 injury in *Brassica oleracea* appeared after 35 days of fumigation with SO_2. Chronic foliar injury was first seen as a greyish-green to dull green, water-soaked appearance which later developed into a marginal and or bifacial interveinal necrosis visible in plants treated with the highest SO_2 concentration (300 ppb) (Figures 4.6a and b). The necrotic areas became ivory to white-coloured upon drying, and became bleached (Figure 4.6c). The white-coloured necrotic symptoms appearing at the leaf margins and the bleached areas extended progressively toward the midrib with increasing severity (concentration and duration) of the SO_2 exposure. This colour symptoms were described (Barrett & Benedict, 1970) as acute symptoms for garden pea (*Pisum sativum*), which have been extensively studied over the years as peas are considered one of the most SO_2-sensitive plants. Although not very noticeable, chronic foliar injury was also visible at the lowest SO_2 (50 ppb) treatment which appeared as interveinal chlorosis with a somewhat silvery appearance. In addition, non-green pigmentation appeared in plants treated at the highest SO_2 concentration. This non-green pigmentation turned purplish with increasing SO_2 concentration and duration of the fumigation practice.

In *Glycine max* chronic foliar injury first occurred after 18 days of fumigation at the 150 ppb level and was most commonly seen as marginal and interveinal chlorosis (yellowing), with the affected areas remaining turgid (Figure 4.7 right). The interveinal chlorosis was more advanced on the older leaves than on the younger leaves (Figure 4.7 right). Acute SO_2 injury on leaves occurred after 28 days at the 300 ppb level, displaying typical whitish-tanned interveinal necrosis with slight dark pigmentation at the margins of the necrotic areas. Pigmentation was present before the necrotic areas appeared. Acute injury was seen as a light-brown necrosis progressing from the leaf edge. The injury became reddish-brown as the symptoms matured. The marginal and interveinal necrotic areas were pigmented, with various shades of brown or reddish-brown dominating (Figure 4.7 right). Acute foliar injury progressed with increasing SO_2 concentration and duration of the fumigation and was mostly visible at the highest (300 ppb) SO_2 treatment (Figure 4.8). Acute SO_2 injury at the time the leaves were expanding caused the leaves to have a distorted appearance (Figures 4.7 left and 4.9 right). Acute and chronic foliar injury symptoms were also present simultaneously. The basal leaflets showed both acute reddish-brown interveinal or dark-brown bifacial necrosis and interveinal marginal chlorosis, while the apical leaflets showed primarily interveinal chlorosis. Although

biotic and abiotic stresses such as drought stress and plant nutritional stress may be the cause of chlorotic and necrotic symptoms similar to that of chronic or acute SO_2 injury, most of the plants exhibited similar symptoms which were noticeable on both well watered and drought stressed plants.



Figure 4.6 Leaves of *Brassica oleracea* after 30 days of fumigation with SO_2 showing chronic foliar injury that developed into interveinal necrosis (a, b). Foliar injury symptoms became acute with increasing concentration and duration of the experiment to divulge white-coloured necrotic symptoms formed at the leaf margins, with bleached areas extending progressively toward the midrib (c).



Figure 4.7 Epinastic growth appearing in youngest leaves of plants exposed to 300 ppb SO_2 (left). Necrotic lesions and leaf thickening visible in fully expanded leaves on the 6th node on the main stem after 20 days of exposure to 300 ppb SO_2 (right).



Figure 4.8 Acute injury seen in fully expanded trifoliate leaves on the 5th node as whitish-tan interveinal necrosis that developed after 20 days exposure to 50 ppb (left), 150 ppb (middle) and 300 ppb SO_2 (right), respectively.



Figure 4.9 Epinasty visible in youngest leaves of plants exposed to 50 ppb SO_2 after 20 days (right) compared to leaves from the control (0 ppb) treatment (left).

4.3.3 Effect of SO_2 on the leaf ultrastructure of *Glycine max*

Figure 4.10 shows a chloroplast with the normal arrangement of grana- and stroma-thylakoids in a soybean leaf that was grown in SO_2-free air. Chloroplasts retained their original shape (Figure 4.10A). No re-arrangement of the internal membranes or changes in size and number of starch granules was observed in the control material. The electron microscopic observation depicted in Figure 4.11 and Figure 4.12 revealed ultrastructural changes that occurred after fumigation with 300 ppb SO_2. Changes in chloroplast shape, damage to internal membranes and damage to the thylakoids were the most notable changes that occurred after 35 days' fumigation with 300 ppb SO_2. Chloroplasts that initially appeared swollen (Figure 4.11) were further deformed (Figure 4.12E) and the arrangement of the internal membrane system was distorted. The chloroplasts appeared to be aggregated (Figure 4.11) and, in some cases, even fused with one another. In severely damaged mesophyll cells the chloroplast envelopes had almost completely disintegrated. It is not clear if the visible foliar injury might be associated with the ultrastructural changes, but the subsequent yellowing and occurrence of darkly pigmented spots on the leaves probably reflect loss of chlorophyll attendant on serious damage to the thylakoids (Figure 4.11B). Electron-dense material was noticeable in contact with or around broken chloroplasts (Figure 4.11C). The frequent appearance of the latter suggests the hypertonic status within the chloroplasts (Whatley, 1971). Sulphur dioxide produces super oxide, hydroxyl radical and other active oxygen species as a consequence of interactions with photosynthetic electron transport (Asada & Kiso, 1973). These active oxygen species may destroy the thylakoid components (Shimazaki *et al.*, 1980). The chloroplast has frequently been regarded as the primary site of many of the disturbances by SO_2 and its products formed in aqueous solution (Ziegler, 1975; Hällgren, 1982).

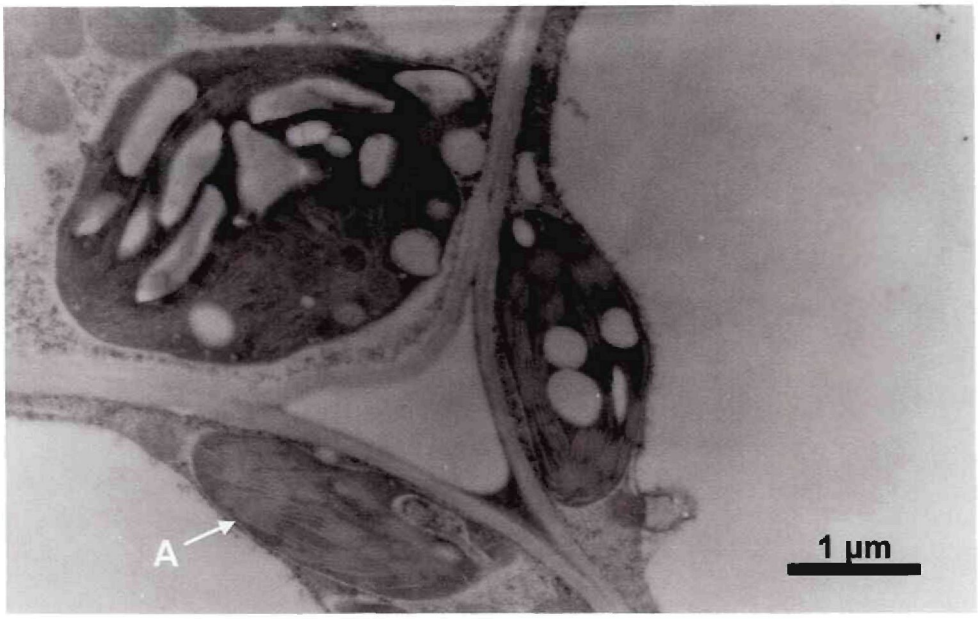


Figure 4.10 Transmission electron micrographs of adaxial mesophyll cells of *Glycine max* leaves grown in SO_2-free air showing normal chloroplasts in the control plants. Arrow A indicates that the control material retained its original shape as well as the normal arrangement of grana and stroma thylakoids within the chloroplast. Scale bar = 1 µm.

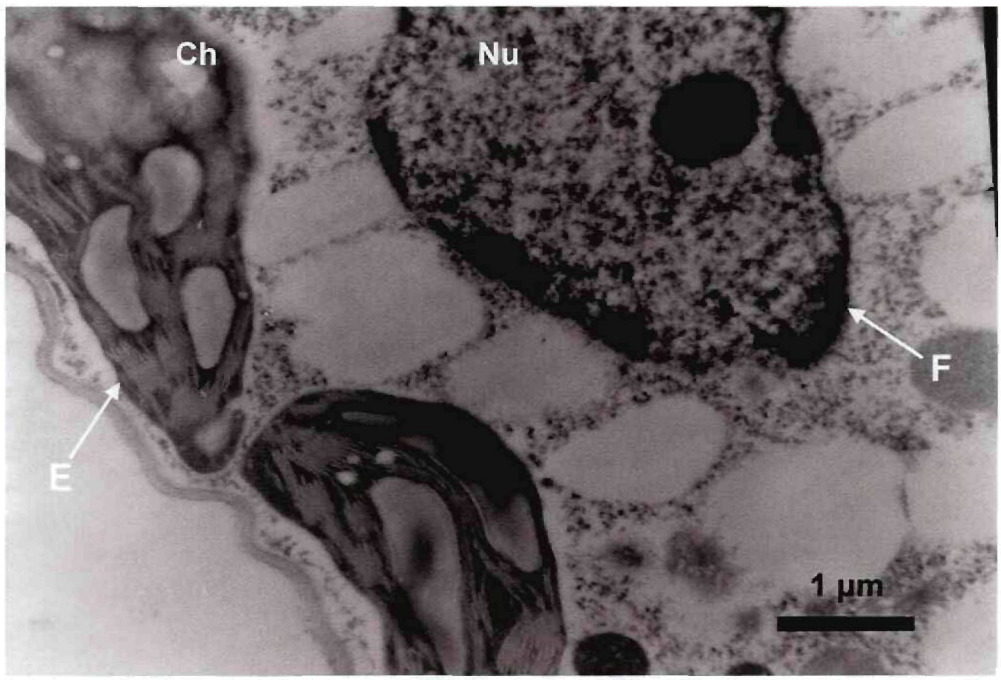


Figure 4.11 Electron micrographs of soybean fumigated with 300 ppb SO_2 after 35 days, where Ch = chloroplast; Nu = Nucleus; arrow E refers to the irregular shape attained by the chloroplasts after fumigation. Arrow F points to the collapse of the nucleus membrane. Scale bar = 1 µm.

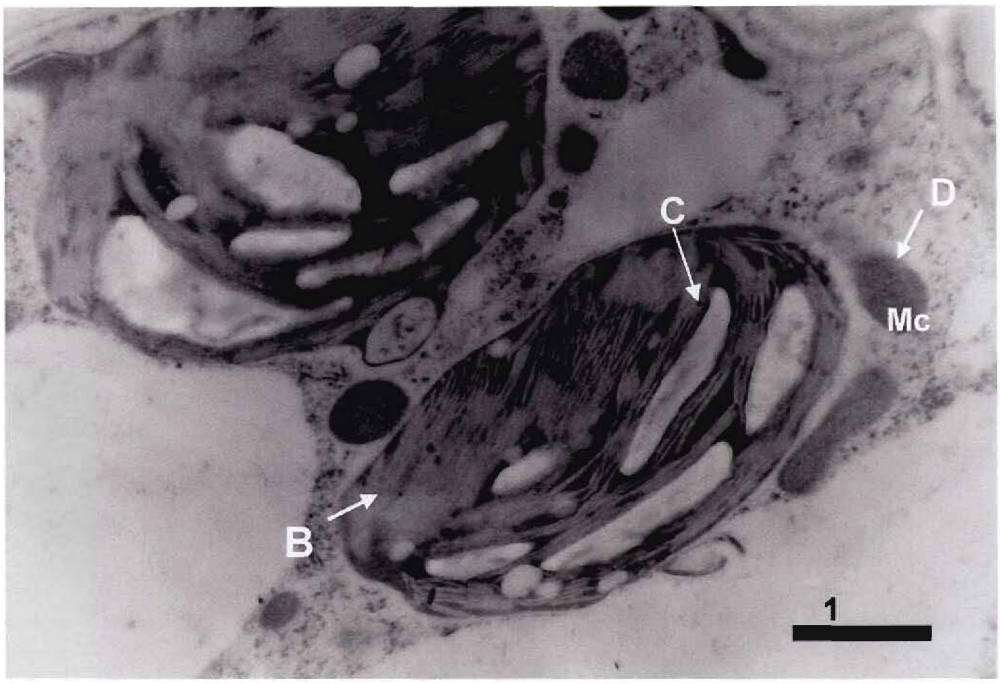


Figure 4.12 **Transmission electron micrograph of chloroplasts present in the adaxial mesophyll cells of *Glycine max* after 35 days fumigation with SO_2, where Mc = mitochondrion; arrow B points at distortion in the thylakoid and disintegration of the chloroplast envelopes and arrow C shows out electron dense material developing in the stroma. Arrow D points to a mitochondrion that appears electron dense.**

4.3.4 Biomass accumulation

4.3.4.1 Effect of SO_2 on biomass accumulation in *Brassica oleracea*

Biomass accumulation of *Brassica oleracea* was markedly affected after 21 days' fumigation with SO_2 (Figure 4.13). Total dry weight of plant organs measured at the final harvest was reduced by 4 %, 4 % and 12 % for 50, 150, and 300 ppb SO_2, respectively. Although not statistically significant, the well watered SO_2 treated plants displayed an increase of 7 % in the shoot dry mass at the lowest SO_2 treatment level of 50 ppb and a decrease of 15 % and 17 % at the 150 and 300 ppb treatments, respectively (Figure 4.13b). This was, however, not the case for the root dry mass. No increase was observed in root dry mass for the well watered SO_2 treated plants. Root dry mass decreased by 16 %, 6 % and 7 % for the 50, 150 and 300 ppb SO_2 treatments from the control plants. However, again not statistically significant, the effect of SO_2 on the shoot and root dry masses led to a stimulation of the shoot to root ratio at the 50 ppb and 150 ppb SO_2 treatments and an inhibition thereof at the

highest SO_2 concentration of 300 ppb. The response of dry mass of *Brassica oleracea* fumigated with SO_2 and simultaneously subjected to drought was severely reduced at all SO_2 treatment concentrations. Shoot dry mass was reduced by 17 %, 18 % and 28 % at the 50, 150 and 300 ppb SO_2 levels, respectively. Although not statistically significant, root dry mass was reduced more severely than shoot dry mass at the lowest treatment level, leading to stimulation in shoot to root ratio. Root dry mass was, however, higher at the intermediate and highest SO_2 treatment levels, resulting in inhibition of the shoot-to-root ratio at the 150 and 300ppb levels, respectively.

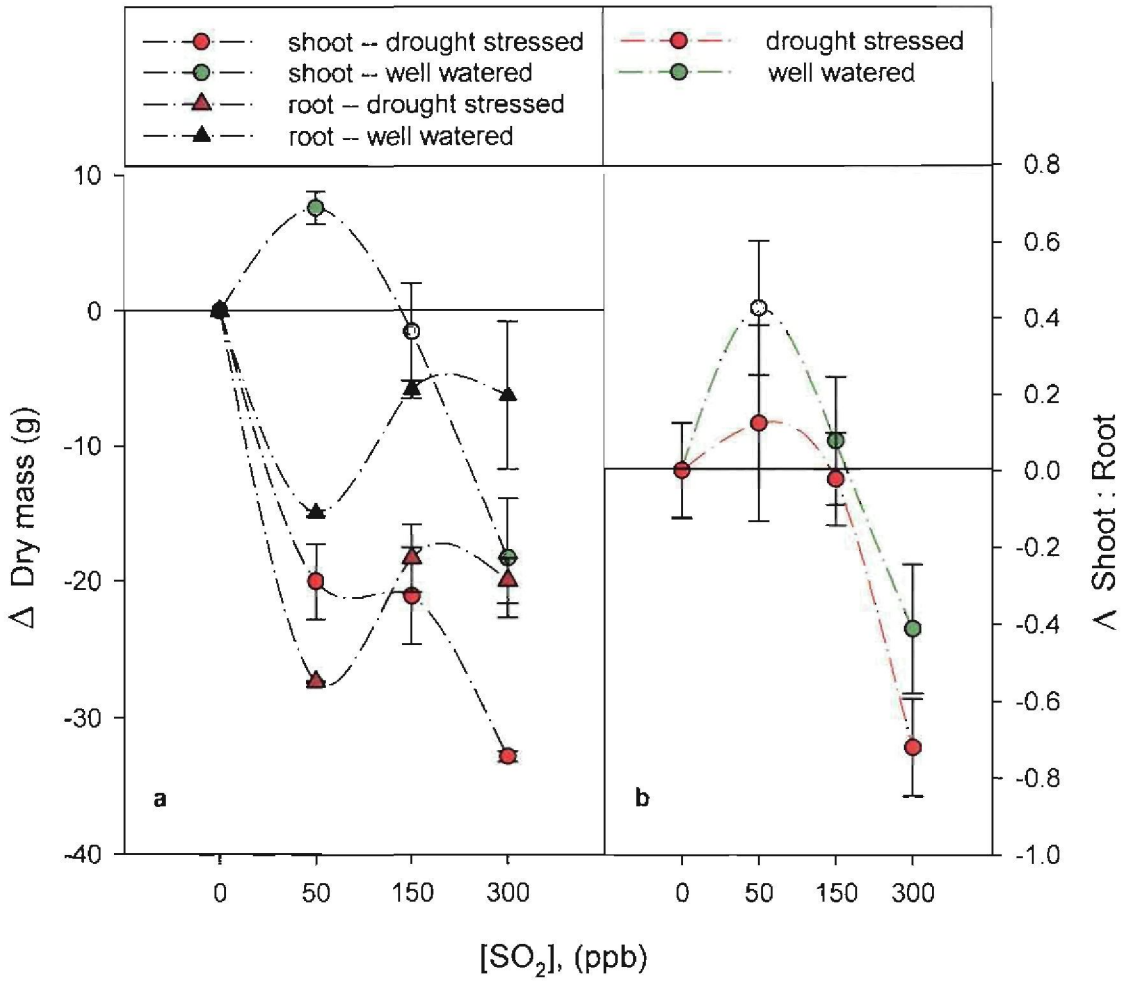


Figure 4.13 Effect of different levels of SO_2, alone and in combination with drought stress, on (a) shoot and root biomass accumulation in *Brassica oleracea* at the final harvest and (b) shoot-to-root ratio, relative to well watered plants grown in SO_2-free air. Each value represents a mean (±SE), where n = 8.

4.3.4.2 Effect of SO_2 on biomass accumulation in *Glycine max*

The vegetative response of *Glycine max* was evaluated from the parameters measured at the midseason harvest. The dry mass (g) of plant organs (i.e. shoots and roots) was markedly affected by SO_2 exposure (Figure 4.14). Plant total dry mass of the well watered plants were reduced by 12 %, 19 % and 23 % at the 50, 150, and 300 ppb SO_2 levels, respectively, compared to the control plants (Figure 4.14a). This decrease in dry mass is attributable to a decrease in both shoot and root mass. Shoot biomass production, however, decreased less than root biomass, leading to an increase in the shoot-to-root ratio (Figure 4.14b). This indicates that root biomass reductions occurred prior to that of shoot biomass reduction. This was, however, not the case for plants fumigated with SO_2 and simultaneously subjected to drought stress. SO_2 fumigation in combination with drought reduced total plant biomass production with 15 %, 32 % and 44 % at the 50, 150, and 300 ppb, respectively. This reduction was due to a reduction in both shoot and root dry mass. Shoot dry mass decreased more than the root biomass, resulting in a reduction in the shoot-to-root biomass (Figure 4.14). The decrease in total biomass was primarily due to a significant reduction in shoot biomass (Figure 4.14a). Shoot dry mass was reduced by 16 %, 42 % and 56 % for the 50, 150 and 300 ppb SO_2 levels, respectively, in plants subjected to drought stress. Although root dry mass was reduced by 14 %, 16 % and 22 % for the 50, 150 and 300 ppb SO_2 levels, respectively, root dry mass for the drought stressed and SO_2 treated plants was less affected than shoot biomass. This finding indicates that SO_2 fumigation with simultaneous drought stress inhibits shoot dry mass production before it affects root dry mass production. This phenomenon is also related to the large inhibition in the shoot-to-root ratio (Figure 4.14b).

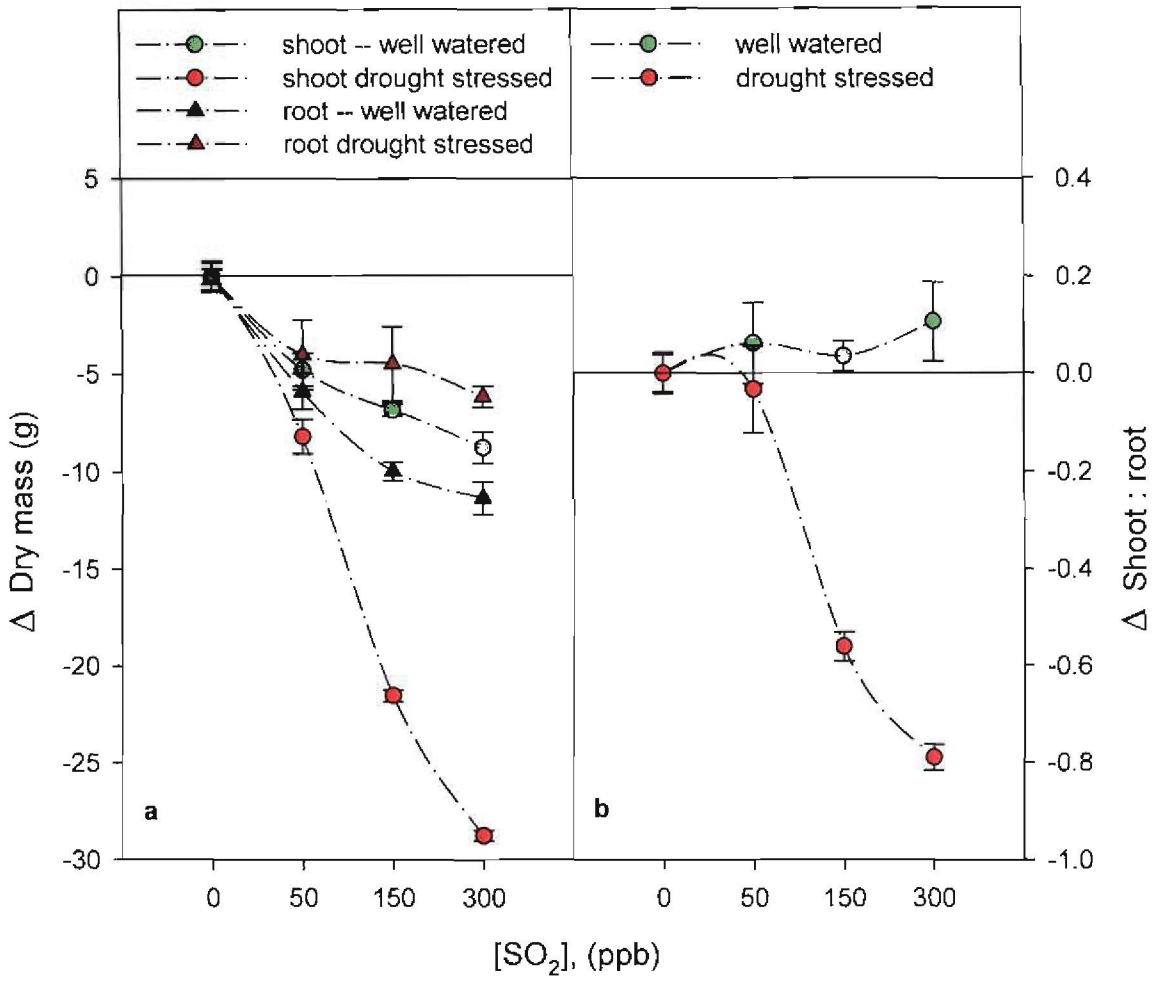


Figure 4.14 Effect of different levels of SO_2 alone and in combination with drought stress on (a) shoot and root biomass accumulation at the final harvest and (b) shoot-to-root ratio, relative to well watered plants grown in SO_2-free air in *Glycine max*. Each value represents a mean (±SE), where n = 4.

4.3.5 Yield attributes

4.3.5.1 Effect of SO_2 on yield production in *Glycine max*

Yield components at the final harvest after 85 days measured in well watered and drought stressed plants fumigated with different SO_2 concentrations were markedly suppressed (Tables 4.1 and 4.2). The number of pods per plant in the well-watered plants was reduced at all SO_2 treatments. The number of pods per plant decreased by 16 % and 37 % at the 150 and 300 ppb treatment level, but increased slightly (6 %) at the lowest treatment level. Pod weight decreased with increasing SO_2 concentration, namely 20 %, 23 %, and 25 % at the 50, 150, and 300 ppb SO_2 levels,

respectively. The same held true for the number of seeds per pod. The number of seeds per pod decreased markedly with 21 %, 24 % and 39 % for the 50, 150 and 300 ppb SO_2 concentrations, respectively. Even though SO_2 caused decreases in the above-mentioned yield components, an increase in individual seed weight occurred at the lowest and intermediate SO_2 concentrations. Although not significant, a 30 % reduction in individual seed weight was measured for the highest treatment level. All yield components decreased markedly when drought was introduced as a co-stress. Yield attributes decreased drastically with an increased SO_2 concentration, indicating the large effect elevated levels of SO_2 have on the plants when drought conditions prevail. Although not significant at all treatment levels used, the number of pods per plant decreased sharply by 38 %, 35 %, 47 % and 57 % at the 0, 50, 150 and 300 ppb SO_2 levels respectively, compared to the well watered plants fumigated with the respective SO_2 concentrations. Individual pod weight also decreased correspondingly with increasing SO_2 concentration. Individual seed weight decreased by 38 %, 42 %, 49 %, and 53 % at the 50, 150 and 300 ppb treatment levels respectively, compared to the well watered SO_2 fumigated plants. This decrease, however, was only significant at the 0 and 50 ppb treatments. The number of seeds per pod decreased by 21 %, 17 %, 8 % and 42 % at the 0, 50, 150 and 300 ppb treatment levels, respectively, compared to the corresponding well watered fumigated plants. Drought stress caused a 10 % reduction in individual seed weight of plants grown in SO_2-free air. Although not significant, fumigation in combination with drought stress suppressed individual seed weight with 11 %, 9 %, and 20 % at the 50, 150 and 300 ppb SO_2 levels, respectively, compared to the corresponding well watered fumigated plants. According to all parameters measured, except the number of immature pods in well watered and drought stressed plants, SO_2 fumigation had a significant effect. The number of immature pods per plant increased with increased SO_2 concentrations (results not shown). The number of pods and seeds per pod of the well watered plants was reduced significantly. Yield components of plants subjected to drought and fumigation simultaneously were reduced significantly. Drought stress caused a higher degree of immature pod abscission. No increase in the number and weight of the filled pods occurred at the lowest SO_2 level as was seen in the well watered plants treated at 50 ppb SO_2. Yield attributes of the well watered plants grown in SO_2-free air did not differ significantly from those of the controls. The number of pods per plant and individual pod weight were respectively 7 % and 18 % higher in plants grown in SO_2-free air as compared to ambient controls. The number of seed per pod increased by

6 % at the 0 ppb level, but individual seed weight at this level was nonetheless reduced with 6 % relative to the ambient grown plants.

Table 4.1 Vegetative and reproductive responses of well watered fumigated *Glycine max* (L.) Merr. cv. PAN 809 (soybean) plants measured at the midseason (after 67 days) and final harvests (after 110 days). The vegetative responses were measured from the midseason harvest and the reproductive responses were taken from the final harvest. Each response value is the mean of 8 plants (four plants in each of two open-top chambers), with * and ** indicating significant differences at $p<0.05$ and $p<0.01$ respectively, compared to control plants.

		0 ppb SO_2	50 ppb SO_2	150 ppb SO_2	300 ppb SO_2	Ambient Control
Vegetative response	Shoot dry wt. (g)	33.66 (0.42)	28.86 (0.83**)	26.82 (0.31**)	24.90 (0.81**)	42.39 (0.50)
	Root dry wt. (g)	53.71 (0.84*)	47.82 (0.92*)	43.75 (0.46**)	42.37 (0.85**)	51.5 (0.50*)
	Shoot : root	1.59 (0.42)	1.65 (0.83*)	1.63 (0.31**)	1.70 (0.81**)	0.82 (0.42)
Reproductive response	Pods / plant	147.3 (10.5)	155.5 (0.7)	123.6 (20.1)	93.5 (9.72**)	136.5 (6.8)
	Individual pod mass (g)	0.56 (0.04*)	0.45 (0.03*)	0.43 (0.04)	0.42 (0.05)	0.46 (0.03*)
	Seed / pod	3.3 (0.2)	2.6 (0.3)	2.5 (0.4*)	2.0 (0.2**)	3.1 (0.3)
	Individual seed mass (g)	0.161 (0.006**)	0.213 (0.003)	0.181 (0.005)	0.113 (0.016)	0.170 (0.08**)

Table 4.2 Vegetative and reproductive responses of drought stressed fumigated *Glycine max* (L.) Merr. cv. PAN 809 (soybean) plants measured at the midseason (after 67 days) and final harvests (after 110 days). The vegetative responses were measured from the midseason harvest and the reproductive responses were taken from the final harvest. Each response value is the mean of 8 plants (four plants in each of two open-top chambers), with * and ** indicating significant differences at $p<0.05$ and $p<0.01$ respectively, compared to control plants.

		0 ppb SO_2	50 ppb SO_2	150 ppb SO_2	300 ppb SO_2	Ambient Control
Vegetative response	Shoot dry wt. (g)	51.8 (0.38)	43.6 (0.88**)	30.3 (0.30**)	23.1 (0.27**)	53.5 (0.5)
	Root dry wt. (g)	28.3 (0.69*)	24.2 (1.8)	23.8 (1.9)	22.1 (0.5**)	55.0 (1.5*)
	Shoot : root	1.83 (0.38)	1.80 (0.88**)	1.27 (0.30**)	1.04 (0.27**)	2.2 (0.34)
Reproductive response	Pods / plant	91.5 (8.2)	95.0 (12.4)	82.0 (12.6)	39.8 (8.31*)	123.3 (9.2)
	Individual pod mass (g)	0.35 (0.04)	0.26 (0.08*)	0.22 (0.07*)	0.19 (0.07)	0.40 (0.04*)
	Seed / pod	2.6 (0.42)	2.15 (0.43)	2.3 (0.3)	1.17 (0.3)	2.6 (0.43)
	Individual seed mass (g)	0.145 (0.005)	0.190 (0.01**)	0.164 (0.007)	0.09 (0.01)	0.14 (0.01)

Although the pods of the well watered plants grown in SO_2-free air were much longer and contained more seeds per pod, the seeds were not as well developed as the seeds in pods of plants treated at 50 and 150 ppb SO_2 (Figure 4.15 - bottom). Most seeds of plants treated at the lowest and intermediate SO_2 concentrations matured earlier than seeds of plants treated at 300 ppb SO_2. Fumigated plants subjected to drought stress had smaller pods; the seeds of the 0, 50 and 150 ppb treatments,

however, were heartier, while most pods of plants treated at 300 ppb SO_2, contained only one seed or were completely immature (Figure 4.15 - top).

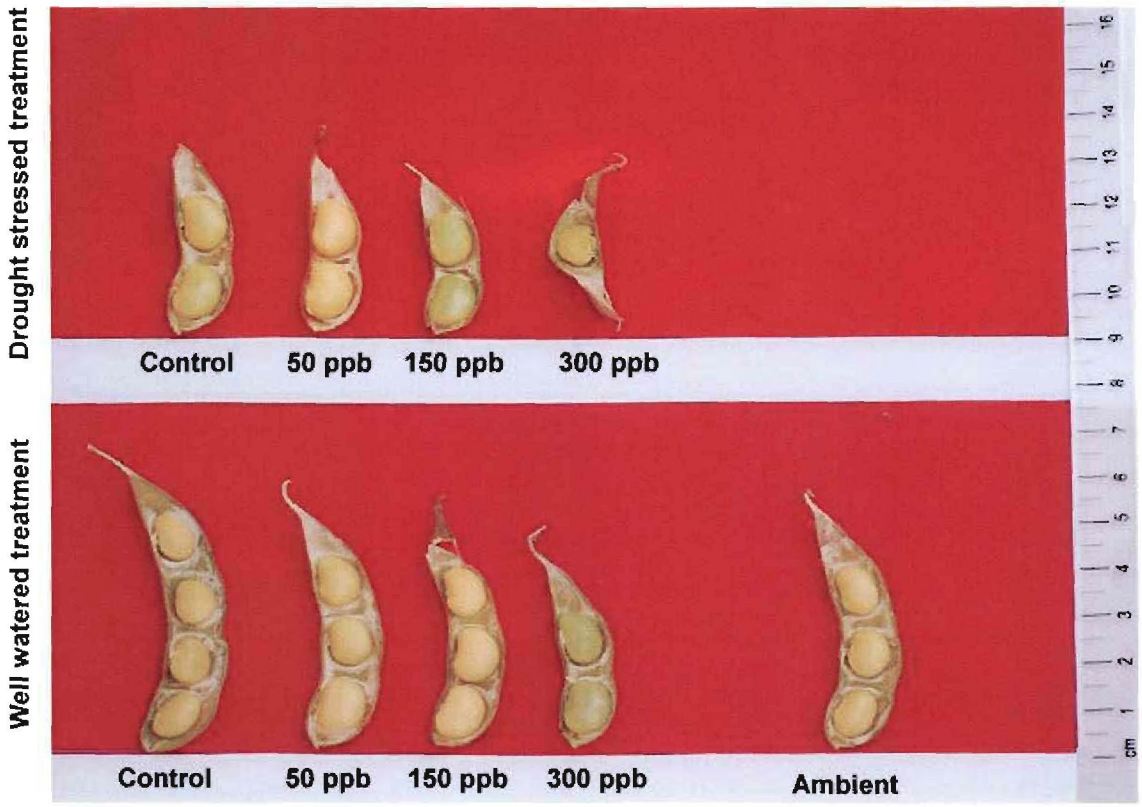


Figure 4.15 **Seed development inside pods of *Glycine max* after 85 days of treatment at different SO_2 concentrations and simultaneously subjected to drought stress (top) and in fumigated plants kept close to field capacity (bottom).**

4.3.6 Chlorophyll content index (CCI)

4.3.6.1 Effect of SO_2 on chlorophyll content index (CCI) in *Brassica oleracea*

The effect of SO_2 on the chlorophyll concentration (Figures 4.16a and b) might help to explain the inhibition of photosynthesis. Although the chlorophyll concentration of the SO_2 fumigated plants was not lower than at the onset of the fumigation experiments (day 0) indicating that no chlorophyll degradation occurred, it could provide information on the changes the different SO_2 concentrations exerted on the plants. SO_2 fumigation caused a concentration dependant decrease in the chlorophyll content index (CCI) of the older leaves of *Brassica oleracea*. The CCI

decreased by 24 %, 30 % and 33 % in well watered plants fumigated for 50 days at 50, 150 and 300 ppb SO_2 respectively, compared to the well watered control plants (Figure 4.16a). When plants were fumigated with SO_2 and subjected to drought stress, CCI increased by 21 % at the 50 ppb level, after which it decreased by 19 % and 25 % at the 150 and 300 ppb levels, respectively, compared to the control plants subjected to drought (Figure 4.16b).

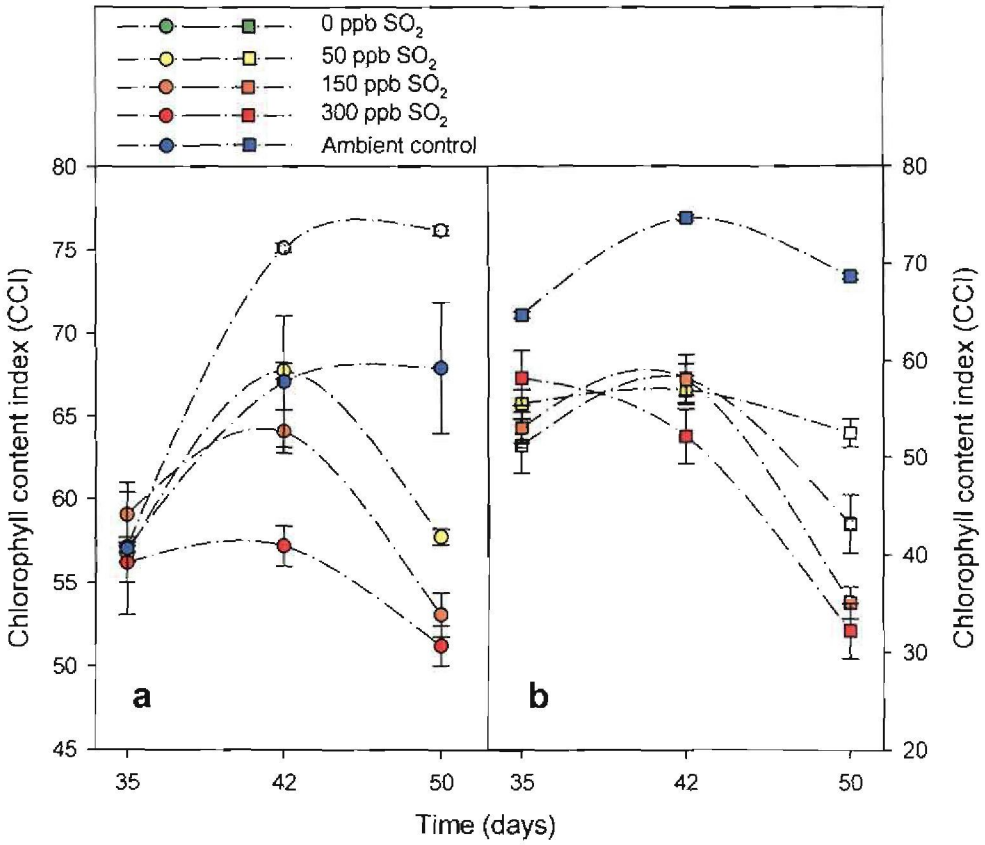


Figure 4.16 The effect of SO_2 fumigation on the chlorophyll content index measured in the 5th leaf of the main stem after 35, 42 and 50 days of treatment in well watered (a) and drought stressed (b) *Brassica oleracea*.

4.3.6.2 Effect of SO_2 on chlorophyll content index (CCI) in *Glycine max*

A strong concentration dependant decrease in CCI for well watered and drought stressed plants were evident after 35 days (Figures 4.17a and b). CCI decreased by 8 %, 9 % and 1 % in 50, 150 and 300 ppb levels respectively in well watered plants

when compared to the control (Figure 4.17a). For plants grown in the presence of drought and fumigated with SO_2, CCI decreased by 2 %, 10 % and 18 % at the 50, 150 and 300 ppb levels, respectively, compared to drought stressed control plants (Figure 4.17b). Exposure to SO_2 reduced the chlorophyll content of older leaves (i.e. leaves situated on the 3rd node) in both well watered and drought stressed plants, implying an SO_2-induced premature senescence. Characteristic necrosis was observed at the beginning of the second week after fumigation commenced of the plants receiving 150 and 300 ppb SO_2. There was a significant difference between *Brassica oleracea* and *Glycine max* plants, with leaves of the *Glycine max* plants having a lower overall CCI than *Brassica oleracea*.

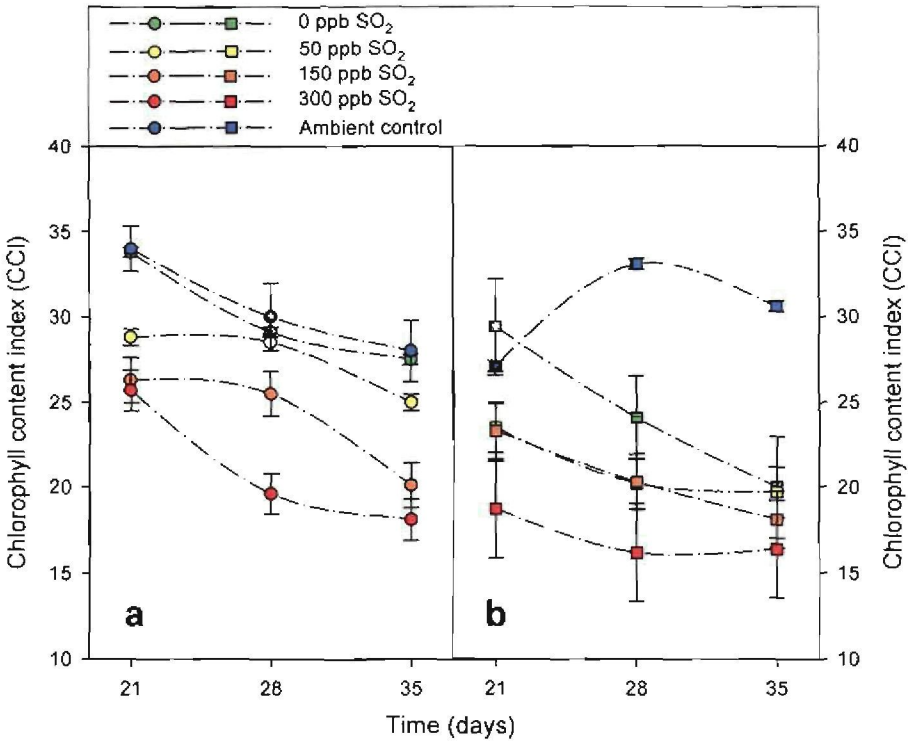


Figure 4.17 The effect of SO_2 fumigation on the chlorophyll content index measured in the 5th leaf of the main stem after 35, 42 and 50 days of treatment in well watered (a) and drought stressed (b) *Glycine max*.

4.3.7 Effect of SO_2 on the nodule ureide content in *Glycine max*

Figure 4.18 depicts the ureide catabolism in soybean nodules after 28 days' fumigation with SO_2 and shows the concentration dependant decrease in ureide content. After 28 days' fumigation with SO_2, nodule ureide content in well watered plants decreased by 28 %, 40 % and 60 % at the 50, 150 and 300 ppb levels,

respectively, compared to the control. In drought stress plants fumigated with SO_2, the ureide content decreased to more than half of that measured in the well watered control plants. Drought stressed caused nodule ureide content to decrease by 25 %, 17 % and 29 % at the 50, 150 and 300 ppb concentrations, respectively, compared to the drought stressed control plants. The nodule ureide content measured in ambiently grown plants did not vary much from the chambered control plants, indicating that the chamber had very little to almost no effect on the symbiotic nitrogen fixation in the potted plants.

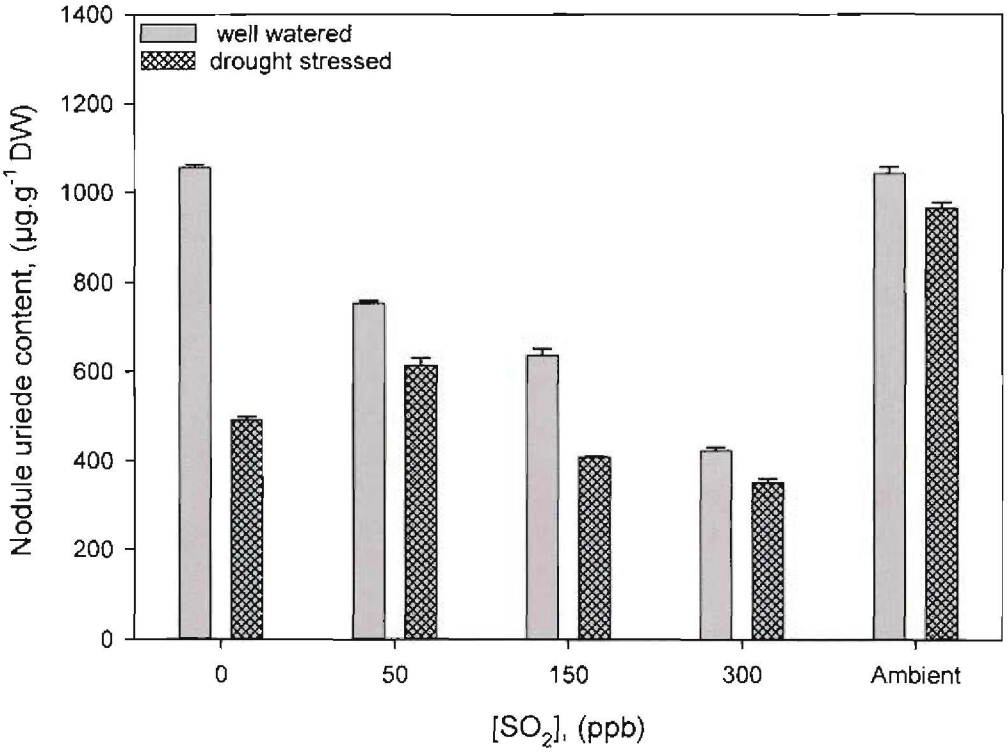


Figure 4.18 Effect of SO_2 fumigation separately and in combination with drought stress on the root nodule ureide content determined after 35 days of fumigation.

4.3.8 Effect of SO_2 on *in vitro* Rubisco activity in *Glycine max*

The results depicted in Figure 4.19 demonstrate that the exposure to different SO_2 concentrations over the entire growth season directly affected the activity of Rubisco, the key enzyme catalysing the carboxylation reactions. The activity of Rubisco activase was determined by measuring the activation state (initial activity) of Rubisco. This measurement provides a valid estimate of the photosynthetic activity of the leaf

because the activation state of Rubisco in the light is a direct consequence of the activity of Rubisco activase (Walker & Osmond, 1986). The total activity displays the activity of the fully carbamylated Rubisco. Studies conducted to illustrate the effects of SO_2 on CO_2 fixation in plants revealed the inhibitory effects SO_3^{2-}. Ziegler (1972) showed that this effect is due to competition between CO_2 and SO_3^{2-} for the active sites of the enzyme ribulose 1,5-bisphosphate carboxylase (Rubisco), central to photosynthetic CO_2 fixation. Higher concentrations of SO_3^{2-} resulted in non-competitive inhibition of the enzyme. Considering this, one could assume that the effect of SO_2 in combination with elevated CO_2 as expected in the coming years could result in decreased sensitivity to SO_2 injury.

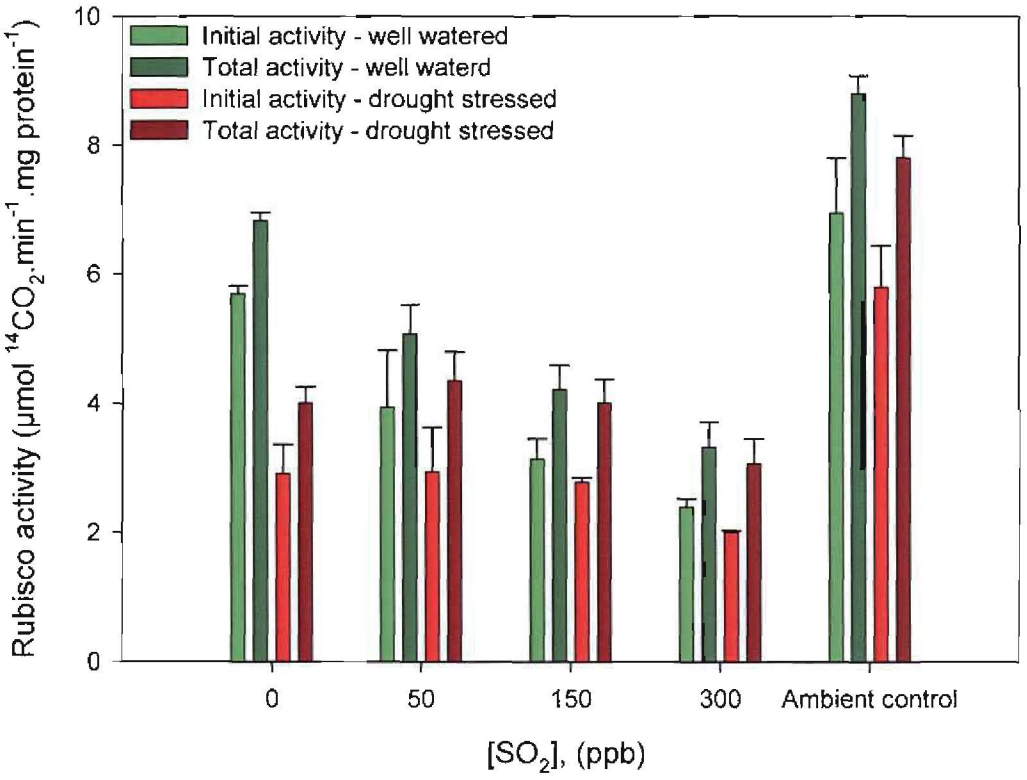


Figure 4.19 **Initial and total Rubisco activity measured in *Glycine max* after 28 days' exposure to different SO_2 concentrations. Green bars represent the initial and total Rubisco activities for well watered plants, while red bars represent the initial and total activities of plants subjected to drought stress. Each value represents the mean of 2 replicates (n = 2) with Rubisco activity expressed as activity µmol CO_2 fixed per minute per milligram protein.**

4.4 Physiological response parameters

4.4.1 Effect of SO_2 on photosynthetic gas exchange in *Brassica oleracea*

For the purpose of determining the response of *Brassica oleracea* to SO_2, numerous parameters, deduced from the $A:C_i$ response curve, were evaluated to compare and characterise the status of the photosynthetic apparatus. SO_2-induced stress caused a very pronounced decrease in the CO_2 assimilation rate at C_i = 350 $\mu mol.mol^{-1}$ (A_0) *after only 35 days' fumigation (Table 4.3; Figure 4.20).* A_0 *decreased with increasing* SO_2 concentration by 22 %, 48 % and 49 % for the 50, 150 and 300 ppb SO_2 levels, respectively. This drastic inhibition of CO_2 assimilation capacity could be ascribed to decreases in the CO_2 saturated rates of photosynthesis (J_{max}), which suggests that SO_2 had an inhibitory effect on the regeneration capacity of RuBP (Figure 4.3.1.1). J_{max} decreased by 9 %, 21 % and 36 % for the 50, 150 and 300 ppb SO_2 levels, respectively. Carboxylation efficiency (CE; slope of the $A:C_i$ response curve at $C_i \leq$ 200 $\mu mol.mol^{-1}$), which is a sensitive indicator of *in vivo* Rubisco activity, was inhibited in excess of 30 %, pointing towards severe mesophyll limitation of photosynthesis. The reduction was even greater after 7 weeks' fumigation, despite the use of a physiological younger leaf, which had been exposed for a shorter period *(Figure 4.20). At an ambient* CO_2 *concentration* (C_a = 350 $\mu mol.mol^{-1}$), Ci_{350} *values in* plants fumigated with 50, 150 and 300 ppb SO_2 remained fairly similar to values recorded at the beginning of the experiment, and were shown to have slightly increased CO_2 concentrations after 35 days' fumigation. Ci_{350} increased by 7 % at the 50 and 150 ppb SO_2 concentration levels and decreased by 35 % at the 300 ppb SO_2 level, while the relative stomatal limitation decreased by 8 %, 11 % and 98 % for the 50, 150 and 300 ppb SO_2 levels, respectively compared to the control (Table 4.3). The supply function which is related to the stomatal conductance at C_a = 350 $\mu mol.mol.^{-1}$ (Gs_{350}) increased with increasing SO_2 concentrations compared to the control (Figure 4.20). Gs_{350} increased by 44 %, 86 % and 99 % for the 50, 150 and 300 ppb SO_2 levels, respectively, compared to the control - corroborating the idea *that inhibition in photosynthesis is mainly due to severe mesophyll limitation. Apart* from the increased stomatal conductance, a concomitant increase in transpiration rate was notable. The transpiration rate at C_a = 350 $\mu mol.mol^{-1}$ (E) increased by 57 %, 77 % and 37 % at the 50, 150 and 300 ppb SO_2 levels, respectively, compared to the control. The increase in E caused an overall reduction in the water use efficiency (WUE) of 66 %, 46 % and 33 % for the respective treatments, even when Ci_{350} was shown to have slightly increased. This reduction in WUE could be explained by the

direct or indirect effect of SO_2 on the stomata and could be detrimental for crops growing under drought near or in the vicinity of SO_2 sources as often occurs on the South African Highveld near petrochemical or electrical power-plants.

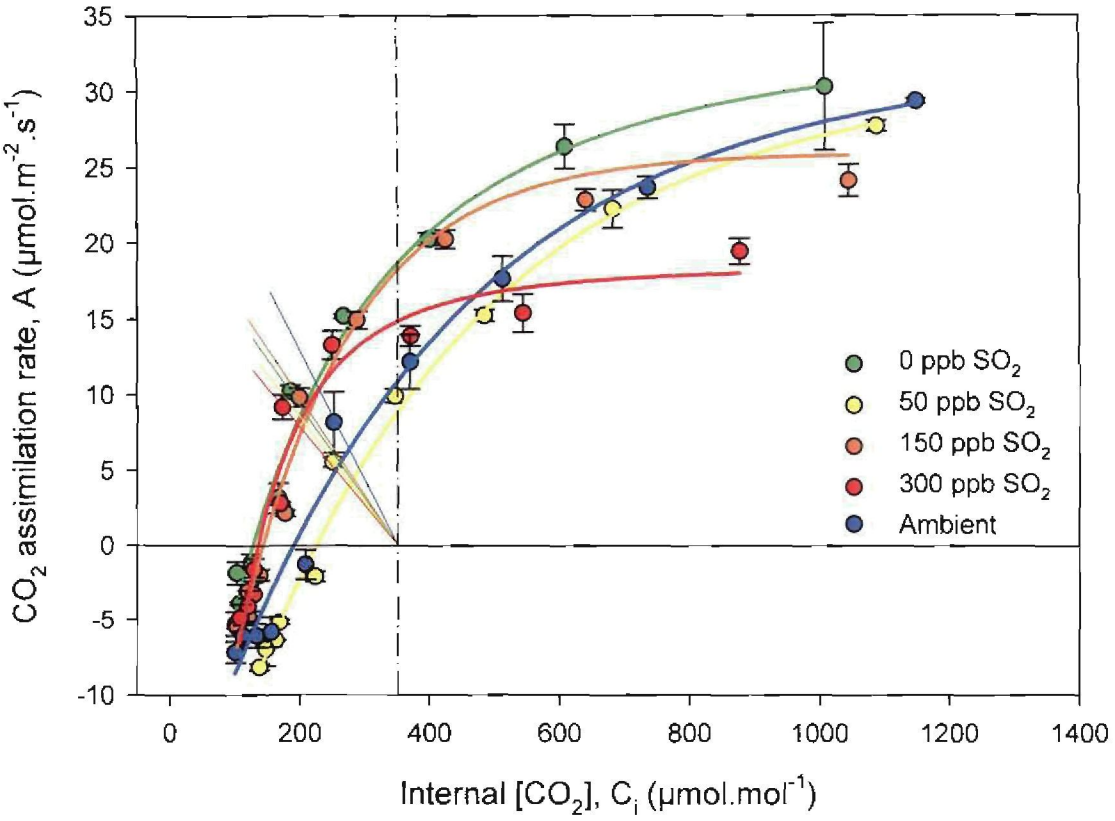


Figure 4.20 CO_2 assimilation rate as a function of intercellular CO_2 concentration of intact well watered leaves of *Brassica oleracea* plants after 35 days' exposure to elevated SO_2 concentrations of 50, 150 and 300 ppb. The 0 ppb SO_2 treatment served as the control. Each value represents a mean (± SE) where n = 2.

Table 4.3 Mean values (± standard errors) of gas exchange parameters measured in well watered leaves of *Brassica oleracea* (n = 2 plants per SO_2 treatment) 35 days after SO_2 fumigation commenced. Symbols: A_{350}, rate of CO_2 assimilation at C_a = 350 µmol.mol^{-1}; Ci_{350}, intercellular CO_2 concentration at C_a = 350 µmol.mol^{-1}; A_0, rate of CO_2 assimilation at C_i = 350 µmol.mol^{-1}; Gs_{350}, stomatal conductance at C_a = 350 µmol.mol^{-1}; CE, carboxylation efficiency at Γ; J_{max}, maximum rate of CO_2 assimilation; Γ, CO_2 compensation concentration; ℓ, percentage stomatal limitation of photosynthesis; WUE, water use efficiency, with * and ** indicating significant differences at $p<0.05$ and $p<0.01$, respectively, compared to control plants.

	0 ppb SO_2	50 ppb SO_2	150 ppb SO_2	300 ppb SO_2	Ambient Control
E (mmol.m^{-2}.s^{-1})	1.7 (0.29*)	2.6 (0.24*)	2.9 (0.34)	2.3 (0.01)	4.3 (0.15)
A_{350} (µmol.m^{-2}.s^{-1})	10.2 (0.67*)	5.5 (0.74)	9.8 (4.33)	9.2 (1.80)	8.2 (0.54)
Ci_{350} (µmol.mol^{-1})	186.5(0.35)	252.0 (3.76*)	200.0 (6.54)	174.0 (1.28*)	253.0(9.34)
A_0 (µmol.m^{-2}.s^{-1})	19.0 (0.73*)	9.6 (0.56)	9.9 (0.56)	14.9 (0.56)	13.9 (0.43)
Gs_{350} (µmol.m^{-2}.s^{-1})	79.0 (0.54)	147.0 (0.63)	157.0 (0.68*)	113.5 (0.55)	197.5(0.64*)
CE (mol.m^{-2}.s^{-1})	0.091(0.07*)	0.062 (0.08)	0.105 (0.06)	0.133 (0.04)	0.050(0.43)
J_{max} (µmol.m^{-2}.s^{-1})	30.3 (0.61)	27.7 (0.51)	24.1 (0.67)	19.4 (0.87*)	29.4 (1.23)
Γ (µmol.mol^{-1})	129.1(4.32*)	217.3 (1.23)	220.2 (4.39**)	136.5 (5.43)	193.8(3.21)
ℓ (%)	46.3 (3.42)	42.7 (5.06)	1.0 (4.33)	98.9 (1.22)	41.4 (2.63)
WUE (mmol.mol^{-1})	6.1 (3.23)	2.1 (0.93**)	3.3 (6.32)	4.1 (10.43)	1.9 (0.76)

In response to SO_2, the photosynthetic rate of *Brassica oleracea* was reduced to almost half the rate measured in control plants. Nevertheless, when drought stresses were introduced in combination with SO_2, the photosynthetic rate was reduced even more than in that of the well watered plants (Table 4.4; Figure 4.21). The CO_2 assimilation rate at C_i =350 $\mu mol.mol^{-1}$ (A_0) decreased by 39 %, 51 % and 91 % at the 50, 150 and 300 ppb SO_2 levels compared to the control plants (Figure 4.21). From the analysis of variations in A in response to changes in C_i, it appears that SO_2 may reduce either the activity or concentration of Rubisco by about 36 % for the 300 ppb SO_2-treated plants compared to the control plants subjected to drought stress. Apart from the reduction in J_{max}, SO_2 also caused the carboxylation efficiency (CE) to decrease corroborating the assumption that SO_2 caused a decrease in the *in vivo* activity of Rubisco. CE decreased by 94 % at the 50 and 150 ppb treatment level and 96 % at the 300 ppb SO_2 concentration. The transient nature of the depression of A already mentioned suggests that a reduction in Rubisco activity was a more likely explanation for a short-term change in A, rather than a change in the amount of RuBP (data not shown). Correspondingly, the compensation concentration (Γ) increased, corroborating the decrease in CE, suggesting that limitations within the mesophyll caused the observed response of photosynthesis to SO_2. The intercellular CO_2 concentration at C_a = 350 $\mu mol.mol^{-1}$, (Ci_{350}) remained constant at the 50 ppb but increased by 17 % and 46 % at the 150 and 300 ppb SO_2 concentrations, respectively, compared to the control. This increase in Ci_{350} emphasises the fact that reductions in A were not due to stomatal constraints, but rather due to constraints within in the mesophyll processes. This increase in Ci_{350} occurred despite the decrease in Gs_{350} (Figure 4.22). Stomatal conductance (Gs_{350}) remained the same at the 50 ppb SO_2 level, but decreased by 53 % and 63 % at the 150 and 300 ppb SO_2 concentration, respectively, compared to the control. However, the calculated percentage of stomatal limitation (ℓ), suggests that reductions in A could also resulted due to stomatal closure. ℓ increased by 8 %, 20 % and 6 % at the 50, 150 and 300 ppb SO_2 concentrations, respectively, compared to the control. SO_2 also decreased the water use efficiency (WUE) of the SO_2 treated plants by 72 %, 67 % and 86 % for the 50, 150 and 300 ppb SO_2 concentrations, respectively, compared to the control plants subjected to drought stress. This decrease in WUE occurred in spite of a reduction in the transpiration rate (E) (Table 4.4). E decreased by 10 %, 48 % and 95 % at the 50, 150 and 300 ppb SO_2 concentrations compared to the control plants subjected to drought stress.

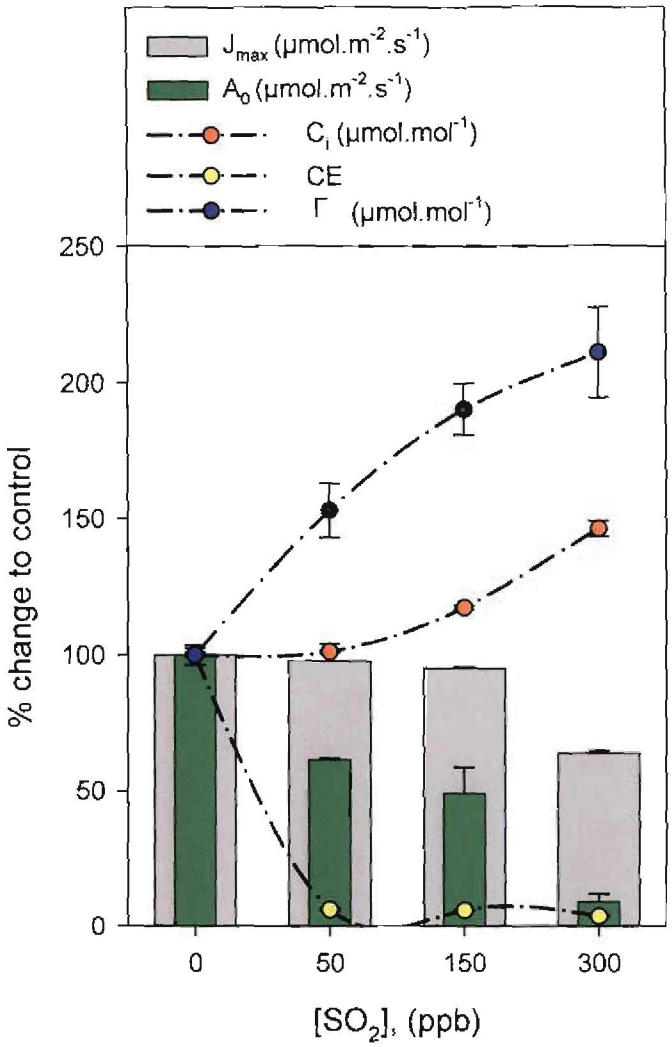


Figure 4.21 **The effect of SO_2 on photosynthetic response parameters measured in drought stressed *Brassica oleracea* after 35 days' fumigation with SO_2. The parameters indicating the broadened effect mesophyll limitation induced in A upon exposure to SO_2. Note the sharp increase in both Γ and Ci_{350}. It appears that photosynthetic reductions resulted from the direct effect of SO_2 upon the photosynthetic processes, rather than any effect on stomatal closure and subsequent reductions of CO_2 movement into the leaf. It seems as if stomatal closure could have resulted from a build-up of CO_2 in the intercellular spaces, due to the photosynthetic depression. The 0 ppb SO_2 treatment served as the control. Each value represents a mean (± SE) where n = 2.**

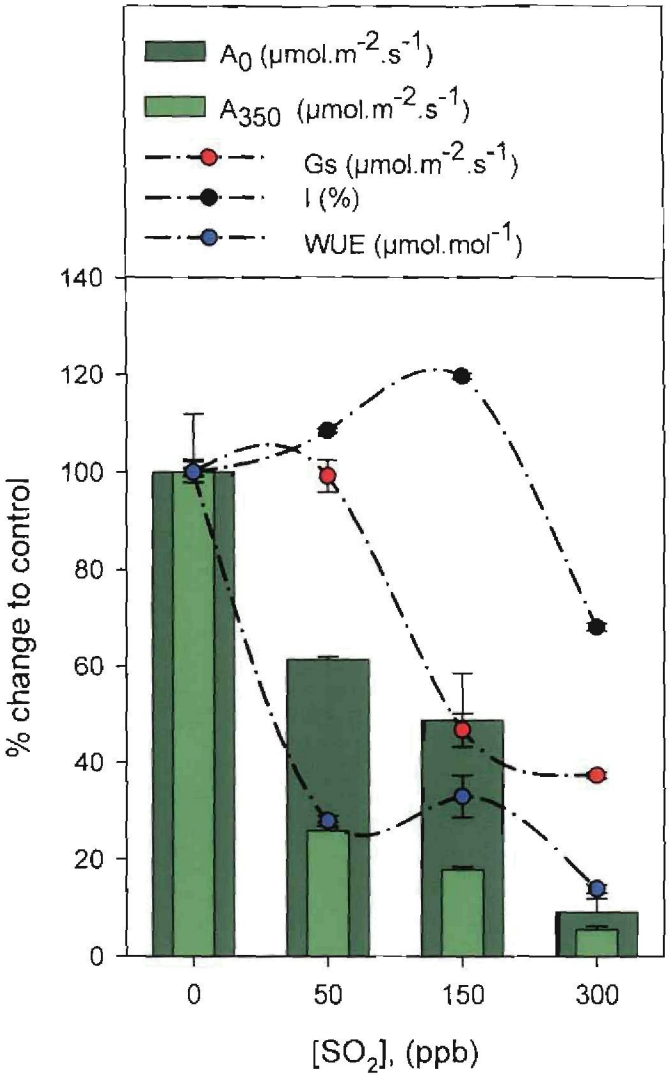


Figure 4.22 The effect of SO_2 exposure on photosynthetic response parameters after 35 days' exposure to 50, 150 and 300 ppb SO_2. The parameters indicate the limitations imposed by stomatal resistance on A. Note the sharp reduction in WUE, explaining the far-reaching effect on the photosynthetic rate in crop plants grown under water deprivation and exposed to SO_2 concentrations as low as 50 ppb. The 0 ppb SO_2 treatment served as the control. Each value represents a mean (± SE) where n = 2.

Table 4.4 Mean values (± standard errors) for gas exchange parameters measured in drought stressed leaves of *Brassica oleracea* (n = 2 plants per SO_2 treatment) 35 days after SO_2 fumigation commenced. Symbols: A_{350}, rate of CO_2 assimilation at C_a = 350 $\mu mol.mol^{-1}$; Ci_{350}, intercellular CO_2 concentration at C_a = 350 $\mu mol.mol^{-1}$; A_0, rate of CO_2 assimilation at C_i = 350 $\mu mol.mol^{-1}$; Gs_{350}, stomatal conductance at C_a = 350 $\mu mol.mol^{-1}$; CE, carboxylation efficiency at Γ; J_{max}, maximum rate of CO_2 assimilation; Γ, CO_2 compensation concentration; ℓ, percentage stomatal limitation of photosynthesis; WUE, water use efficiency, with * and ** indicating significant differences at $p<0.05$ and $p<0.01$ respectively, compared to control plants.

	0 ppb SO_2	50 ppb SO_2	150 ppb SO_2	300 ppb SO_2	Ambient Control
E ($mmol.m^{-2}.s^{-1}$)	2.1 (1.21*)	1.9 (0.17)	1.1 (0.003**)	0.1 (0.13)	4.1 (0.7*)
A_{350} ($\mu mol.m^{-2}.s^{-1}$)	16.3 (11.8)	4.2 (1.8*)	2.9 (0.61*)	0.9 (0.75)	4.4 (6.5)
Ci_{350} ($\mu mol.mol^{-1}$)	162.5 (0.54*)	164.5 (0.34)	190.5 (0.67)	237.5 (2.89)	203.5 (1.08*)
A_0 ($\mu mol.m^{-2}.s^{-1}$)	8.8 (2.52)	5.4 (0.56*)	4.3 (9.65)	0.8 (2.85)	5.5 (0.97)
Gs_{350} ($\mu mol.m^{-2}.s^{-1}$)	95.1 (2.12)	94.3 (3.21)	44.5 (3.45)	35.5(0.65*)	188.2 (0.36)
CE ($mol.m^{-2}.s^{-1}$)	0.701(0.03)	0.043 (0.53*)	0.041 (0.12)	0.026 (0.35**)	0.045(0.46)
J_{max} ($\mu mol.m^{-2}.s^{-1}$)	17.7 (1.09*)	17.3 (6.3)	16.8 (0.64)	11.3 (0.97*)	23.6 (6.46)
Γ ($\mu mol.mol^{-1}$)	134.0(3.56)	205.0 (10.07*)	255.0(9.46)	283.0 (16.54*)	247.0(7.45)
ℓ (%)	-86.3 (0.87)	22.1 (0.46)	33.3 (0.65)	-18.8 (0.76)	20.1 (0.21)
WUE ($mmol.mol^{-1}$)	7.9 (0.64)	2.2 (1.03*)	2.6 (4.32)	1.1 (0.87)	1.0 (0.98*)

Repeated chronic exposure of *Brassica oleracea* to SO_2 at different concentrations indicated that the rate of photosynthesis decreased with increasing SO_2 concentration and decreased overall with the duration of the fumigation practice (Table 4.5; Figure 4.23). The CO_2 assimilation rate at C_i = 350 $\mu mol.mol^{-1}$ (A_0) decreased with increasing SO_2 concentration. A_0 decreased by 6 %, 25 % and 38 % at 50, 150 and 300 ppb SO_2 concentrations, respectively. Similar to A_0, the CO_2 assimilation rate at C_i = 350 $\mu mol.mol^{-1}$ (A_{350}) also decreased by 6 %, 29 % and 32 % at 50, 150 and 300 ppb SO_2 concentrations compared to the control. A depression of the CO_2 saturation level (J_{max}), which indicates a reduction in the RuBP regeneration capacity, was more pronounced with increased SO_2 treatment concentration. J_{max} decreased by 10 %, 37 % and 42 % at the 50, 150 and 300 ppb SO_2 concentrations, respectively, compared to the control plants. CE, which is a sensitive indicator of *in vivo* Rubisco activity, decreased by 3 %, 38 % and 10 % for 50, 150 and 300 ppb SO_2 levels, respectively, compared to the control plants. On the other hand, the supply function, which is related to stomatal conductance, shows that Gs_{350} increased by 36 %and 25 % at 50, 150 SO_2 levels and decreased by 38 % at the 300 ppb SO_2 level, indicating that changes in stomatal response to SO_2 may partially account for reductions in A. This suggests that in addition to Gs, biochemical changes in the mesophyll were also limiting carbon acquisition at the greatest SO_2 concentration. This finding is corroborated by reduction in the stomatal limitation (ℓ). ℓ decreased by 15 %, 18 % and 8 % at the 50, 150 and 300 ppb SO_2 levels, compared to control plants. Further, the CO_2 compensation concentration (Γ) increased for all SO_2 treatment levels, corroborating the idea that reductions in A were mainly due to the effect of SO_2 on components of the mesophyll. Γ increased by 18 %, 4 % and 5 % for the 50, 150 and 300 ppb SO_2 concentrations, respectively, compared to the control plants. As mentioned previously, SO_2 can influence the WUE of plants by the direct or indirect action on the stomata. The WUE decreased with increasing treatment concentration by 17 %, 49 % and 50 % at the 50, 150 and 300 ppb SO_2 treatments, respectively, compared to the control plants. The decrease in WUE could be due to enhanced Gs leading to increases in E of 26 %, 39 % and 31 % at the respective treatment levels.

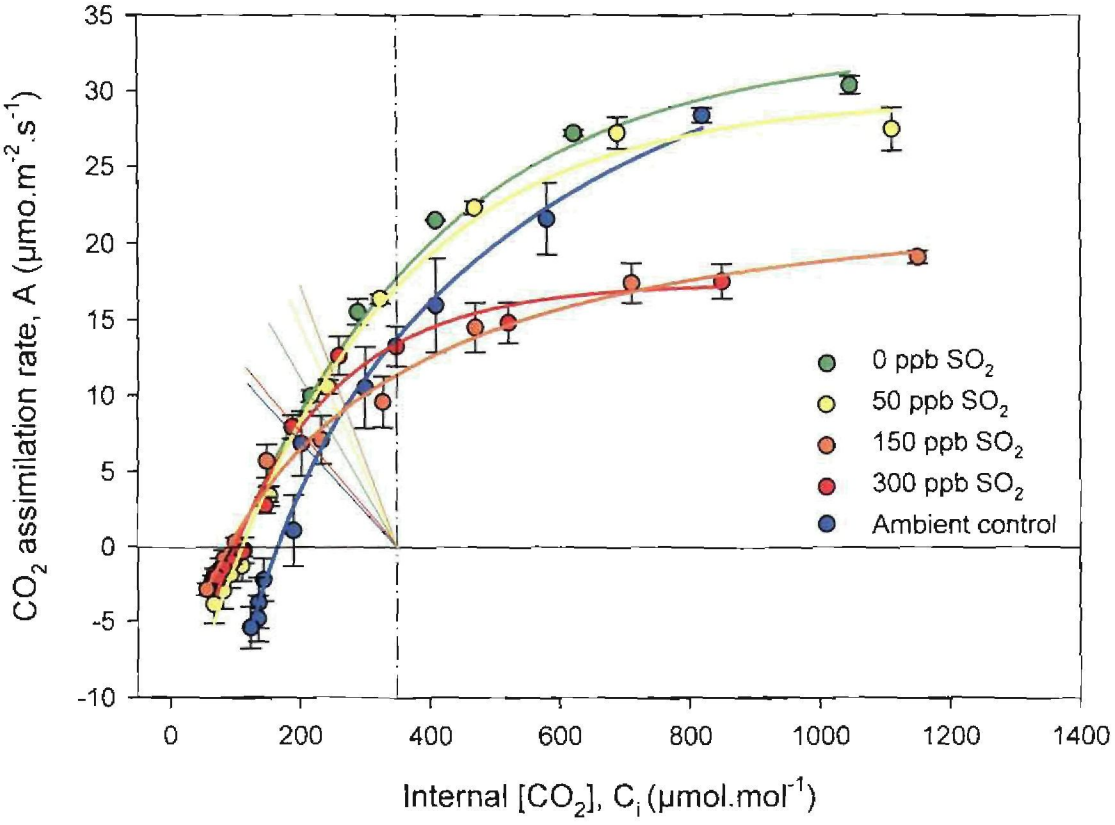


Figure 4.23 CO_2 assimilation rate as a function of intercellular CO_2 concentration of intact well watered leaves of *Brassica oleracea* plants after 50 days' exposure to elevated SO_2 concentrations of 50, 150 and 300 ppb. The 0 ppb SO_2 treatment served as the control. Each value represents a mean (± SE) where n = 2.

Table 4.5 Mean values (± standard errors) for gas exchange parameters measured in well watered intact leaves of *Brassica oleracea* (n = 2 plants per SO_2 treatment) 50 days after SO_2 fumigation commenced. Symbols: A_{350}, rate of CO_2 assimilation at C_a = 350 $\mu mol.mol^{-1}$; Ci_{350}, intercellular CO_2 concentration at C_a = 350 $\mu mol.mol^{-1}$; A_0, rate of CO_2 assimilation at C_i = 350 $\mu mol.mol^{-1}$; Gs_{350}, stomatal conductance at C_a = 350 $\mu mol.mol^{-1}$; CE, carboxylation efficiency at Γ; J_{max}, maximum rate of CO_2 assimilation; Γ, CO_2 compensation concentration; ℓ, percentage stomatal limitation of photosynthesis; WUE, water use efficiency, with * and ** indicating significant differences at $p<0.05$ and $p<0.01$ respectively, compared to control plants.

	0 ppb SO_2	50 ppb SO_2	150 ppb SO_2	300 ppb SO_2	Ambient Control
E ($mmol.m^{-2}.s^{-1}$)	2.44 (0.51*)	3.08 (0.293)	3.38 (0.183)	1.67 (0.226)	2.46 (0.148*)
A_{350} ($\mu mol.m^{-2}.s^{-1}$)	9.95 (0.98)	10.55 (1.45*)	7.05 (0.75)	7.9 (1.20)	6.8 (0.75)
Ci_{350} ($\mu mol.mol^{-1}$)	217.1 (0.43)	242.5 (4.65)	233.1(11.64)	188.5 (3.54)	202.5 (10.04)
A_0 ($\mu mol.m^{-2}.s^{-1}$)	18.1 (1.20)	17.1 (2.03*)	11.2 (0.74)	13.5 (0.36)	13.9 (0.76)
Gs_{350} ($\mu mol.m^{-2}.s^{-1}$)	134 (0.22)	182(0.13)	206 (0.22)	83 (0.12)	111 (0.34*)
CE ($mol.m^{-2}.s^{-1}$)	0.069 (0.01)	0.975 (1.01)	0.095 (1.03)	0.067 (0.33**)	0.098 (0.57)
J_{max} ($\mu mol.m^{-2}.s^{-1}$)	30.4 (6.57)	27.5 (5.43)	19.1 (8.53)	17.5 (0.46)	28.4 (1.04*)
Γ ($\mu mol.mol^{-1}$)	96.1 (0.45)	113.1 (1.29)	92.1 (3.27*)	101.0 (0.56)	165.5 (4.36)
ℓ (%)	45.0 (0.48)	38.3 (0.34)	37.0 (0.65)	41.5 (1.08*)	51.1 (0.04)
WUE ($mmol.mol^{-1}$)	4.1 (0.98)	3.4 (0.87)	2.1 (0.94)	4.7 (0.36*)	2.7 (0.29)

In order to partition photosynthetic inhibition between stomatal and non-stomatal factors more precisely, photosynthetic response parameters were calculated and plotted in relation to SO_2 fumigation concentrations (Table 4.6; Figure 4.24 and Figure 4.25). The CO_2 assimilation rate at C_i = 350 $\mu mol.mol^{-1}$ (A_0), decreased by 86 %, 55 % and 63 % for the 50, 150 and 300 ppb SO_2 concentrations, respectively, compared to the control plants subjected to drought stress. These reductions in A_0 could be ascribed to a decrease in the activity or amount of Rubisco. This assumption is corroborated by the decrease in J_{max}, which is a sensitive indicator of the regeneration capacity of RuBP and hence the activity of Rubisco. J_{max} decreased by 26 %, 30 % and 42 % at the 50, 150 and 300 ppb SO_2 concentrations, respectively, compared to the drought stressed plants grown in SO_2-free air. The carboxylation efficiency (CE) decreased by 34 %, 45 % and 51 % at the 50, 150 and 300 ppb SO_2 concentrations, respectively, pointing to reduced activity of Rubisco. Concurrently, increases in the compensation concentration (Γ) of 92 %, 114 % and 122 % at the 50, 150 and 300 ppb SO_2 concentrations corroborate the decreases in CE, pointing to severe mesophyll limitation. Despite the decreases in Gs_{350} (Figure 4.24) of 37 % and 55 % at the 50 and 150 and 300 ppb concentrations, respectively (Figure 4.24); Ci_{350} increased, indicating that reductions in A were due to the mesophyll limitation, rather than stomatal limitation. Ci_{350} increased by 39 %, 51 % and 76 % for the 50, 150 and 300 ppb SO_2 concentrations, respectively, compared to the drought stressed plants grown in SO_2-free air. Stomatal limitation decreased by 12 %, 43 % and 17 % for the 50, 150 and 300 ppb SO_2 concentrations, respectively, indicating that the reduction in the CO_2 assimilation rate was not caused by stomatal limitation, but was due to constraints with in the mesophyll processes (Figure 4.25). SO_2 stress also induced reductions in the WUE of plants under drought stress (Figure 4.25). Although WUE increased by 13 % at the 50 ppb SO_2 concentration, WUE decreased by 19 % and 17 % at the 150 and 300 ppb SO_2 concentrations, respectively. The decrease in WUE occurred in spite of decreased transpiration rate (E) of 13 %, 25 % and 48 % at the 50, 150 and 300 ppb SO_2 concentrations, respectively, compared to the control plants subjected to drought stress.

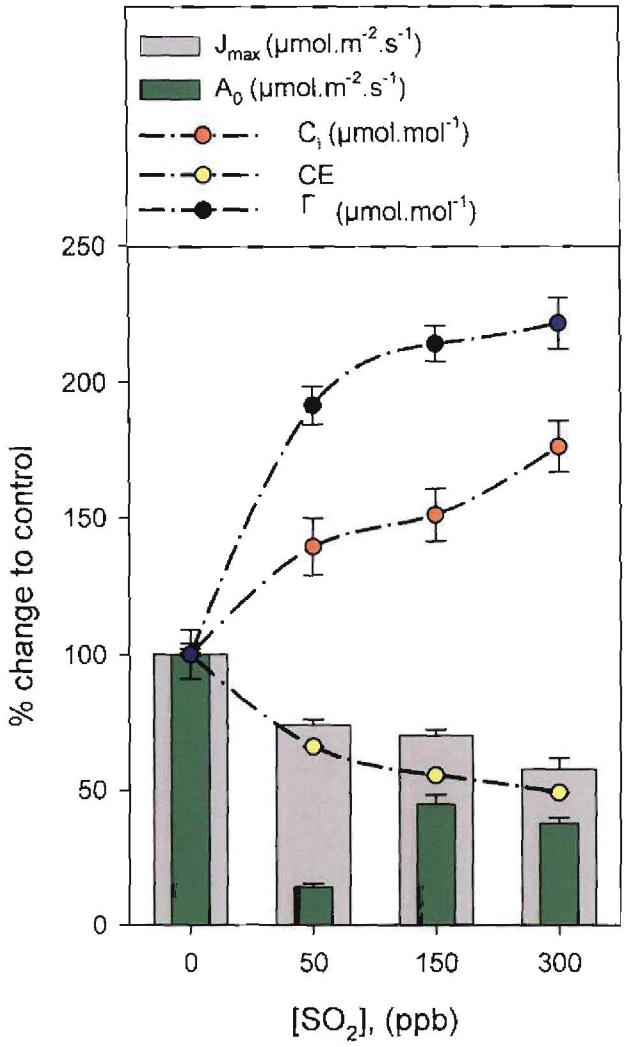


Figure 4.24 The effect of SO_2 on photosynthetic response parameters measure in drought stressed *Brassica oleracea* after 50 days' fumigation with SO_2. The parameters indicate the broadened effect mesophyll limitation induced in A upon exposure to SO_2. Note the sharp increase in both Γ and Ci_{350}. It appears that photosynthetic reductions resulted from the direct effect of SO_2 upon the photosynthetic processes, rather than any effect on stomatal closure and subsequent reductions of CO_2 movement into the leaf. It seems as if stomatal closure could have resulted from a build-up of CO_2 in the intercellular spaces, due to the photosynthetic depression. The 0 ppb SO_2 treatment served as the control. Each value represents a mean (± SE) where n = 2.

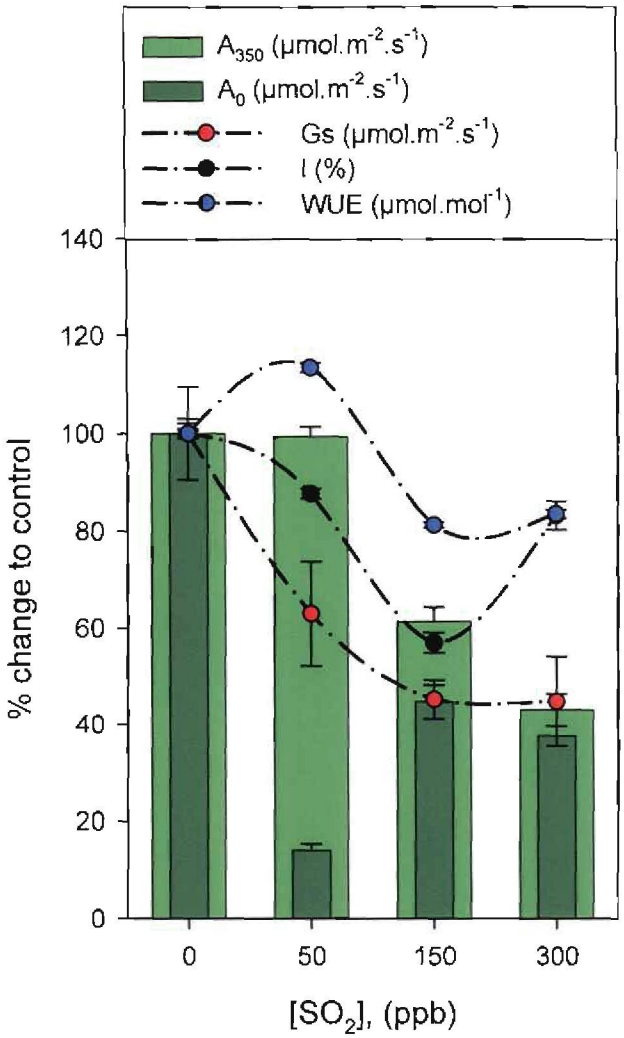


Figure 4.25 The effect of SO_2 exposure on photosynthetic response parameters after 50 days' exposure to 50,150 and 300 ppb SO_2. The parameters indicate the limitations imposed by stomatal resistance on A. Note the sharp reduction in WUE, explaining the far-reaching effect on the photosynthetic rate in crop plants grown under water deprivation and exposed to SO_2 concentrations as low as 50 ppb. The 0 ppb SO_2 treatment served as the control. Each value represents a mean (± SE) where n = 2.

Table 4.6 Mean values (± standard errors) for gas exchange parameters measured in drought stressed leaves of *Brassica oleracea* (n = 2 plants per SO_2 treatment) 50 days after SO_2 fumigation commenced. Symbols: A_{350}, rate of CO_2 assimilation at C_a = 350 $\mu mol.mol^{-1}$; Ci_{350}, intercellular CO_2 concentration at C_a = 350 $\mu mol.mol^{-1}$; A_0, rate of CO_2 assimilation at C_i = 350 $\mu mol.mol^{-1}$; Gs_{350}, stomatal conductance at C_a = 350 $\mu mol.mol^{-1}$; CE, carboxylation efficiency at Γ; J_{max}, maximum rate of CO_2 assimilation; Γ, CO_2 compensation concentration; ℓ, percentage stomatal limitation of photosynthesis; WUE, water use efficiency, with * and ** indicating significant differences at $p<0.05$ and $p<0.01$ respectively, compared to control plants.

	0 ppb SO_2	50 ppb SO_2	150 ppb SO_2	300 ppb SO_2	Ambient Control
E ($mmol.m^{-2}.s^{-1}$)	1.99 (0.37*)	1.74 (0.65*)	1.49 (0.36)	1.03 (2.04)	1.02 (1.56)
A_{350} ($\mu mol.m^{-2}.s^{-1}$)	7.1 (3.00)	7.05 (2.07*)	4.35 (2.94)	3.05 (3.34)	3.4 (0.57)
Ci_{350} ($\mu mol.mol^{-1}$)	179.5(0.57)	250 (10.46)	271 (9.85)	316.5 (9.43)	45 (10.6)
A_0 ($\mu mol.m^{-2}.s^{-1}$)	13.2 (2.04)	11.85 (1.29*)	5.9 (3.45)	4.95 (2.10)	7.4 (10.46)
Gs_{350} ($\mu mol.m^{-2}.s^{-1}$)	118.4(9.46)	74.5 (10.75)	53.5 (4.04)	53.0 (9.32)	78 (7.42)
CE ($mol.m^{-2}.s^{-1}$)	0.047(0.004*)	0.031 (0.06)	0.026 (0.03**)	0.023 (0.03*)	0.019 (0.75)
J_{max} ($\mu mol.m^{-2}.s^{-1}$)	22.9 (4.05*)	16.95 (1.94)	16.05 (2.07)	13.2 (4.03)	17.5 (2.98)
Γ ($\mu mol.mol^{-1}$)	93.0 (9.02)	178.1 (7.00)	199.0 (6.54)	206.1(9.47)	142.3(11.73)
ℓ (%)	46.2 (0.98)	40.5 (1.04*)	26.3 (2.06)	38.4 (2.93)	54.0 (2.38*)
WUE ($mmol.mol^{-1}$)	3.57 (0.46)	4.05 (0.98*)	2.90 (0.56)	2.98 (0.85)	3.33 (0.59*)

4.4.2 Effect of SO_2 on photosynthetic gas exchange in *Glycine max*

Repeated measurements of photosynthetic gas exchange rates for leaves of similar position and age on *Glycine max* plants grown in SO_2-free air, prior to the start of fumigation, indicated that these rates were comparable and reproducible for all test plants (Figure 4.3.2.1; Table 4.3.1.1). Note the small standard error obtained for all plants that represented the different SO_2 treatments after fumigation commenced.

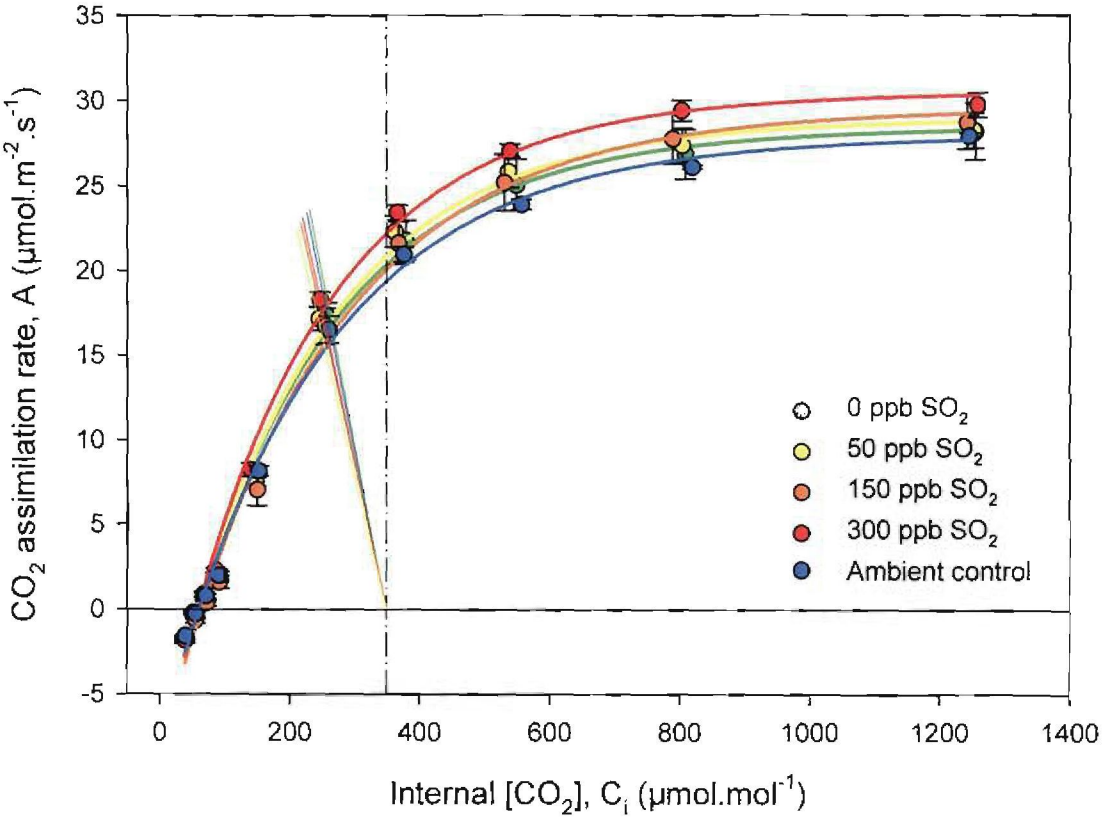


Figure 4.26 The A:C_i response curve for plants exposed to SO_2-free air prior to the start of SO_2 fumigation. Intact leaves on the 4th node of the individual plants were selected on the basis of their uniformity for gas exchange measurements. The response of each plant was measured at increasing ambient CO_2 concentrations to assess the effects of fumigation on the different photosynthetic gas exchange parameters. Each value represents a mean (± SE) where n = 8.

According to the A and J_{max} values (Table 4.7; Figure 4.26) obtained, all plants were at the same physiological status prior to the start of SO_2 fumigation treatment. From

the A:C_i response curves it can be seen that the plants allocated for the highest SO_2 concentration treatment, i.e. 300 ppb SO_2, performed even 5 % better than the plants allocated for the 0 ppb treatment grown in SO_2-free air. Also note that the stomatal conductance for all the test plants was very similar. The effects of SO_2 on *Glycine max* in absence and in combination with drought stress were evaluated by analysis of their respective A:C_i and light response curves. Photosynthetic gas-exchange parameters were measured after 7 and 28 days of fumigation with SO_2. Photosynthetic light-response curves were constructed from measurements taken 14 and 35 days after fumigation with SO_2. During the course of fumigation of non water-stressed plants, i.e. plants watered to 80 % of field capacity, a progressive decrease of CO_2 assimilation rates was evident (Figure 4.26)

Table 4.7 Means (± standard errors) for gas exchange parameters measured in intact leaves of *Glycine max* (n = 4 plants per SO_2 treatment) before fumigation commenced (Day 0). Symbols: A_{350}, rate of CO_2 assimilation at C_a= 350 µmol.mol^{-1}; Ci_{350}, intercellular CO_2 concentration at C_a= 350 µmol.mol^{-1}; A_0, rate of CO_2 assimilation at C_i = 350 µmol.mol^{-1}; Gs_{350}, stomatal conductance at C_a= 350 µmol.mol^{-1}; CE, carboxilation efficiency at Γ; J_{max}, maximum rate of CO_2 assimilation; Γ, CO_2 compensation point; ℓ, stomatal limitation of photosynthesis; WUE, water use efficiency, with * and ** indicating significant differences ($p<0.05$ and $p<0.01$ respectively) compared to control plants.

	0 ppb SO_2	50 ppb SO_2	150 ppb SO_2	300 ppb SO_2	Ambient Control
E (µmol.m^{-2}.s^{-1})	6.4 (0.21)	5.7 (0.24)	6.0 (0.31*)	6.2 (0.32*)	5.26 (0.05**)
A_{350} (µmol.m^{-2}.s^{-1})	17.3 (0.81)	18.3 (0.24*)	16.7 (0.38)	18.3 (0.23*)	16.5 0.28)
Ci_{350} (µmol.mol^{-1})	257.5 (0.42)	235.0 (0.11)	255.5 (0.47*)	247.0 (0.12)	260.5 (0.41)
A_0 (µmol.m^{-2}.s^{-1})	19.6 (0.12)	20.6 (0.31)	17.5 (0.17)	20.3 (0.33)	19.52 (0.41**)
Gs_{350} (µmol.m^{-2}.s^{-1})	437.5 (0.41)	358.5 (0.12)	406.5 (0.36)	401.8 (0.23*)	394 0.25)
CE (mol.m^{-2}.s^{-1})	0.09 (0.753)	0.09 (0.362*)	0.082 (0.233)	0.097 (0.259)	0.088 (0.293*)
J_{max} (µmol.m^{-2}.s^{-1})	28.1 (0.64)	29.8 (0.33**)	28.7 (0.42*)	29.7 (0.23*)	27.9 0.45*)
Γ (µmol.mol^{-1})	61.3 (0.21)	56.5 (0.13)	64.3 (0.12*)	59.3 (0.21)	60 (0.32*)
ℓ (%)	11.6 (0.33)	11.0 (0.42**)	4.5 (0.03*)	9.0 (0.23)	15.5 0.19)
WUE	2.7 (0.22)	3.2 (0.13)	2.8 (0.32*)	2.9 (0.21*)	3.1 (0.05)

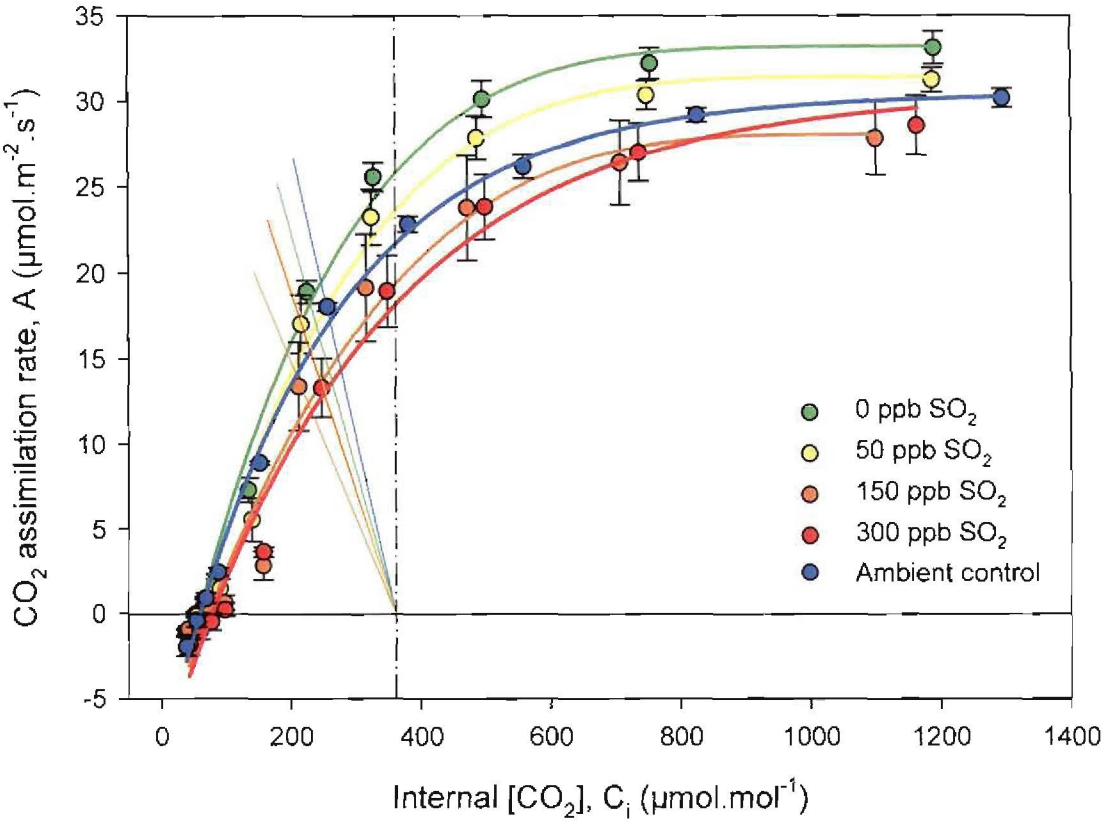


Figure 4.27 CO_2 assimilation rate as a function of intercellular CO_2 concentration of intact leaves of well watered *Glycine max* plants after 7 days' exposure to elevated SO_2 concentrations of 50, 150 and 300 ppb. The 0 ppb SO_2 treatment served as the control. Each value represents a mean (± SE) where n = 4.

One week after starting fumigation of well watered test plants with 50 ppb, 150 ppb and 300 ppb SO_2 respectively, the CO_2 saturated rates of photosynthesis, (J_{max}) increased by 5 % at the 50 ppb level and decreased slightly by only 3 %, and 4 % for the 150 ppb and 300 ppb levels, respectively, as compared to values measured prior to the onset of fumigation (Table 4.8; Figure 4.27). At the same time the control plants, i.e. the 0 ppb treatment, performed 18 % better. This depression of the CO_2 saturation level observed in plants treated at 150 and 300 ppb points at a reduction in RuBP regeneration capacity which limits net photosynthesis (A). Similar to J_{max}, the rate of CO_2 assimilation at C_a = 350 µmol.mol^{-1} (A_{350}), decreased by 10 %, 29 %, and 30 % at the 50, 150 and 300 ppb SO_2 levels, respectively. The same trend was evident for the rate of CO_2 assimilation at C_i = 350 µmol.mol^{-1} (A_0) decreasing by 10 %, 30 % and 33 %, respectively with increasing SO_2 concentration. The corresponding carboxylation efficiency (CE), determined from the initial linear slope

of the demand function of the A:C_i response curve ($\delta A/\delta C_i$) (Figure 4.27), was reduced at all SO_2 treatments (Table 4.8). The decline in CE was smallest at the 50 ppb treatment showing a reduction of 25 %, but increased with increasing SO_2 treatment by 51 % and 49 %, at the 150 and 300 ppb SO_2 treatments respectively, compared to the values recorded prior to fumigation with SO_2. The calculated carboxylation efficiency is a sensitive indicator of *in vivo* Rubisco activity (Walker *et al.*, 1986). The inhibition of the CE with concomitant reduction in J_{max}, points towards severe and irreversible damage to the mesophyll processes (i.e. biochemical reactions of photosynthesis) which ultimately limits photosynthesis. At the same time, the supply function, which is related to the stomatal conductance at C_a = 350 $\mu mol.mol^{-1}$ (Gs_{350}), decreased at 50 ppb and 150 ppb SO_2 levels respectively, and remained the same at the 300 ppb SO_2 level, in spite of concomitant decreases in A_{350} and A_0 at this SO_2 concentration (Table 4.8; Figure 4.27). Gs_{350} decreased by 8 % and 30 % at the 50 ppb and 150 ppb treatments respectively, and increased very slightly (1 %) at the 300 ppb SO_2 treatment. The intercellular CO_2 concentration at C_a = 350 $\mu mol.mol^{-1}$, (Ci_{350}) remained comparable to values recorded for the control plants at the beginning before SO_2 fumigation commenced. Ci_{350} decreased slightly by 4 % and 6 % at the 50 and 150 ppb treatments, respectively, and increased by 10 % at the 300 ppb SO_2 treatment. The relative stomatal limitation (ℓ), however, decreased in excess of 70 %, indicating that the reduction in A was due to mesophyll limitation rather than stomatal limitation. This assumption is corroborated by the increases in the CO_2 compensation concentration point (Γ) of 5 %, 31 %, and 39 % at the 50, 150 and 300 ppb SO_2 levels, respectively. The small increase in stomatal conductance induced by exposure to SO_2 probably resulted from a combination of immediate effects on the activity of certain key enzymes in the epidermis, and delayed effects arising from the inhibition of photosynthesis in the mesophyll (Müller *et al.*, 1979). Decreases in the rate of photosynthesis in the mesophyll probably led to accumulation of CO_2 in the intercellular spaces, affecting stomatal movement (Raschke, 1979). Our data indicated that the transpiration rate decreased by 11 %, 30 % and 8 % at 50 ppb, 150 ppb and 300 ppb SO_2, respectively. Decreases in water use efficiency (WUE) of 105 % at both 50 ppb and 150 ppb SO_2 treatments and 103 % at 300 ppb SO_2 treatment, indicate that the measured decreases in transpiration were not caused by reduced water availability, but rather to stomatal closure, due to impairment of proper functioning of the stomata by SO_2. It is evident (Figure 4.26) that the control plants receiving 0 ppb SO_2, performed 8 % better than those grown under ambient conditions (chamber effect control), pointing at a stimulating effect occurring inside the chambers. This can be ascribed to night

temperatures dropping below 10°C outside during the first two weeks of October. At that time the minimum temperature inside the chamber never dropped below 15 °C (data not shown).

Table 4.8 Mean values (± standard errors) for gas exchange parameters measured in well watered leaves of *Glycine max* (n = 4 plants per SO_2 treatment) 7 days after fumigation commenced. Symbols: A_{350}, rate of CO_2 assimilation at C_a = 350 µmol.mol^{-1}; Ci_{350}, intercellular CO_2 concentration at C_a = 350 µmol.mol^{-1}; A_0, rate of CO_2 assimilation at C_i = 350 µmol.mol^{-1}; Gs_{350}, stomatal conductance at C_a = 350 µmol.mol^{-1}; CE, carboxilation efficiency at Γ; J_{max}, maximum rate of CO_2 assimilation; Γ, CO_2 compensation concentration; ℓ, stomatal limitation of photosynthesis; WUE, water use efficiency, with * and ** indicating significant differences at p<0.05 and p<0.01 respectively, compared to control plants.

	0 ppb SO_2	50 ppb SO_2	150 ppb SO_2	300 ppb SO_2	Ambient Control
E (mmol.m^{-2}.s^{-1})	5.595 (0.286*)	4.968 (0.630)	3.883 (0.936*)	5.155 (0.849*)	6.315 (0.415*)
A_{350} (µmol.m^{-2}.s^{-1})	18.925 (0.663*)	17.025 (1.698*)	13.375 (2.587*)	13.3 (1.723*)	18.450 (0.250*)
Ci_{350} (µmol.mol^{-1})	225.5 (5.515*)	216.0 (9.283)	212.250 (13.098*)	247.75 (16.075)	252.0 (5.000*)
A_0 (µmol.m^{-2}.s^{-1})	23.875 (0.740*)	21.463 (1.455)	16.663 (1.976**)	15.9 (2.435*)	22.5 (2.100*)
Gs_{350} (µmol.m^{-2}.s^{-1})	300.0 (37.674*)	275.25 (51.476)	209.75 (64.280)	303.0 (78.727**)	429.5 (61.5)
CE (mol.m^{-2}.s^{-1})	0.091 (0.006*)	0.067 (0.018)	0.036 (0.011**)	0.05 (0.005**)	0.097 (0.014)
J_{max} (µmol.m^{-2}.s^{-1})	33.1 (0.957)	31.225 (0.303)	27.85 (2.150*)	28.575 (1.722*)	33.3 (2.1*)
Γ (µmol.mol^{-1})	57.375 (1.028)	60.75 (3.119)	75.25 (6.7*)	79.75 (8.901*)	65.5 (0.500)
ℓ (%)	19.936 (1.44*)	20.947 (4.428)	22.313 (7.468*)	14.353 (8.312*)	17.844 (1.668*)
WUE (mmol.mol^{-1})	3.329 (0.08)	3.478 (0.235*)	3.566 (0.262*)	2.724 (0.396)	2.922 (0.001)

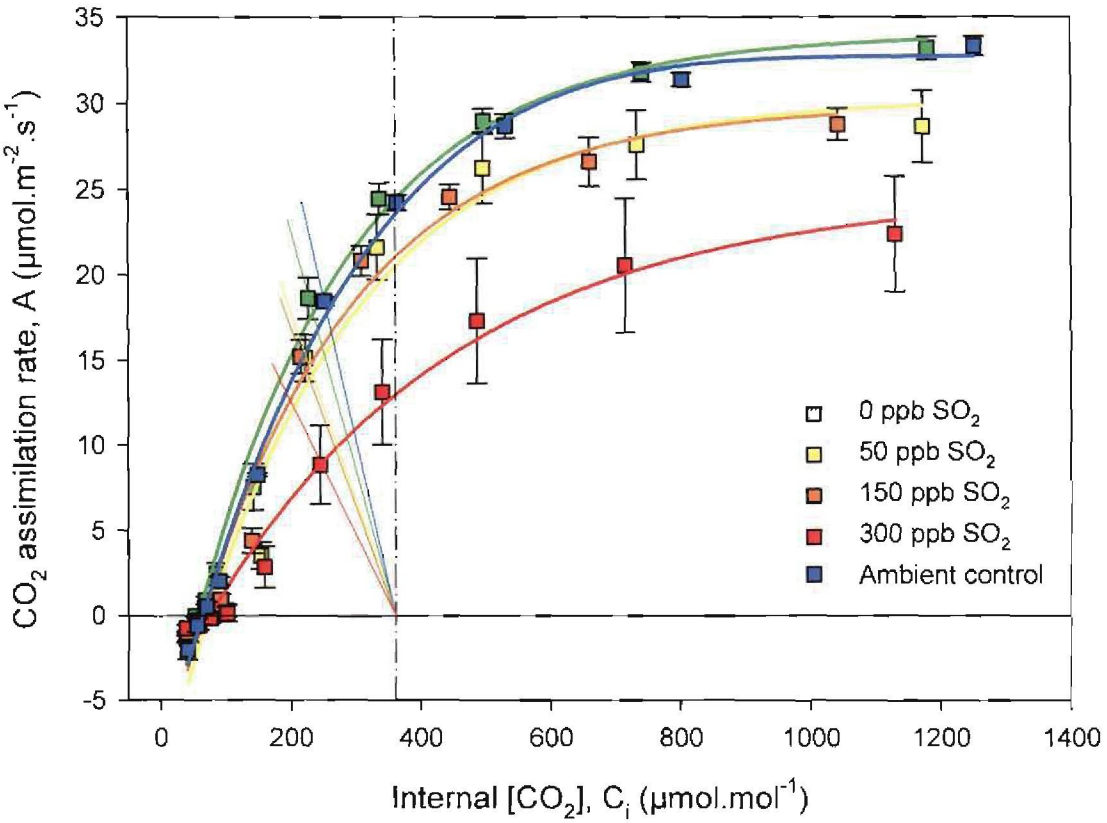


Figure 4.28 CO_2 assimilation rate as a function of intercellular CO_2 concentration for leaves of drought stressed *Glycine max* plants after 7 days' exposure to elevated SO_2 concentrations of 50, 150 and 300 ppb. The 0 ppb SO_2 treatment served as the control. Each value represents a mean (± SE) where n = 4.

Plants fumigated and simultaneously subjected to drought stress were severely affected at all SO_2 concentrations after 7 days (Table 4.9; Figure 4.28). The inhibition of photosynthesis is often regarded as the first sign of SO_2 action on plants (Bell & Turner, 2002). After 7 days' SO_2 fumigation in combination with drought stress, the A:C_i response curves indicated that CO_2 saturated rates of photosynthesis, (J_{max}), which is an indicator of the RuBP regeneration capacity of the Calvin cycle, were inhibited by 13 % at both 50 ppb and 150 ppb SO_2 treatments and decreased by 32 % at the 300 ppb level, respectively, compared to the chamber control plants, after only one week's treatment. Concurrently the CO_2 assimilation rate at C_a = 350 µmol.mol^{-1} (A_{350}) decreased by 19 % at the 50 ppb treatment, 18 % at the 150 ppb SO_2 treatment and very pronouncedly by 53 % at the 300 ppb

treatment. The CO_2 assimilation rate at C_i = 350 $\mu mol.mol^{-1}$ (A_0), also showed decreases of 20 %, 18 % and 48 % at the 50, 150, and 300 ppb SO_2 treatments, respectively. The respective decreases in CE were 47 %, 32 % and 57 %. This decrease in CE may be due to SO_2-induced constraints on the *in vivo* activity of Rubisco. The concurrent respective increases in the CO_2 compensation concentration (Γ) of 42 %, 10 % and 42 % corroborate this finding. A further indication of mesophyll limitation was the fact that the intercellular CO_2 concentration at C_a = 350 $\mu mol.mol^{-1}$, (Ci_{350}) remained nearly constant, showing a decrease of 2 % at 50 ppb SO_2 treatment and 6 % at the 150 ppb SO_2 treatment respectively, an increase of 8 % at the 300 ppb SO_2 treatment. The stomatal conductance at C_a = 350 $\mu mol.mol^{-1}$ (Gs_{350}), increased slightly by 3 % at the 50 ppb SO_2 treatment, decreased by 6 % at the 150 ppb SO_2 treatment and decreased more profoundly with 31 % at the 300 ppb SO_2 treatment. The 300 ppb treatment showed an 8 % increase in Ci_{350} with a concomitant decrease in Gs_{350} of more than 30 %. This suggests that in addition to Gs, biochemical changes in the mesophyll were also limiting carbon assimilation at higher SO_2 concentrations. This phenomenon is corroborated by a decrease in the calculated percentage stomatal limitation (ℓ): (Table 4.9). The percentage stomatal limitation decreased by 55 % relative to the control, at the 50 ppb, 46 % at the 150 ppb and to a lesser extent, namely 32 %, at the 300 ppb SO_2 treatment. At the same time it should be noted that the transpiration rate at C_a = 350 $\mu mol.mol^{-1}$, (E) decreased significantly at all SO_2 levels, showing a 94 % reduction at the 50 ppb and 150 ppb levels and a 96 % decrease at the 300 ppb SO_2 level. This decrease in the E was the result of stomatal closure due to reduced availability of water, and resulted in improved water use efficiency (WUE). The WUE of the test plants increased at all treatments, but was higher at the lowest and intermediate levels. The increases were 116 % at 50 ppb, 118 % at the 150 ppb and, less significantly, 80 % at the 300 ppb treatment. This observation suggests that the SO_2 and drought-induced decrease in A measured at all SO_2 levels was mainly due to stomatal limitation. Note that the Gs_{350} decreased by more than 30 % at the highest treatment and analogous to this, the percentage stomatal limitation (ℓ) decreased to a lesser extent at this particular treatment level. However, the WUE proved to be 35 % lower in the drought stressed plants treated at 300 ppb SO_2. It has been reported that various aspects of stomatal functioning can be modified by air pollutants, and in some cases pollutant concentration can cause significant disturbances that cause the plant to lose control of its water relations (Mansfield, 1998). Although the decrease in Gs_{350} was not very drastic, reductions in *A* at all SO_2 levels were affected by stomatal limitation. However, if A is inhibited mainly by mesophyll limitation, increases in C_i

might be expected, as is seen at the 300 ppb treatment (Figure 4.28). Although a decrease in Gs_{350} points to stomatal limitation, the decrease in the calculated percentage stomatal limitation suggests otherwise. The increase in Ci_{350} at the 300 ppb level as well as the decrease in CE and a corroborating increase in Γ suggests that reductions in A must mainly be ascribed to mesophyll limitation. Thus, SO_2 induced reductions in CO_2 assimilation (A), must be ascribed mainly to non-stomatal, i.e. mesophyll constraints.

Table 4.9 Means (± standard errors) for gas exchange parameters measured in drought stressed leaves of *Glycine max* (n = 4 plants per SO_2 treatment) after 7 days of fumigation with SO_2. Symbols: A_{350}, rate of CO_2 assimilation at C_a = 350 $\mu mol.mol^{-1}$; Ci_{350}, intercellular CO_2 concentration at C_a = 350 $\mu mol.mol^{-1}$; A_0, rate of CO_2 assimilation at C_i = 350 $\mu mol.mol^{-1}$; Gs_{350}, stomatal conductance at C_a = 350 $\mu mol.mol^{-1}$; CE, carboxilation efficiency at Γ; J_{max}, maximum rate of CO_2 assimilation; Γ, CO_2 compensation point; ℓ, stomatal limitation of photosynthesis; WUE, water use efficiency, with * and ** indicating significant differences ($p<0.05$ and $p<0.01$ respectively) compared to control plants.

	0 ppb SO_2	50 ppb SO_2	150 ppb SO_2	300 ppb SO_2	Ambient Control
E ($\mu mol.m^{-2}.s^{-1}$)	4.93 (0.78*)	4.61 (0.428)	4.50 (0.396)	3.45 (0.548)	6.31(0.465)
A_{350} ($\mu mol.m^{-2}.s^{-1}$)	18.62 (1.217)	15.12 (1.379)	15.21 (0.992*)	8.82 (2.320**)	18.45 (0.465)
Ci_{350} ($\mu mol.mol^{-1}$)	227.00 (6.494*)	222.5 (18.693)	215.5 (8.539)	245.5 (25.659)	252.1 (5*)
A_0 ($\mu mol.m^{-2}.s^{-1}$)	23.35 (0.718)	18.48 (1.67*)	19.25 (0.83**)	12.12 (2.99**)	22.51 (2.12)
Gs_{350} ($\mu mol.m^{-2}.s^{-1}$)	244.6 (88.107)	251.5 (27.786)	230.5 (30.829)	168.1 (26.935)	429.5 (61.5)
CE ($mol.m^{-2}.s^{-1}$)	0.087 0.016)	0.046 (0.011*)	0.059 (0.011)	0.037 (0.016*)	0.097 (0.014)
J_{max} ($\mu mol.m^{-2}.s^{-1}$)	33.17 (0.654)	28.67 (2.093)	28.81 (0.930)	22.42 (3.396)	33.34 (2.1)
Γ ($\mu mol.mol^{-1}$)	58.37 (2.322)	82.75 (8.4**)	64.51 (2.398*)	82.75 (12.072*)	65.52 (0.5)
ℓ (%)	39.04 (21.629)	17.46 (3.310)	21.04 (4.141)	26.52 (3.628)	17.84 (1.668)
WUE ($mmol.mol^{-1}$)	1.55 (0.941)	3.37 (0.504)	3.40 (0.151)	2.80 (0.714)	2.92 (0.001)

From the A:C_i response curves depicted in Figures 4.29 and 4.30 it is evident that after 28 days of fumigation with SO_2 singly (Table 4.10; Figure 4.29) and in combination with drought stress (Table 4.11; Figure 4.31) photosynthetic gas exchange parameters were severely inhibited.

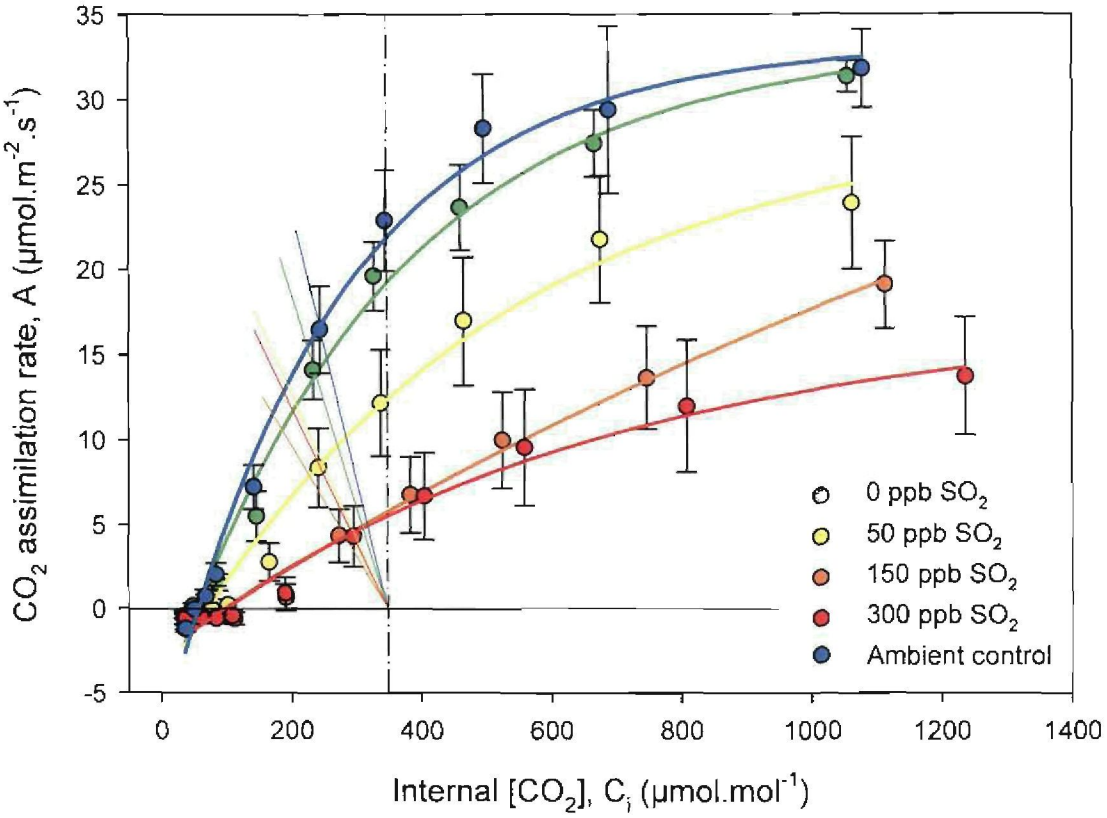


Figure 4.29 CO_2 assimilation rate as a function of intercellular CO_2 concentration of intact leaves of well watered *Glycine max* plants after 28 days' exposure to elevated SO_2 concentrations of 50, 150 and 300 ppb. The 0 ppb SO_2 treatment served as the control. Each value represents a mean (± SE) where n = 4. (Drought stress meaning $\Psi_{MD} \approx$ -1.4 MPa; $\Psi_{PD} \approx$ -0.4 MPa.)

After 28 days' fumigation with SO_2 of well watered plants, all gas exchange parameters were severely affected (Table 4.10; Figure 4.29). At the 50 ppb and 150 ppb SO_2 concentrations (Table 4.10; Figure 4.29) the CO_2 saturated rates of photosynthesis, (J_{max}) decreased by 23 % and 25 %, respectively. At the 300 ppb SO_2 level, even despite the fact that the measurement was carried out on a physiologically younger leaf which had been exposed for a shorter period, the decrease was 54 %. The rate of CO_2 assimilation at C_a = 350 µmol.mol^{-1} (A_{350}) also decreased severely from 41 % at the 50 ppb treatment to 69 % and 70 % at the 150

ppb and 300 ppb SO_2 treatments respectively. The rate of CO_2 assimilation at C_i = 350 µmol.mol^{-1} (A_0), decreased by 35 %, 66 % and 70 % at the 50, 150 and 300 ppb treatments respectively. The corresponding decreases in CE were 45 %, 81 % and 74 %, respectively, at 50, 150 and 300 ppb SO_2 concentrations. The concomitant increases in the compensation concentration (Γ) of 37 %, 102 % and 143 %, respectively, corroborates the decreases in CE and point to an increasing mesophyll limitation and reduced activity of Rubisco. The intercellular CO_2 concentration at C_a = 350 µmol.mol^{-1}, (Ci_{350}) increased slightly by 4 % at the lowest concentration and by 17 % and 27 % at the intermediate and highest SO_2 concentrations. These increases took place in spite of the strong decreases in Gs_{350}, indicating that *limitations within the mesophyll are the dominant cause of reduction in A.* The stomatal conductance at C_a = 350 µmol.mol^{-1} (Gs_{350}), decreased drastically, by 49 %, 57 % and 51 % at 50, 150, and 300 ppb SO_2 treatments respectively. It appears, however, that mesophyll limitation was more evident at the intermediate and highest concentrations. This contention is corroborated by the values calculated for stomatal limitation (ℓ), revealing that the 50 ppb treatment induced the highest percentage limitation (41 %). Stomatal limitation increased by only 7 % and 11 % at the 150 ppb and 300 ppb SO_2 treatments respectively. The water use efficiency decreased by 12 %, 39 % and 56 % at the 50, 150, and 300 ppb SO_2 treatments, respectively. According to the gas exchange data, it is clear that after treatment to 50 ppb SO_2, reductions in A were due to a decreased supply of CO_2 through the stomata. Further support for the above-mentioned argument is the large increase in stomatal limitation at this level which was more than five times higher than the level obtained at the intermediate and highest SO_2 treatments. At the 150 ppb and 300 ppb SO_2 treatments, reductions in CO_2 assimilation (A), must be ascribed mainly to limitations within the mesophyll. This finding is supported by the large decrease in J_{max} and CE. Increases in stomatal limitation at the 150 and 300 ppb treatments were small compared to the values calculated for plants treated with 50 ppb SO_2 (Table 4.10; Figure 4.29).

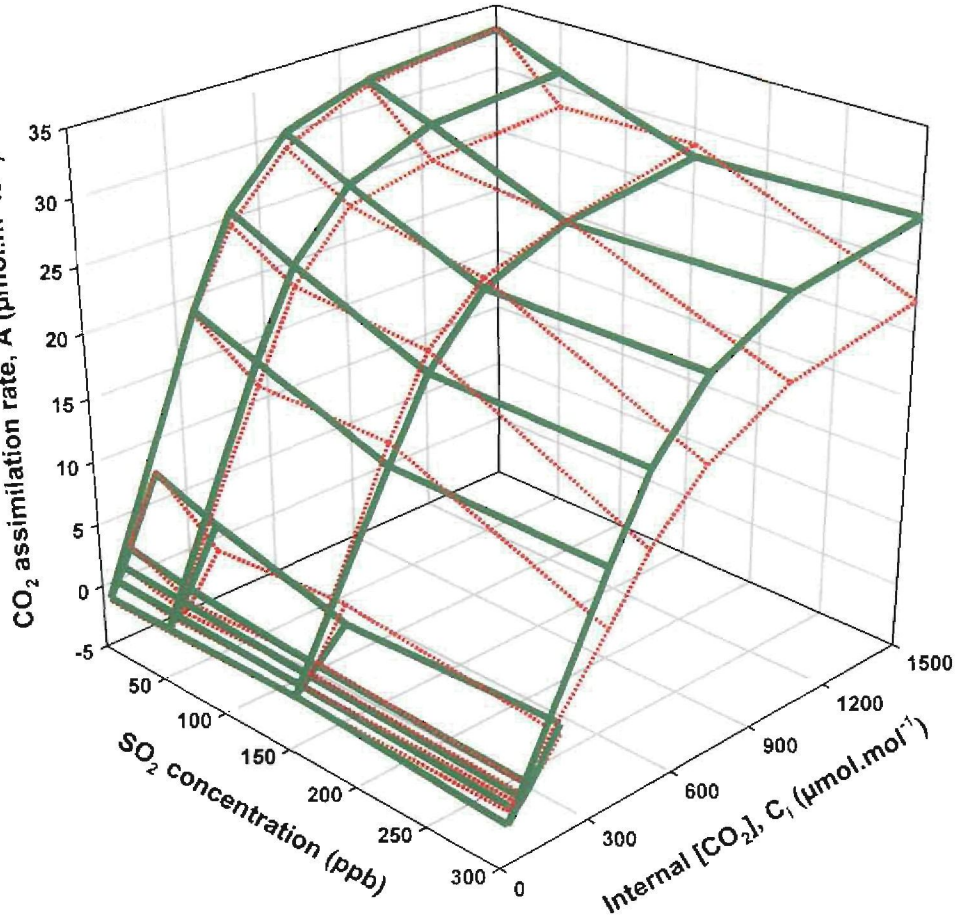


Figure 4.30 Three-dimensional representation of the affect of different SO_2 fumigation levels on the A:C_i response of well watered (green) and drought stressed (red) *Glycine max* plants after 7 days' fumigation.

Table 4.10 Means (± standard errors) for gas exchange parameters measured in well watered leaves of *Glycine max* (n = 4 plants per SO_2 treatment) after 28 days' fumigation. Symbols: A_{350}, rate of CO_2 assimilation at C_a = 350 $\mu mol.mol^{-1}$; Ci_{350}, intercellular CO_2 concentration at C_a = 350 $\mu mol.mol^{-1}$; A_0, rate of CO_2 assimilation at C_i = 350 $\mu mol.mol^{-1}$; Gs_{350}, stomatal conductance at C_a = 350 $\mu mol.mol^{-1}$; CE, carboxilation efficiency at Γ; J_{max}, maximum rate of CO_2 assimilation; Γ, CO_2 compensation point; ℓ, stomatal limitation of photosynthesis; WUE, water use efficiency, with * and ** indicating significant differences ($p<0.05$ and $p<0.01$ respectively) compared to control plants.

	0 ppb SO_2	50 ppb SO_2	150 ppb SO_2	300 ppb SO_2	Ambient Control
E ($\mu mol.m^{-2}.s^{-1}$)	4.113 (0.686)	2.570 (0.503*)	2.243 (0.542*)	2.453 (0.393*)	5.378 (0.623)
A_{350} ($\mu mol.m^{-2}.s^{-1}$)	14.1 (1.493)	8.325 (2.335*)	4.325 (1.560*)	4.275 (1.799**)	17.37 (85.247)
Ci_{350} ($\mu mol.mol^{-1}$)	233.33 (14.751)	241.5 (16.215)	273.5 (20.234)	295.75 (21.053*)	248.75 (7.341)
A_0 ($\mu mol.m^{-2}.s^{-1}$)	18.45 (1.089*)	11.963 (2.859*)	6.213 (2.403*)	5.55 (2.441**)	23.675 (1.601*)
Gs_{350} ($\mu mol.m^{-2}.s^{-1}$)	268 (77.780)	137.5 (32.702)	114.5 (26.850)	130.25 (19.12)	399.5 (85.247)
CE ($mol.m^{-2}.s^{-1}$)	0.056 (0.013*)	0.030 (0.012)	0.011 (0.008*)	0.014 (0.008*)	0.087 (0.087*)
J_{max} ($\mu mol.m^{-2}.s^{-1}$)	31.33 (0.808*)	24.075 (3.965)	23.575 (3.011)	14.5 (3.745**)	6.976 (6.516*)
Γ ($\mu mol.mol^{-1}$)	56 (2.598)	76.5 (10.071*)	113.250 (19.551*)	136.25 (39.398)	56.5 (2.217)
ℓ (%)	23.959 (4.423)	33.801 (5.541)	25.699 (9.855)	26.659 (17.669)	43.998 (21.027)
WUE ($mmol.mol^{-1}$)	3.513 (0.192*)	3.074 (0.532)	2.133 (0.615)	1.561 (0.650*)	1.198 (0.688*)

Investigating the interaction of SO_2 fumigation and drought stress revealed the enormous contribution that co-stress may have on the constraints imposed on plants cultivated in SO_2 polluted areas, especially on crops near high-emission sources.

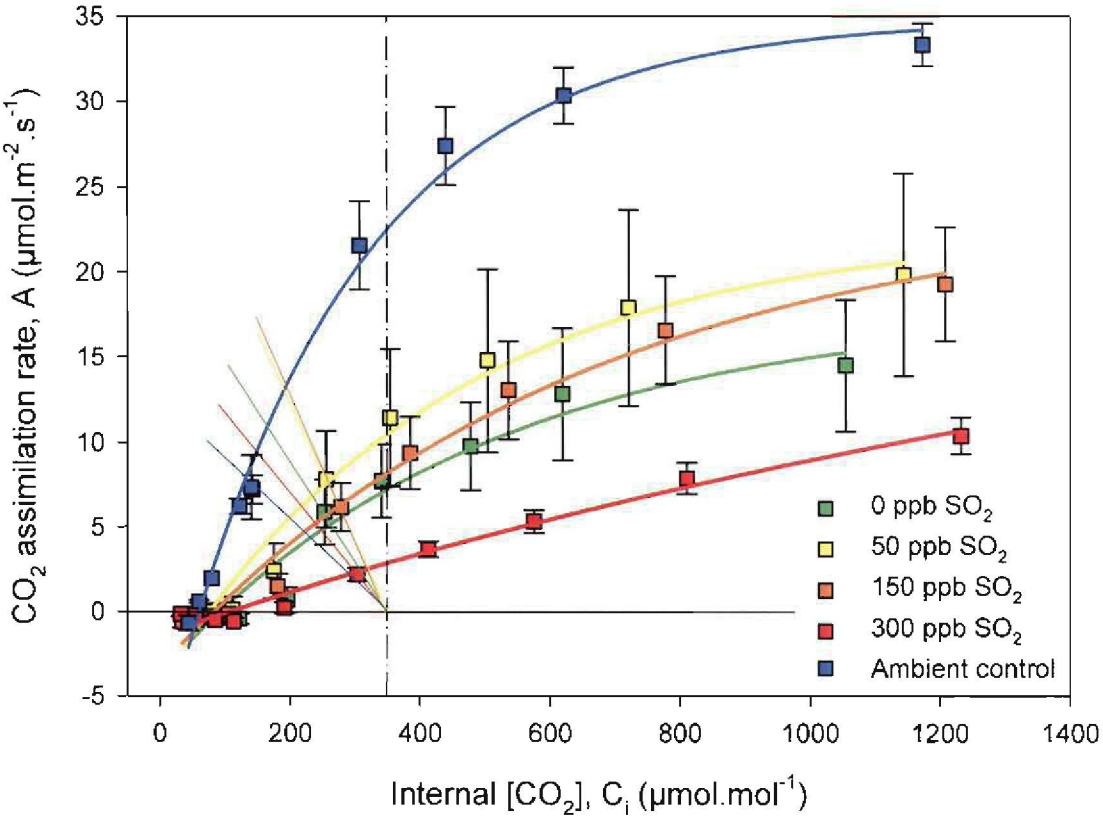


Figure 4.31 CO_2 assimilation rate as a function of intercellular CO_2 concentration for leaves of drought stressed *Glycine max* plants after 28 days' exposure to elevated SO_2 concentrations of 50, 150 and 300 ppb. The 0 ppb SO_2 treatment served as the control. Each value represents a mean (± SE) where n = 4.

From the analysis of the response of A upon changes in C_i (Table 4.11; Figure4.31) it appears that *Glycine max* plants treated with 50, 150 and 300 ppb SO_2 and simultaneously subjected to drought were severely injured. The CO_2-saturated rates of photosynthesis, (J_{max}) decreased at all SO_2 levels used. The decreases were most obvious at the 300 ppb SO_2 treatment, revealing a 54 % decrease relative to the well watered 0 ppb treatment. J_{max} decreased 18 % more at the 50 ppb and 150 ppb treatments compared to the well watered plants treated at the 50 ppb SO_2 level. J_{max} decreased 29 % more than the well watered plants (i.e. 67 %) at the 300 ppb treatment when grown in combination with drought stress. Correspondingly, the rate

of CO_2 assimilation at C_a = 350 µmol.mol^{-1} (A_{350}), also decreased severely, namely 59 % in plants grown in SO_2-free air and simultaneously subjected to drought. This means drought stress alone had a marked effect on the test plants. However, A_{350} remained constant at the 50 ppb treatment and increased by 42 % and 49 % at the 150 ppb and 300 ppb treatments, respectively, when subjected to drought. The rate of CO_2 assimilation at C_i = 350 µmol.mol^{-1} (A_0), decreased by 60 % at the 0 ppb treatment, remained constant at the 50 ppb treatment, and increased by 29 % and 48 % at the 150 ppb and 300 ppb treatments, respectively. This increase in C_i suggests that reductions in A are due to non-stomatal constraints; i.e. constraints within the mesophyll processes. The ambient control treatment was not subjected to drought due to the prevailing seasonal rain. The induction of drought on the plants caused a 54 % decrease in the carboxylation efficiency (CE) at the 0 ppb treated plants, once again showing the large effect of drought stress. The same trend was evident at the 300 ppb SO_2 treatment with CE decreasing by 71 % in relation to the well watered plants. CE, however, decreased only by 10 % at the 50 ppb treatment and then increased drastically with 55 % at the 150 ppb treatment, indicating that the plants performed better than the drought stressed 0 ppb control plants when the regeneration capacity of RuBP is taken into consideration. The decrease in J_{max} and CE at the 0 ppb and 300 ppb treatment is indicative of the fact that RuBP regeneration capacity became limiting and that the activity of Rubisco decreased. Taking the 38 % increase in the compensation concentration (Γ) into consideration, it is evident that mesophyll limitation played a major role in the inhibition of photosynthetic gas exchange in plants subjected to drought stress at the lowest SO_2 treatment (50 ppb). Γ decreased by 25 % and 18 % in the 150 ppb and 300 ppb drought stressed treatments, respectively. Γ increased by 11 % in the 0 ppb drought stressed plants compared to the well watered plants. The stomatal conductance at C_a = 350 µmol.mol^{-1} (Gs_{350}) decreased by 31 % and 65 % at the 0 ppb and 300 ppb SO_2 treatments, remained constant at the 50 ppb treatment and increased by 41 % at the 150 ppb treatment. Although Gs_{350} of the drought stressed plants increased in relation to the well watered treatment at the 150 ppb treatment, it decreased by 30 % from the values measured 7 days after treatment commenced. At the same time an increase of 67 % occurred in stomatal limitation (ℓ) at the 150 ppb treatment, indicating that the reduction in A is not only due to non-stomatal constraints. Water use efficiency (WUE) decreased with all treatments, and most severely at the 150 ppb treatment (25 %), regardless of the increased Gs_{350} at this treatment level. The intercellular CO_2 concentration at C_a = 350 µmol.mol^{-1}, (Ci_{350}) remained nearly constant, presenting a small increase of less than 5 % with all treatments.

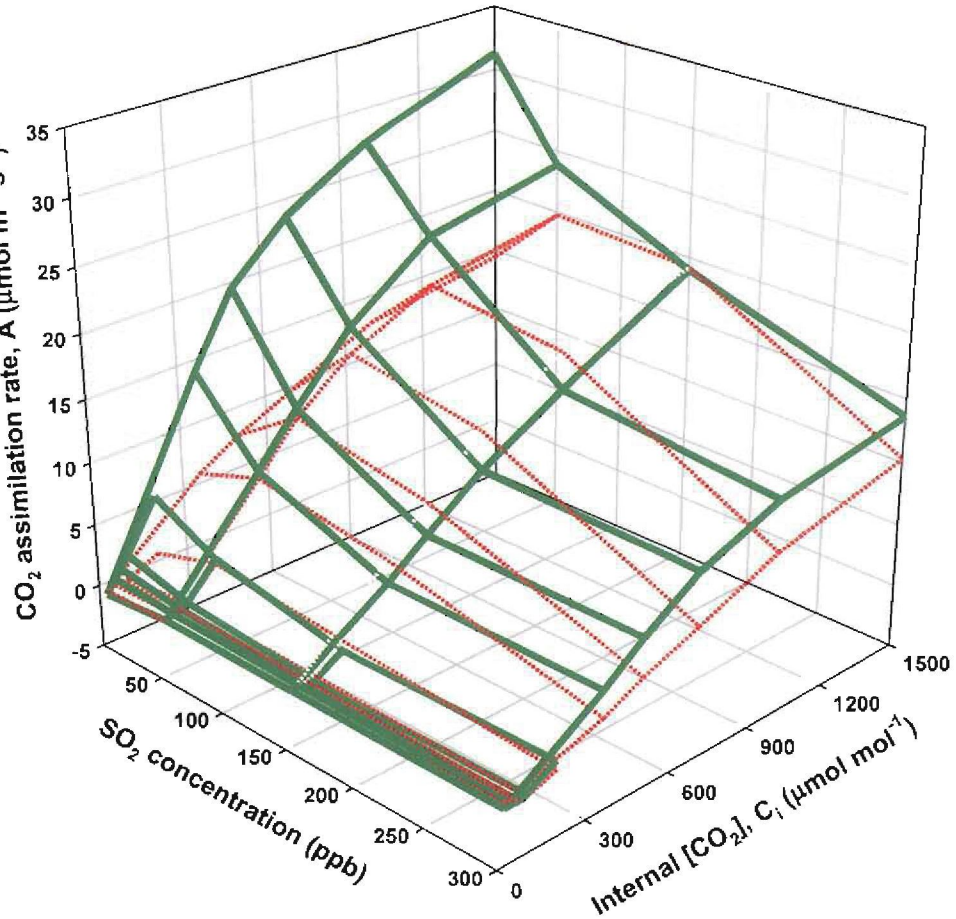


Figure 4.32 Three dimensional representation of the affect of different SO_2 fumigation levels on the A:C_i response of well watered (green) and drought stressed (red) *Glycine max* plants after 28 days' fumigation.

Table 4.11 Means (± standard errors) for gas exchange parameters measured in drought stressed leaves of *Glycine max* (n = 4 plants per SO_2 treatment) after 28 days. Symbols: A_{350}, rate of CO_2 assimilation at C_a = 350 µmol.mol^{-1}; Ci_{350}, intercellular CO_2 concentration at C_a = 350 µmol.mol^{-1}; A_0, rate of CO_2 assimilation at C_i = 350 µmol.mol^{-1}; Gs_{350}, stomatal conductance at C_a = 350 µmol.mol^{-1}; CE, carboxilation efficiency at Γ; J_{max}, maximum rate of CO_2 assimilation; Γ, CO_2 compensation point; ℓ, stomatal limitation of photosynthesis; WUE, water use efficiency, with * and ** indicating significant differences ($p<0.05$ and $p<0.01$ respectively) compared to control plants. Drought stressed means: Ψ_{MD} = -0.6; Ψ_{PD} = -0.2.

	0 ppb SO_2	50 ppb SO_2	150 ppb SO_2	300 ppb SO_2	Ambient Control
Evap (µmol.m^{-2}.s^{-1})	1.81 (0.002**)	2.345 (0.325)	2.718 (0.134)	1.783 (0.479)	5.378 (0.002**)
A_{350} (µmol.m^{-2}.s^{-1})	5.850 (0.001**)	7.8 (0.323)	6.150 (0.409)	2.175 (0.056)	17.375 (0.001**)
Ci_{350} (µmol.mol^{-1})	252.5 (0.429)	255 (0.401)	278 (0.151)	303 (0.033*)	248.75 (0.429)
A_0 (µmol.m^{-2}.s^{-1})	7.288 (0.001**)	10.898 (0.220)	8 (0.386)	2.887 (0.058)	23.675 (0.001**)
Gs_{350} (µmol.m^{-2}.s^{-1})	93 (0.007**)	136.250 (0.228)	161.5 (0.088)	90.5 (0.466)	399.5 (0.007**)
CE (mol.m^{-2}.s^{-1})	0.010 (0.006**)	0.027 (0.269)	0.017 (0.192)	0.004 (0.177)	0.087 (0.006**)
J_{max} (µmol.m^{-2}.s^{-1})	14.475 (0.180)	19.8 (0.187)	19.250 (0.231)	10.35 (0.172)	6.976 (0.180)
Γ (µmol.mol^{-1})	115.5 (0.077)	105.250 (0.239)	85.5 (0.235)	112 (0.466)	56.6 (0.077)
ℓ (%)	20.728 (0.159)	29.849 (0.099)	42.949 (0.487)	22.027 (0.448)	43.998 (0.159)
WUE	2.876 (0.056)	2.978 (0.291)	1.612 (0.209)	1.260 (0.022*)	1.198 (0.056)

4.4.3 Effect of SO_2 on photosynthetic light response in *Glycine max*

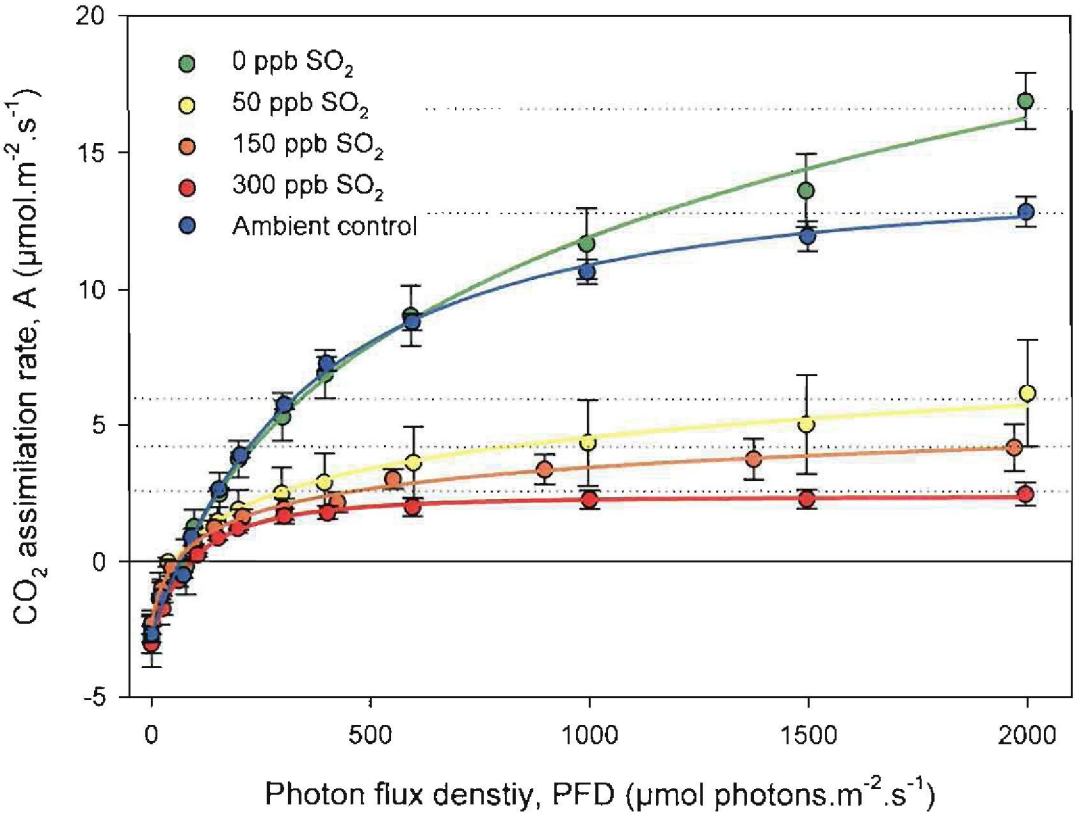


Figure 4.33 Photosynthetic light response curve of CO_2 assimilation rate (A) to photon flux density (PFD) measure in well watered leaves of soybean (*Glycine max*) plants after 14 days of treatment to different SO_2 concentrations. Each value represents a mean (± SE), where n = 4.

Light response curves (A:Q) were obtained for intact leaves following 14 and 35 days' exposure to SO_2 to determine to what extent the incident quantum yield (Φ), or the light saturation point (A_{max}) was affected by fumigation with SO_2 (Table 4.12; Figure 4.33 and Table 4.13; Figure 4.34). The incident quantum yield (Φ) determined from the slope of the initial linear phase (δA/δQ) of the light response curves indicated that SO_2 inhibited Φ severely at all SO_2 levels. Light saturated rates of photosynthesis (A_{max}) reflect the ability of the photosynthetic apparatus to utilise light to fix CO_2 (Genty & Harbinson, 1996). With increasing irradiance (PFD), A increased linearly as CO_2 fixation and electron transport processes are proportional to the photons captured. As expected, A_{max} and Φ increased with increased PDF as photorespiration was gradually overcome. The light saturated rates of net CO_2

uptake (A_{max}), decreased severely with increasing SO_2 concentration, indicating that the CO_2 assimilation capacity was decreased by 68 %, 76 % and 78 % at the 50, 150 and 300 ppb SO_2 levels, respectively, compared to the 0 ppb (Table 4.12; Figure 4.33). This inhibition of the activity of Rubisco could be ascribed to the competitive inhibition of Rubisco for HCO_3^- (Zeigler, 1972). The initial slope of the curve ($\delta A/\delta Q$), is a measure of the photochemical efficiency, Φ or quantum yield (moles CO_2 fixed per moles photons absorbed), specifying the ability of the photosynthetic system to utilise photons for CO_2 fixation at the greatest efficiency when the flux is zero. From the A:Q curves it is clear that the initial slope decreased with increasing SO_2 concentration, indicating that the efficiency to utilise photons for fixing CO_2 decreased. The quantum yield of photosynthesis decreased by 36 %, 9 %, and 9 % at 50 ppb, 150 ppb and 300 ppb, respectively (Table 4.12; Figure 4.33). According to Farquhar *et al.* (1980), CO_2 assimilation is limited at low light by the rate of electron transport and at high light by the capacity of Rubisco. The position of the breaking point between these two limitations determines the convexity, Θ. If the light activation of Rubisco proceeds over the extended light range, the transition becomes more gradual, and will become somewhat lower than expected given a sharp truncation of the electron transport curve by Rubisco. Values listed in Table 4.12 show the severe increase in Θ with increasing SO_2 concentration. Θ increased from 0.014 for the 0 ppb treatment to 0.09 for the 50 ppb and 150 ppb SO_2 levels to 0.6 for the 300 ppb level. This increase in Θ suggested a lower capacity of Rubisco relative to that of electron transport, and the earlier transition to A_{max}. The light compensation point (I_c), i.e. the PFD at which CO_2 uptake is equal to CO_2 release, decreased by 19 % and 16 % at the 50 and 150 ppb treatments, respectively, and increased by 15 % at the 300 ppb treatment. From the A:Q curves conducted for well watered plants, the ambient control plants performed 30 % poorer than the 0 ppb treatment with respect to A_{max} (Table 4.12; Figure 4.33). The Φ value, however, remained similar to the 0 ppb SO_2 treatment. The Θ of the curve for the ambient treatment decreased slightly to 0.04 compared to the 0 ppb SO_2 treatment, suggesting a lower capacity of Rubisco relative to electron transport. The I_c of the ambient treatment increased by 7 % from the 0 ppb SO_2 treatment. A_{max} decreased by 30 % with respect to the 0 ppb treatment. This indicates that the 0 ppb treatment performed better with regard to Rubisco activity and the ability of the photosynthetic system to utilise absorbed photons for CO_2 fixation than the ambient treatment.

Table 4.12 Mean values (± standard errors) for gas exchange parameters measured in well watered leaves of *Glycine max* (n = 4 plants per SO_2 treatment) after 14 days' fumigation with SO_2. Symbols: A_{max}, the asymptote indicating the light-saturated rate of A, (rate of CO_2 assimilation at 2000 µmol photons.$m^{-2}.s^{-1}$); Φ, linear phase (δA/δQ) represents the maximum quantum yield of photosynthesis; Θ, represents the convexity which describe the transition from light limited to light saturated photosynthesis; Ic, light compensation point. * and ** indicate significant differences ($p<0.05$ and $p<0.01$ respectively) compared to control plants.

	0 ppb SO_2	50 ppb SO_2	150 ppb SO_2	300 ppb SO_2	Ambient Control
Φ (mol photons.$m^{-2}.s^{-1}$)	0.03 (0.005*)	0.02 (0.005**)	0.03 (0.01*)	0.04 (0.004*)	0.04 (0.01*)
A_{max} (µmol.$m^{-2}.s^{-1}$)	24.4 (1.0*)	7.83 (2.21)	5.94 (0.42*)	5.29 (0.56*)	17.0 (2.5)
Θ	0.014 (0.03)	0.09 (0.02*)	0.09 (0.04)	0.65 (0.04*)	0.04 (0.02)
I_c (µmol.mol^{-1})	58.3 (0.23)	47.5 (0.34*)	49.0 (0.13)	66.9 (0.65)	62.1 (0.05)
Light sat est (µmol.$m^{-2}.s^{-1}$)	790 (0.32)	428 (0.27)	254 (0.87)	193 (0.65*)	484 (0.75)

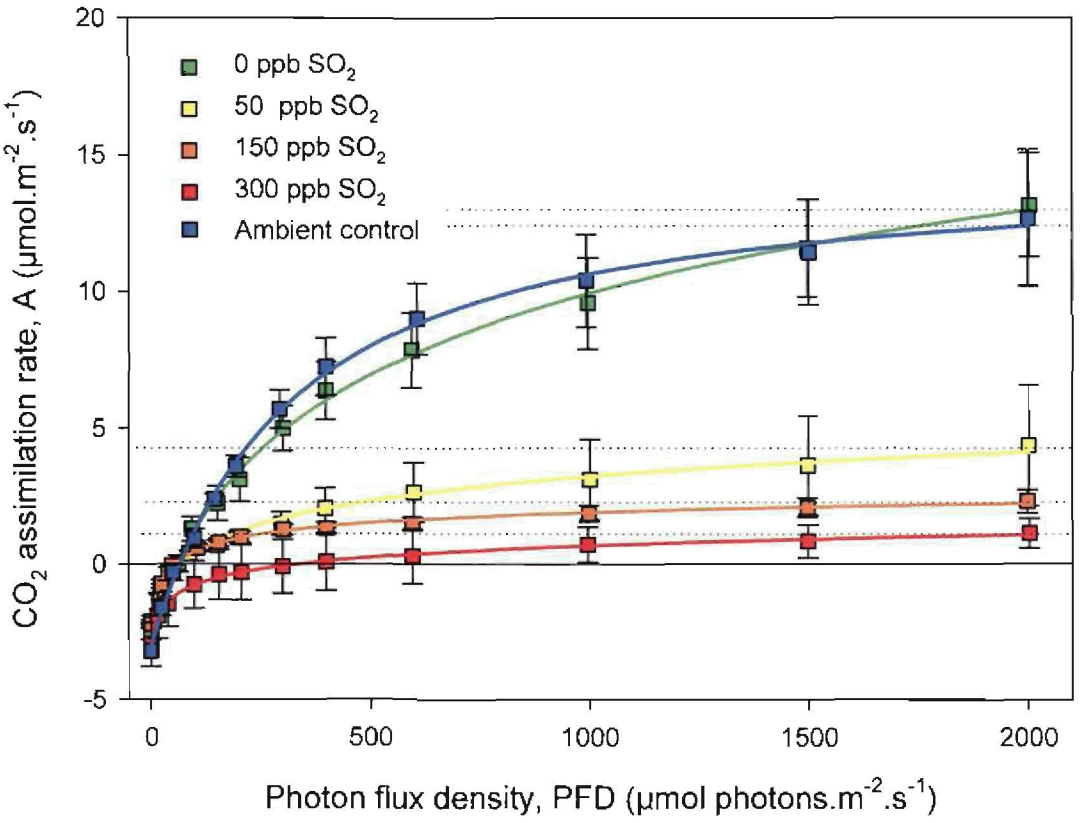


Figure 4.34 Photosynthetic light response curve of CO_2 assimilation rate (A) to photon flux density (PFD) measured in intact drought stressed leaves of soybean (*Glycine max*) plants after 14 days of treatment to different SO_2 concentrations. Each value represents a mean (±SE), where n = 4.

Fumigation with SO_2 in combination with drought stress modified all gas exchange parameters (Table 4.13; Figure 4.34). The light saturation rate of photosynthesis (A_{max}) decreased severely with increasing SO_2 concentration. The light saturated rate of photosynthesis measured in drought stressed plants decreased by 67 %, 81 % and 82 % relative to the control for the 50, 150 and 300 ppb from the 0 ppb drought stressed treatment, respectively. The light saturation rate of photosynthesis for the drought stressed plants decreased to 25 %, 23 %, 43 % and 38 % of the well watered treatments, 0, 50, 150 and 300 ppb SO_2, respectively (Table 4.13; Figure 4.34). The quantum yield of photosynthesis (Φ) determined from the initial linear phase ($\delta A/\delta Q$) of the light response curve was drastically inhibited at all levels of SO_2 fumigation. This means that SO_2 fumigation reduced the efficiency of the test plants to utilise captured photons for CO_2 fixation. The Φ decreased by 63 %, 29 % and 50 % at the 50 ppb, 150 ppb and 300 ppb SO_2 concentrations, respectively. The

transition from the light limited to light saturated photosynthesis indicated by the convexity (Θ) of the curves, increased with increasing SO_2 concentrations, pointing to a decrease in the capacity of Rubisco relative to the capacity of electron transport. The Θ increased from 0.005 to 0.03, 0.04 and 0.05 at the 50, 150, and 300 ppb SO_2 concentration. The Θ was even larger in the drought stressed SO_2 treated plants compared to the well watered plants. The light compensation point (I_c), increased by 15 % at the 50 ppb level, but decreased by 26 % at the 150 ppb level. Even though I_c increased at the 150 ppb level, I_c increased severely to almost double that of the 0 ppb treatment by 97 % at the 300 ppb level. I_c measured in drought stressed plants increased by more than 80 % at the 300 ppb level, compared to that measured in well watered plants at the same level. There was not a large difference between the ambient grown plants and the 0 ppb treated plants subjected to drought stress. Due to the high annual rainfall, the ambient control plants did not experience drought stress opposed to the drought stress induced in the 0 ppb chamber plants.

Table 4.13 Mean values (± standard errors) for gas exchange parameters measured in drought stress leaves of *Glycine max* (n = 4 plants per SO_2 treatment) after 14 days' fumigation. Symbols: A_{max}, the asymptote indicating the light-saturated rate of A (rate of CO_2 assimilation at); Φ, linear phase (δA/δQ) represents the maximum quantum yield of photosynthesis; Θ represents the convexity which describe the transition from light limited to light saturated photosynthesis; and light compensation point, with * and ** indicating significant differences (p<0.05 and p<0.01 respectively) compared to control plants.

	0 ppb SO_2	50 ppb SO_2	150 ppb SO_2	300 ppb SO_2	Ambient Control
Φ (mol photons.$m^{-2}.s^{-1}$)	0.038 (0.004*)	0.014 (0.003)	0.027 (0.01)	0.019 (0.005)	0.043 (0.318)
A_{max} (μmol.$m^{-2}.s^{-1}$)	18.30 (0.58)	6.02 (0.331*)	3.41 (0.252)	3.28 (0.168**)	16.70 (0.795)
Θ	0.005 (0.01)	0.03 (0.03*)	0.04 (0.02*)	0.05 (0.03)	0.009 (0.04)
I_c (μmol.mol^{-1})	56.40 (0.02)	64.8 0 (0.03*)	41.50 (0.01*)	111.00 (0.2)	58.10 (0.03*)
Light sat est (μmol.$m^{-2}.s^{-1}$)	541 (0.23)	492 (0.45)	169 (1.23)	287 (0.98)	443 (0.64)

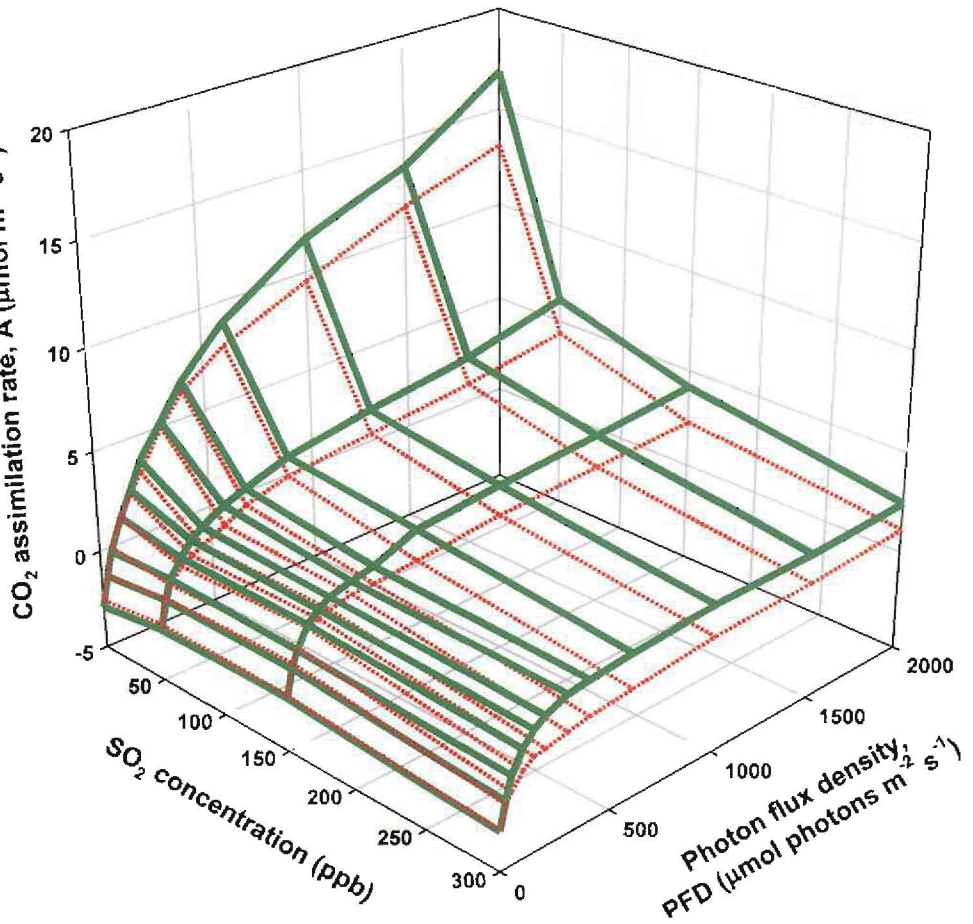


Figure 4.35 Light response curve of plants subjected to 14 days' fumigation with SO_2. Interaction between CO_2 assimilation capacity, light intensity and SO_2 fumigation level of soybean plants which were well watered (green) and drought stressed (red). Note that at all the SO_2 levels, the drought stressed plants were affected more severely. Values calculated for ambient grown plants are not shown.

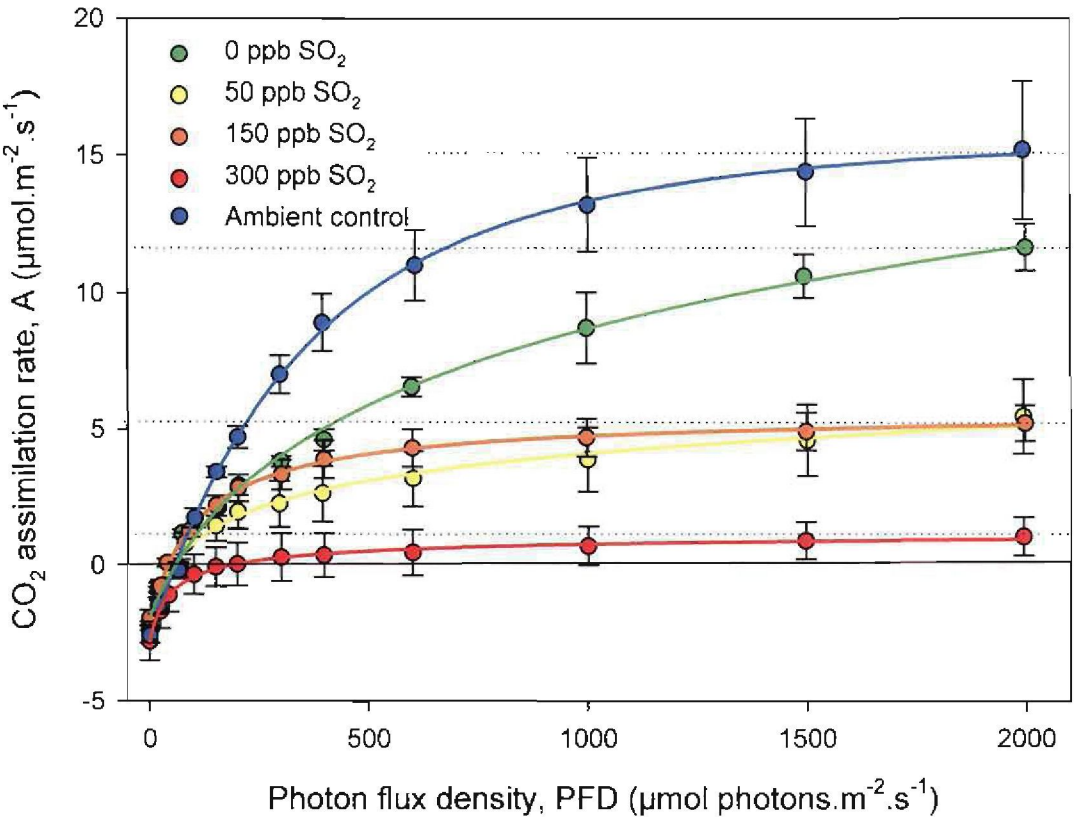


Figure 4.36 Photosynthetic light response curve of CO_2 assimilation rate (A) to photon flux density (Q) measure in well watered leaves of soybean (*Glycine max*) plants after 35 days of fumigation with SO_2. Each value represents a mean (±SE), where n = 4.

Photosynthetic light response curves obtained after 35 days of fumigation with SO_2 show that photosynthesis became saturated at a substantially lower PDF, indicating that factors such as electron transport, Rubisco activity, or the metabolism of triose phosphates have become limiting (Genty & Harbinson, 1996). The light saturation rate of photosynthesis (A_{max}), decreased by 41 %, 40 % and 70 % at the 50 ppb, 150 ppb and 300 ppb concentrations, respectively (Table 4.14; Figure 4.36). At the light saturation point, photosynthesis is regarded as CO_2 limited (Farquhar & Sharky, 1982), reflecting the inability of the carbon metabolism enzymes to fully utilise the absorbed light energy. It is evident that exposure to even the lowest SO_2 level used in this experiment inhibited photosynthesis severely. The initial slope (in the light limited range) of the light response curve yielding the linear relationship between photon flux density and photosynthetic rate, gives the maximum quantum yield of photosynthesis (Farquhar & Sharky, 1982). The decrease in the maximum quantum

yield of photosynthesis measured in plants exposed to SO_2 indicates that SO_2 impaired the ability of the photosynthetic system to utilise the required number of absorbed photons required to fix one molecule of CO_2, to evolve one molecule of O_2, or to initiate a photochemical event. Therefore, the point at which photosynthetic CO_2 uptake exactly balances CO_2 release by photorespiration, namely the light compensation point, increased with increasing SO_2 concentration (Coombs *et al.*,1987). The light compensation concentration increased by 10 % at the 50 ppb SO_2 level, and unexpectedly decreased by 11 % at the 150 ppb treatment (Figure 4.36 ; Table 4.14). Although the I_c decreased at the 150 ppb level, it increased severely, as expected, by 78 % at the 300 ppb level, compared to the 0 ppb control plants.

Table 4.14 Mean values (± standard errors) for gas exchange parameters measured in well watered leaves of *Glycine max* (n = 4 plants per SO_2 treatment) after 35 days' fumigation with SO_2. Symbols: A_{max}, the asymptote indicating the light-saturated rate of A, (rate of CO_2 assimilation at 2000 µmol photons.m^{-2}.s^{-1}); Φ, initial linear phase (δA/δQ) represents the maximum quantum yield of photosynthesis; Θ, represents the convexity which describe the transition from light limited to light saturated photosynthesis; I_c, light compensation point. * and ** indicate significant differences ($p<0.05$ and $p<0.01$ respectively) compared to the control plants.

	0 ppb SO_2	50 ppb SO_2	150 ppb SO_2	300 ppb SO_2	Ambient Control
Φ (mol photons.m^{-2}.s^{-1})	0.04 (0.004*)	0.039 (0.012)	0.034 (0.005*)	0.023 (0.01)	0.04 (0.003)
A_{max} (µmol.m^{-2}.s^{-1})	12.5 (0.682*)	7.32 (0.465*)	7.52 (0.119*)	3.74 (0.126**)	19.5 (0.432)
Θ	0.001 (0.05*)	0.006 (0.08)	0.05 (0.45*)	0.072 (0.03*)	0.002 (0.07*)
I_c (µmol.mol^{-1})	56.2 (0.08)	62.1 (0.03*)	50.1 (0.23*)	100 (0.54*)	57.0 (0.87)
Light sat est (µmol.m^{-2}.s^{-1})	584 (0.09)	230 (0.07*)	154 (0.65)	101 (0.54)	481 (0.04)

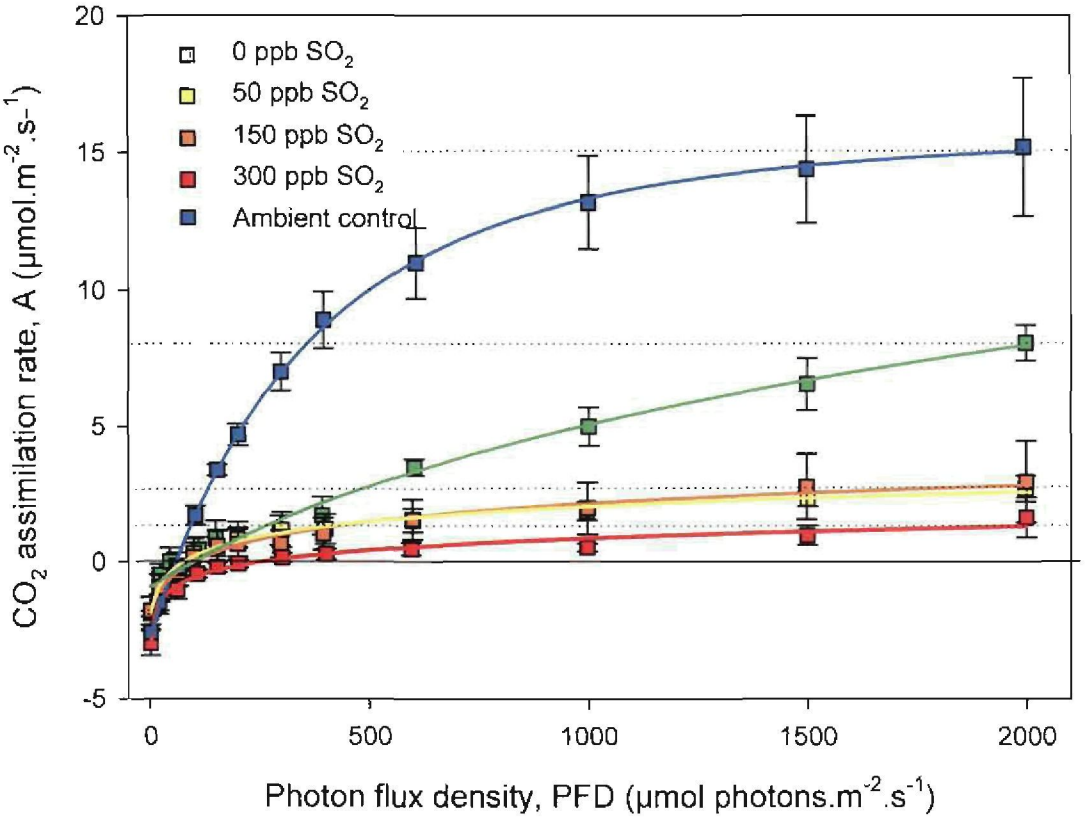


Figure 4.37 Photosynthetic light response curve of CO_2 assimilation rate (A) to photon flux density (Q) measure in drought stressed leaves of soybean (*Glycine max*) plants after 35 days of treatment to different SO_2 concentrations. Each value represents a mean (±SE), where n = 4.

According to the data presented in Table 4.15, drought stress enhanced the inhibitory effect of SO_2 on the photosynthetic rate of the treated plants. Although the 0 ppb treated plants were also severely affected by drought stress, the drought stressed SO_2 treated plants performed 48 %, 43 % and 56 % poorer with respect to the light saturation rates of photosynthesis for the 50 ppb, 150 ppb and 300 ppb treatments, respectively, compared to the 0 ppb drought stressed plants. The light saturation rate of photosynthesis decreased with 35 %, 42 % 38 % and 4 % for the 0, 50, 150 and 300 ppb SO_2 treated plants, respectively, compared to the 0, 50, 150 and 300 ppb well watered SO_2 treatments, respectively. The quantum yield of photosynthesis for the drought stressed plants decreased by 50 %, 49 %, 44 % and 13 % for the 0, 50, 150 and 300 ppb SO_2 treatments, respectively, compared to the well watered plants treated at the same SO_2 concentrations, respectively. It is thus evident that drought stress in combination with SO_2 had a much larger inhibitory effect on the plants than the SO_2 or drought alone. This was evident from the very large decrease

in the initial slopes of the light response curves of the drought stressed fumigated plants (Table 4.15; Figure 4.37). The Φ of the SO_2 treated and drought stressed plants did not differ much from the values calculated for the 0 ppb drought stressed plants, but decreased severely by 50 %, 49 %, 44 % and 13 % for 0, 50, 150 and 300 ppb SO_2 treated plants, respectively, compared to the values calculated for the well watered plants treated at the same SO_2 concentrations. The increase in convexity of the light response curves of the drought stressed SO_2 treated plants with increasing SO_2 concentration was more than in the case of the well watered plants treated to the corresponding concentration of SO_2 (Table 4.15; Figure 4.37). The compensation concentration, representing the point where CO_2 uptake equals CO_2 release by mitochondrial respiration and photorespiration, increased by 21 % at the 150 ppb level and increased severely with 121 % at the 300 ppb SO_2 treatment, compared to the 0 ppb drought stressed treatment. The I_c increased even more when compared to the well watered SO_2 treated plants. I_c increased by 22 % for the 0 ppb drought stressed treatment compared to the 0 ppb well watered treatment, and increased severely with 66 % and 59 % at the 50 and 300 ppb levels for the drought stressed plants, respectively, compared to the well watered plants treated to the same SO_2 concentrations.

Table 4.15 Mean values (± standard errors) for gas exchange parameters measured in drought stressed leaves of *Glycine max* (n = 4 plants per SO_2 treatment) after 35 days' fumigation with SO_2. Symbols: A_{max}, the asymptote indicating the light-saturated rate of A, (rate of CO_2 assimilation at); Φ, linear phase ($\delta A/\delta Q$) represents the maximum quantum yield of photosynthesis; Θ, represents the convexity which describe the transition from light limited to light saturated photosynthesis; I_c, light compensation point. * and ** indicate significant differences ($p<0.05$ and $p<0.01$ respectively) compared to control plants.

	0 ppb SO_2	50 ppb SO_2	150 ppb SO_2	300 ppb SO_2	Ambient Control
Φ (mol photons.m^{-2}.s^{-1})	0.007 (0.269*)	0.03 (0.008)	0.017 (0.006*)	0.0331 (0.003)	0.046 (0.003)
A_{max} (µmol.m^{-2}.s^{-1})	8.16 (1.75)	4.25 (0.240*)	4.67 (0.375**)	3.61 (0.74*)	19.5 (0.432)
Θ	0.007 (0.24)	0.08 (0.79*)	0.09 (0.45)	0.9 (0.04*)	0.007 (0.86)
I_c (µmol.mol^{-1})	159 (0.09)	54.9 (0.01*)	83.4 (0.06*)	72.1 (0.07*)	57.0 (0.03)
Light sat est (µmol.m^{-2}.s^{-1})	1336 (0.23)	195 (0.34)	356 (0.54)	181 (0.55)	481 (0.67)

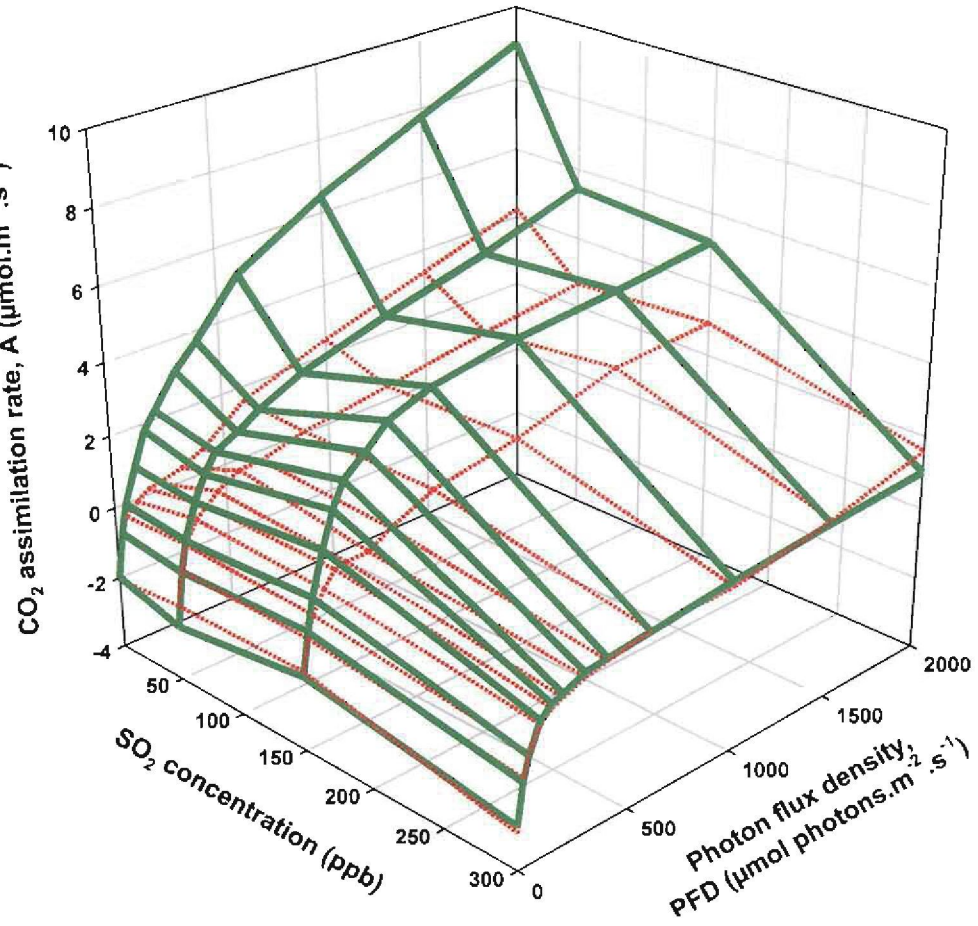


Figure 4.38 Light response curve after 35 days' fumigation with SO_2. Interaction between CO_2 assimilation capacity, light intensity and SO_2 fumigation level of well watered (green) and drought stressed (red) soybean plants. Note that at all the SO_2 levels the drought stressed plants were affected more severely. Each value represents a mean (±SE), where n = 4.

4.4.4 Effect on stomatal conductance

4.4.4.1 Effect of SO_2 on stomatal conductance in *Brassica oleracea*

SO_2 has been documented to both open and close stomata, depending upon species, SO_2 concentration and environmental conditions, e.g. drought. After 28 days of fumigation, stomatal conductance in well watered *Brassica oleracea* increased drastically by 86%, 99% and 44% at the 50, 150 and 300 ppb

concentrations, respectively, compared to the control. It was already apparent that stomata opened to a lesser degree in plants treated with the 300 ppb concentration. After 35 days, stomatal conductance increased again drastically by 36% and 54% at the 50 and 150 ppb levels, but decreased severely by 38% at the 300 ppb SO_2 concentration. This would indicate that high concentrations result in partial stomatal closure and low or intermediate concentrations (i.e. 50 ppb and 150 ppb) increase conductance. Drought stress induced partial stomatal closure at all SO_2 concentration levels. After 28 days, stomatal conductance decreased by 1 %, 54 % and 63 % at the 50, 150 and 300 ppb SO_2 levels, respectively, compared the drought stressed control. After 35 days, stomatal conductance in drought stressed plants decreased by 35 %, 58 % and 76 % at the 50, 150 and 300 ppb levels, respectively, compared to the drought stressed control.

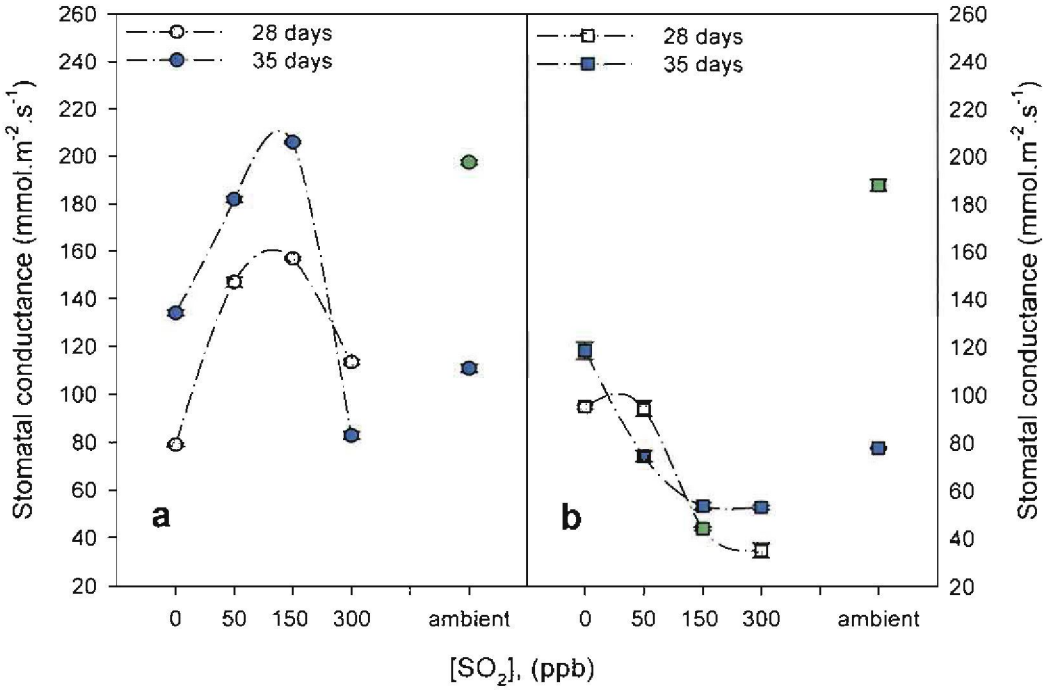


Figure 4.39 Porometric stomatal conductance measured in well watered (a) and drought stressed (b) *Brassica oleracea* plants after 28 days' (green) and 35 days' (blue) SO_2 fumigation.

4.4.4.2 Effect of SO_2 on stomatal conductance in *Glycine max*

Stomtal conductance measured in well watered *Glycine max* plants indicates that stomata responded much different to SO_2 fumigation compared to the well watered

Brassica *oleracea* plants. After 7 days, stomatal conductance of well watered *Glycine max* decreased drastically by 8 % and 30 % at the 50 and 150 ppb levels, respectively, compared to the control. Stomatal response in the 300 ppb treated plants did not differ from the control plants. After 28 days, stomatal conductance in well watered *Glycine max* decreased drastically at all treatment levels. Stomatal conductance decreased by 9 %, 4 % and 57 % at the 50, 150 and 300 ppb concentrations, respectively, compared to the control plants. The drought stressed plants displayed the opposite. After seven days' fumigation, stomatal conductance of the drought stressed *Glycine max* increased by 3 % at the 50 ppb level, after which it decreased by 6 % and 31 % at the 150 and 300 ppb levels, respectively, compared to the drought stressed control plants. After 28 days, stomatal conductance increased slightly by 3 % at the 50 ppb level, after which it increased drastically by 67 % and 61 % at the 150 and 300 ppb concentrations, respectively, compared to the drought stressed control plants.

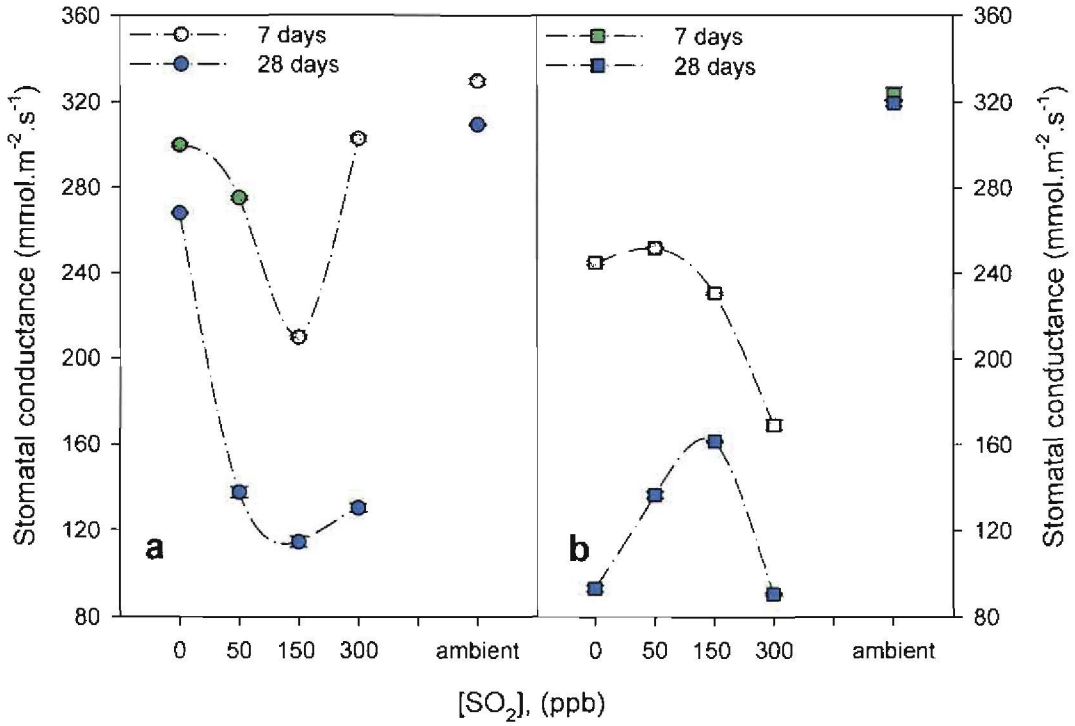


Figure 4.40 Porometric stomatal conductance measured in well watered (a) and drought stressed (b) *Glycine max* plants after seven days' (green) and 28 days' (blue) SO_2 fumigation.

4.4.5 Effect of SO_2 on fast phase *chlorophyll a* fluorescence kinetics

Chlorophyll a fluorescence transients (O-J-I-P) were recorded weekly on dark-adapted intact leaves of *Brassica oleracea* and *Glycine max.* When plotted on a logarithmic time scale, the *Chl a* fluorescence transients started from an initial level of F_0 and increased up to a maximum F_M (peak P), which can be considered as representing the maximum fluorescence yield, since the light applied (600 $W.m^{-2}$, peak at 650 nm) is high enough to ensure the closure of all the reaction centres. Translation of the measured O-J-I-P fluorescence transients by the Biolizer computer programme (Manoldo-Rodriguez, 2002) provided the biophysical parameters that quantified the energy fluxes through PSII as well as the performance index.

4.4.5.1 Effect of SO_2 on PSII in *Brassica oleracea*

The multi-parametric description of structure and function of PSII of the treatments, presented by an octagonal line, provided a direct visualisation of the behaviour of the plants under different water regimes in the absence of, and in combination with drought stress (Figures 4.41 and 4.42). Changes occurred in the phenomenological energy fluxes (per cross section) when well watered plants were fumigated with SO_2. Well watered *Brassica oleracea* plants displayed decreases in the electron transport per cross section (ET_0/CS_0), as well as a concomitant decrease in the density of the reaction centres (RC/CS_0) (Figure 4.41). The phenomenological trapping flux also decreased. The results show that the specific energy fluxes (per reaction centre) through PSII were rather insensitive to SO_2 treatment (Figure 4.41). However, when drought was induced (Figure 4.42), ABS/RC, which is regarded as a measure of "antenna size" (Krüger *et al.*, 1997; Strasser *et al.*, 2004) increased by 3 %, 5 % and 8 % at the 50, 150 and 300 ppb SO_2 levels after 28 days of fumigation. These increases in antenna size compensated for the concomitant decrease in the density of the reaction centres (RC/CS_0) due to inactivation of the reaction centres. At the same time the specific trapping flux (TR_0/RC) increased slightly when drought was induced (Figure 4.42). As a result, the quantum yield of primary photochemistry ($\varphi P_0 = F_V/F_M$) remained almost constant with increasing SO_2 concentration (Figure 4.42). The inhibitory effect of the combined SO_2 and drought stress was, however, evident in the decrease in density of reaction centres (RC/CS) with increasing SO_2 levels, which resulted in a corresponding decrease in electron transport per cross section (ET_0/CS) (Figure 4.42).

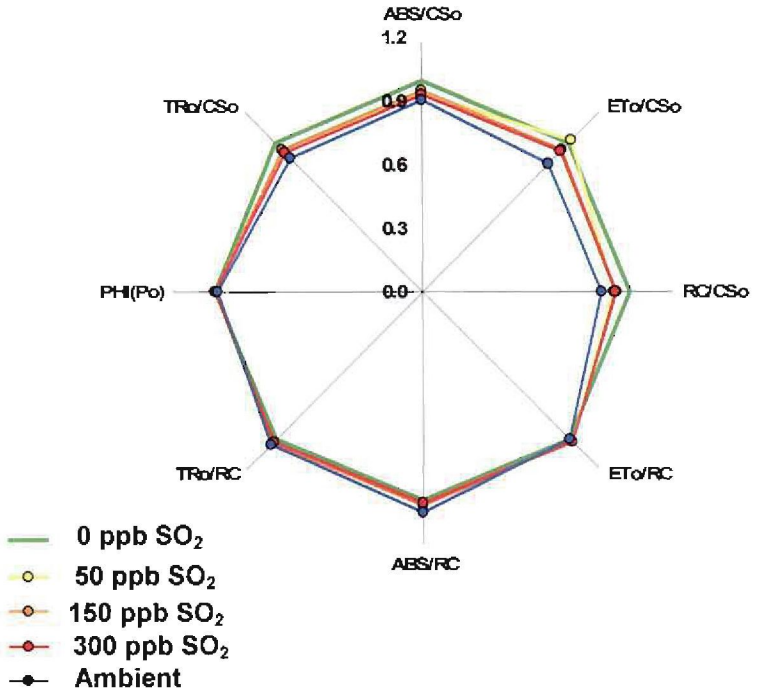


Figure 4.41 Fractional changes in specific and phenomenological energy fluxes through PSII measured in intact leaves of well watered *Brassica oleracea* plants after 28 days of fumigation with SO_2.

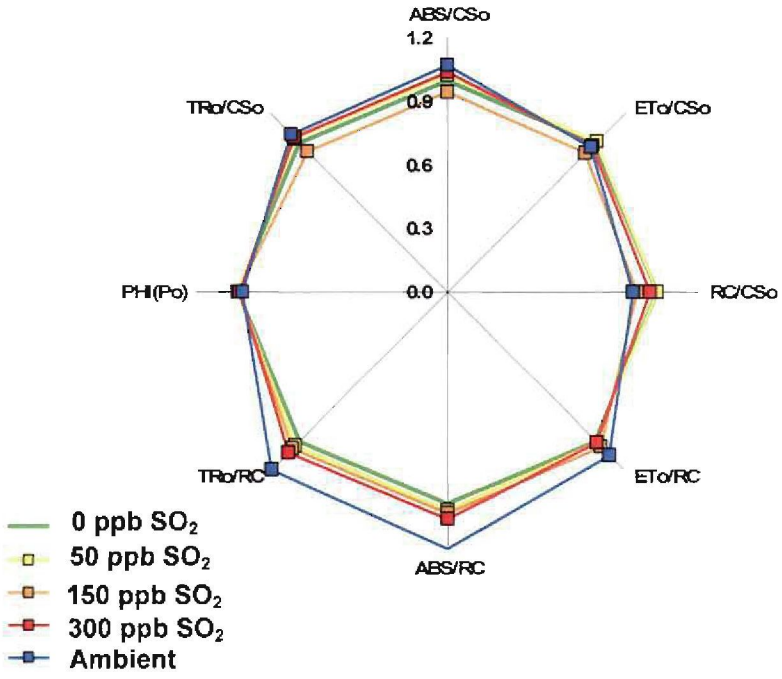


Figure 4.42 Fractional changes in specific and phenomenological energy fluxes through PSII measured in intact leaves of drought stressed *Brassica oleracea* plants after 28 days of fumigation with SO_2.

The performance index (PI_{TOT}) which is a multiparametric expression taking into consideration four independent parameters, namely efficiency of absorption of light energy (RC/ABS) (chlorophyll concentration), quantum efficiency of trapping of excitation energy [$\varphi_{Po}/(1-\varphi P_o)$], conversion of trapped excitation energy to electron transport [$\Psi_0/(1-\Psi_0)$] and the probability for reduction of end acceptors [$(\delta_0 / 1-\delta_0)$] (e.g. NADP) is the most sensitive parameter for detection and quantification of most stresses (Strasser *et al.*, 1999; Smit *et al.*, 2008). The data show that SO_2 had a concentration-dependant effect on PI_{TOT} in *Brassica oleracea* (Figures 4.43a and 4.43b). After 28 days, the PI_{TOT} for well watered SO_2 fumigated plants decreased by 12 %, 13 % and 23 % at the 50, 150 and 300 ppb SO_2 concentrations, respectively; compared to the 0 ppb SO_2 treated plants that were well watered (Figure 4.43a). After 35 days, however, no concentration dependant relationship was evident. The explanation for the decline in effect may be found in the concomitant reduction in stomatal conductance at the corresponding SO_2 levels (Figure 4.39a), resulting in a much reduced conductance of also SO_2 and finally reduced inhibition of the electron transport rate. It has been shown that when the stomata close, CO_2 is entirely replaced by O_2 as an acceptor of electrons from PSII (Cornic, 1994). Furthermore, similar patterns with regard to the effect of different SO_2 concentrations in combination with drought were visible for drought stressed plants after 28 days. After 35 days' fumigation, PI_{TOT} increased in excess of 40 % in plants subjected to drought stress (Figure 4.43b).

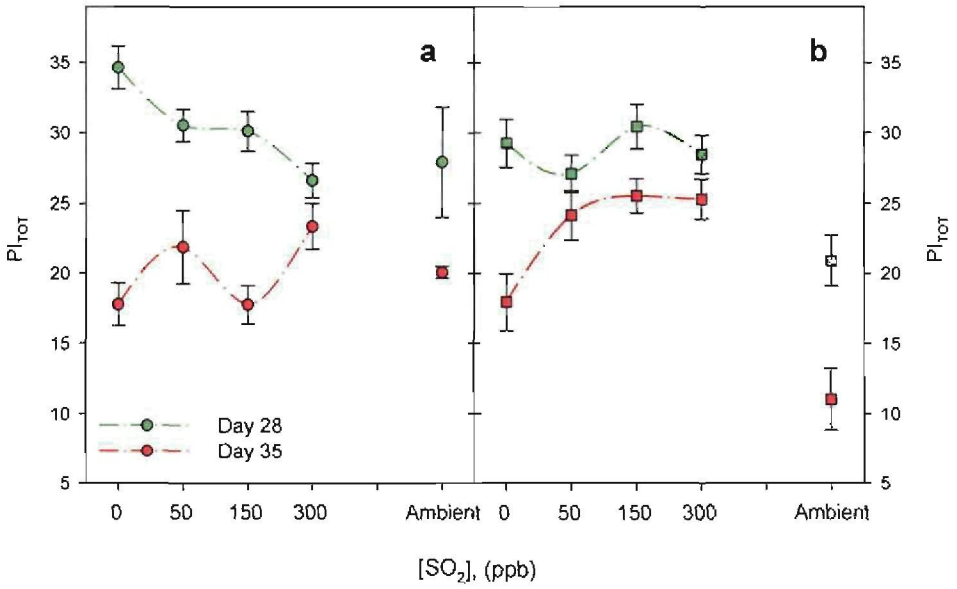


Figure 4.43 Performance index total (PI_{TOT}) measure after 28 and 35 days' fumigation with SO_2 in well watered (a) and drought stressed (b) *Brassica oleracea* plants. Each value represents a mean (± SE), where n = 6.

Using PI_{TOT} as a measure of SO_2 (drought) induced stress, it was possible to differentiate between the effects of SO_2 alone and SO_2 in combination with drought, on the individual constituent parameters of the driving force (Figure 4.44a and 4.44b). PI_{TOT} is based on the following equation (for the conceptual approach and derivation of the equation see Strasser *et al.*, 1999; Van Heerden *et al.*, 2003; Smith *et al.*, 2008):

$$\Delta DF_{TOT} = \Delta\log(PI_{TOT}) = \Delta\log\left(\frac{RC}{ABS}\right) + \Delta\log\left(\frac{\varphi P_0}{1-\varphi P_0}\right) + \Delta\log\left(\frac{\Psi_0}{1-\Psi_0}\right) + \Delta\log\left(\frac{\delta_0}{1-\delta_0}\right)$$

Figure 4.5.4 presents the changes in the constituent partial driving forces expressed as difference, (ΔDF) with respect to their corresponding control [ΔDF_{TOT} = ((DF_{SO2} – $DF_{control}$) / $DF_{control}$)]. (Thus, the logarithm of the performance index (PI_{TOT}), defined as the driving force of photosynthesis, DF_{TOT} = log [PI_{TOT}] summarise the four driving forces: $\Delta DF_{TOT} = \Delta DF_{RC} + \Delta DF_{\varphi P0}\, \Delta DF_{\psi 0} + \Delta DF\ \delta_0$).

Twenty eight days of SO_2 fumigation in well watered *Brassica oleracea* resulted in inhibition of all parameters of the DF_{TOT} (Figure 4.44a). The efficiency of absorption of light energy (RC/ABS) decreased by 2 %, 3 % and 4 % at the 50, 150 and 300 ppb levels, respectively, to the control, indicating that the efficiency of light absorption was almost not affected. The same was true for the drought stressed plants: RC/ABS decreased by 3 %, 1 % and 3 % at the 50, 150 and 300 ppb levels, respectively, relative to the drought stressed control plants. In the well watered plants, trapping of excitation energy [$\varphi P_o/(1-\varphi P_o)$] decreased slightly by 1 %, 1 % and 2 % at the 50, 150 and 300 ppb levels, respectively, compared to the control plants, indicating the low sensitivity of this parameter towards SO_2 stress. The conversion of excitation energy to electron transport [$\Psi_0/(1-\Psi_0)$], however, decreased by 7 %, 9 % and 17 % at the 50, 150 and 300 ppb levels, respectively, compared to the control plants. The probability for formation of reducing equivalents [(δ_0 / 1- δ_0)] proved not to be very sensitive to SO_2 treatment. This parameter remained almost constant relative to the control plants at the 50 and 150 ppb level, but increased slightly by 3 % at the 300 ppb level, compared to the well watered control plants.

In *Brassica oleracea* plants fumigated with SO_2 and simultaneously subjected to drought (Figure 4.44b), trapping of excitation energy [$\varphi P_o/(1-\varphi P_o)$] decreased by 2 % at the 50 ppb level, remained the same at the 150 ppb and increased by 5 % at the 300 ppb level, when compared to the control subjected to drought only. [$\Psi_0/(1-\Psi_0)$] increased drastically by 20 % and 35 % at the 50 and 300 ppb levels, respectively,

but remained the same at the 150 ppb level, when compared to the drought stressed control plants. $[\Psi_0/(1- \Psi_0)]$, representing the probability for the conversion of trapped excitation energy to electron transport proved to be a very sensitive parameter also in the case of the drought stressed treatment, which largely contributed to the change in DF_{TOT} at the 300 ppb SO_2 level (Figures 4.44a and b). In SO_2-fumigated drought stressed plants, $[\delta_0 / (1- \delta_0)]$ showed a SO_2 concentration dependant decrease. $[\delta_0 / (1- \delta_0)]$ decreased by 4 %, 6 % and 8 % at the 50, 150 and 300 ppb levels, respectively, compared to the drought stressed control plants. The partial driving forces most affected, in both well watered and drought stressed SO_2-fumigated plants, thus were the probability for conversion of trapped excitation energy to electron transport beyond Q_A, namely log $[\Psi_0 / (1- \Psi_0)]$ (green line), and secondly the probability for reduction of end acceptors log $[\delta_0 / (1- \delta_0)]$ (black line). The comparison of the chamber treated plants with ambient grown plants indicated that the chambered plants were stimulated by the higher temperatures inside the chambers over the winter period. All constituent components of the DF_{TOT} for the ambient plants were much lower compared to the chambered control plants, indicating harsher conditions outside. Also here, $[\Psi_0 / (1- \Psi_0)]$ was the most sensitive parameter (results not shown).

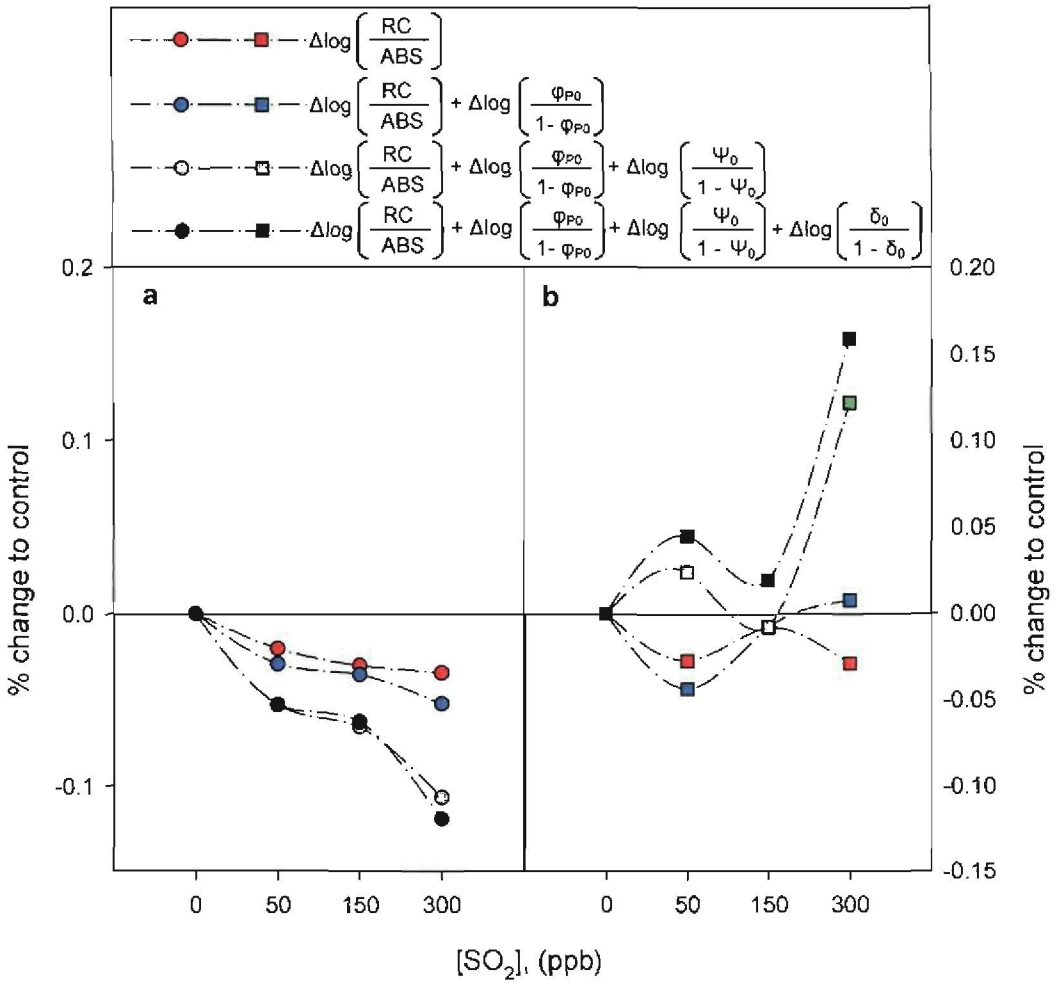


Figure 4.44 Driving force total (DF_{TOT}) measure after 28 days' fumigation with SO_2 in well watered (a) and drought stressed (b) *Brassica oleracea* plants. Each value represents the mean, where n = 6.

4.4.5.2 Effect of SO_2 on PSII in *Glycine max*

The behaviour of the photosynthetic apparatus of *Glycine max* subjected SO_2 exposure under well watered and drought stressed conditions was quantified by the analysis of the recorded fluorescence transients according to the JIP-test. An important future to point out is the fact that F_0 of the *chlorophyll a* fluorescence transients of the test plants at day 0, before fumigation commenced, were remarkably similar. F_0 indicates that the plants were completely dark adapted (i.e. RC fully open) and physiologically very homogenous. The *chlorophyll a* fluorescence kinetics once again showed that SO_2 has a concentration dependant inhibitory effect, as was seen

in data previously presented in this chapter. The *chlorophyll a* fluorescence kinetics pointed out that drought aggravated the inhibitory effect of SO_2.

The average fast fluorescence transients presented on a logarithmic scale and normalised on 50µs (F_0) and 2ms (F_J) of *Glycine max* (Figures 4.45 and 4.46) of plants treated with different SO_2 concentrations under two watering regimes, indicate that the major effect of SO_2 alone or in combination with drought, mainly occurred in the multiple turn-over events of PSII function, i.e. in the transition J (2ms) to P (700ms). The transition from O to J represents the single turnover range of the transient (i.e. Q_A only reduced once) which reflects mainly photochemical reactions leading to the reduction of the electron acceptor Q_A, while the J to P part of the transient is strongly affected by the subsequent dark reactions in the electron transport chain (Strasser *et al.*, 1999). Normalised transients of both well watered and drought stressed *Glycine max* plants showed a concentration depended decrease in the multiple turn-over phase of PS II. Well watered plants fumigated with SO_2 showed an inhibition in the transients at the 150 and 300 ppb SO_2 levels. It is worth noting that the transients (yellow circles) of the well watered plants (Figure 4.47) indicate a stimulation of PSII-activity at the lowest (50 ppb) SO_2 level, a phenomenon also pointed out by other measures of growth used in this study (Section 4.3). However, in plants that were fumigated at 50 ppb and simultaneously subjected to drought (Figure 4.48), no stimulation occurred. The concentration dependant effect was reversed, i.e. the 300 ppb treated plants performed better than the 150 ppb treatment, while the 50 ppb treatment was inhibited the most. This phenomenon could be due to induced stomatal closure at intermediate and high SO_2 levels (Darrall, 1989). It is well known that low concentrations of SO_2 may directly or indirectly disturb stomatal mechanisms, resulting in impaired stomatal closure even when water deprivation prevails (Heath, 1980).

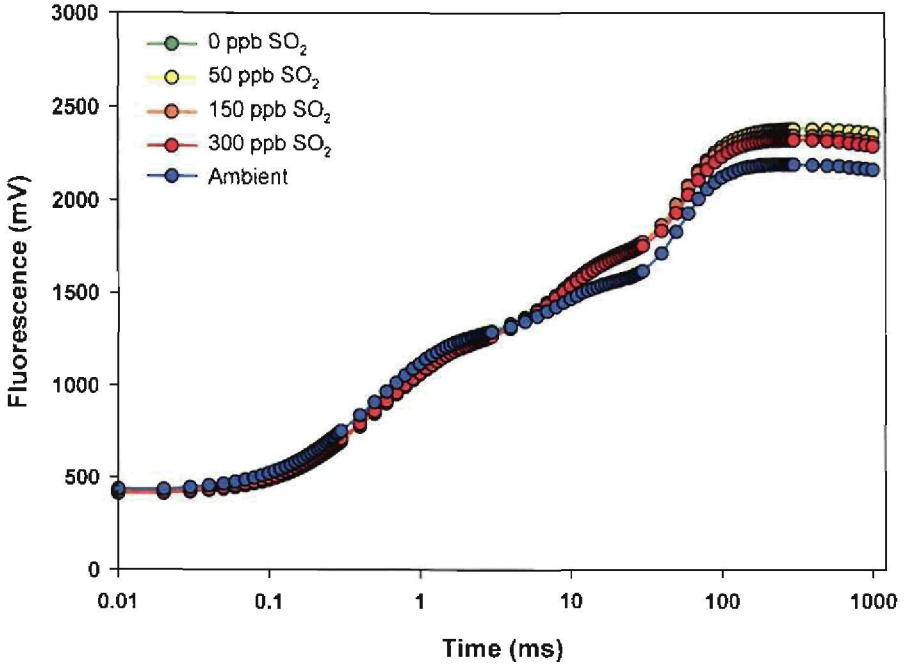


Figure 4.45 Raw *chlorophyll a* fluorescence transients measured in intact leaves of well watered *Glycine max* plants before fumigation commenced.

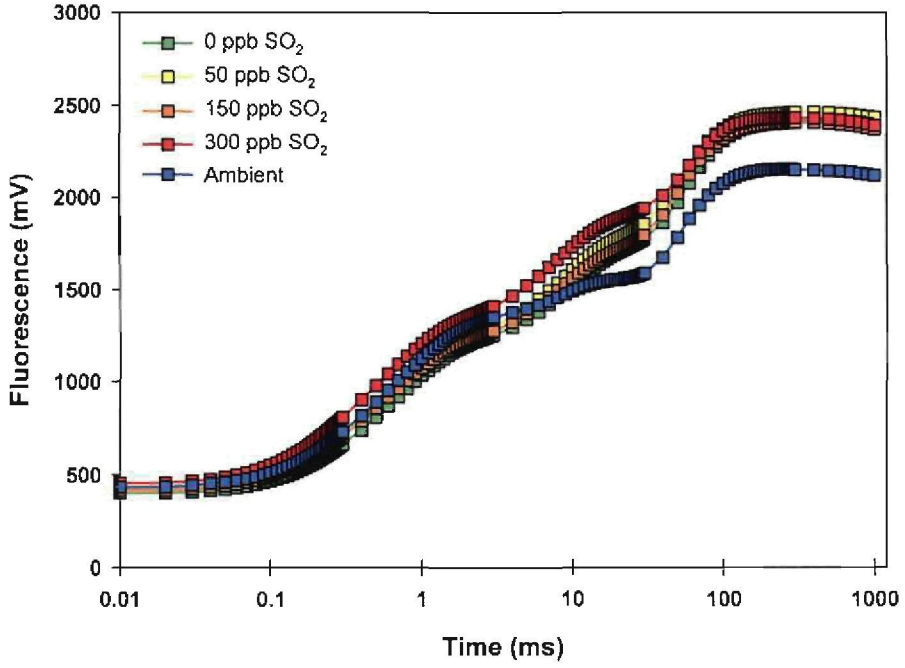


Figure 4.46 Raw *chlorophyll a* fluorescence transients measured in intact leaves of drought stressed *Glycine max* plants before fumigation commenced.

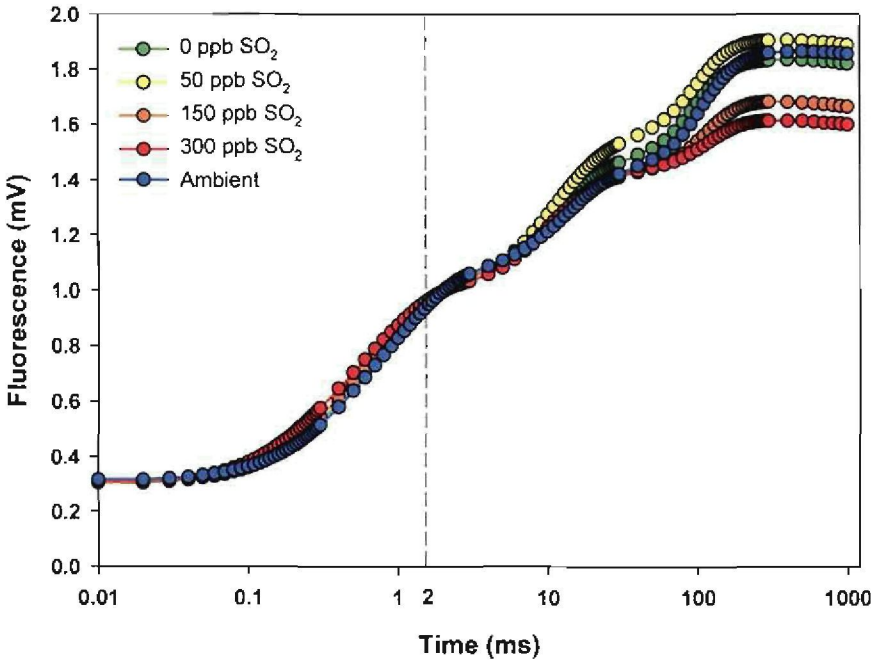


Figure 4.47 ***Chlorophyll a*** **fluorescence transients normalised between 0.05 and 2 ms for well watered** ***Glycine max*** **plants after 28 days' fumigation with SO_2, indicating the relative change in the single turnover phase (0 – 2 ms) and the multiple turnover phase (2 ms – 1 000 ms).**

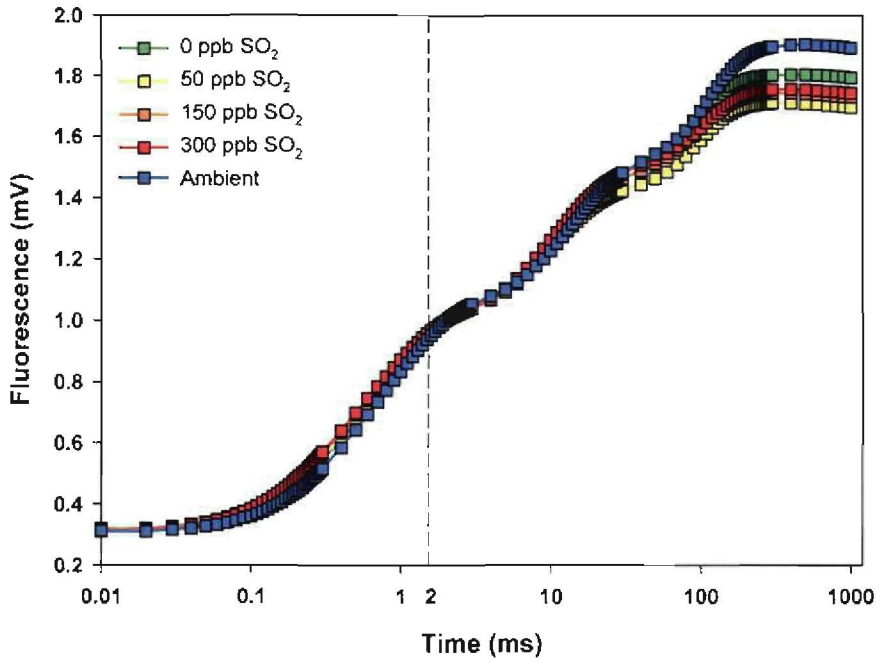


Figure 4.48 ***Chlorophyll a*** **fluorescence transients normalised between 0.05 and 2 ms for drought stressed** ***Glycine max*** **plants after 28 days' fumigation with SO_2, indicating the relative change in the single turnover phase (0 – 2 ms) and the multiple turnover phase (2 ms – 1 000 ms).**

The multiparametric radar plots depicted in Figure 4.49 and Figure 4.50 show SO_2 and drought stress-induced changes that occurred after 28 days of fumigation in selected JIP-test parameters which describe PSII structure and function at 28 days of SO_2 fumigation. Values of all parameters are expressed relative to the 0 ppb treatment (regular octagonal [green] line). Plants that were well watered and treated with SO_2 (Figure 4.49) showed a stimulation in electron transport per excited cross section (ET_0/CS) at the lowest (i.e. 50 ppb) treatment level and decreased with increasing concentration by 6 % and 14 % at the 150 and 300 ppb levels, respectively, compared to the control plants. These reductions in ET_0/CS at the intermediate and high treatment levels were mainly due to a decrease in the density of reaction centres per excited cross section (RC/CS). Increased SO_2 concentrations led to a decrease in the density of active PSII reaction centres (RC/CS). RC/CS decreased by 4 %, 4 % and 18 % at the 50, 150 and 300 ppb levels, respectively, compared to the control plants (Figure 4.49). Figure 4.59 also indicates a concomitant increase in antenna size (ABS/RC) with increasing SO_2 concentrations in well watered plants. ABS/RC increased by 2 %, 8 % and 24 % at the 50, 150 and 300 ppb levels, respectively, compared to the control plants. The maximum trapping flux (TR_0/RC) also increased by 2 %, 6 % and 20 % at the 50, 150 and 300 ppb levels, respectively, compared to the control plants. This concomitant concentration dependent increases in apparent antenna size (ABS/RC) and specific trapping flux (TR_0/RC) compensated for decreases in ET_0/CS and RC/CS, resulting in no or very little change in the quantum efficiency of primary photochemistry [$\varphi_{P0}/(1- \varphi_{P0})$] at all SO_2 concentrations. This phenomenon suggests that the primary processes of photosynthesis are regulated at a level of the reaction centres (RC/CS) which may be activated or "switched off" at the level of trapping of excitation energy (TR_0/RC) and the level of transformation of trapped excitation energy to electron transport ($ET_0/TR = \Psi_0$) and finally the reduction of end electron acceptors (RE/ABS) (Krüger *et al.*, 1997; Van Heerden *et al.*, 2003; Smith *et al.*, 2008). The relation between absorbed light energy (ABS), density of reaction centres (RC/CS), electron transport (ET_0/CS) and dissipation of energy (DI_0/CS) that occurred in the test plants after 28 days' fumigation at 300 ppb is depicted by the energy pipeline model depicted in Figure 4.51. This is indicated by the large deactivation of the density of the (active) reaction centres expressed as a relative number of reaction centres per cross section of the sample (RC/CS) as well as the decrease in electron transport (ET_0/CS) mainly at the 300 ppb SO_2 concentration (Figure 4.51).

Figure 4.5.10 indicates the effects in plants fumigated with SO_2 and subjected to drought stress. When drought was induced in plants fumigated with SO_2, no stimulation occurred in ET_0/CS at any SO_2 level. At all SO_2 levels, a concentration dependant decrease was evident in ET_0/CS. The situation did not differ much from that of the well watered plants. The data (Figure 4.51) shows a SO_2-induced decrease in the density of reaction centres per excited cross section (RC/CS) being responsible for reductions in ET_0/CS. Also in this case "switching off" of a fraction of RCs was compensated for by an increase in the specific trapping flux (TR_0/RC) and the apparent antenna size (ABS/RC), leading to only a very moderate decrease in φ_{P0} (F_V/F_M). Only moderate changes occurred in the selected fluorescence parameters of the ambient control plants. The small decreases evident in parameters shown in Figure 4.49 are mainly due to the somewhat higher temperatures inside the chambers during July to September 2007.

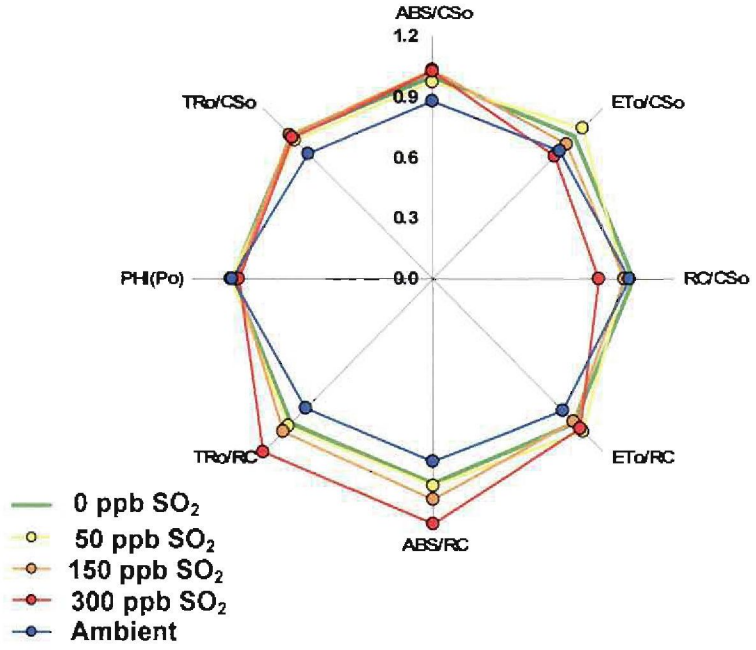


Figure 4.49 Fractional changes in specific and phenomenological energy fluxes through PSII measured in intact leaves of well watered *Glycine max* plants after 28 days of fumigation with SO_2.

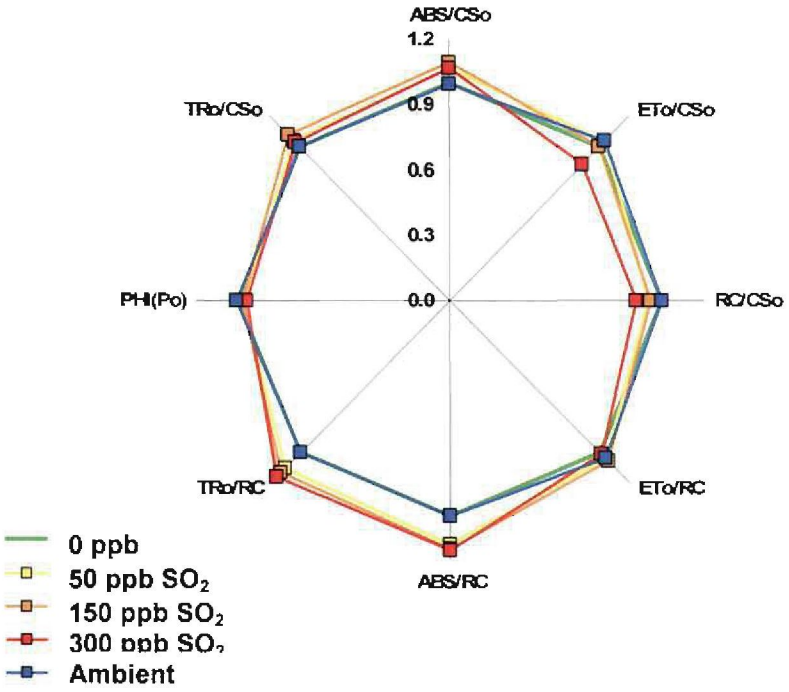


Figure 4.50 **Fractional changes in specific and phenomenological energy fluxes through PSII measured in intact leaves of drought stressed *Glycine max* plants after 28 days of fumigation with SO_2.**

The change in the derived energy fluxes per reaction centre (membrane model) or per cross section (leaf model) is displayed by the pipeline model (Figure 4.51). The leaf model provides a visualisation of the inactivation of RCs upon SO_2 fumigation, while the membrane model demonstrates the associated increase of the ABS/RC, both as flux and as antenna size. ABS/RC has been regarded as providing a measure of antenna size (Strasser & Strasser, 1995), based on the relation $TR_0/RC = \varphi P_0 \times ABS/RC$. The pipeline model is a dynamic model in which the value of each energy flux is expressed by the appropriately adjusted width of the corresponding arrows. Two types of models have been shown; one deals with the specific energy (per RC, Membrane Model), and the other refers to the cross section of a leaf (per CS, Leaf Model). In the membrane model (Figure 4.51 - top), the antenna size, which corresponds with the ABS/RC, has been demonstrated. In the leaf model (Figure 4.51 - bottom), the active RC per cross section (RC/CS) is indicated by open circles, and the inactive ones by closed circles. It is clear from these visual presentation (Figure 4.51) that after 28 days of SO_2 treatment, SO_2 inactivated the RC (see the closed circles in the leaf model), which resulted in the associated increase in the ABS/RC (Figures 4.49 and 4.50), both as flux and as average antenna size. This

resulted in the 300 ppb treated plants having a much lower electron transport per leaf cross section than the control.

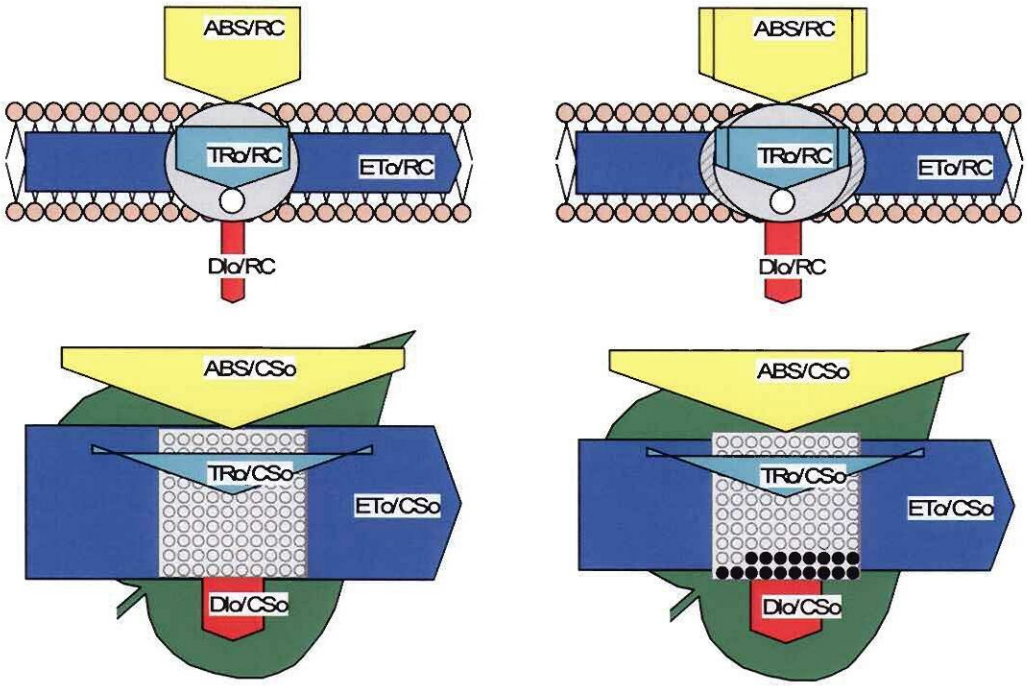


Figure 4.51 **Energy pipeline models of the control (left) and 300 ppb SO_2 treated (right) plants after 28 days of fumigation. The membrane models (top) represent the specific activities, expressed as fluctuations per reaction centre (RC). The leaf models (bottom) show the phenomenological fluctuations, expressed as per leaf cross section (CS). The relative magnitude of each activity or fluctuation is shown by the width of the corresponding arrow. The average antenna size is given as ABS/RC. This expresses the total absorption flux of PSII antenna chlorophyll divided by the number of active reaction centres. Thus, the antenna of PSII complexes with non-Q_A reducing RCs (heat sink centres) are graphically added to the antenna of the active reaction centres. The absorption and trapping by PSII units with a heat sink centre is indicated as the hatched parts of the arrows ABS/RC and TR_0/RC. The antenna belonging to the PSII units with heat sink centres is drawn in black while the antenna which belongs to the active (QA reducing) centres is drawn in white. In the shaded zones of the model, the Q_A reducing RCs per cross section are indicated by open circles and the non-Q_A reducing RCs (heat sink or silent RCs) are indicated by the closed circles. The colouration of the foliage indicates the chlorophyll concentration per leaf cross section.**

PI_{TOT} values calculated after 14, 21 and 28 days of fumigation showed that photosynthesis in both the well watered and drought stressed *Glycine max* experimental plants was increasingly inhibited with increasing SO_2 concentration, i.e. the decrease was concentration dependent. After 14 days, and to a lesser extent after 21 days of fumigation, a stimulatory effect was evident at the 50 ppb SO_2 treatment (Figure 4.52a). Such stimulation did not occur with drought as co-stress (Figure 4.5.12b). The overall decrease in PI_{TOT}, however, was more pronounced in the plants that were subjected to drought (Figure 4.52b). After 14 days, the PI_{TOT} in well watered plants (Figure 4.52a) increased by 19 % at the 50 ppb concentration, and decreased by 1 % and 18 % for the 150 and 300 ppb SO_2 concentrations, respectively, relative to the 0 ppb well watered plants. Although a very slight stimulation of 3 % was evident at the 50 ppb SO_2 concentration, the inhibitory effect of SO_2 reflected by PI_{TOT} progressed with time (number of days), increasing by 44 % and 62 % for the 150 and 300 ppb SO_2 concentrations, respectively, compared to the 0 ppb well watered plants after 28 days. PI_{TOT} in drought stressed plants decreased by 9 %, 21 % and 39 % for the 50, 150 and 300 ppb SO_2 concentrations, respectively, compared to the control plants subjected to drought stress (Figure 4.52b). After 28 days this decrease was even greater. PI_{TOT} decreased by 34 %, 38 % and 36 % for the 50, 150 and 300 ppb SO_2 concentrations, respectively, compared to the 0 ppb SO_2-treated plants subjected to drought.

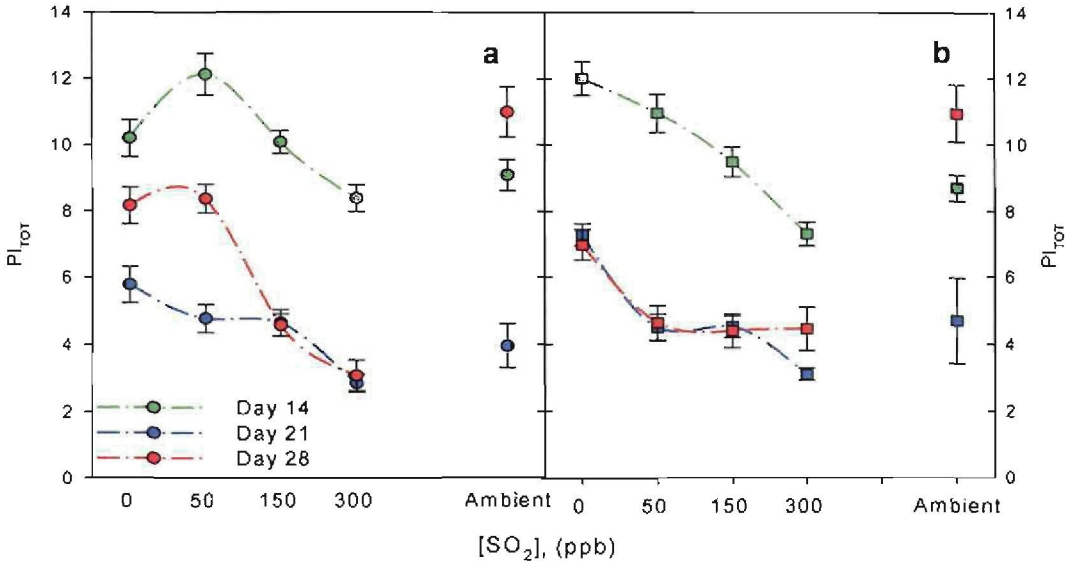


Figure 4.52 **Performance index total (PI_{TOT}) measure after 14, 21 and 28 days' fumigation with SO_2 in well watered (a) and drought stressed (b) *Glycine max* plants. Each value represents a mean (±SE), where n = 6.**

The total driving force for photosynthetic activity (DF_{TOT}), created by summation of the logarithm of the partial driving forces for efficiency of absorption of light energy [log(RC/ABS)], trapping of excitation energy [$\log(\varphi P_o/(1-\varphi P_o)$], the conversion of excitation energy to electron transport [$\log(\Psi_0/(1-\Psi_0)$] and the formation of reducing equivalents [$\log(\delta_0 / 1-\delta_0)$], was used to determine the effect SO_2 alone, and in combination with drought on the individual partial processes of PSII function (Figure 4.53a and 4.53b). The efficiency of absorption of light [log(RC/ABS)] in well watered plants (Figure 4.53a – red line) decreased by 1 %, 4 %, and 10 % at the 50, 150 and 300 ppb SO_2 levels, respectively, compared to the control plants. The quantum efficiency of primary photochemistry [$\log(\varphi P_o/(1-\varphi P_o)$] in well watered plants (Figure 4.53a – blue line) displayed an initial stimulation of 1 % at the 50 ppb level, after which it decreased by 6 % and 13 % at the 150 and 300 ppb SO_2 levels, respectively, compared to the control. The quantum efficiency of the conversion of excitation energy to electron transport [$\log(\Psi_0/(1-\Psi_0)$] (Figure 4.53a – green line) in the well watered plants, however, displayed a marked increase of 31 % at the lowest treatment (50 ppb SO_2), after which it decreased drastically with 69 % and 128 % at the 150 and 300 ppb levels, respectively, compared to the control plants, and this points to the vulnerability of this partial process of primary photosynthesis. The quantum efficiency of the formation of the reducing equivalents [$\log(\delta_0/1-\delta_0)$] (Figure 4.53a – black line) decreased noticeably by 1 %, 10 % and 26 % at the 50, 150 and 300 ppb SO_2 levels, respectively, compared to the control. As the PI_{TOT} suggested, no stimulation of any of the partial processes of primary photochemistry occurred at any SO_2 level in drought stressed soybean (Figure 4.513b). In drought stressed plants the efficiency of absorption of light (RC/ABS) (Figure 4.53b – red line) decreased by 4 %, 7 % and 8 % at the 50, 150 and 300 ppb SO_2 levels, respectively, compared to the drought stressed control treatment. The quantum efficiency of primary photochemistry (Figure 4.53b – blue line) decreased by 7 %, 11 % and 6 % at the 50, 150 and 300 ppb SO_2 levels, respectively, compared to the control plants subjected to drought. The conversion of excitation energy to electron transport (Figure 4.53b – green line), however, decreased drastically with 90 %, 65 % and 71 % at the 50, 150 and 300 ppb SO_2 levels, respectively, compared to the drought stressed control plants. The quantum efficiency of the formation of the reducing equivalents [$\log(\delta_0/1-\delta_0)$] (Figure 4.53b – black line) decreased more drastically in drought stressed plants. The latter parameter decreased by 11 %, 13 % and 17 % at the 50, 150 and 300 ppb levels, respectively, compared to the control plants subjected to drought. It was evident that among the partial processes of primary photosynthesis, SO_2 caused the greatest reduction in the conversion of excitation

energy to electron transport [$\log(\Psi_0 /(1- \Psi_0)$] and secondly in the efficiency of the formation of reducing equivalents [$\log(\delta_0/1- \delta_0)$]. This finding corroborates the gas exchange data that showed a strong decrease in J_{max} (measure of the regeneration capacity of RuBP) at all treatment levels and secondly, the large SO_2 dependant decreases in the carboxylation efficiency (CE) (see Section 4.4.2). This evidence strongly indicates that the inhibitory effect of SO_2 was mainly due to mesophyll limitation. The most striking difference in the response between the SO_2 and the SO_2 plus drought treatments, as indicated by the DF, was that in absence of drought, photosynthesis was stimulated at the 50 ppb treatment, and thereafter the increase in inhibition was concentration dependent (Figure 4.53a). No stimulation, however, occurred in any parameter of the DF at any of the SO_2 concentration for the drought stressed plants (Figure 4.53b). Indeed at the 50 ppb SO_2 level all parameters of the DF were already markedly inhibited. Secondly, in the drought stressed plants the direct relationship between SO_2 concentration and inhibition of photosynthesis declined at SO_2 concentrations higher than 50 ppb.

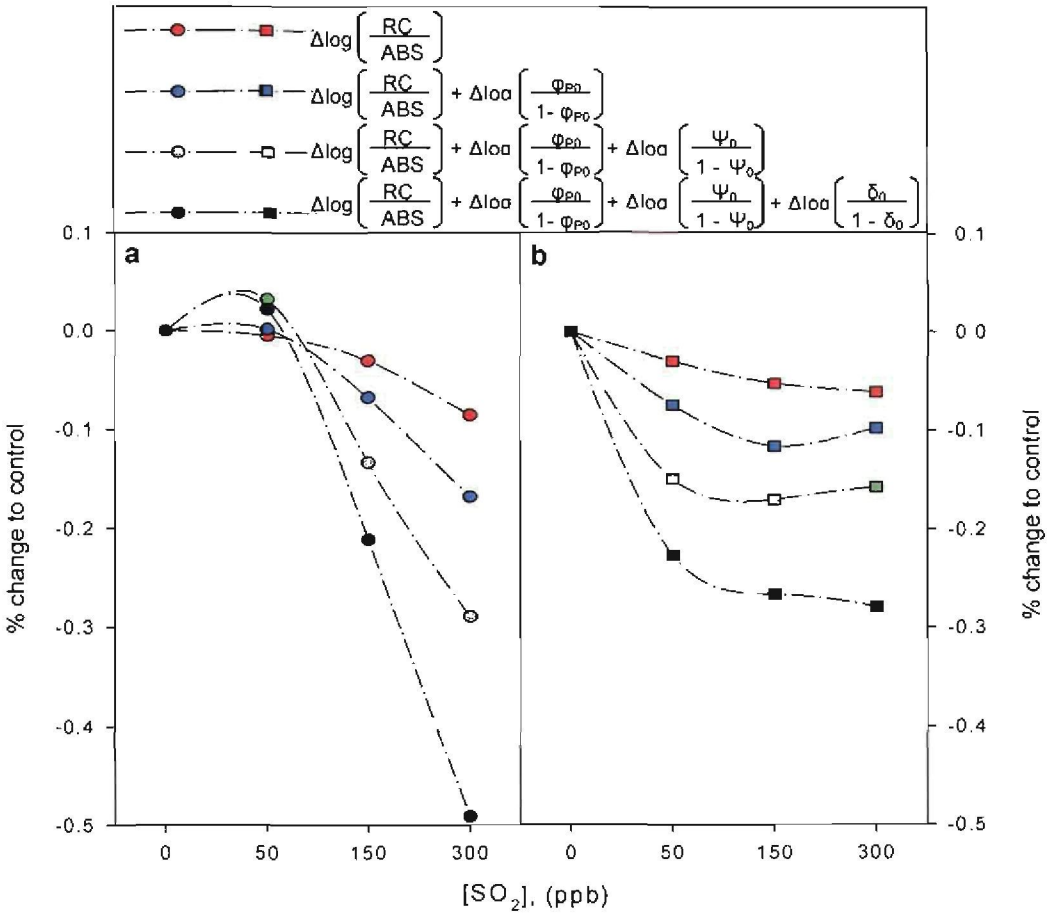


Figure 4.53 Driving force total (DF_{TOT}) measure after 28 days' fumigation with SO_2 in well watered (a) and drought stressed (b) *Glycine max* plants. Each value represents the mean, where n = 6.

The subtraction of the normalised (V_t) transients (normalised between F_0 and F_M, i.e. V) of the control plants from the treatments of the stressed plants provided the difference in fluorescence (ΔV) plots and, in the case of the transients, normalised between F_0 and F_2 ms, providing the ΔW plots (Strasser *et al.*, 2007). In the plots of the difference in relative variable fluorescence between the average transients of the treatments and their respective controls, the ΔW plots (Figures 4.54a and b; Figures 4.55a and b) and ΔV (Figure 4.54c; Figure 4.55c) are presented. The ΔV and ΔW plots revealed bands hidden in the J and I steps of the fluorescence kinetics which are much richer in information than the original O-J-I-P. From these plots, information such as integrity of the OEC, accumulation of Q_A^- and reduction of end electron acceptors of the photosynthetic electron transport chain as affected by the treatment could be obtained (Strasser *et al.*, 2007). The plot of the transients as V-curves and W-curves facilitates the comparison of the effects of the treatment relative to the control, as only the dynamic accumulation of Q_A in its reduced form Q_A^- is considered. By observing the differences of the relative variable fluorescence between F_0 and F_M (Figure 4.54 and Figure 4.55), the well watered and drought stressed SO_2 treated plants (Figure 4.54b and c) showed a marked SO_2 dependent increase in fluorescence intensity in the multiple turnover range. The increased fluorescence intensity in this region indicates biochemical inhibition beyond the redox couple Q_A / Q_A^-.

However, when closely analysed by normalising the transients between F_0 and 2ms and plotting the ΔW transients, a noticeable K-band, which in the ΔV plot hidden behind the J-step (Figures 4.54a, 4.55a, 4.56a, and 4.57a) was revealed. The K-step emerged very clearly after 14 days' (Figure 4.54a) fumigation in well watered SO_2 fumigated plants and became even more apparent after 28 days of fumigation (Figure 4.56a). On the contrary, the drought stressed plant fumigated with SO_2 for 14 days showed a marked -ΔK-peak, pointing at stimulation of the OEC relative to the control (Figure 4.55a). After 28 days, these –ΔK-peaks became prominent +ΔK-peaks (Figure 4.57a). The occurrence of a K-peak is the consequence of an increase in fluorescence, probably due to the short-lived accumulation of reduced electron carriers such as $Pheo^-$, which, in turn, is caused by the dissociation of the OEC, resulting in an imbalance between the electron flow from the OEC to the RC and towards the acceptor side of PSII in the direction of PSI (Strasser, 1997). Uncoupling of the OEC enables an alternative internal electron donor such as ascorbate or proline (instead of H_2O) to donate electrons to PSII. This leads to a short-lived increase in the reduced Pheo/Q_A concentration, creating a K-peak

appearing between 100 and 300 µs and increasing with intensity of the stress (De Ronde *et al.*, 2004). The first reduction of Q_A and the subsequent reduction of $P680^+$ require one electron which is normally present on the secondary electron donor of PS II (Tyr161, situated on the D1 protein of PSII) (Diener & Babcock, 1996); and there is no necessary involvement of the OEC. Both SO_2 treated and water stressed SO_2 treated plants exhibited an obvious increase in the K-band (300 – 400 µs), indicating a partial block on the water splitting side or uncoupling of the oxygen evolving complex (OEC).

By analysing the relative fluorescence transients normalised between 2 ms and F_M (Figures 4.54b, 4.55b, 4.56b and 4.57b), a clearly visible I-band provided information on the activation state of ferredoxin $NADP^+$ reductase (FNR) and possible accumulation of end electron acceptors such as NADPH and Fd (red). After 14 days of fumigation a definite +ΔI-peak was visible, illustrating the concentration dependent effect SO_2 has once more. The prominent I-peak also supports results shown in Section 4.4.2, indicating an inhibition in the CO_2 saturated rates of photosynthesis (J_{max}) that occurred with increasing SO_2 concentration and correlates well with decreases observed in $[\log(\delta_0 / 1- \delta_0)]$ that represent the quantum efficiency of the formation of reducing equivalents and form a component that constitute part of the DF_{TOT}. This indicated that photosynthesis was mainly inhibited due to a decrease in the formation of NADPH. Furthermore, the SO_2 dependent appearance of the +ΔI-peaks thus corroborates the concomitant decreases that occurred in J_{max} (regeneration capacity of RuBP) in the carboxylation efficiency (CE; which is a measure of the *in vivo* Rubisco activity, and the *in vitro* Rubisco activity).

The relative fluorescence transients of the drought stressed plants showed a -ΔJ-peak after 14 days' fumigation at the 300 ppb level (Figure 4.55c). Contrarily, a +ΔJ was evident after 14 and 28 days for well watered plants fumigated with 50 ppb SO_2 (Figures 4.55c and 4.56c). The J-peak indicates an accumulation of Q_A^- due to inhibition of the dark reactions responsible for the reoxidation of the Q_A^- pool.

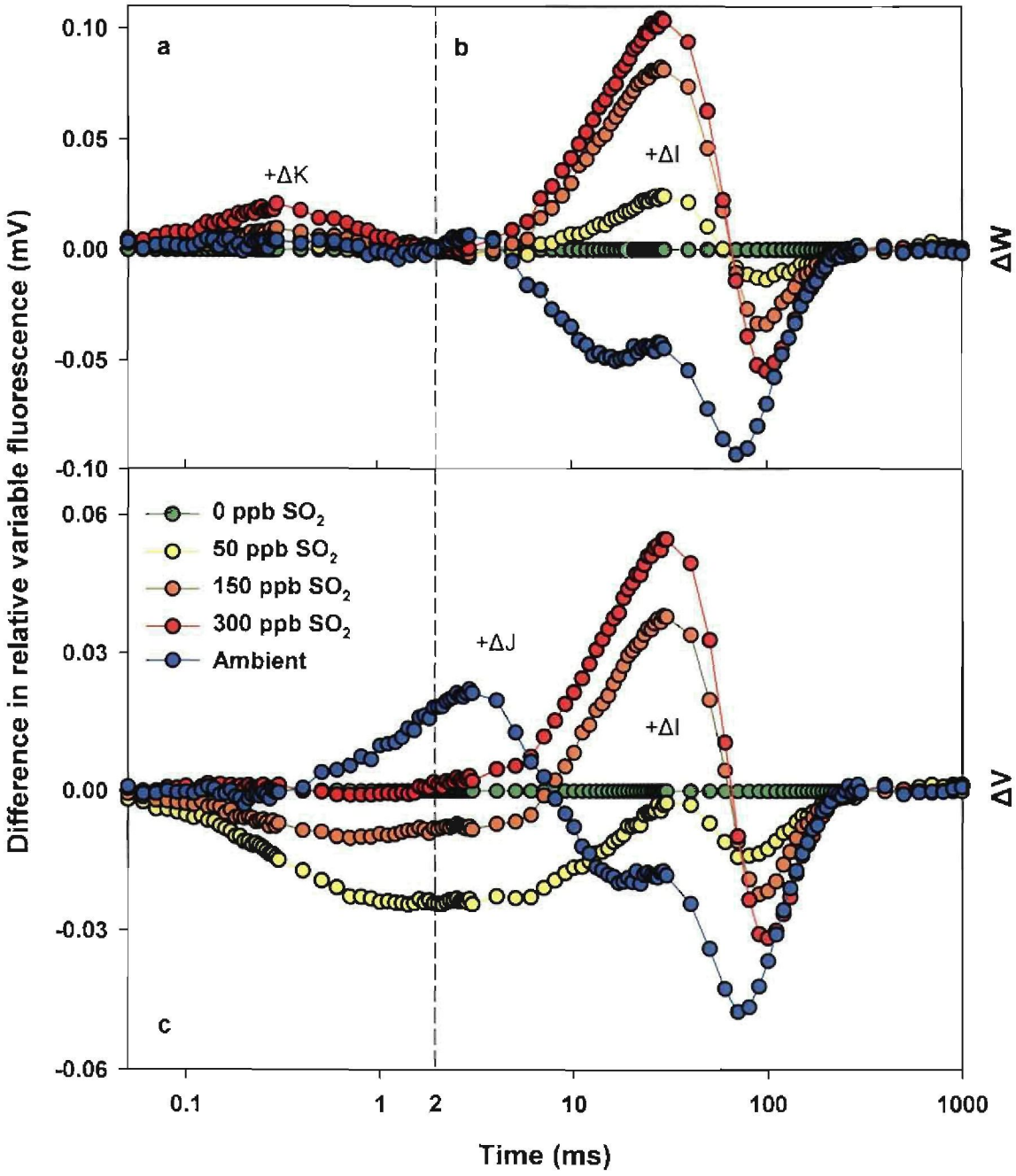


Figure 4.54 Changes in difference in the relative variable *chlorophyll a* fluorescence transients ($\Delta W = W_{treatment} - W_{control}$ and $\Delta V = V_{treatment} - V_{control}$) recorded in well watered *Glycine max* plants after 14 days' fumigation with SO_2 (expressed as W = f(t)) normalised between fluorescence extremes F_0 and FJ (2ms) ($W = (F-F_0)/(F_J-F_0)$, $\Delta W = W_{treatment} - W_{control}$) and between (a) FJ (2ms) and F_M ($W = (F_0-F_J)/(F_M-F_J)$, $\Delta W = W_{treatment} - W_{control}$) (b) and between F_0 and F_m ($V = (F-F_0)/(F_m-F_0)$, $\Delta V = V_{treatment} - V_{control}$) (c).

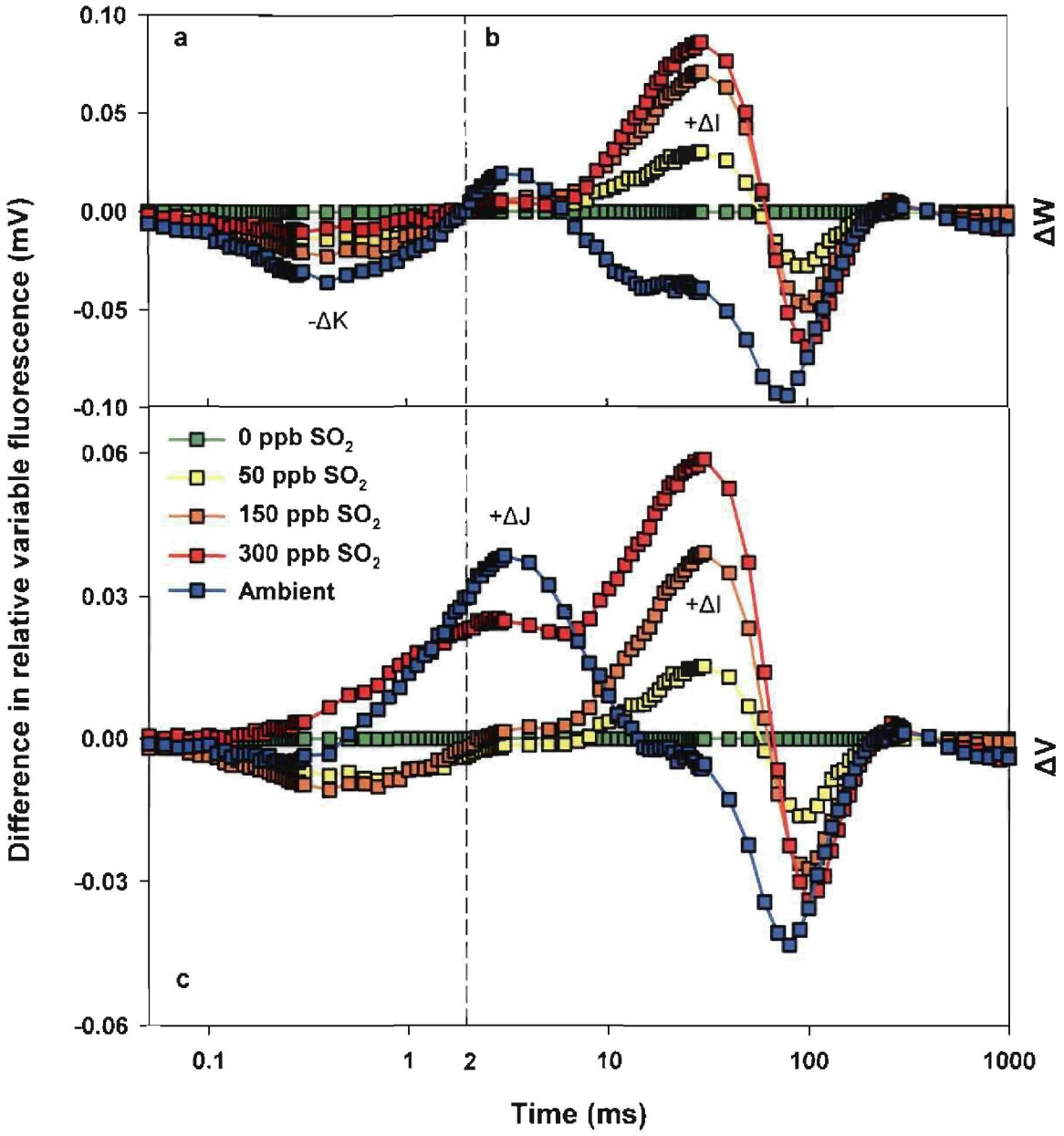


Figure 4.55 Changes in difference in the relative variable *chlorophyll a* fluorescence transients ($\Delta W = W_{treatment} - W_{control}$ and $\Delta V = V_{treatment} - V_{control}$) recorded in drought stressed *Glycine max* plants after 14 days' fumigation with SO_2 (expressed as $W = f(t)$) normalised between fluorescence extremes F_0 and FJ (2ms) ($W = (F-F_0)/(F_J-F_0)$, $\Delta W = W_{treatment} - W_{control}$) and between (a) FJ (2ms) and F_M ($W = (F_0-F_J)/(F_M-F_J)$, $\Delta W = W_{treatment} - W_{control}$) (b) and between F_0 and F_m ($V = (F-F_0)/(F_m-F_0)$, $\Delta V = V_{treatment} - V_{control}$) (c).

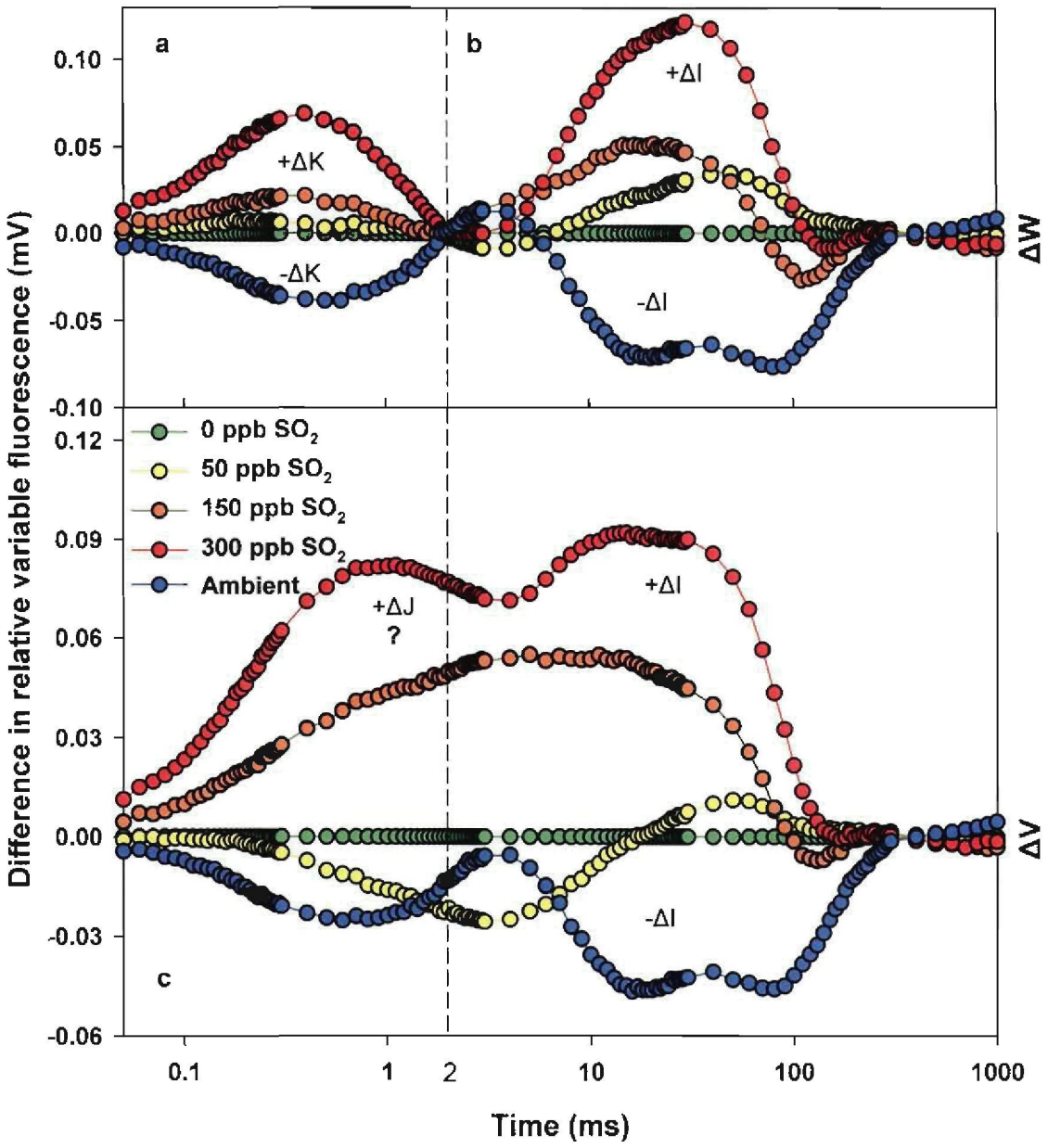
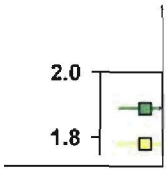


Figure 4.56 **Changes in difference in the relative variable *chlorophyll a* fluorescence transients ($\Delta W = W_{treatment} - W_{control}$ and $\Delta V = V_{treatment} - V_{control}$) recorded in well watered *Glycine max* plants after 28 days' fumigation with SO_2 (expressed as W = f(t)) normalised between fluorescence extremes F_0 and FJ (2ms) ($W = (F-F_0)/(F_J-F_0)$, $\Delta W = W_{treatment} - W_{control}$) and between (a) FJ (2ms) and F_M ($W = (F_0-F_J)/(F_M-F_J)$, $\Delta W = W_{treatment} - W_{control}$) (b) and between F_0 and F_m ($V = (F-F_0)/(F_m-F_0)$, $\Delta V = V_{treatment} - V_{control}$) (c).**



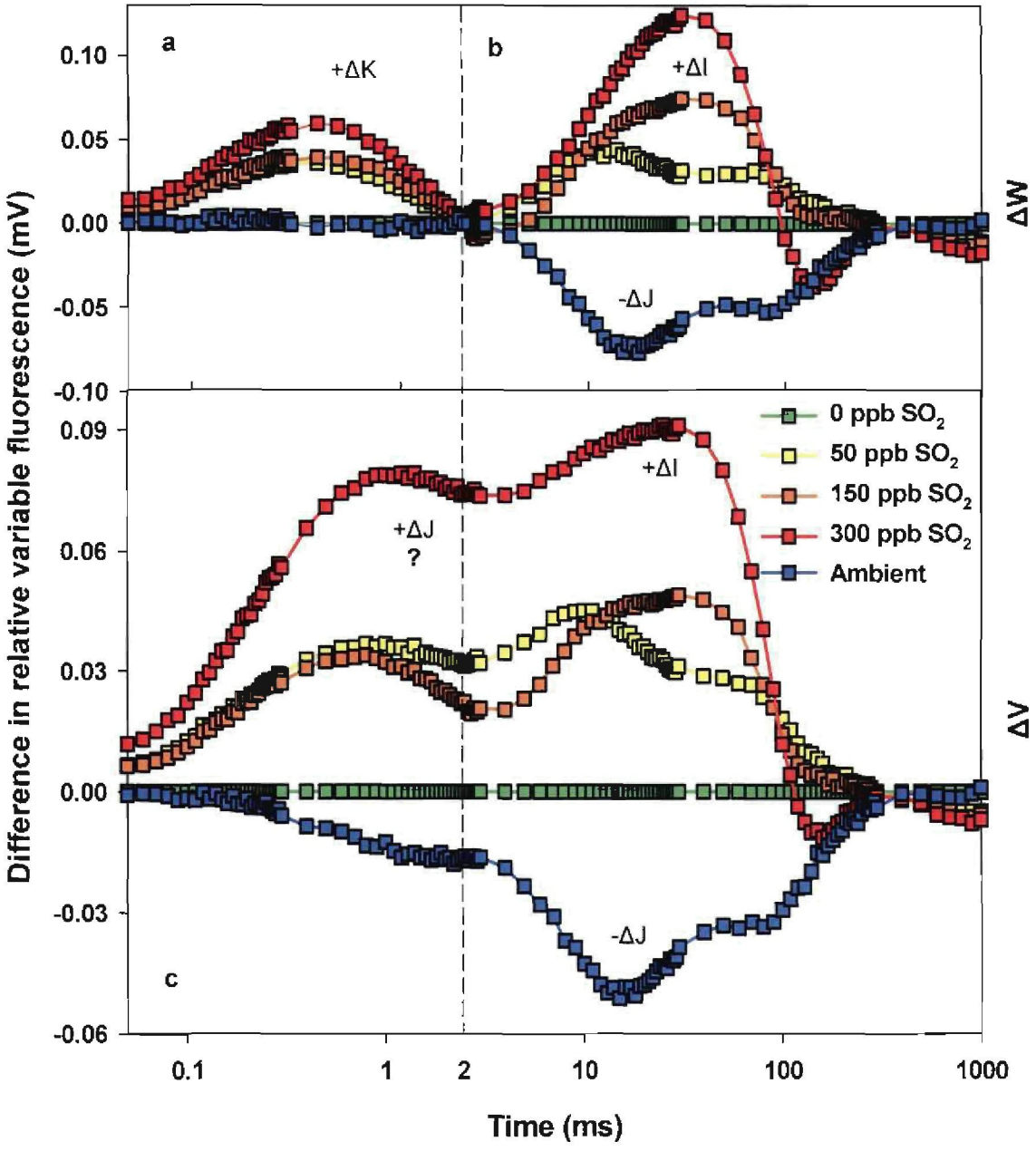


Figure 4.57 Changes in difference in the relative variable *chlorophyll a* fluorescence transients ($\Delta W = W_{treatment} - W_{control}$ and $\Delta V = V_{treatment} - V_{control}$) recorded in drought stressed *Glycine max* plants after 28 days' fumigation with SO_2 (expressed as W = f(t)) normalised between fluorescence extremes F_0 and FJ (2ms) ($W = (F-F_0)/(F_J-F_0)$, $\Delta W = W_{treatment} - W_{control}$) and between (a) FJ (2ms) and F_M ($W = (F_0-F_J)/(F_M-F_J)$, $\Delta W = W_{treatment} - W_{control}$) (b) and between F_0 and F_m ($V = (F-F_0)/(F_m-F_0)$, $\Delta V = V_{treatment} - V_{control}$) (c).

Chapter 5

Discussion

Opposed to what the flux based model attempt to achieve (Emberson *et al*, 2000) the recorded data with respect to the SO_2 concentration in the OTCs (Section 4.1) only reflects the SO_2 concentrations in the OTCs at the height of the soybean canopy and does not give a direct measure of uptake by the plants. However, the data indicates the strong concentration dependant inhibition SO_2 caused (Chapter 4) and is generally substantiated by the calculated gas-exchange parameters, *chlorophyll a* fluorescence parameters, and *in vitro* measurement of Rubisco activity values measured on the test plants. The data showed that after only seven days at low SO_2 (i.e. 50 ppb) concentrations after only seven days, photosynthesis was reduced, without accompanying visible symptoms. Visible symptoms only appeared after 14 days of fumigation.

5.1 Meteorological growth conditions in the open-top chambers

The open-top chamber facility described in Chapter 2 and Chapter 4, Section 4.1, proved to be very well suited to the purpose for which they were designed; namely the generation of controllable test atmospheres of elevated SO_2 (or other gaseous pollutants) at the height of the canopy of the test plants. Fan speed, size and shape of the chambers, and number and size of the perforations in the manifold of toroids (lay-flat tubing) at the height of the plant canopy, were carefully considered in the design of the chambers. The aim was to provide uniformly dispersed, elevated concentrations of SO_2 (1 ppb = 1 part in 10^9 by volume) across the plant canopy, while maintaining temperature, relative humidity and solar radiation close to those measured outside. The recorded average temperature inside the open top chambers was generally approximately 2° C higher than ambient and occurred at midday on warm, sunny days. Night-time average temperatures inside the chambers were approximately 1 °C higher than ambient.

5.2 Growth

Apart from the appearance of necrotic and chlorotic injury symptoms, severe deformity of the youngest growth was noticeable. The susceptibility of leaves to SO_2

changed systematically during development (Guderian, 1977). In many species, young leaves are resistant to injury from chronic and later acute exposure to SO_2, while mature leaves are sensitive (Bressan *et al.*, 1978). This resistance is not attributable to an uptake difference, because younger leaves actually absorb SO_2 at a higher rate than mature leaves (Bressan *et al.*, 1979). This deformity of the youngest leaves, known to occur as epinasty, indicated that SO_2 could be the cause for a change in hormonal levels. Epinasty of new growth occurs due to disturbed leaf expansion and cell division caused by changes in the auxin levels (Ursin & Bradford, 1989). Epinastic movement of the younger petioles is a result of greater expansion of the adaxial cells as compared to abaxial cells in specific regions of the petiole (Kang, 1979; Palmer, 1985). It is not known if epinastic growth was induced by the direct action of SO_2, or indirectly, by a change in auxin activity or levels. Epinasty is a growth deformity that occurs due to the formation aminocyclopropane carboxylic acid (ACC) in the roots of the plant from where it is then transported via the xylem to the leaves where it is converted to ethylene (Yang & Hoffman, 1984). The production of ethylene is synonymous with SO_2-injured plants and has been described by numerous authors (Bressan *et al.*, 1978; 1979; Peiser & Yang, 1979). Peiser and Yang (1979) have shown that ethylene is produced in relative low amounts by plants under normal conditions, but when plants are perturbed or injured by SO_2, elevated ethylene production rates occurred.

5.3 Biomass accumulation

Biomass accumulation showed a SO_2 concentration dependant decrease in shoot dry mass production. Biomass measured for *Brassica oleracea* at the final harvest indicated that low concentrations of SO_2 caused stimulation in biomass production of well watered plants. However, when drought was induced, no stimulation in biomass production occurred at the 50 ppb level. When plants were fumigated with 150 and 300 ppb SO_2, shoot biomass production was reduced severely, resulting in a sharp decline in the shoot-to-root ratio. This was the case in both well watered and drought stressed *Brassica oleracea* plants. The root biomass production of the drought stressed plants was affected less severely than that of the shoots. In *Glycine max*, no stimulation in dry mass production occurred, not even at the lowest treatment level. This suggests that *Glycine max* is more sensitive towards SO_2 than *Brassica oleracea,* even though both species are referred to as relatively sensitive (Legge *et al.*, 1998). In *Glycine max,* the same trend was observed regarding the shoot-to-root ratio when drought was induced. SO_2 fumigation in combination with drought stress

reduced shoot dry mass production more drastically as compared to that of the roots, resulting in a sharp decrease in the shoot-to-root ratio. It appears that the roots rather than the shoots acted as a sink for photosynthate when plants fumigated with SO_2 experienced water deprivation. This extra investment in root biomass production could provide a mechanism to ensure a better acquisition of mineral nutrients and water to maintain photosynthesis (Deepak & Agrawal, 2001). The retardation in growth and reduction in biomass accumulation due to SO_2 exposure might be ascribed to the diversion of photoassimilates for repair and detoxification or a reduction in photosynthetic rate (Rao & De Kok, 1994; Verma & Agrawal, 1996).

5.4 Yield

The reduction in yield of SO_2 exposed, well watered or drought stressed *Glycine max* plants was a result of the reduction in number of pods per plant and number of seeds per pod, rather than the weight of individual pods or seeds. Reduction in soybean yield due to SO_2 exposure has previously been described by Sprügel *et al.* (1980) and Verma and Agrawal (1996) who found an 18 % reduction in yield per plant in soybean exposed to $0.06\mu l.l^{-1}$ (ppm = 60 ppb). It has been suggested that exposure to SO_2 may lead to reduction in yield that can be directly related to tissue damage, and occurs only when visible injury appears (Brisley *et al.*, 1959), while other studies indicate that yield reduction may occur in the absence of visible injury (Heck & Brandt, 1977). A reduction in CO_2 assimilation rate (Section 4.2) was observed at all SO_2 treatment levels used in this study. The effect was most severe at the highest treatment level (i.e. up to a 57 % reduction in yield was observed). Importantly, both chronic and acute foliar injury symptoms occurred throughout the summer at the intermediate and high concentrations applied. At the lowest treatment level, reductions in CO_2 assimilation rate occurred without accompanying visible injury. Constraints in photosynthesis were measured in uninjured leaves with no visible symptoms in plants treated with 50 ppb SO_2, indicating that permanent physiological damage may occur in the absence of visible injury. These observations suggest a physiological basis for the occurrence of yield reduction independent of visible injury (Sprügel *et al.*, 1978).

5.5 Chlorophyll content

Exposure to SO_2 reduced the chlorophyll content of *Brassica oleracea* and *Glycine max*. The CCI in well watered *Brassica oleracea* increased significantly at the 50 and

150 ppb levels after 42 days, but remained nearly the same as was measured after 35 days at the 300 ppb level. After 50 days fumigation of well watered *Brassica oleracea*, the CCI decreased drastically at the 150 and 300 ppb levels respectively, but remained unaffected at the 50 ppb level. The CCI of the drought stressed *Brassica oleracea* plants was unaffected at the 50 and 150 ppb levels, but decreased quickly at the 300 ppb level after 42 days of fumigation. After 50 days of exposure, the CCI in drought stressed *Brassica oleracea* decreased even more at the 150 and 300 ppb levels, but remained unchanged at the 50 ppb level. *Glycine max* seemed to be more sensitive to SO_2 exposure with respect to the CCI. The CCI of well watered and drought stressed plants showed strong decreases at the 150 and 300 ppb levels respectively, but remained constant at the 50 ppb level after 28 days of exposure. CCI showed strong decreases at all treatment levels after 35 days of SO_2 exposure and drought stress. The reduction in the chlorophyll content might be ascribed to the photooxidation of sulphite to sulphate in the chloroplasts that gives rise to super oxide radicals. Superoxide radicals are known to destroy chlorophyll when it is not quickly rendered harmless by superoxide dismutase (SOD).

5.6 Photosynthesis

Fumigation with SO_2 caused a very strong concentration dependant inhibition of photosynthetic gas exchange of *Brassica oleracea* and *Glycine max* plants (Chapter 4). This inhibitory effect, however, was larger in *Glycine max* plants. Although the SO_2 concentration dependant decrease in photosynthetic rate occurred in both well watered and drought stressed treatments, photosynthesis of drought stressed plants was reduced even more drastically, i.e. up to 50 % more, than in well watered plants. In previous work, working with isolated protoplasts, Pfanz *et al.* (1987b) showed that SO_2 can inhibit photosynthesis by different mechanisms even at very low cellular concentrations. The inhibitory effect of SO_2 at very low concentrations may be very small, but when acidification could not be compensated for by pH stabilising cellular mechanisms, it was the major element contributing to SO_2 toxicity. At higher cellular SO_2 concentrations, anion toxicity was thought to be the major cause of inhibition. Sulfite (SO_3^{2-}) and metabolising (HSO_3^-) that accumulate in the cellular tissue react with disulphite bonds, disrupting membranes and proteins. SO_2 and its oxidation products, SO_3^{2-} and HSO_3^-, are known to cleave disulfide linkages – a mechanism proposed by Puckett *et al.* (1973) – which could inactivate enzymes, destroy protein structures and influence cell permeability. Among the consequences of SO_2 injured membranes were effects on structural changes in thylakoid membranes and altered

stomatal function and stromal metabolism (Huttunen & Soikkeli, 1984). Ultrastructural studies of Glycine max fumigated with 300 ppb SO_2, revealed damage to occur mainly in the chloroplast. These chloroplasts that initially appeared swollen, showed severe deformity after 35 days. Chloroplasts appeared to be aggregated and the arrangement of the internal membrane system was severely distorted. In severely damaged mesophyll cells, the chloroplast envelopes had almost completely disintegrated and the thylakoids showed severe damage with electron dense material being noticeable in the stroma. This damage to the thylakoid components could be due to super oxide, hydroxyl radical and other active oxygen species that formed as a consequence of interactions with photosynthetic electron transport (Shimazaki *et al.*, 1980).

The physiological and biochemical inhibition of photosynthesis in *Brassica oleracea* plants, seem to be located at different sites within the chloroplast, as is indicated in the schematic presentation shown in Figure 5.1. In well watered and drought stressed *Brassica oleracea*, the inhibition of photosynthesis by SO_2 could mainly be ascribed to mesophyll limitation, i.e. constraints on PSII function, photosynthetic electron transport, and enzymatic reactions of CO_2 assimilation. According to the data of the present study, stomatal limitation played a secondary role. The physiological and biochemical mode of inhibition by SO_2 and its oxidation products is depicted in Figure 5.1. The proposed sites of inhibition of photosynthesis are numbered in the schematic presentation (Figure 5.1).

1. In well watered plants, the stomatal conductance (Gs) of the test plants initially increased with increasing SO_2 concentrations, a phenomenon also reflected by a decrease in the calculated percentage stomatal limitation. The increase in stomatal conductance resulted in an increase in the transpiration rate and a severe reduction of the water use efficiency (WUE). With prolonged exposure to SO_2 (i.e. 50 days), the stomatal conductance decreased at the high (i.e. 300 ppb) SO_2 level. When drought was induced in *Brassica oleracea*, the stomatal conductance decreased severely, leading to an increase in the calculated percentage stomatal limitation. After 35 days' fumigation, water use efficiency (WUE = A/E) decreased at all concentration levels, regardless of the increase in percentage stomatal limitation. These reductions in water use efficiency took place even though the transpiration rate decreased. This phenomenon shows that the decrease in CO_2

assimilation rates (A) was higher than the corresponding decrease in the transpiration rate (E).

2. In well watered and drought stressed *Brassica oleracea* plants, biochemical constraints within the mesophyll were primarily responsible for reductions in the CO_2 assimilation rate (A). Barton *et al.* (1980), Taylor *et al.* (1986) and Sison *et al.* (1981) found that mesophyll resistance, rather than stomatal constraints, was important in SO_2 induced inhibition of photosynthesis. Mesophyll limitation contributed markedly to the reduction in photosynthetic rate. The action of the oxidation products of SO_2 in leaves is known to have several effects at the biochemical and cellular level. The carboxylation efficiency (CE) measured in intact leaves of well watered and drought stressed *Brassica oleracea* indicated that SO_2 caused a concentration dependant decrease in the activity or concentration of Rubisco (Section 4.4.1). Rubisco, which is associated with the stroma of chloroplasts and which assimilates CO_2 in the first step in the C_3 pathway of photosynthesis, is thought to be inhibited through the competitive action of SO_3^{2-} and HSO_3^- with CO_2 and HCO_3^- for the binding sites in Rubisco (Ziegler, 1972).

3. The reduction in the maximum CO_2 assimilation rate (J_{max}) in both well watered and drought stressed *Brassica oleracea* plants indicated that SO_2 inhibited the regeneration capacity of RuBP (Farquhar & Sharkey, 1982) (Section 4.4.1). The latter may be due to a reduction in the formation of reducing equivalents by the electron transport chain, as was indeed indicated by the fluorescence data (Section 4.4.5.1). Constraints on photosynthetic electron transport may also have led to a decrease in photophosphorylation. The resulting effect is thus a decrease in NADPH, necessary to promote glyceraldehydes – 3 – phosphate dehidrogenase and ATP necessary for phosphoglycerate kinase and Ribulose – 5 – phosphate kinase. ATP is also needed in the detoxification of toxic oxidation products (SO_3^{2-}, HSO_3^-) of SO_2 in the sulphate reduction pathway (Garsed & Read, 1977). Reduced ferredoxin, that reduces bound sulphite to bound sulphide, is largely formed in the chloroplasts in the light, although an amount may also be formed in the dark by ferredoxin-NADP-oxidoreductase (FNR) (Hennies, 1975).

4. Analysis of *chlorophyll a* fluorescence transients, showed that an initial stimulation in PSII activity occurred at the lowest SO_2 concentration in

particular, but not at the higher SO_2 concentrations (Figures 4.41 & 4.43). This stimulation only occurred in well watered plants and could be ascribed to the possible nutritional role of the sulphate reduction pathway in metabolising SO_2 (Garsed & Read, 1977). Well watered *Brassica oleracea* fumigated with 150 and 300 ppb SO_2, displayed decreases in the electron transport per cross section (ET_0/CS_0), as well as a concomitant decrease in the density of the reaction centres (RC/CS_0). Concurrently, ABS/RC, which is regarded as a measure of "antenna size" (Krüger *et al.*, 1997; Strasser *et al.*, 2004), increased. This increase was not necessarily due to stimulation by SO_2, but rather points to shrinking of the leaf material and chlorophyll concentration possibly due to turgor loss (De Ronde *et al.*, 2004). This might explain why the reduction in ET/CS_0 in the drought stressed plants was minimal. The increase in the performance index (PI_{TOT}) of the drought stressed *Brassica oleracea* plants that occurred after 28 and 35 days, most probably resulted due to a corresponding decrease in stomatal conductance that occurred after 28 and 35 days of fumigation (Figure 4.43). This decrease in stomatal conductance suppressed the influx of SO_2 into the leaf decreasing the damage to the mesophyll. Cornic, (1994) showed that CO_2 is entirely replaced by O_2 as an electron acceptor from PSII when stomatal conductance was minimal.

6. SO_2 and its oxidation products, SO_3^{2-} and HSO_3^- are known to be capable of inhibiting photosynthetic electron transport between PS I and PS II, restricting the production of end electron acceptors such as NADPH as well as the production of ATP necessary to drive photosynthesis (Nieboer *et al.*, 1976; Horsman & Wellburn, 1976). The data of the present study convincingly corroborates this finding. A decrease in the efficiency for the formation of reducing equivalents in well watered *Brassica oleracea*, is illustrated by the decrease in partial driving force of photosynthesis, namely the quantum efficiency of the formation of reducing equivalents (φRE) component $\log[\delta/(1-\delta)]$ in well watered *Brassica oleracea* (see Section 4.4.5.1 and Figure 4.44a).

The detrimental effects of SO_2 pollution on *Glycine max* are well documented in the literature (Verma & Agrawal, 1996; Deepak & Agrawal, 2001). The result of the present study show that SO_2 inhibited photosynthesis of well watered and drought stressed plants at different locations in the chloroplast, as is explained schematically in Figure 5.1. The proposed sites of inhibition are numbered accordingly:

1. SO_2 fumigation reduces stomatal conductance in well watered plants treated with 50 and 150 ppb SO_2. This could be due to the direct action of the oxidation products of SO_2 on the stomata (Biscoe *et al.*, 1973), or could be due to accumulation of CO_2 in the intercellular spaces, thereby affecting stomatal movement, as was indicated by an increase in C_i values measured in SO_2 fumigated leaves (Section 4.3). Stomatal closure may result from a build-up of CO_2 in the intercellular spaces due photosynthetic depression (Hill & Bennett, 1970). Despite stomatal closure, the WUE also decreased even though E decreased. It has previously been recognised that SO_2 can influence the control of plant water relations greatly (Mansfield, 1998). Even though drought could have caused severe stomatal limitation at the lowest and intermediate SO_2 levels, the stomatal conductance remained similar to that of the control plants and even increased at the highest SO_2 level applied. Unsworth, Biscoe and Pinckney (1972) showed that stimulation of stomatal conductance was most pronounced in water stressed plants exposed to relatively high SO_2 concentrations. This observation was also described by numerous other authors (Unsworth *et al.*, 1972; Black & Unsworth, 1980). High concentrations of SO_2 are known to stimulate stomatal opening and thereby not only to reduce the WUE of the plant, but also to increase the access of SO_2 to the mesophyll where the damage caused was the greatest. This phenomenon became more profound when drought was induced (Table 4.11).

2. As mentioned above, accumulation of CO_2 in the intercellular spaces, indicated by increasing C_i value (Section 4.4.2), suggests that mesophyll limitation was mainly responsible for the SO_2 induced reduction in the photosynthetic rate. The calculated percentage stomatal limitation also decreased with increasing SO_2 concentrations and increased duration of the exposure, indicating that non-stomatal constraints (i.e. constraints in the mesophyll) were mainly responsible for the reduction in the photosynthetic rate. Changes in Rubisco activity of the test plants, measured by *in vitro* analysis, indicated a concentration dependant decrease (Figure 4.19). The corresponding *in vivo* Rubisco activity (CE), also decreased with increasing SO_2 concentration, decreased even more when plants were subjected to drought (Section 4.4.2). The decrease in Rubisco activity could be ascribed

to the affinity of SO_3^{2-} and HSO_3^- for the active sites where CO_2 or HCO_3^- normally binds, competitively inhibiting Rubisco (Ziegler, 1972).

3. SO_2 caused a concentration dependent reduction in the capacity to regenerate RuBP (Section 4.4.2). This can be ascribed to the direct inhibition Calvin cycle enzymes or a decrease in the efficiency in formation of reducing equivalents of electron transport (Section 4.4.5.2; Figure 4.53). Inhibition of photosynthetic electron transport not only results in decreased formation of reduced end acceptors such as NADPH that promotes glyseraldehyde–3-phosphate dehidrogenase, but also the production of ATP-promoting phosophoglycerate kinase and Ribulose–5–phosphate kinase. The photosynthetic light response data corroborated the above mentioned findings, indicating a sharp concentration dependent decrease in the light saturation point at all SO_2 levels, reflecting the inability of the carbon metabolism enzymes to fully utilise the absorbed light energy.

4. In depth analysis of the kinetics of the relative variable fluorescence transients (Section 4.4.5.2; Figure 4.55 a) clearly showed an initial stimulation in the OEC (appearance of the –ΔK-band) of SO_2 exposed drought stressed plants. This initial stimulation diminished after 28 days of fumigation (Figure 4.57a). The +ΔK-bands that developed after 28 days of fumigation indicate that SO_2 caused uncoupling of the OEC from PSII. This uncoupling of the OEC could be due to conformational changes induced in proteins by the oxidation products of SO_2 (Shimazaki & Sugahara, 1979).

5. The above-mentioned SO_2 induced reduction in the probability for formation of reducing equivalents of electron transport (Section 4.4.5.2), namely ATP and NADPH, are indicated by +ΔI-peaks occurring in the double normalised *chlorophyll a* fluorescence plots (Figure 4.54b; Figure 4.55 b; Figure 4.56 b and Figure 4.57b). These peaks point to an inhibition of electron flow further down from the reduced intersystem electron acceptors of the electron transport chain to the PSI and electron acceptors. ATP is also used in the sulphate reduction pathway for the phosphorylation of adenosine-5-phosphosulphate (APS) used in the biosynthesis of organic compounds such as cycteine, glutathione and methionine, constricting the major soluble SH component of normal cells (Schiff & Hodson, 1973). It has earlier been suggested that the inhibitory effect of SO_2 might be connected with impaired

phosphorylation (Sji & Swanson, 1974). The ATP content measured in pine tree hybrids was shown to decrease linearly with increasing SO_2 concentration (Harvey & Legge, 1979). The effect of SO_2 on ATP production and ATP content might alter metabolic pathways leading to synthesis and/or degradation of macromolecules in the chloroplast. Rubisco synthesis in particular is known to have a large energy demand and material requirement (Raven, 1977).

6. Analysis of the chlorophyll fluorescence transients also revealed an +ΔJ-peak indicating SO_2-induced inhibition of electron transport beyond Q_A resulting in accumulation of Q_B^- due to the inability of plastoquanone (PQ) to bind to the D1 protein in PSII for electrons to enter the PQ pool. It is not sure whether SO_2 has a direct effect on the D1 binding site on PSII. The dominating +ΔI peaks, displayed as the second phase of the OKJIP transient, reflected changes in electron withdrawal from PSII, depending on the activity of PSI (Shansker *et al.*, 2005). This possibility was also confirmed by the new parameter $\varphi(R_0)$ introduced by Tsimilli-Michael and Strasser (2008) that showed a sharp decrease in the reducing capacity of the PSI end electron acceptors (Figure 4.44a).

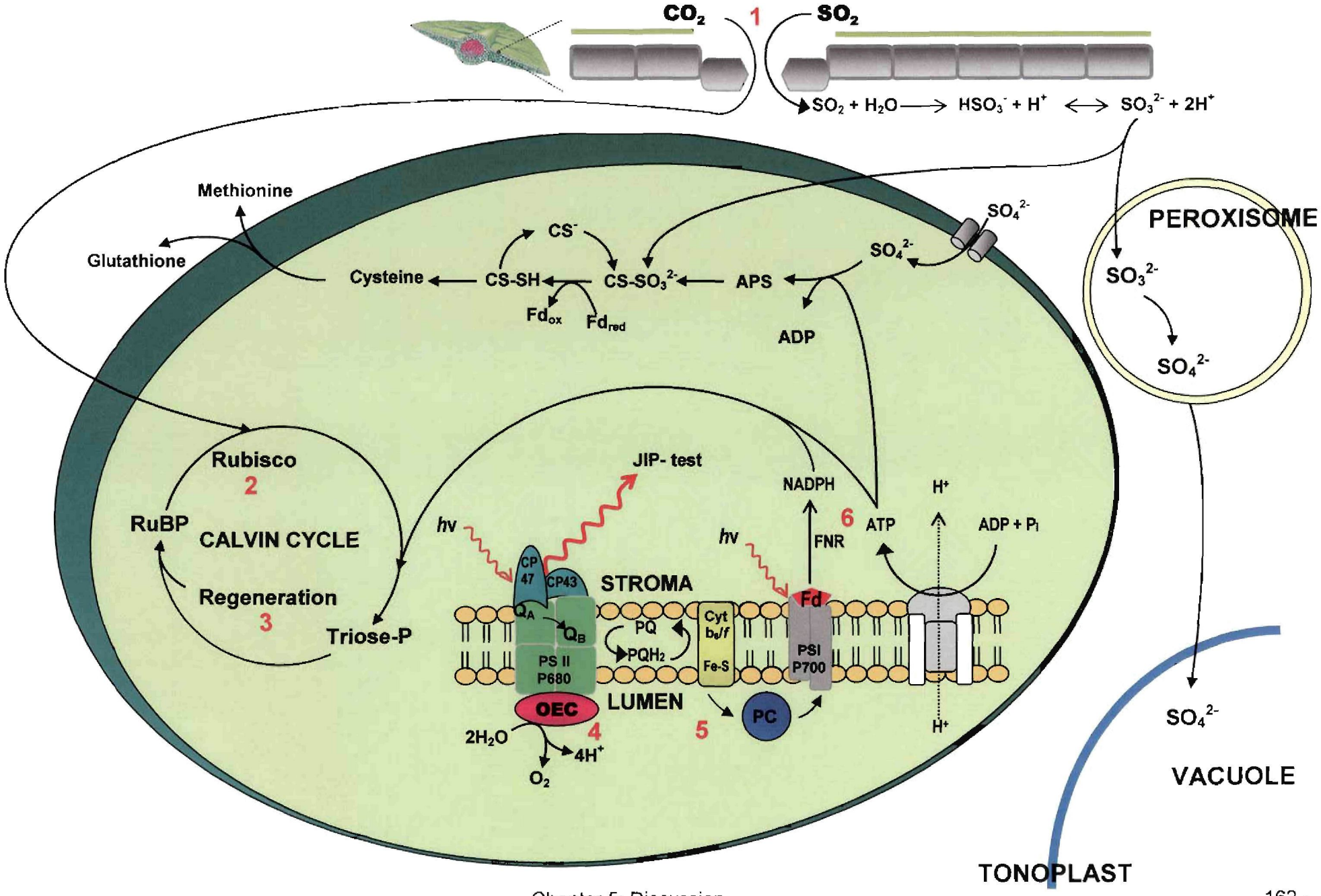

CO2
1
SO2
SO2 + H2O → HSO3- + H+ ↔ SO3 2- + 2H+
Methionine
Glutathione
Cysteine
CS-SH
CS-SO3 2-
CS-
APS
SO4 2-
SO4 2-
Fdox
Fdred
ADP
PEROXISOME
SO3 2-
SO4 2-
Rubisco
2
RuBP
CALVIN CYCLE
Regeneration
3
Triose-P
JIP- test
hv
hv
NADPH
6
FNR
ATP
H+
ADP + Pi
CP 47
CP43
STROMA
QA
QB
PQ
PQH2
Cyt b6/f
Fe-S
Fd
PSI P700
PS II P680
OEC
LUMEN
PC
2H2O
4
4H+
O2
5
H+
SO4 2-
VACUOLE
TONOPLAST

Figure 5.1 schematises some of the important features of photosynthetic events as they occur within the chloroplast. These include the biochemistry of CO_2 fixation, electron transport and sulphur metabolism through the sulphur reduction pathway.

5.7 Constraints on photosynthesis

5.7.1 Stomatal constraints

The data of the present study clearly illustrates that the physiological and biochemical constraints responsible for SO_2 induced reductions in photosynthetic rate, though mainly due to non-stomatal (mesophyll) constraints, can partly be ascribed to stomatal limitations.

We could provide evidence that, in both well watered *Brassica oleracea* and *Glycine max*, the stomatal conductance of the SO_2 fumigated plants was higher than that of the controls. When drought was induced, the stomatal conductance of the *Brassica oleracea* test plants decreased. In *Glycine max*, however, with continuation of fumigation, stomatal conductance increased noticeably at all SO_2 levels, even in the presence of drought stress. Increased stomatal conductance in bean plants exposed to SO_2 has also been reported by Bonte *et al.* (1989). The concomitant increase in transpiration rate could explain the sharp decrease in the WUE of the plants, especially in those simultaneously subjected to SO_2 and drought stress. This phenomenon must be regarded as a serious threat to crop production in the highly industrialised areas of Mpumalanga (Marshall, 2000). The prospects become even worse when the prediction of future increases in temperatures and drought, associated with increasing global warming is considered (Kickert *et al.*, 1999). Stomatal closure of SO_2 fumigated plants could be induced by (i) the direct effect of SO_2 on the guard cells and surrounding epithelial cells (Darrall, 1989), or/and (ii) the indirect effect of SO_2 within the mesophyll processes, contributing to a decrease in CO_2 assimilation rate and resulting in an unchanged or elevated internal CO_2 concentration (C_i) (Brodribb, 1996), as was evident from the results of the present study. It is important to note that stomatal response towards a pollutant (e.g. SO_2) may differ according to seasonal conditions, species response as well as the gaseous pollutant concentration and duration of fumigation. Several studies on different plant species have confirmed that SO_2 can disturb stomatal functioning (Black & Black, 1979). The effect of SO_2 on the mechanical functioning of stomata varies. There has been a considerable degree of confusion about the effects of SO_2

on the mechanistic opening and closing of the stomata, amidst evidence that drought may both increase and decrease the tolerance of plants (Unsworth *et al.*, 1972). Research on soybeans indicated that soil moisture stress may interact with O_3 to cause major reductions in yields (Heggestad *et al.*, 1985). Contrary to this, various investigations conducted in the USA have suggested that water stress can reduce injury to O_3. It is known that the resistance of leaves to water vapour diffusion, i.e. evaporation, may decrease upon exposure to SO_2 (Majernik & Mansfield, 1971; Biscoe *et al.*, 1973). However, it has also been shown that SO_2 exposure may induce stomatal closure under certain conditions besides these differences, stomatal behaviour may be affected by the water status of the plants (Sij & Swanson 1974; Farrar, Relton & Rutter, 1977). Majernik and Mansfield (1971) have shown that stomatal opening is stimulated by SO_2 when the relative humidity is above 40 %. In contrast to this, Unsworth, Biscoe and Pinckney (1972) showed that stimulation of stomatal opening is most pronounced in water stressed plants.

The results reported here, suggest that stomatal behaviour is not the major cause of the observed response of photosynthesis to SO_2 exposure in plants with or without simultaneous drought stress, but rather the indirect effect of SO_2 on the photosynthetic processes. This is in contrast to the reported behaviour of stomata of plants exposed to O_3. In the latter case, stomatal closure precedes photosynthetic depression and apparently causes reduction in the photosynthetic rate (Hill & Littlefield, 1969). Reductions in stomatal conductance may thus only partially explain reductions in photosynthetic rate, suggesting that in addition to reduced stomatal conductance, inhibited biochemical reactions in the mesophyll significantly contributes to limitation of carbon acquisition.

The results of the present study show that drought stress interact with moderate and high levels of SO_2 to reduce leaf photosynthetic capacity of the winter crop *Brassica olearcea* and the summer crop *Glycine max*. Under drought conditions, the photosynthetic capacity of plants grown in the presence of SO_2 decreased much more than when grown in SO_2 free air. All data seem to fit the same propensity. The water balance of the leaves is controlled by water loss through the epidermis via the stomata and water supply from the soil via the roots. Stomatal mechanisms or other mechanisms that control water uptake could be affected in some way by the action of SO_2. The data presented in Section 4.4.2 indicates that WUE decreased severely in well watered and especially in drought stressed plants when fumigated with SO_2, even when the stomata conductance and the rate of transpiration were low. Water

deprived plants showed a more severe decrease in WUE even though stomatal conductance decreased by more than 90 % in plants fumigated at the highest SO_2 level (Table 4.4; Figure 4.6). Experiments performed by Maas *et al.* (1987) revealed that continuous fumigation with SO_2 resulted in an increase in dark period transpiration rates. Although these have been proven to be only minor increases, the increase in dark-period transpiration was still large enough to affect the water status of the plants, since the increased transpiration was not accompanied by increased water uptake. The authors also suggested that cells of plants that transpire relatively large quantities of water during the night, as indicated by increased percentage dark-period transpiration, cannot build up enough turgor pressure to expand during the first hours of the light period. This then resulted in a reduced fresh weight yield and a higher dry matter content. However, this observed yield reduction of fresh weight can only be explained by increased dry matter content. Effects of SO_2 on transpiration and water uptake have been reported by numerous others such as Majernik and Mansfield (1971); Black and Unsworth (1980); Taylor *et al.* (1985) and Temple *et al.* (1985).

5.7.2 Non-stomatal constraints

The present study convincingly demonstrated that limitations within the mesophyll were primarily responsible for the reduction in the rate of photosynthesis. This pointed at the important role of SO_2 and its oxidation products within the mesophyll. Additional direct indications of mesophyll damage were associated with ultrastructural damage to chloroplasts all over the mesophyll (Figures 4.11, 4.12). It is not yet clear what contribution biochemical modifications present to reduce net photosynthesis, and the actual occurrence of oxidative stress which causes a higher demand of energy to support repair and maintenance processes. The most likely reasons for the decline in photosynthesis caused by SO_2, seems to be the inactivation of RuBP (Atkinson & Winner, 1987) and stomatal closure (partly a consequence of the former). The transient nature of the depression in photosynthesis reported for increasing SO_2 levels can be interpreted as a reduced RuBP activity or the amount thereof or the turnover rate of the leaf enzymes. The decline in carboxylation efficiency (CE) can be ascribed to be offset by increases in RuBP regeneration capacity (J_{max}). Barton *et al.* (1980), Taylor *et al.* (1986) and Sison *et al.* (1981) all found residual (mesophyll) resistance to be much more important than stomatal resistance in SO_2 inhibition of photosynthesis. Barton *et al.* (1980) found that mesophyll resistance in bean leaves contributed to 99 % of the

total leaf resistance at high humidity and to 89 % with low humidity. Kropff (1987) confirmed for *Vicia faba* that SO_2 did not affect stomata (except indirectly through the feedback loop between net photosynthesis and internal CO_2 concentration, indicating that SO_2 only inhibited photosynthesis through increased residual (mesophyll) resistance. He suggested changes in the affinity of ribulose-1,5-bisphostphate-carboxylase-oxiginase (Rubisco) towards oxygen. Rubisco would thus be relatively inhibited in its CO_2 scavenging function. Several other authors reported on the inhibitory effect of SO_2 upon RuBP (Von Caemmerer & Farquhar, 1981; Winner *et al.*, 1985).

Photosynthesis declined gradually with duration of fumigation which was evident even when no visible leaf necrosis was noticeable. This was also reported by others (Saxe, 1990, Rao *et al.*, 1983). Visible injury occurred in plants treated with higher SO_2 doses (150 and 300 ppb) and was first discernible at the 150 ppb SO_2 level after 20 days of fumigation. Thus, the effect of SO_2 on RuBP does not fully explain the observed inhibition of photosynthesis. The fact that SO_2 had a marked effect on photosynthesis at low quantum flux densities, shows that the effect of SO_2 can be directly connected with the primary photoreactions (i.e. the electron transport and photophosphorylation). Declines in photosynthesis may thus be due to biochemical factors, although biochemical responses to SO_2 do not necessarily affect net photosynthesis.

5.8 The influence of the chamber effect

The ambient plots used in this investigation made the evaluation of the "chamber effect" on the crop possible. It is noteworthy that the presence of the chamber had opposite effects on biomass accumulation and yield of *Brassica oleracea* grown during the winter and *Glycine max* grown during the summer. The average shoot and root dry mass measured in *Brassica oleracea* were respectively 42 % less in the external plots in comparison with the well watered 0 ppb chambered control. The experiment on *Brassica oleracea* was conducted during the winter months, when the low ambient temperature may have been a limiting factor for growth. Under these conditions the plants in the OTCs performed better that those in the ambient plots. In the second experiment which was conducted during the summer of 2007, the chamber effect on yield was somewhat negative. During the summer months, *Glycine max* plants in the external plots yielded higher than those in the chambers, probably due to the slight increased temperature in the chambers.

Chapter 6

Concluding comments and future perspectives

Many scientists have contributed in resolving the mechanism by which SO_2 becomes phytotoxic in plants, but still there is little real information as to how essential physiological and biochemical processes are affected in SO_2 exposed plants. In order to generate an in depth assessment, immense endeavor was put into designing, commissioning and optimising a battery of 12 state-of-the-art open top chambers. The meteorological data inside the chambers were continually recorded and weekly analysed and evaluated with that recorded at ambient so that the necessary adjustments could be made to eliminate possible modification the 'chamber effect' might present. The data presented at the beginning of Chapter 4 convincingly illustrated that this OTC facility was very well suited for generating test atmosphere of elevated SO_2 concentrations, and could maintain the climatic environment within the chambers very close to the natural situation. Although the OTC facility presented some operational challenges (Chapter 2), the reproducibility of the data highlighted the significance of such a facility in air pollution research; making it a world class one. In depth analysis of the data persistently and clearly demonstrated the concentration dependant inhibition of SO_2 on the physiological and biochemical processes of the test plants. Some parameters in the *chlorophyll a* fluorescence data showed stimulation in well watered and drought stressed *Brassica oleracea* and *Glycine max* test plants. These reductions occurred largely at the lowest treatment level in well watered test plants. However, this stimulation by SO_2 was not the norm. SO_2 fumigation of test plants resulted in large inhibitions and this inhibition was more severe in drought stressed plants. The data presented in Chapter 4 was analysed with great sophistication and revealed that the physiological and biochemical basis for SO_2-induced decreases in photosynthesis should be ascribed to the following:

1. Inhibition of growth

Inhibition of growth was apparent in both *Brassica oleracea* and *Glycine max* plants that were exposed to SO_2, applied separately and in combination with drought stress. Biomass data indicated that root growth in both species was more affected than shoot growth when plants were adequately watered.

However, when plants were exposed to SO_2 and simultaneously subjected to drought, the opposite was true. In drought stressed plants exposed to SO_2, shoot growth was affected more severely than root growth, resulting in stimulation of the shoot-to-root ratio ratio. In *Glycine max*, SO_2 exposure brought about a large decrease in the formation of yield attributes (Figure 4.15 present good visual evidence). Yield decreased severely in well watered plants exposed to SO_2, but decreased even more, by as much as 57 %, when SO_2 exposed plants were simultaneously subjected to drought. Apart from the above mentioned inhibition, SO_2 also brought about a disturbance of leaf expansion and cell division that caused deformity of the youngest petioles.

2. Root nodule ureide content

Root nodule ureide content, which serves as a measure of the affectivity of the nitrogen metabolism in symbiotic nitrogen fixing plants, (i.e. *Glycine max*), decreased at all SO_2 concentrations in well watered and drought stressed plants. It could be assumed that this reduction in ureide content contributed to the decreases in growth and yield production.

3. Decrease in chlorophyll content index (CCI)

The chlorophyll content of both *Brassica oleracea* and *Glycine max* was decreased by SO_2 treatment. Chlorophyll content in well watered *Brassica oleracea* showed an initial increase at all SO_2 treatment levels after 42 days' fumigation, whereafter it decreased severely at the 150 and 300 ppb levels. No stimulation of chlorophyll content occurred in *Brassica oleracea* plants exposed to SO_2 and simultaneously subjected to drought stress. The chlorophyll content of both well watered and drought stressed *Glycine max* plants exposed to SO_2, were inhibited at all SO_2 concentrations. Also in this case, no stimulation was apparent at any SO_2 concentration administered and the inhibitory effect however was most severe in plants simultaneously subjected to drought stress.

4. Ultrastructural decay/degradation/deterioration

Ultrastructural investigations of leaf material of the 300 ppb fumigated *Glycine max* plants revealed that SO_2-induced damage was most apparent in the

chloroplasts. Changes in chloroplast shape, damage to internal membranes and damage to the thylakoids, were the most notable changes that occurred after 35 days' fumigation with 300 ppb SO_2.

5. Changes in stomatal conductance

Stomatal conductance was severely altered in both *Brassica oleracea* and *Glycine max* plants fumigated with SO_2 separately or simultaneously subjected to drought stress. Stomatal conductance increased in well watered *Brassica oleracea*. This increase led to an increased transpiration rate resulting in a severe reduction of the water use efficiency of the plants. Stomatal conductance in drought stressed *Brassica oleracea* were reduced at all treatment levels. The reduction in stomatal conductance and transpiration rate however did not increase the water use efficiency (WUE = A/E) of the test plants, indicating that CO_2 assimilation rate was severely inhibited. This decrease in stomatal conductance occurred due to an accumulation of CO_2 in the substomatal cavity as indicated by the Ci_{350} that remained constant or even increased. However, drought stressed *Glycine max* that was exposed to the same SO_2 concentrations (i.e. 50 and 150 ppb), showed a drastic increase in stomatal conductance resulting in decreased water use efficiency. This indicates the severity of SO_2 pollution when conditions of drought prevail. Thus, the hypothesis (Chapter 1) claiming that closing of stomata protects plants against further uptake of injurious SO_2 was proven wrong.

6. Inhibition of Rubisco activity

According to Majernik & Mansfield (1970), stomatal conductance is considered to be the primary factor controlling SO_2 flux into leaves and subsequent reductions in photosynthetic rate. Our results however convincingly demonstrated that physiological and biochemical inhibition by SO_2 mainly resulted from limitations within the mesophyll (biochemical) processes. In the present study it was demonstrated that the loss in photosynthetic capacity may be associated with a loss in Rubisco activity. In part, inhibition is induced by direct damage to Rubisco, or in part due to a down-regulation of electron transport and the reduction in the probability for the formation of end electron acceptors, namely NADPH and ATP. The carboxylation efficiency (CE), which is considered to be a

sensitive *in vivo* measure of Rubisco activity, showed a strong concentration dependent decrease. The decreased *in vitro* Rubisco activity strongly corroborated this finding. The CO_2 compensation concentration increased drastically with increasing SO_2 exposure concentration, further indicating that injury resulted mainly from limitations in the mesophyll processes.

7. Inhibition of RuBP regeneration

The drastic concentration dependent inhibition of CO_2 assimilation capacity could be ascribed to decreased CO_2 saturated rates of photosynthesis (J_{max}), which suggests that SO_2 had an inhibitory effect on the regeneration capacity of RuBP (Farquhar & Sharkey, 1982). This inhibition may have been caused by the reduction in Calvin-cycle enzyme reaction rates. These reaction rates are highly dependent on ATP to promote phosphoglycerate kinase and ribulose-5-phosphate kinase and NADPH to promote glyceraldehyde-3-phosphate dehydrogenase. The concomitant reduction in the quantum yield of electron transport from Q_A^- to PSI end electron acceptors (φR_0), resulting in a reduction of NADPH and ATP production, corroborates the decrease in CO_2 assimilation found.

8. Inhibition of photosynthetic transport

In depth analysis of the difference relative variable *chlorophyll a* fluorescence O-K-J-I-P transients revealed hidden bands, namely ΔK, ΔJ and ΔI -peak which is much richer in information than the original O-J-I-P. The occurrence of a K-peak is the consequence of an increase in fluorescence, probably due to the short-lived accumulation of reduced electron carriers such as $Pheo^-$, which, in turn, is caused by the dissociation of the OEC, resulting in an imbalance between the electron flow from the OEC to the RC and towards the acceptor side of PSII in the direction of PSI (Strasser, 1997). The difference relative *chlorophyll a* fluorescence transients of drought stressed *Glycine max* plants revealed a -ΔK-peaks that pointed to initial stimulation of the oxygen evolving complex (OEC) that took place after 14 days' fumigation (Figure 4.55). After 28 days' fumigation, +ΔK-peaks developed, indicating that SO_2 caused uncoupling of the OEC from PSII. Uncoupling of the OEC enables an alternative internal electron donor such as ascorbate or proline (instead of H_2O) to donate electrons to PSII. Both SO_2

treated and water stressed SO_2 treated plants exhibited an obvious increase in the K-band (300 – 400 µs), after 28 days' fumigation, indicating a partial block on the water splitting side or uncoupling of the oxygen evolving complex (OEC). Analysis of the chlorophyll fluorescence transients of drought stressed *Glycine max* plants also revealed a +ΔJ-peak that developed after 14 days' fumigation with 300 ppb SO_2 (Figure 4.55). The development of +ΔJ-peak indicated an accumulation of Q_A^- due to inhibition of the dark reactions responsible for the reoxidation of the Q_A^- pool. The ΔJ peak (Figure 4.55) suggests the possibility that SO_2 inhibited electron transport beyond Q_A, which resulted in the accumulation of Q_B^-. Clearly visible +ΔI-peaks that developed after 14 and 28 days' fumigation in both well watered and drought stressed *Glycine max* plant provided information on the activation state of ferredoxin $NADP^+$ reductase (FNR) and possible accumulation of end electron acceptors such as NADPH and Fd (red). The developed +Δ-peaks suggested an inhibition of electron flow further down from the reduced intersystem electron acceptors of the electron transport chain to the PSI and electron acceptors. The concomitant decrease in the quantum efficiency of electron transport from Q_A^- to the PSI end electron acceptors (φR_0), which reflects the reduction capacity of the PSI end electron acceptors, (Tsimilli-Michael & Strasser, 2008; Yordanov *et al.*, 2008) corroborated the above mentioned finding.

Future perspectives

Although the aims of this study were adequately reached, the following aspects however need further investigation:

- Determination of ATP and NADPH levels in isolated chloroplasts to confirm the inhibition of their formation by SO_2;
- Determination of the contribution of the sulphate-reduction pathway by determination of the glutathione levels;
- Determination of SOD (superoxide dismutase) and POD (peroxidase) activity in SO_2 exposed plants;
- Confirmation of the ultrastructural study; and
- To study the effect of SO_2 on symbiotic nitrogen fixation.

REFERENCES

ADAROS G, WEIGEL HJ, JÄGER HJ (1988). Effects of sulphur dioxide and acid rain alone or in combination on growth and yield of broad bean plants. New Physiologist, 108: 67-74.

ADAROS G, WEIGEL HJ & JÄGER HJ (1989). Environment in open-top chambers and its effects on growth and yield of plants. i. Measurement of microclimatic parameters. Gartenbauwissenschaft, 54(4): 165 -171.

AGRAWAL M & VERMA M (1997). Amelioration of sulphur dioxide phytotoxicity in wheat cultivars by modifying NPK nutrients. Journal of Environmental Management, 49: 231–244.

AGRAWAL M (2000). Researches on air pollution impacts on vegetation in India: a review. The Botanica, 50: 76 – 85.

ALLEN LH, Jr. (1990). Plant responses to rising carbon dioxide and potential interactions with air pollutants. Journal of Environmental Quality, 19: 15 -34.

ASADA K & KISO K. (1973). Initiation of aerobic oxidation of sulfite by illuminated spinach chloroplasts. European Journal of Biochemistry, 33: 253-257.

ASADA K. Formation and scavenging of superoxides in chloroplast, with relation to injury by sulphur dioxide, In: N.I.E.S (1980) pp. 165-179.

ASHMORE MR & MARSHALL FM (1998). Direct impacts of pollutant gasses on crops and forests. In KUYLENSTIERNA J & HICKS K (eds.) Regional air pollution in developing countries, Stockholm Environmental Institute, York, pp. 21 -33.

ATKINSON CJ & WINNER WE (1987). Gas exchange characteristics of *Heteromeles arbutfolia* during fumigation with sulphur dioxide. New Phytotlogist, 106:423-136.

ATKINSON CJ, WOOKEY PA, MANSFIELD TA (1991). Atmospheric pollution and the sensitivity of stomata on barley leaves to abscisic acid and carbon dioxide. New Phytologist, 117: 535-541.

BARRETT TW & BENEDICT HM (1970). Sulfur dioxide. In: J. S. JACOBSON & A. C. HILL. Recog- nition of air pollution injury to vegetation: a pictoral atlas. (Eds.). Air Pollution Control Assn., Pittsburgh, pp. C1-C5.

BARTON JR, MCLAUGHLIN SB, MCCONATHY RK (1980). The effects of SO2 on componenets of leaf resistance to gas exchange. Environmental Pollution, 21:255-265.

BEADLE CL, LUDLOW MM, HONEYSETT, JL (1993). Water relations. In: HALL DO, SCURLOCK JMO, BOLHAR-NORDENKAMPF RC & LONG SP (eds.) Photosynthesis and production in a changing environment. A field and laboratory manual. Chapman & Hall, London, pp. 121–123; 156-159.

BELL JNB & THRESHOW H (2002). Air pollution and plant life, John Wiley & Sons, New York. 87–118.

BELL JNB & TURNER M. (2002). Air pollution and plant life. 2nd Ed. John Wiley & Sons, Ltd., New York.

BENTON, J. FUHRER, B.S. GIMENO, L. SKÄRBY, D. PALMER-BROWN, G. BALL, C. ROADKNIGHT, G. MILLS (2000). An international cooperative programme indicates the widespread occurrence of ozone injury on crops. Agriculture, Ecosystems and Environment 78, pp. 19–30.

BIGGS K & FRY C (1987). Phenolic cross-linking in the cell wall. In: Physiology of cell expansion during plant growth In COSGROVE DJ & KNIEVEL DP (eds.) pp. 46-57. American Society of Plant Physiologists, Rockville, MD.

BISCOE PV, UNSWORTH MH & PINCKNEY HR (1973). The effects of low concentrations of sulphur dioxide on stomatal behaviour in *Vicia faba*. New Phytologist, 72(6): 1299–1306.

BLACK CR & BLACK VJ (1979). The effects of low concentrations of sulphur dioxide on stomatal conductance and epidermal cell survival in field bean (*Vicia Faba* L.). Journal of Experimental Botany, 30:291-298

BLACK VJ & UNSWORTH MH (1979). Resistance analysis of sulphur dioxide fluxes to *Vicia faba*. Nature, 282: 68-69.

BLACK VJ & UNSWORTH MH (1980). Stomatal responses to sulphur dioxide and vapour pressure deficit. Journal of Experimental Botany, 31:667-677.

BOLHÁR-NORDENKAMPF HR & ÖQUIST G (1993). Chlorophyll fluorescence as a tool in photosynthesis research. In: HALL DO, SCURLOCK JMO, BOLHÁR-NORDENKAMPF HR, LEEGOOD RC, LONG SP (eds.) Photosynthesis and production in a changing environment: a field and laboratory manual. Chapman & Hall, London, pp. 193-206.

BONTE J, CANTUEL J, GALAUP S & LOUGUET P (1989). Effects of ambient ozone on yield and physiological parameters of bean (*Phaseolus vulgaris*, cultivar Lt). In: BONTE J & MATHY P (eds.) The European Communities research project on open-top chambers. Results on agricultural crops 1987-1988. Commission of the European Communities, Brussels, pp. 26-42.

BOUBEL RW, FOX, DL, TURNER DB, STERN AC. (1994). Fundamentals of air pollution (3rd ed.), Academic Press, New York.

BRADFORD MM (1976). A rapid and sensitive method for the quantification of microgram quantities of protein utilising the principle of protein dye binding. Analytical Biochemistry, 72: 248-254.

BRESSAN RA, LECUREUX L, WILSON LG, FILNER P (1979). Emission of ethylene and ethane by leaf tissue exposed to injurious concentrations of sulfur dioxide or bisulfite ion. Plant Physiology, 63: 924-930.

BRESSAN RA, WILSON LG, LECURAUX L, FILNER P (1978). Use of ethylene and ethane emission to assay injury by S02. Plant Physiology, 61: S-59.

BRIMBLECOMBE P, HAMMER C, RODHE HI, RYABOSHAPKO A, BOUTTRON CF (1989). Human influence on the sulphur cycle. In: BRIMBLECOMBE P & LIEN AY (eds.) Evolution of the global biogeochemical sulphur cycle. Scope, 39, 77-121. John Wiley & Sons, New York.

BRISLEY HR, DAVIS CR, BOOTH JA (1959). Sulphur dioxide fumigation of cotton with special reference to its effect on yield. Agronomy Journal, 51:77-80.

BRODRIBB T (1996). Dynamics of changing intercellular CO_2 concentration (C_i) during drought and determination of minimal functional C_i. Plant Physiology, 111: 179-185

BUCKENHAM AH, PARRY MA, WHITTINGHAM CP, YOUNG AT (1981). An improved open-topped chamber for pollution studies on crop growth. Environmental Pollution, (Ser. B), 2: 475-82.

CHAVES MM (1991) Effects of water deficits on carbon assimilation. Journal of Experimental Botany, 42: 1-16.

CLARKE K & MURRAY F (1990). Stimulatory effects of SO_2 on growth of *Eucalyptus rudis.* Endl. New Phytologist, 115: 633-637.

COLVILL KE, BELL RM, ROBERTS TM, BRADSHAW AD (1983). The use of open top chambers to study the effects of air pollutants, in particular sulphur dioxide, on the growth of rye grass *Lolium perenne* L. Part II. The long term effect of filtering polluted urban air or adding SO_2 to rural air. Environmental Pollution, 31: 35–55.

HALL DO, SCURLOCK JMO, BOLHAR-NORDENKAMPF HR, LEEGOOD RC, LONG SP (1995). Photosynthesis and production in a changing environment: A field and laboratory maual. (Eds.). Chapman & Hall, London, pp. 166-159.

CORNIC G (1994). Drought stress and high light effects on leaf photosynthesis. In BAKER NR & BOWYER JR (eds.) Photoinhibition of photosynthesis. Bios Scientific Publishers, Oxford, UK. pp. 297-313.

CRITICAL LOADS ADVISORY GROUP (1996). Critical levels of air pollutants for the United Kingdom. Institute of Terrestrial Ecology, Edinburgh Research Station, UK.

CRITTENDEN PD & READ DJ (1978). The effects of air pollution on plant growth with special reference to sulphur dioxide. II. Growth studies with *Lolium perenne* L. New Phytologist, 80: 49–62.

CULLIS CF & HIRSHLER MM (1980). Atmospheric sulphur: Natural and man-made sources. Atmospheric Environment, 14: 1263-1278.

DARALL NM (1986). The sensitivity of net photosynthesis in several plant species to short term fumigation with sulphur dioxide. Journal of Experimental Botany, 37: 1313-1322.

DARALL NM (1989). The effects of air pollutants on physiological processes in plants. Plant Cell and Environment, 12: 1-30.

DEEPAK SS & AGRAWAL M (1999). Growth and yield responses of wheat plants to elevated levels of CO_2 and SO_2, singly and in combination. Environmental Pollution, 104: 411-419.

DEEPAK SS & AGRAWAL M (2001). Influence of elevated CO_2 on the sensitivity of two soybean cultivars to sulphur dioxide. Environmental and Experimental Botany, 46: 81-91.

DE KOK LJ. 1990. Sulfur metabolism in plants exposed to atmospheric sulfur. In: RENNENBERG H, BRUNOLD C, DE KOK LJ, STULEN I (eds.) Sulfur Nutrition and Sulfur Assimilation in Higher Plants. The Hague,The Netherlands: SPB Academic Publishing, pp. 111-130.

DENMEAD OT, DUNIN FX, WONG SC, GREENWOOD EAN (1993). Measuring water use efficiency of Eucalypt trees with chambers and micrometeorological techniques. Journal of Hydrology. 150: 649-664.

DE RONDE JA CRESS WA KRüGER GHJ STRASSER RJ, VAN STADEN J (2004). Photosynthetic response of transgenic soybean plants containing the *Arabidopsis P5CR* gene, during heat and drought stress. Journal of Plant Physiology, 161:1211-1224

DE SILVA M, PURCELL LC, KING CA (1996). Soybean petiole ureide response to water deficits and decreased transpiration. Crop Science, 36: 611–616.

DIENER BA & BABCOCK GT (1996). Structure, dynamics, and energy conversion efficiency in Photosystem II. In: ORT DR & YOCUM F (Eds.). Oxygenic Photosynthesis; the Light Reactions, Kluwer Academic Publishers, Dordrecht, the Netherlands, pp 213-247.

DRAKE GB, LEADLEY PW, ARP WJ, NASSIRY D, CURTIS PS (1989). An open top chamber for field studies of elevated atmospheric CO_2 concentration on saltmarsh vegetation. Technical Report. Functional Ecology, 3: 363-371.

DUNIN FX & GREENWOOD EAM (1986). Evaluation of the ventilated chamber for measuring evaporation from a forest. Hydro. Proc., 1:47-62.

EMBERSON LD, ASHMORE MR, BAMBRIDGE H, TUOVINEN JP & SIMPSON D (2000). Moddeling stomatal flux across Europe. Environmental Pollution, 109:403-413.

ENSER U & HEBER U (1980). Metabolic regulation by pH gradients. Inhibition of photosynthesis by indirect photon transfer across the chloroplast envelope. Biochemical and Biophysical Acta, 592: 577-591.

EPITALAWAGE N, EGGENBERG P, STRASSER RJ (2003). Use of fast chlorophyll a fluorescence technique in detecting drought and salinity tolerant chickpea *(Cicer arietinum L)* varieties. Archives des Sciences, 56 : 79-93

ERICKSON RO & MICHELINI FJ (1957). The plastochron index. American Journal of Botany, 44: 297-305.

FARQUHAR GD, SCHULZE E-D, KÜPPERS M (1980). Response to humidity by stomata of Nicotiana gluuca L. and Corylus avellana L. are consistent with the optimisation of carbon dioxide uptake with respect to water loss. Australian Journal of Plant Physiology, 7:315-327.

FARQUHAR GD & SHARKEY TD (1982). Stomatal conductance and photosynthesis. Annual Review of Plant Physiology, 33: 317-345.

FARRAR JF, RELTON J, RUTTER AJ (1977). Sulphur dioxide and the growth of *Pinus sylvestris*. Journal of Applied Ecology, 14:861-875.

FINLAYSON-PITSS BJ & PITTS JN (1999). Chemistry of the upper and lower atmosphere. Academic Press, New York.

FLEXAS J, DIAZ-ESPEJO A, GALMES J, KALDENHOFF R, MEDRANO H, RIBAS-CARBO M (2007). Rapid variations of mesophyll conductance in response to changes in CO_2 concentration around leaves. Plant Cell & Environment, 10:1284-1298.

FORCE L, CRITCHLEY C, VAN RENSEN JJS (2003). New fluorescence parameters for monitoring photosynthesis in plants. Photosynthesis Research, 78: 17-33.

GARSED SG & READ DJ (1977). Sulphur dioxide metabolism in soy-bean *Glycine max* var. Biloxi. I. Effects of light and dark on the uptake and translocation of $^{35}SO_2$. New Phytologist, 78: 111.

GENTY B & HARBINSON J (1996). Regulation of light utilisation for photosynthetic electron transport. In: BAKER NR (Eds.). Photosynthesis and Environment Kluwer Academic Publications, The Netherlands. pp 67-99.

GODZIK S & KRUPA SV (1982). Effects of sulphur dioxide on growth and productivity of crop plants. In: UNSWORTH MH & ORMROD DP (eds.) Air pollution in agriculture and horticulture. Butterworth, London. pp. 474–575.

GOVINDJEE XUC, SCHANSKER G, VAN RENSEN, JJS (1997). Chloroacetates as inhibitors of photosystem II: Effects on electron acceptor side. Journal of Photochemistry and Photobiology B: Biology, 37: 107-117.

GOVINDJEE XUC (2004) Robert Emerson and Eugene Rabinowitch: understanding photosynthesis. In: HODDESON L (eds.) No Boundaries: University of Illinois Vignettes, Chapter 12, pp 181–194. Board of Trustees, University of Illinois, Urbana and Chicago

GUDERIAN R (1977). Air pollution. Springer-Verlag, Berlin. pp. 42–49.

GUISSÉ B, SRIVASTAVA A, STRASSER RJ (1995). The polyphasic rise of the chlorophyll a fluorescence (OKJIP) in heat-stressed leaves. Archives of Science Geneva, 48: 147-160.

HÄLLGREN J-E & GEZEKIUS K (1982). Effects of SO_2 on photosynthesis and ribulose bisphosphate carboxilase in pine tree seedlings. Physiologia Plantarum, 54:153-161.

HARVEY GW & LEGGE AH (1979). The effect of sulphur dioxide upon the metabolic level of adenosine triphosphate. Canadian Journal of Botany, 57:759-764.

HEAGLE AS, BODY DE, HECK WW (1973). An open-top field chamber to assess the impact of air pollution on plants. Journal of Environmental Quality, 2: 365-72.

HEAGLE AS, PHILBECK RB, ROGERS HH, LETCHWORHT MB (1979). Dispensing and monitoring ozone in open-top field chambers for plant-effects studies. Phytopathology, 69: 15-20.

HEAGLE AS, PHILBECK RB, FERREL RE, HECK WW (1989). Design and performance of a large, field exposure chamber to measure effects of air quality on plants. Journal of Environmental Quality, 18: 361-368.

HEATH RL (1980). Initial events in injury to plants by air pollutants. Annual Review of Plant Physiology. 31: 395-431.

HEBER U, YIN Z-H, DITTRICH A, GHISI R, WAGNER U (1989b). Response to mesophyll cells and its organelles to the stresses produced by the atmospheric pollutant SO_2. In: TAZAWA M, KATSUMI M, MASUDA Y,

OKAMOTO H (eds.) Plant water relations and growth under stress. Yamada Science Foundation and My KK, Tokyo. pp. 93-100.

HECK WW & BRANDT CS (1977). Effects on vegetation: Native crops, forests. In: Air Pollution. 3rd Ed. Volume II, Academic Press, New York. pp. 158-299.

HECK WW, TAYLOR OC, TINGLEY D (1988). Assessment of crop loss from air pollutants. Elsevier Applied Science, London.

HEGGESTAD HE, HEAGLE AS, BENNETT JP, KOCH EJ (1980) The effects of photochemical oxidants on the yield of snap beans. Atmospheric Environment, 14: 317-326.

HEGGESTAD HE, GISH TJ, LEE EH, BENNETT JH, DOUGLAS LW (1985). Interaction of soil moisture stress and ambient ozone on growth and yields of soybean. Phytopathology, 75:472-477.

HENNIES HH (1975). Die sulfitreduktase aus Spinacea oleracea ein Ferredoxin-abhangiges Enzym. Z. Naturforsch C, 30:359.

HILL AC & BENNETT JH (1970). Inhibition of apparent photosynthesis by nitrogen oxides. Atmospheric Environment, 4:341-348.

HILL AC & LITTLEFIELD N (1969). Ozone: Effect on apparent photosynthesis, rate of transpiration and stomatal closure in plants. Environmental Science and Technology, 3:52-56

HOAGLAND DR & ARNON DI (1950). The water culture method for growing plants without soil. California Agricultural Experiment Station Circular, 347.

HOPKINS WG (1999). Introduction to plant physiology, 2nd Ed. John Wiley & Sons, Inc. New York. pp. 200-206.

HORSMAN DC & WELLBURN AR (1976). In: Effects of air pollutants on plants. (Eds.). MANSFIELD TA. Cambridge University Press. New York. pp. 185-199.

HUTTEN S & SOIKKELI S (1984). Effects of various gaseous pollutants on plant cell ultrastructure. In: KOZIOL MJ & WHATLEY FR (Eds.). Gaseous air pollutants and plant metabolism.Butterworths, London.

HYODO H, KURODA H, YANG SF (1978). Introduction of phenylalanine ammonia-lyase and increase in phenolics in lettuce leaves in relation to the development of russet spotting caused by ethylene. Plant Physiology, 62: 31-35.

IPCC (Intergovernmental Panel on Climate Change). (2001). Climate Change 2001: The Scientific Basis. Contribution of Working Group I to the Third Assessment Report of the Intergovernmental Panel on Climate Change. HOUGHTON JT, DING Y, GRIGGS DJ, NOGUER M, VAN DER LINDEN PJ, DAI X,

MASKELL K, AND JOHNSON CA. (eds.) Cambridge University Press, Cambridge.

JÄGER H-J, UNSWORTH M, DE TEMMERMAN L, MATHY P (eds.) Effects of air pollution on agricultural crop in Europe. Air Pollution report 46, Commission of the European Communities, Brussels.

JETTEN TH (1992) Physical description of transport processes inside an open-top chamber in relation to field conditions. PhD thesis, Agricultural University of Wageningen, The Netherlands.

JOSIPOVIC M, ANNEGARN HJ, KNEEN MA, PIKETH SJ, PIENAAR JJ (2007). A regional-scale passive monitoring study of SO_2, NO_2 and ozone in South Africa. Newsletter of the International Global Atmospheric Chemistry Project, 36:6-13.

KAISER G & HEBER U (1983). Photosynthesis of leaf cell protoplasts and permeability of the plasmalemma to some solutes. Planta, 157: 462 -470.

KANG BG (1979). Epinasty. In HAUPT W, FEINLAB ME (eds.) Encyclopaedia of Plant Physiology, Vol. 7. Springer-Verlag, Berlin, pp. 647-667.

KAUTSKY H & HIRSCH A (1931). Neue Versuche zur Kohlensäureassimilation. Naturwissenschaften, 19: 96.

KELLER T (1984). Direct effects of sulphur dioxide on trees. Philosophical Transactions of the Royal Society of London. London Series B, 305: 317–326.

KEYS AJ & PARRY MAJ (1990). Ribulose bisphosphate carboxylase/oxygenase and carbonic anhydrase. Methods in Plant Biochemistry, 3: 1-15.

KICKERT RN, TONELLA G, SIMONOV A, KRUPA SV (1999). Predictive modeling of effects under global change. Environmetal Pollution, 100: 87-132.

KIRSCHBAUM MUF & FARQUHAR GD (1987). Investigation of the CO_2 dependence of quantum yield and respiration in *Eucalyptus pauciflora*. Plant Physiology, 83:1032–1036.

KOCH GW, WINNER WE, NARDONE A, MOONEY HA (1987). A system for controlling the root and shoot environment for plant growth studies. Environmental and Experimental Botany 27: 365–377.

KRAUSE GH & WEISS E (1991). Chlorophyll fluorescence and photosynthesis: the basics. Annual Review of Plant Physiology, 42: 313-349.

KRISHNAYYA NSR & DATE MV (1996). The impact of SO_2 and SO_2 + ascorbic acid treatments on growth and partitioning of dry matter in *Trigonella Foenum – graecum* L. Environmental Pollution, 91: 121-125.

KROPFF MJ, MOOI J, GOUDRIAAN J, SMEETS , LEEMANS A, KLIFFEN C, VAN DER ZALM JA (1989). The effects of long-term open-air fumigation with SO_2 on a field crop of broad bean (Vicia faba L.) I. Depression of growth and effects on leaf area development. New Phytologist, 113: 337-344.

KRÜGER GHJ, TSIMILLI-MICHAEL M, STRASSER RJ (1997). Light stress provokes plastic and elastic modifications in structure and function of photosystem II in camellia leaves. Physiologia Plantarum, 101: 265-277.

KRUPA SV (1996). The role of atmospheric chemistry in the assessment of crop growth and productivity. In: YUNUS M & IQBAL M (eds.) Plant response to air pollution. pp. 35–73. John Wiley & Sons, Chichester, England.

KURKDJIAN A & GUERN J (1989). Intracellular pH measurement and importance in cell activity. Annual Review of Plant Physiology, Plant Molecular Biology, 40: 271-303.

LANGE OL, HARLEY PC, BEYSCHLAG W, TENHUNEN JD (1987). Gas exchange methods for characterizing the impact of stress on leaves. In: TENHUNEN JD (ed.) Plant response to stress. Springer-Verlag, Heidelberg, Germany. pp. 3-22.

LAVOREL J & ETIENNE AL (1977). *In vivo* chlorophyll fluorescence. Topics in Photosynthesis, 2: 203-268.

LAZÁR D & ILÍK P (1997). High-temperature induced chlorophyll fluorescence changes in barley leaves: Comparison of the critical temperatures determined from fluorescence induction and from fluorescence temperature curve. Plant Science, 124: 159-164.

LEEGOOD RC KOBAYASHI J, NEIMANIS S, WALKER DA, HEBER U (1982). Cooperative activation of chloroplast fructose-1,6-bisphosphatase by reductant, pH and substrate. Biochemical and Biophysical Acta, 682: 168-178.

LEGGE AH, JÄGER HJ, KRUPA SV (1998) Sulphur dioxide. In: FLAGER RB (ed.) Recognition of air pollution injury to vegetation: A pictorial atlas, 2nd Ed. Air and Waste Management Association, Pittsburgh, PA. pp. 311-342.

LEGGE AH, KRUPA SV. 2002. Effects of sulphur dioxide. In: BELL JNB, TRESHOW M, (eds.).Air pollution and plant life, 2nd edn. Chichester: John Wiley, pp. 135–162.

LEUNING R & FOSTER IJ (1990). Estimation of transpiration by single trees: comparison of a ventilated chamber, leaf energy budgets and a combination equation. Agricultural and Forest Meteorology, 51: 63-86.

LEVERENZ JW (1987). Chlorophyll content and the light response curve of shade-adapted conifer needles. Plant Physiology, 71: 20–29.

LONG SP (1985). Leaf gas exchange. In: BARBER J & BAKER NR (eds.) Photosynthetic mechanisms and the environment. Elsevier, Amsterdam. pp. 453-500.

LONG SP & HÄLLGREN JE (1993). Measurement of CO_2 assimilation by plants in the field and the laboratory. In: HALL DO *et al.* (eds.) Photosynthesis and production in a changing environment: a field and laboratory manual. Chapman & Hall, London. pp. 129-167.

MAAS FM, KOK LJ, DE HOFFMANN I, KUIPER JC (1987). Plant responses to H_2S and SO_2 fumigation. I. Effects on growth, transpiration and sulphur content of spinach. Physiologia Plantarum, 70:713-721.

MAIER-MAERCKER U (1989). Delignification of subsidiary and guard cell walls of *Picea abies* (L.) Karst by fumigation with ozone. Trees, 3: 57-64.

MAJERNIK O & MANSFIELD TA (1970). Effects of SO2 pollution on stomatal movement in *Vicia Faba* L. Phytopathologische Zeitschrift, 71:123-128.

MALDONADO-RODRIGUEZ R. (2002). Web-published. www.unige.ch/sciences/biologie/bioen/bioindex.html

MALHOTRA SS & HOCKING D (1976). Biochemical and cytological effects of sulphur dioxide on plant metabolism. New Phytologist, 76: 227.

MANDL RH, WEINSTEIN LH, MCCUNE DB, KEVENY M (1973). A cylindrical, open-top chamber for exposure of plants to air pollutants in the field. Journal of Environmental Quality, 2: 371-376.

MANDL RH, LAURENCE JA, KOHUT RJ (1989). Development and testing of open-top chambers for exposing large perennial plants to air pollutants. Journal of Environmental Quality, 18: 534-540.

MANSFIELD TA (1998). Stomata and plant water relations: Does air pollution create problems? Environmental Pollution, 101: 1-11.

MARSHALL FM, ASHMORE MR, BELL JNB, MILNE E (1998). Air pollution impacts on crop yield in developing countries – a serious but poorly recognized problem? In: Paper of 11th World Clean Air and Environment Congress, Durban, 13–18 Sept. Vol. 5, 13E-2, 6 pp.

MARSHALL FM, TE LINTELO DJH, WILDIG Z, STONEHOUSE J, BELL JNB, ASHMORE MR, BATTY K (2000). The impacts of policy implications on crops in developing countries. Final Technical Report: Department of International Development, Environment Research Programme. R6992. Imperial College of Science, Technology and Medicine, London.

MAXWELL K & JOHNSON GN (2000). Chlorophyll fluorescence – a practical guide. Journal of Experimental Botany, 51(345): 659-668.

MCANISH MR, EVANS NH, MONTGOMERY LT, NORTH KA (2002). Calcium signalling in stomatal response to pollutants. New Phytologist, 153: 441-447.

MOONEY HA, KUPPERS M, KOCH G, GORHAM J, CHU C, WINNER WE (1988). Compensating effects to growth of carbon partitioning changes in response to SO_2-induced photosynthetic reduction in radish. Oecologia, 75: 502-506.

MORGAN PW & FOWLER JL (1972). Ethylene: Modification of peroxidase activity and iso-zyme complement in cotton (Gossypium hirsutum L). Plant and Cell Physiology, 13: 727-736.

MUDD JB & KOZLOWSKI TT (1975). Response of plants to air pollution. Academic Press, New York.

MULLER RN, MILLER JE, SPRÜGEL DG (1979). Photosynthetic response of field-grown soybean to fumigations with sulphur dioxide. Journal of Applied Ecology, 16:567-576.

NEUBAUER C & SCHREIBER U (1987). The polyphasic rise of chlorophyll fluorescence upon onset of strong continuous illumination: I. Saturation characteristics and partial control by Photosystem II acceptor side. Z Naturforsch, 42c: 1246–1254.

NIEBOER E, RICHARDSON DHS, PUCKETT KJ, TOMASSINI FD (1976). In: Effects of air pollutants on plants. (Eds.). MANSFIELD TA. Cambridge University Press. New York. pp. 61-85.

NORRIS TS & BAILEY BJ (1996). Use of simulation analysis to improve the design of open-top chambers. Agricultural and Forest Meteorology, 78: 259-275.

NORRIS TS, BAILEY BJ, LEES MJ, YOUNG PC (1996). Design of a controlled-ventilation open-top chamber for climate change research. Journal of Agricultural Engineering Research, 78: 279-288.

OLSZYK DM, TIBBITTS TW, HERTZBERG WM (1980). Environment in open-top field chambers utilised for air pollution studies. Journal of Environmental Quality, 9(4): 610-615.

OLSZYK DM, BYTNEROWICZ A, KATS G, DAWSON PJ, WOLF J, Thompson CR (1986). Effects of sulphur dioxide and ambient ozone on winter wheat and lettuce. Journal of Environmental Quality, 15: 363- 369.

OUTLAW WH (2003). Integration of cellular and physiological function of guard cells. Critical Review of Plant Science, 22: 503-529.

PALMER JH (1985). Epinasty, hyponasty, and related topics. In PHARIS RP & REID DM (eds.) Encyclopaedia of Plant Physiology, Vol. 11. Springer-Verlag, Berlin, pp. 139-168.

PAPAGEORGIOU J (1975). Chlorophyll fluorescence: an intrinsic probe of photosynthesis. In: GOVINDJEE XUC (ed.). Bioenergetics of Photosynthesis. Academic Press, New York. pp. 319-371.

PEISER GD & YANG SF (1979). Ethylene and ethane production from sulfur dioxide-injured plants. Plant Physiology, 63: 142-145.

PERCY KE, MCQUATTIE CJ, REBBECK JA (1994). Effects of air pollutants on epicuticular wax chemical composition. In: PERCY KE, CAPE JN, JAGELS R, SIMPSON CJ (Eds.). Air Pollutants and the Leaf Cuticle. Heidelberg, Springer-Verlag, 67-79.

PFANZ H & HEBER U (1986). Buffer capacities of leaves, leaf cells and leaf cell organelles in relation to fluxes of potentially acidic gases. Plant Physiology, 81: 597–602.

PFANZ H, MARTINOLA E, LANGE OL & HEBER U (1987b) Flux of SO_2 into leaf cells and cellular acidification by SO_2. Plant Physiology, 85: 928–933.

PFANZ H, DIEZ KJ, WEINERTH J, OPPERMANN B (1990). Detoxification of sulphur dioxide by apoplastic peroxidases. In: RENNENBERG H, BURNOLD C, DE KOK LJ, STULEN I. (eds.) Sulphur nutrition and sulphur assimilation in higher plants. SPB Academic Publishers, The Hague, The Netherlands. pp. 229-233.

PRATT GC, KROMROY KW, KRUPA SV (1983). Effects of ozone and sulphur dioxide on injury and foliar concentrations of sulphur and chlorophyll in soybean *Glycine max*. Environmental Pollution, 32: 91-99.

PUCKETT KJ, NIEBOER E, FLORA WP, RICHARDSON DHS (1973). Sulphur dioxide: its effects on photosynthetic C^{14} fixation in lichens and suggest mechanisms of phototoxictiy. New Phytologist, 72: 141.

RAJPUT M, AGRAWAL M, SINGH J (1995). Interaction of soil fertility levels and sulphur dioxide on growth, assimilate partitioning and yield of wheat. Journal of Environmental Biology, 16: 265–275.

RAVIN JA (1977). Ribulose bisphosphate carboxylase activity in terrestrial plant: significance of O_2 CO_2 diffusion - Commentaries in Plant Science No3. Current Advances in Plant Science, 9:579-590.

ROA IM & ANDERSON LE (1983). Light and stomatal metabolism. I. Possible involvement of light modulation of enzymes in stomatal movement. Plant Physiology, 71: 451-455.

ROA IM & ANDERSON LE (1983). Light and stomatal metabolism. II. Effects of sulfite and arsenite on stomatal opening and light modulation of enzymes in epidermis. Plant Physiology, 71: 456-459.

RAO MV & DE KOK LJ (1994). Interactive effects of high CO_2 and SO_2 on growth and antioxidant levels in wheat. Phyton, 36: 279-290.

RASCHKE K (1979). Movements of stomata. In: HAUPT W & FEINLEIB ME (eds.) Encyclopaedia of Plant Physiology (New Series) 7: 383-441. Springer-Verlag, Berlin.

RENNENBERG H (1984). The fate of excess sulphur in higher plants. Annual Review of Plant Physiology, 35: 121-153.

RENNENBERG H & HERSCHBACH C (1996). Responses of plants to atmospheric sulphur. In YUNYS M & IQBAL M (eds.) Plant responses to air pollution. John Wiley & Sons, Chichester, UK. pp. 285-294.

ROBINSON MF, HEATH J, MANSFIELD TA. (1998). Disturbances in stomatal behaviour caused by air pollutants. Journal of Experimental Botany, 49: 461-470.

RORICH RP & GALPIN JS (1998). Air quality in the Mpumalanga Highveld region, South Africa. South African Journal of Science, 94: 109-114.

SANDERS GE, CLARK AG, COLLS JJ (1991). The influence of open-top chambers on the growth and development of field bean. New Phytologist, 117: 439-447.

SAXE H (1990). Photosynthesis and stomatal responses to polluted air, and the use of physiological and biochemical responses for early detection and diagnostic tools. Advances in Botanical Research, 18: 2-129.

SCHANSKER G, TOTH S, STRASSER RJ (2005). Methylviologen and dibromothymoquinone treatments of pea leaves reveal the role of photosystem I in the Chl a fluorescence rise OJIP. Biochim Biophys Acta, 1706: 250-261.

SCHIFF JA & HODSON RC (1973). The metabolism of sulfate. Annual Review of Plant Physiology, 24: 381.

SCHOLANDER PF, HAMMEL HT, BRADSTREET ED (1965). Sap pressure in vascular plants. Science, 148: 339-346.

SCHREIBER U & NEUBAUER C (1987). The polyphasic rise of chlorophyll fluorescence upon onset of strong continuous illumination: II Partial control by Photosystem II donor side and possible ways of interpretation. Z Naturforsch 42c: 1255–1264.

SHARP RE, MATTHEWS MA, BOYER JS (1984). Kok effect and the quantum yield of photosynthesis: light partially inhibits dark respiration. Plant Physiology, 75: 95–101.

SHIMAZAKI K & SUGAHARA K (1979). Active oxygen participation in chlorophyll destruction and lipid peroxidation in SO_2-fumigated leaves of spinach. Plant & Cell Physiology, 21: 1193-1204.

SHIMAZAKI K, SAKAKI T, KONDO N, SUGAHARA K (1980). Active oxygen participation in chlorophyll destruction and lipid peroxidation in SO_2-fumigated leaves of spinach. Plant & Cell Physiology, 21: 1193-1204.

SINGSAAS E, ORT DR, DeLUCIA EH (2001). Variation in measured values of photosynthetic quantum yield in ecophysiological studies. Oecologia, 128: 15-23.

SJI JW & SWANSON CA (1974). Short-term kinetic studies on the inhibition of photosynthesis by sulphur dioxide. Journal of Environmental Quality, 3:103-107.

SISON WB, BOOTH JA, THRONBERRY GO (1981). Absorption of SO_2 by pecan [*Carya illinoensis* (Wang) K Koch] and alfalfa (*Medicago sativa* L.) and its effect on photosynthesis. Journal of Experimental Botany, 32:523-534.

SMITH M, KRÜGER G, VAN HEERDEN P, PIENAAR J, WEISSFLOG L, STRASSER R (2008). Effect of trifluoracetate, a persistent degradation product of fluorinated hydrocarbons, on C3 and C4 crop plants. In: ALLEN J, GANTT E, GOLBECK J, OSMOND B (eds.) Photosynthesis. Energy from the sun: 14th international congress on photosynthesis. 1501 -1504. Springer, England.

SPRÜGEL DG, MILLER JE, MULLER RN, SMITH HJ, XERIKOS PB (1978). Effects of sulfur dioxide fumigation on development and yield of field-grown soybeans. Argonne National Laboratory, Radiological and Environmental Research Division Annual Report, January- December ANL-77-65-III, pp. 7-11.

SPRÜGEL DG, MILLER JE, MULLER RN, SMITH HJ, XERIKOS PB (1980). Sulfur dioxide effects on yield and seed quality in field-grown soybeans. Phytopathology, 70: 1129-1133.

STRASSER RJ & GOVINDJEE XUC (1992). On the OJIP fluorescence transient in leaves and DI mutants of *Chlamydomonas reinhardtii*. In: MURATA N (ed.). Research in Photosynthesis. Kluwer Academic Publishers, Dordrecht. pp. 29-32.

STRASSER RJ & STRASSER BJ (1995). Measuring fast fluorescence transients to address environmental questions: The JIP-test. In: MATHIS P (ed.). Photosynthesis: From light to biosphere. Kluwer Academic Publishers, The Netherlands. pp. 977-980.

STRASSSER RJ, SRIVASTAVA A, GOVINDJEE XUC (1995). Polyphasic chlorophyll a fluorescence transients in plants and cyanobacteria. Journal of Photochemistry and Photobiology, 61: 32-42.

STRASSER RJ, TSIMILLI-MICHAEL M, PÊCHEUX M (1999). Perpetual adaptation in a perpetually changing environment as a survival strategy of plants: a case study in foraminifers concerning coral reef bleaching. Photosynthetica, 37 (1): 71-85.

STRASSER RJ, SRIVASTAVA A, TSIMILLI-MICHAEL M (2004). Analysis of the chlorophyll fluorescence transient. In: PAPAGEORGIOU G & GOVINDJEE XUC (eds.) Chlorophyll fluorescence a signiture of photosynthesis. Kluwer Academic Publishers, The Netherlands. 19: 321-362.

STRAUSS AJ, KRÜGER GHJ, STRASSER RJ, VAN HEERDEN PDR (2006). Ranking of dark chilling tolerance in soybean genotypes probed by the chlorophyll a fluorescence transient O-J-I-P. Environmental and Experimental Botany, 56: 147–157.

TAKAHAMA U (1993). Regulation of peroxidase-dependent oxidation of phenolics by ascorbic acid: different effects of ascorbic acid on the oxidation of coniferyl alcohol by the apoplastic soluble and cell wall-bound peroxidases from epicotyls of *Vigna angularis*. Plant and Cell Physiology, 34: 809-817.

TAYLOR SE & TERRY N (1984) Limiting factors in photosynthesis. V. Photochemical energy supply co-limits photosynthesis at low values intercellular CO_2 concentration. Plant Physiology, 75: 82-86.

TAYLOR GE, TINGEY DT, GUNDERSON CA (1985). Photosynthesis, carbon allocation, and growth of sulphur dioxide eco-types of *Geranium carolinianum* L. Oecologia, 68:350-357.

TAYLOR HJ, ASHMORE MR, BELL JNB (1986). Air pollution injury to vegetation. Institution of Environmental Health Officers.

TEMPLE PJ, Fa CH & TAYLOR OC (1985). Effects of SO_2 on stomatal conductance and growth of Phaseolus vulgaris. Environmental Pollution (series A), 37:267-279.

TINGEY DT, NEELY GE, GUMPERTZ ML (1980). The effects of low concentrations of sulphur dioxide on the growth, quality and nitrogen fixation of alfalfa. In: PRESTON EM & GUINN DWO (eds.) The bioenvironmental impact of a coal

fired plant, fifth intrim report. EPA, Corvallis, EPA – 600/3-80-052. pp. 279 - 291.

TSIMILLI-MICHAEL M, PÊCHEUX M, STRASSER RJ (1999). Light and heat stress adaptation of the symbionts of coral reef and temperate foraminifers probed *in hospite* by the chlorophyll a fluorescence kinetics O-J-I-P. Zeitschrift Naturforsch, 54C: 671-680.

TSIMILLI-MICHAEL M & STRASSER R (2008). In vivo assessment of stress impact on plants' vitality: applications in detecting and evaluating the beneficial role of Mycorrhization on host plants. (In press).

TURNER CR (1990). A five year study of air quality in the Highveld region. Eskom Report No TRR/S90/002, Eskom, TRI, Johannesburg.

TYREE MT & JARVIS PG (1982). Water in tissue and cells. In: Encyclopaedia of Plant Physiology, New Series Vol. 12B (LANGE OL, NOBEL PS, OSMOND CB, ZEIGLER H (eds.) Springer-Verlag, Berlin pp. 35 -77.

TYSON PD, KRUGER FJ, LOUW CW (1988). Atmospheric pollution and its implications in the eastern Transvaal highveld. South African National Scientific Programmes, Report No 150, CSIR, Pretoria.

UNSWORTH MH & PICKNEYHR (1972). Nature, 239:458-459.

UNSWORTH MH, BISCOE PV, BLACK V (1976). Analysis of gas exchange between plants and polluted atmospheres. In: MANSFIELD TA (eds.). Effects of air pollutants on plants. Cambridge University Press. NewYork. pp. 5-16.

UNSWORTH M.H. (1982) Exposure to gaseous pollutants and uptake by plants. In: UNSWORTH MH & ORMROD DP (eds.) Effects of gaseous air pollution in agriculture and horticulture. Butterworth Scientific, London, pp. 43-63.

UNSWORTH MH (1986). Principles of microclimate and plant growth in open-top chambers. In: Commission of the European Communities, Air Pollution Research Report 5: Microclimate and plant growth in open-top chambers. pp. 16-29.

URSIN VM & BRADFORD KJ (1989). Auxin and ethylene regulation of petiole epinasty in two developmental mutants of tomato, diageotropica and epinatic. Plant Physiology, 90: 1341-1346.

VAN HEERDEN PDR, TSIMILLI-MICHAEL M, KRÜGER GHJ, STRASSER RJ (2003). Dark chilling effects on soybean genotypes during vegetative development: parallel studies of CO_2 assimilation, chlorophyll a fluorescence kinetics O-J-I-P and nitrogen fixation. Physiologia Plantarum, 117: 476-491.

VAN HEERDEN PDR, STRASSER RJ, KRÜGER GHJ (2004). Reduction of dark chilling stress in N2-fixing soybean by nitrite as indicated by chlorophyll a fluorescence kinetics. Physiologia Plantarum, 121: 239-249.

VAN TIENHOVEN AM & SCHOLES MC (2003). Air pollution impacts on vegetation in South Africa. In: EMBERSON L, ASHMORE M, MURRAY F (eds.) Air pollution impacts on crops and forests – a global assessment. Imperial College Press, London, UK. pp. 237–262.

VERMA M & AGRAWAL M (1996). Alleviation of injurious effects of SO_2 on soybean by modifying NPK nutrients. Agricultural Ecosystem and Environment, 57: 49-55.

VON CAEMMERER S & FARQUHAR GD (1981). Some relationships between the biochemistry of photosynthesis and the gas exchange of leaves. Planta, 153: 376–387.

WALKER DA & OSMOND CB (1986). Measurement of photosynthesis in vivo using a leaf disc electrode:Correlations between light dependence of steady-state photosynthetic O2 evolution and chlorophyll a fluorescence transients. Proc. R. Soc. Lond. B 227:267-280.

WATSON RT, RODHE H, OESCHGER H, SIENGENTHALER U (1990). Greenhouse gases and aerosols. In: HOUGHTON JT, JENKINS GJ, EPHRAUMS JJ (eds.) Climate change – The IPCC Scientific Assessment. Cambridge University Press, Cambridge, UK. pp. 1-40.

WEIGEL HJ & JÄGER HJ (1988). Zur Ökotoxikologie von Luftschadstoffen. II. Aufbau und Funktionweise einer Expositionsanlage aus open-top kammern zur Untersuchung von Immissionswirkungen auf Pflanzen. Landbauforschung Völkenrode, 38(3): 182-195.

WEINSTOCK L, KENDER WJ, MUSSELMAN RC (1982). Microclimate within open-top air pollution chambers and its relation to grapevine physiology. Journal of the American Society of Horticultural Science, 107:923-929.

WELLBURN AR, MAJERNIK O, WELLBURN FAM (1972). Effects of SO_2 and NO_2 polluted air upon the ultrastructure of chloroplasts. Environmental Pollution, 3: 37-49.

WELLBURN AR (1985). SO_2 effects on stomatal and thylakoid function. In: WINNER WE, MOONEY HA, GOLDSTEIN RA (eds.) Sulphur dioxide and vegetation - physiology, ecology and policy issues. Stanford University Press, Stanford, CA. pp. 133-147.

WELLBURN A (1994). Air pollution and climate change: the biological impact. Harlow, UK: Longman Scientific Publishers.

WHATLEY JM (1971). Ultrastructural changes in chloroplasts of Phaseolus vulgaris during development under conditions of nutrient deficiency. New Physiologist, 70: 725-742.

WHITEHEAD D, HOGAN KP, ROGERS GND, BYERS JN, HUNT JE, MCSEVENY TM, HOLLINGER DY, DUNGAN RJ, EARL WB, BOURKE MP (1995). Performance of large open-top chambers for long-term investigations of tree response to elevated carbon dioxide concentration. Journal of Biogeography, 22: 307-313.

WINNER WE, MOONEY HA, WILLIAMS K, VON CAEMMERER S (1985). Measuring and assessing SO_2 effects on photosynthesis and plant growth. In: WINNER WE, MOONEY HA, GOLDSTEIN RA. (eds.) Sulphur dioxide and vegetation - physiology, ecology and policy issues. Stanford University Press, Stanford, CA. pp. 118-132.

WINNER WE (1994). Mechanistic analysis of plant responses to air pollution. Ecological Applications, 4(4): 651-661.

WOLFENDEN J, PEARSON M, FRANCIS J (1991). Effects of overwinter fumigation with sulphur and nitrogen oxides on biochemical parameters and spring growth in red spruce (Pecea rubens Sarg.). Plant Cell and Environment, 14: 35-45.

WORTHINGTON AG & COLLS JJ (1998). Validation and use of a computer model of the solar radiation regime in open-top chambers. Journal of Agricultural Research, 71: 137-145.

YANG SF & HOFFMAN NE (1984). Ethylene biosynthesis and its regulation in higher plants. Annual Review of Plant Physiology, 35: 155-189.

YORDANOV I, GOLTSEV V, STEFANOV D, CHERNEV P, ZAHARIEVA I, KIROVA M, GECHEVA V, STRASSER RJ (2008). Preservation of photosynthetiuc electron transport from senescence-induced inactivation in primary leaves after decapitation and defoliation of bean plants. Journal of Plant Physiology (In press).

YOUNG EG & CONAY CF (1942). On the estimation of Aln by the Rimini-Schrever reaction. Journal of Biological Chemistry, 142: 839-853.

ZIEGLER I (1972). The effect of SO_3^{2-} on the activity of ribulose-1, 5-diphosphate carboxylase in isolated spinach chloroplasts. Planta, 103: 155-163.

ZIEGLER I (1973) Effect of sulphite on phosophoenolpyrovate carboxylase and malate formation in extracts of Zea mays. Phytochemistry, 12:1027-1030.

ZIEGLER I (1975). The effects of SO_2 pollution on plant metabolism. Residues Reviews, 56: 79 -105.